STOCHASTIC ANALYSIS OF SOLUTE TRANSPORT IN HETEROGENEOUS AQUIFERS SUBJECT TO RANDOM RECHARGE AND CONTAMINANT SOURCE FIELDS

By

LIYONG LI

A DISSERTATION PRESENTED TO THE GRADUATE SCHOOL
OF THE UNIVERSITY OF FLORIDA IN PARTIAL FULFILLMENT
OF THE REQUIREMENTS FOR THE DEGREE OF
DOCTOR OF PHILOSOPHY

UNIVERSITY OF FLORIDA

1998

ACKNOWLEDGEMENTS

First, my heartfelt thanks and appreciations go to Dr. Wendy Graham and Dr. Suresh Rao for their kind help and patience in guiding me through the preparation of this dissertation. They recruited me to the hydrological science group of University of Florida and made my education here possible.

Dr. Graham's weekly meetings are a stimulating working and valuable studying opportunities, which help me to mature in a professional sense. Her technical and moral supports have been sincerely appreciated.

I would like to thank Dr. P. S. C. Rao for his invaluable help and guidance throughout the course of this research. Dr. Rao has provided me with opportunities to look inside the physical processes behind the theoretical analysis. I appreciate the many intellectual and challenging discussions we had over the years.

Special thanks also go to Dr. Kirk Hatfield, Dr. Michael D. Annable, and Dr. Kenneth L. Campbell for serving as my committee members, and for their insightful comments provided during many research meetings. I learned many technical skills from Dr. Hatfield's courses, which have turned out to be highly valuable in my research work.

I thankfully acknowledge the education I received from the Civil Engineering Department at Helsinki University of Technology prior to my transfer to Florida, special thanks go to Professor P. Vakkilainen for his guidance and support during my stayings in the hydraulic laboratory of HUT.

I am thankful beyond words to Dr. DongPing Dai for assisting me at U.F., for her support and friendship.

I would also like to thank Dr. Andy I. James and Dr. Ashie Akpoji for their valuable input to this research. In addition, my gratitude goes to my fellow graduate students in the Hydrological Sciences Academic Cluster for their help and friendship; Dr. Yan Zhang, George G. Demmy, Xavier Foussereau.

I am especially grateful to my family for their love, encouragement, counsel, and support in my pursuit of this dream.

Financial support for this research was provided in part by the University of Florida Department of Agricultural And Biological Engineering–Hydrologic Sciences Academic Cluster Research Assistantship Program.

TABLE OF CONTENTS

ACKNOWLEDGEMENTS ii

LIST OF TABLES vii

LIST OF FIGURES viii

ABSTRACT xi

CHAPTERS

1 BACKGROUND 1
1.1 Introduction 1
1.2 Deterministic Models 2
1.2.1 Basic Assumptions 2
1.2.2 Limitations of the ADE 4
1.3 Stochastic Models 5
1.3.1 Concepts and Assumptions 5
1.3.2 Main Stochastic Methods 6
1.4 Scope for the Dissertation 12

2 SPATIALLY RANDOM RECHARGE 15
2.1 Introduction 15
2.2 Derivation of the Unconditional Moment Equations 18
2.2.1 Head Field 18
2.2.2 Velocity Field 20
2.2.3 Concentration Field 21
2.3 Solution of the Unconditional Moment Equations 23
2.3.1 Head and Pore Water Velocity Moment Equations 23
2.3.2 Concentration Plume Moments 34
2.3.3 Analysis of Higher-Order Concentration Covariance Approximations 46
2.4 Summary 49

3 TRANSIENT RANDOM RECHARGE 54
3.1 Introduction 54
3.2 Unconditional Flow-related Moment Equations 58
3.2.1 Head Field 58
3.2.2 Velocity Field 60
3.3 Solutions for Unconditional Flow-related Moment Expressions . . 61
3.3.1 Solutions of Head-log Transmissivity and Head-Recharge Cross-Covariances 63
3.3.2 Solutions of Head Covariances 64

3.3.3 Solutions of the Velocity Covariance . . . 67
3.4 Moment Equations for Solute Transport . . . 79
3.4.1 Governing Equations . . . 79
3.4.2 Concentration Moment Equations Under Transient Velocity Field . . . 79
3.4.3 Integration Expressions . . . 82
3.5 Solutions in Laplace-Fourier Domain . . . 87
3.5.1 Mean Concentration and Macrodispersive Flux Solutions 87
3.5.2 Concentration Variance Solution . . . 90
3.5.3 Fast Fourier Transform Algorithm . . . 91
3.6 Comparisons of Standard Deviation Computations . . . 91
3.7 Example Problems . . . 94
3.7.1 Problem Description . . . 94
3.7.2 Concentration Plume Moments by Fast Fourier Transform 97
3.8 Summary . . . 107

4 UNCERTAIN SOURCE CONDITIONS . . . 111
4.1 Introduction . . . 111
4.2 Governing Equations . . . 113
4.3 Ensemble Moment Equations . . . 115
4.4 Cross-covariance between Source and Concentration . . . 122
4.5 Moment Solutions in Laplace-Fourier Domain . . . 124
4.5.1 Mean Concentration and Macrodispersive Flux Solutions 124
4.5.2 Uncertain Contaminant Source . . . 128
4.6 Example Problems . . . 131
4.6.1 Problem Settings . . . 131
4.6.2 Concentration Plume Moments . . . 133
4.7 Summary . . . 147

5 SUMMARY AND CONCLUSIONS . . . 150
5.1 Assumptions and Limitations . . . 150
5.2 Conclusions and Applications . . . 153
5.2.1 Spatio-temporally Random Recharge . . . 153
5.2.2 Spatio-temporally Random Contaminant Source . . . 156
5.3 Suggestions for Future Research . . . 158

APPENDIXES

A DERIVATION FOR THE HEAD-RELATED STATISTICS . . . 160
A.1 Fourier Transform . . . 160
A.2 Basic Equations . . . 160
A.3 P_{HY} derivation . . . 161
A.4 P_{HH} derivation . . . 163
A.5 Derivation for $P_{v_i v_j}$ . . . 166

B DERIVATION FOR THE TRANSIENT HEAD-COVARIANCE . . . 170
B.1 P_{HY} derivation . . . 170
B.2 P_{HR} derivation . . . 171
B.3 P_{HH} derivation . . . 174
B.4 Derivation for $P_{v_i v_j}$ . . . 179

C MOMENTUM METHOD . . . 183
C.1 General Integration Expressions for Initial Condition . . . 183
C.2 General Integration Expressions for Non-homogeneous P.D.E.s . 184

D LAPLACE AND FOURIER TRANSFORM 187
D.1 Definiation 187
D.2 Two-Dimensional Convolution 188
D.3 Some Useful Laplace and Fourier Transform Pairs 189
D.4 Derivative Properties of Fourier Transform 191

REFERENCES 192

BIOGRAPHICAL SKETCH 201

LIST OF TABLES

2.1 Input parameters for different simulation cases. 35
3.1 Input parameters for head and velocity correlation function. 67
3.2 Input parameters for different simulation cases. 95
4.1 Input parameters for different simulation cases. 132

LIST OF FIGURES

2.1 The head correlation function vs normalized separation distance in the direction of mean flow (Note: Curves for Cases 2 and 3 coincide with the curve of Case 1) 27

2.2 The head correlation function vs normalized separation distance transverse to the direction of mean flow(Note: Curves for Cases 2 and 3 coincide with the curve of Case 1) 28

2.3 Comparison of x_1-velocity correlation functions (equation (2.9)) to x_1-velocity correlation functions derived by Rubin and Bellin (1994) in the direction of mean flow for Cases 1 through 4. 32

2.4 Comparison of x_2-velocity correlation functions (equation (2.9)) to x_2-velocity correlation functions derived by Rubin and Bellin (1994) in the direction of mean flow for Cases 1 through 4. 33

2.5 Mean concentration at 225 days after release, (a) for Case 1, (b) for Case 2, (c) for Case 3, (d) for Case 4. 37

2.6 Concentration plume for single replicate at 225 days after release, (a) for Case 1, (b) for Case 2, (c) for Case 3, (d) for Case 4. 39

2.7 Concentration plume for single replicate at 225 days after release, (a) for Case 1, (b) for Case 2, (c) for Case 3, (d) for Case 4. 40

2.8 Concentration standard deviation at 225 days after release, (a) for Case 1, (b) for Case 2, (c) for Case 3, (d) for Case 4. 42

2.9 a. Normalized first moment, MX_1, vs time (days); b. Second centralized moment, MX_2, vs time (days); c. Second centralized moment, MY_2, vs time (days). 45

2.10 Comparison of the higher-order estimate of concentration standard deviation (equation (2.30)) and the first order estimate of concentration standard deviation (equation (2.15)) for Case 1 at 170 days. 50

3.1 The head correlation function $P_{HH}(0,0,\tau)/\sigma_H^2$ vs normalized time lag resulting from the spatiotemporally random recharge field 68

3.2 The head correlation function $P_{HH}(\xi_1,0,0)/\sigma_H^2$ vs normalized separation distance resulting from different recharge fields, in which s_y =0.15 69

3.3 The head variance σ_H^2 vs the temporal correlation scale; $\bar{R}$=0. 70

3.4 The head correlation function $P_{HH}(\xi_1, 0, \tau)/\sigma_H^2$ vs normalized time lag subject to different aquifer storativities; (a), σ_Y^2=0.29; (b), σ_Y^2=0. . . 71

3.5 The velocity covariance vs normalized spatial separation distance subject to different temporal correlation scales; $I_t = \infty$ in Temporally uniform, spatially random R. 74

3.6 The velocity covariance vs normalized temporal separation lag subject to different temporal correlation scales; $I_t = \infty$ in Temporally uniform, spatially random R. 75

3.7 The velocity variance $\sigma_{v_1}^2$ vs the temporal correlation scale; $\bar{R}$=0. . . 77

3.8 The velocity covariance vs (a) normalized temporal lag and (b) normalized spatial separation distance subject to different aquifer storativities; $\bar{R}$=0. 78

3.9 Standard deviation at 85 days after release for case 1: (a), the integration method; (b), the finite element method; (c), the fast Fourier transform method 94

3.10 (a), (b), (c), (d), and (e) represent Mean Concentration of Cases 1, 2, 3, 4, and 5 respectively at 85 days after release; (f), (g), (h), (i), and (j) represent Concentration Standard Deviation of Cases 1, 2, 3, 4, and 5 respectively at 85 days after release 98

3.11 The first normalized moments at x_1 direction for each case 102

3.12 The second normalized moments at x_1 direction for each case 103

3.13 The second normalized moments at x_2 direction for each case 104

3.14 (a), (b), and (c) represent Mean Concentration of Case 2 with mean recharge $\bar{R}$ equals 0., -0.003, and 0.003, respectively; (d), (e), and (f) represent Concentration Standard Deviation of Case 2 with mean recharge $\bar{R}$ equals 0., -0.003, and 0.003 meter/day, respectively; . . . 106

4.1 (a) Mean Concentration at 85 days after release for Case 1; (b) Mean Concentration at 85 days after release for Case 2; (c) Mean Concentration at 85 days after release for Case 3. Source size is 2.0 meters * 2.0 meters. 135

4.2 (a) Mean Concentration at 85 days after release for Case 1; (b) Mean Concentration at 85 days after release for Case 2; (c) Mean Concentration at 85 days after release for Case 3. Source size is 4.0 meters * 2.0 meters. 136

4.3 (a) Mean Concentration at 85 days after release for Case 1; (b) Mean Concentration at 85 days after release for Case 2; (c) Mean Concentration at 85 days after release for Case 3. Source size is 2.0 meters * 4.0 meters. 137

4.4 The second normalized moments at x_1 direction for each case. 138

4.5 The second normalized moments at x_1 direction for each case. 139

4.6 (a) Concentration variance at 85 days after release for Case 1; (b) Concentration variance at 85 days after release for Case 2; (c) Concentration Variance at 85 days after release for Case 3. Source size is 2.0 meters * 2.0 meters. 141

4.7 (a) Concentration variance at 85 days after release for Case 1; (b) Concentration variance at 85 days after release for Case 2; (c) Concentration Variance at 85 days after release for Case 3. Source size is 4.0 meters * 2.0 meters. 142

4.8 (a) Concentration variance at 85 days after release for Case 1; (b) Concentration variance at 85 days after release for Case 2; (c) Concentration Variance at 85 days after release for Case 3. Source size is 2.0 meters * 4.0 meters. 143

4.9 (a) Concentration variance resulting from the random velocity field at 85 days after release for Case 2; (b) Concentration variance resulting from the random contaminant source field at 85 days after release for Case 2; (c) Total concentration Variance at 85 days after release for Case 2. Source size is 2.0 meters * 2.0 meters. 144

4.10 (a) Concentration variance resulting from the random velocity field at 85 days after release for Case 3; (b) Concentration variance resulting from the random contaminant source field at 85 days after release for Case 3; (c) Total concentration Variance at 85 days after release for Case 3. Source size is 2.0 meters * 2.0 meters. 145

4.11 Cross-covariance between source strength in the source zone and concentration throughout the domain at 85 days after release for Cases 2 (a) and 3 (b); $\mathbf{x}^{\star}$ =(4,10); Source size is 2.0 meters * 2.0 meters. . . . 146

4.12 Cross-covariance between source strength in the source zone and concentration throughout the domain at 85 days after release for Cases 2 (a) and 3 (b); $\mathbf{x}^{\star}$ =(4,12); Source size is 2.0 meters * 2.0 meters. . . . 147

Abstract of Dissertation Presented to the Graduate School
of the University of Florida in Partial Fulfillment of the
Requirements for the Degree of Doctor of Philosophy

STOCHASTIC ANALYSIS OF SOLUTE TRANSPORT IN HETEROGENEOUS AQUIFERS SUBJECT TO RANDOM RECHARGE AND CONTAMINANT SOURCE FIELDS

By

Liyong Li

May 1998

Chairman: Dr. Wendy D. Graham
Cochairman: Dr. Palakurthi S.C. Rao
Major Department: Agricultural and Biological Engineering

This dissertation derives and solves approximate unconditional moment equations for head, velocity, and concentration in a two-dimensional heterogeneous aquifer subject to random recharge and random contaminant source fields, in which nonuniform (linear trending) velocity and transient velocity are established due to the spatially variable or spatiotemporally variable recharge, respectively.

Under a steady-state recharge field, closed-form expressions are derived for the unconditional, nonstationary auto-covariances for head and velocity, and the cross-covariances between velocity, head, recharge, and log-transmissivity based on a system of coupled first-order partial differential moment equations and assumed hole-type input covariance functions for log-transmissivity and recharge. The unconditional flow related moment equations are incorporated into a system of solute transport moment equations, which are solved using a Galerkin finite element algorithm. A constant

positive mean recharge yields a mean velocity gradient which enhances the ensemble mean plume spreading in the longitudinal direction, similar to results found by Rubin and Bellin (1994). Spatial variability in recharge further enhances the spreading of the ensemble mean plume, especially in the lateral direction. Uncertainty in the spatial distribution of recharge also increases the extent of the ensemble standard deviation plume, particularly in the lateral direction, and increases the coefficient of variation of solute concentration. The uncertainty in the prediction of solute transport increases with increasing recharge variance and spatial correlation scale.

The research is then extended to deal with the unconditional moments of head, velocity, and concentration under transient flow conditions, which are assumed to be caused by a spatiotemporally random recharge. Semi-analytical solutions are derived for the unconditional covariances for transient velocity with a constant mean recharge using the Fourier transform approach. Results demonstrate that the velocity covariance derived for the steady-state random recharge field is a limiting case of the spatiotemporally variable velocity covariance with an infinite temporal correlation scale. Another limiting case with an infinite spatial correlation scale indicates that introduction of temporally variable but spatially uniform recharge has no effect on the velocity covariances, and thus no effect on the ensemble mean concentration plume spreading or the concentration prediction uncertainty.

Following Deng et al. (1993), the equations for mean concentration and macrodispersive flux under zero mean transient recharge are decoupled in the Laplace-Fourier domain and solved using a fast Fourier transform algorithm, which significantly reduces the computational demand. The first-order concentration variance is solved using three different approximate techniques: an approximate fast Fourier transform technique, a finite element method [Graham and McLaughlin, 1989a, 1989b, 1991], and a direct numerical integration. The simulation results show that introduction of a spatiotemporally random recharge enhances both longitudinal

and lateral mean concentration plume spreading compared to the no recharge case. However, transient recharge produces less spreading and less concentration prediction uncertainty than the steady-state spatially random recharge case (Li and Graham, 1998). Increasing recharge variance or temporal correlation scale results in increased concentration prediction uncertainty. The magnitude of aquifer storativity has little effect on the evolution of the concentration field moments.

Finally, the joint effects of uncertain contaminant source and random velocity fields on the evolution of concentration moments are investigated. The continuous mass-release rate in a contaminant source zone is assumed to be a random field, which can be correlated or uncorrelated with the random velocity field. Steady-state unconditional velocity and mass release rate covariances were incorporated into the decoupled mean macrodispersive flux equations, and solved using the fast Fourier transform algorithm to compute the concentration moments. The results confirm the previous result by Zhang and Neuman (1995a) that uncertain mass release rate has little impact the ensemble mean concentration plume spreading. A new term, the covariance between random mass release rate and concentration, is introduced in this work to characterize the correlation between mass release rate and concentration in the source zone. This term serves to transfer the mass release rate uncertainty to the concentration prediction uncertainty, and quantifies the information that local resident concentrations contain regarding source strength throughout the source region. Results also show that a mass release rate which is correlated with local velocity will cause higher concentration prediction uncertainty than an uncorrelated mass release rate will, especially for a larger source area.

CHAPTER 1
BACKGROUND

1.1 Introduction

Groundwater is an important water resource which supplies people with drinking, industrial, and agricultural water around the world. Development of groundwater resources and maintenance of groundwater quality is receiving increasing public attention due to the current and potential environmental contamination resulting from industrial, municipal, radioactive waste disposals and agricultural activities. For many years, groundwater flow and solute transport models have served as management tools in water resource and water quality management activities. These activities include the interpretation of data collected in field investigations, the appraisal and assessment of water resources and their corresponding quality, the prediction of potential contaminant transport associated with contaminant disposal, the design and comparison of remediation alternatives, and the determination of the adequacy of monitoring and compliance networks.

Like models in other areas, the groundwater flow and solute transport models are a simplification or abstraction of the subsurface system. Therefore, a successful groundwater flow and solute transport model requires an adequate knowledge of the fundamental properties of porous media and interactions among the major physical, chemical, and biological processes in the system of concern. Unfortunately, the availability of field data to describe such fundamental properties and interaction relationships is limited in groundwater systems. The problem is further complicated by the fact that the natural properties related to groundwater systems can be highly variable in space and time.

1.2 Deterministic Models

One of the well-known deterministic models for solute transport in aquifers is the physically based advection-dispersion equation (ADE) for an inert solute transport in porous media. This model is derived from the principle of mass conservation, in which advection and dispersion are treated as major physical processes [Bear, 1979]. The advection-dispersion equation is written:

$$\frac{\partial \theta c(\mathbf{x},t)}{\partial t} = \nabla \cdot [\theta \mathbf{D}(\mathbf{x}) \cdot \nabla c(\mathbf{x},t)] - \nabla [\mathbf{q}(\mathbf{x})\, c(\mathbf{x},t)] \quad \mathbf{x} \in D \tag{1.1}$$

where $c(\mathbf{x},t)$ ($[ML^{-3}]$) is the resident concentration of solute in the aqueous phase; θ ($[L^3L^{-3}]$) is the volumetric moisture content; D is a three-dimensional domain; $\mathbf{x} = (x_1, x_2, x_3)$ is a point in D. Also, $\mathbf{D}(\mathbf{x})$ ($[L^2T^{-1}]$) is the dispersion tensor representing the hydrodynamic dispersion coefficients, and $\mathbf{q}(\mathbf{x})$ is the Darcy flux with components q_1, q_2, and q_3.

1.2.1 Basic Assumptions

One of the fundamental assumptions of equation (1.1) is the continuity of its components and medium properties. It is implemented by introducing the continuum concept, in which a real, possibly discontinuous porous medium is replaced by a hypothetical but representative continuum [Bear, 1979]. Therefore the physical variables and properties are perceived as some known spatially and temporally continuous variables, which are differentiable and measurable over some specified domain (area or volume) that is of large extent compared to the pore scale heterogeneity, i.e., 10^{-1} to 1 meter. The pore scale is typically assumed to be on the order of 10^{-5} m to 10^{-1} m [Zhang, 1997].

The properties defined on this specific area or volume basis are macroscopic properties, whose estimation involves an averaging process over this area or volume.

For any physical variable P of concern, its average value at a vector point $\mathbf{x}$ can be written as,

$$P(\mathbf{x}) = \frac{1}{V}\int_0^V p(\mathbf{x}')d\mathbf{x}' \tag{1.2}$$

where $p(\mathbf{x}')$ is an infinitesimal quantity of P integrated over V and is implicitly related to the geometry of pore scale heterogeneities [Bear, 1972]; and V usually represents Representative Elementary Volume (REV) or Representative Elementary Area (REA). The estimation of these parameters assumes that the averaging processes were performed at their Representative Elementary Volume (REV) in order to warrant consistency of measurements or estimations. Therefore, the physically based models describing the groundwater systems are scale-dependent. The ADE (1.1) is a macroscopic partial differential equation for solute transport through porous media. It is reasonable to assume that the validity of this equation holds at the formation local scale for an extent of the flow domain from 10^1 - 10^2 meters [Dagan, 1986].

The second assumption typically underlying groundwater flow and transport models is that the flow regime of the porous media follows the linear Darcy's Law, which is valid for the Reynolds number not exceeding values between 1 and 10 [Bear, 1972]. Widely used in fluid mechanics, the Reynolds number is a dimensionless parameter that expresses the ratio of inertial to viscous forces during the flow, and distinguishes the laminar flow due to low velocities from turbulent flow due to high velocities. Finally, derivation of the ADE assumes that the solute dispersion is similar to a diffusion process, but only in a mathematical sense since dispersion is not due to a gradient in solute concentration. Therefore, dispersion is represented by Fick's First Law.

1.2.2 Limitations of the ADE

Representative Elementary Volume

REV (or REA) choice is usually based on the criteria of indifference to property, insensitivity to experimental method, and invariance to space and time [Bear, 1979]. A fundamental issue lies in that REV is assumed to be significantly smaller than the simulation domain. A common REV for all the physical variables satisfying the ADE is an ideal situation. The possibility of different REVs in real situations could limit explanation of the prediction results and applications of the models.

Natural Heterogeneities

The prediction accuracy of the flow and solute transport models is strongly dependent on the adequate knowledge of physical parameters such as hydraulic conductivity, transmissivity, and recharge. Unfortunately the direct application of the ADE is impractical in natural conditions because porous medium properties can vary dramatically over space. Incorporating detailed data on physical variables into the ADE would require enormous computational resources and more importantly, intensive collection of measurements is too costly to be possible in practice. Therefore, the ignorance of the spatial distribution of the physical variables limits the application of the ADE in subsurface conditions.

Dispersion

It has been observed that the field scale dispersion is many times greater than that observed in the laboratory, and increases with solute travel time or travel distance [Gelhar, 1993]. This is called the scale-dependent dispersion and violates the Fickian assumption [Frind, 1987]. This phenomenon reduces the application range of the ADE.

1.3 Stochastic Models

1.3.1 Concepts and Assumptions

The increasing awareness of natural variability and heterogeneity in groundwater systems and the resulting prediction uncertainty of deterministic models has led researchers to resort to stochastic modelling techniques to deal progressively with the problems in groundwater systems. In contrast to deterministic models, which use known parameters and make single valued predictions of variables at particular locations and times, stochastic methods treat parameters such as hydraulic conductivity, head, velocity, and concentration as random variables or random fields, make predictions of the distribution of values at particular locations and times, and present the statistical characteristics of these variables of concern.

A random variable is different from a random field or random process. The former can be described completely by its probability density function, however, the latter requires a joint probability density function between all points in space to describe the process or processes completely. Field data [Freeze, 1975; Delhomme, 1979; Clifton and Newman, 1982] show that the irregular medium properties often exhibit some spatial correlation between adjacent points, rather than occurring as completely independent random variables. Therefore, random fields are extensively used to characterize the heterogeneity of porous medium. Unfortunately field data are typically not sufficient to estimate these joint probability density functions for medium properties. A more practical approach is to consider certain statistical moments of the joint density functions, such as the covariance and cross-covariance, to describe random field continua. These statistical moments are measures of the variability and spatial or temporal correlation structure of the medium properties.

The treatment of physical aquifer characteristics such as hydraulic conductivity as random fields implies that resulting head, velocity, and solute concentration also are spatiotemporally random processes. Deriving and determining the statistical

ensemble moments of head, velocity, and solute concentration which satisfy head, flow, and solute transport equations in heterogeneous subsurface conditions is the main objective of the stochastic approach. The ensemble mean, variance, covariance, and cross-covariance of these variables are the main statistical moments used to characterize these random fields. For a random field, its ensemble mean, or the expected value (which is a measure of the central tendency of the random field), is found by taking the first moment [Gelhar, 1993]. The macrodispersive flux, variance, covariance, and cross-covariance (which quantify expected deviations from the ensemble means) can be found by taking the second moment of a random variable either with respect to itself or another random variable.

1.3.2 Main Stochastic Methods

During the past 20 years, the field of stochastic analysis of flow and solute transport in porous media has experienced tremendous growth. Stochastic modelling techniques developed and applied to flow and solute transport in both unsaturated and saturated porous media include: Monte Carlo simulations [Warren and Price, 1961; Freeze, 1975; Smith and Freeze, 1979a, 1979b; Ammozegar-Fard et al., 1982], Random Walk approaches [Ahlstrom et al., 1977; Tompson et al., 1987; Valocchi et al., 1989], Transfer function methods [Jury et al., 1982, 1986], Lagrangian perturbation techniques [Dagan, 1982b, 1984, 1986, 1987; Rubin and Dagan, 1987a, 1987b; Rubin and Bellin, 1994; Neuman and Zhang, 1990; Zhang and Neuman, 1990], Eulerian perturbation analysis [Gelhar, 1976; Bakr et al., 1978; Gutjahr et al., 1978; Gelhar et al., 1979; Mizell et al., 1982; Gelhar and Axness, 1983; Yeh et al., 1985a, 1985b; Mantoglou and Gelhar, 1987a, 1987b, 1987c; Graham and McLaughlin, 1989 a, 1989b; Graham and Tankersley, 1994; Kapoor and Gelhar, 1994a, 1994b; Li and Graham, 1998], and Eulerian-Lagrangian theory [Neuman, 1993; Zhang and Neuman, 1995a, 1995b, 1995c, 1995d] and others. Here we present a brief review of these methods.

Monte Carlo Simulations

Monte Carlo simulation is a straightforward, easy-to-implement method. It consists three major parts: 1) generating the random fields for input parameters representing the heterogeneous properties and forcing terms according to the identified or postulated porous medium structures; 2) repeating simulations of flow and solute transport governing equations incorporating the random parameters and forcing terms; and 3) determining ensemble moments for a population of dependent variables resulting from the repeated simulation results.

One of the well-known advantages of Monte Carlo simulations is that this method offers almost no limitations as far as the modeled equations and/or distributional assumptions of input parameters are concerned. However, the applications of this method are restricted by its high computational demands, and the problem-specific nature of its results.

Transfer Function Method

Jury et al. (1982, 1986) proposed a transfer function approach for describing solute movement in unsaturated soils. They tried to characterize transfer-functions between measured inputs and outputs for a soil unit based on the principle of superposition and solute mass balance. This is a kind of black box model which requires site-specific measurements to estimate an appropriate transfer function. It has the advantages of encompassing all linear solute transport models, and being calibrated by actual data. However, there has been difficulty demonstrating that transfer functions fit to specific domains can be extrapolated to other cases.

Lagrangian Perturbation Techniques

In Lagrangian formalism, the inert solute is viewed as a set of infinitesimal particles, dM, which are regarded as macroscopic at the pore-scale, but small at the formation scale. A particle initially located at the vector position $\mathbf{x}_0$ at time t_0, moves

along a Lagrangian trajectory coordinate, $\mathbf{x} = \mathbf{X}_t(\mathrm{t};\, t_0,\, \mathbf{x}_0)$, which can be decomposed as [Dagan, 1984]:

$$\mathbf{X}_t(t; \mathbf{x}_0, t_0) = \mathbf{X}(t; \mathbf{x}_0, t_0) + \mathbf{X}_d(t; t_0) \tag{1.3}$$

The particle trajectory satisfies the fundamental kinetic differential equation:

$$\frac{d\mathbf{X}_t}{dt} = \mathbf{V}_t = \mathbf{U}_t(\mathbf{X}_t, t) + \mathbf{u}(\mathbf{X}_t, t) + \mathbf{v}_d \tag{1.4}$$

where $\mathbf{V}_t$ is the particle velocity, $\mathbf{U}_t$ is the mean or expected velocity, $\mathbf{u}$ is the random velocity perturbation and $\mathbf{v}_d$ is a Brownian motion velocity associated with pore-scale dispersion. Once $\mathbf{X}_t$ is known, the concentration field can be written as follows:

$$dC(\mathbf{x}, t, \mathbf{x}_0, t_0) = \frac{dM}{\theta}\delta\left[\mathbf{x} - \mathbf{X}_t(t, \mathbf{x}_0, t_0)\right] \tag{1.5}$$

where dC stands for a differential increment of concentration, δ is the Dirac function, and $C_0\theta_0 d\mathbf{x} = dM$. Then the concentration at a position $\mathbf{x}$ and at time t over a volume V of which $\mathbf{x}$ is the centroid, becomes [Dagan, 1984]:

$$C(\mathbf{x}, t) = \int_0^{V_0} \frac{\theta_0}{\theta}\delta\left[\mathbf{x} - \mathbf{X}_t(t, \mathbf{x}_0, t_0)\right] C_0(\mathbf{x}_0, t_0) d\mathbf{x}_0 \tag{1.6}$$

where $C_0(\mathbf{x}_0, t_0)$ is the initial solute concentration, and θ_0 is the porosity in the initial volume of the source V_0.

Assuming that velocity $\mathbf{U}_t$ and particle displacement $\mathbf{X}_t$ are random functions, Dagan (1984, 1986, 1987, 1989) derived the approximate expressions for ensemble particle displacement, first-order approximation solutions for ensemble particle displacement statistics and ensemble mean and variance of solute concentration in a

steady state flow field with a uniform mean hydraulic gradient. Dagan's work suggests that the ensemble longitudinal macrodispersivity increases with time and travel distance and reaches an asymptotic value at later times.

Following Dagan's lead, Lagrangian perturbation techniques have been extensively applied and extended for stochastic analysis of inert or reactive solute concentration and solute flux in both saturated and unsaturated zones [Dagan, 1984, 1986, 1987, 1989; Dagan et al, 1992; Rubin, 1990; Bellin et al., 1993, 1996; Cvetkovic et al., 1992; Dagan et al., 1992]. The advantage of Lagrangian perturbation techniques is its mathematical elegance and potential for analytical solution which offers a great quantitative tool for hydrologists. The successful interpretation of the tracer experiments at the Borden site in Canada enhances its acceptance for use in field applications [Sposito and Barry, 1987]. However, the assumption of steady-state flow condition can restrict the application of this approach. Furthermore, the requirement of neglecting local dispersivity in deriving concentration variance casts doubts on the accuracy of the resulting concentration variance. The numerical solutions of the particle displacement and concentration moments can be highly computational demanding in multidimensional cases since they require double integration for each space dimension.

Eulerian Perturbation Techniques

Since the infinite-domain spectral theory was introduced into the subsurface hydrology by Gelhar (1974), it has been applied to a great variety of problems to characterize large-scale spatially variable flow and concentration fields. This method decomposes any random field into a sum of its mean function and a perturbation function and assumes that the perturbation is uniquely represented in terms of the Fourier-Stieltjes integral transform [Gelhar and Axness, 1983; Gelhar 1984, 1986, 1987a, and 1987b].

By invoking stationarity and using the unique conjugate property of Fourier-Stieltjes transform, Gelhar and his co-workers have derived close-form expressions for the head covariance, velocity covariance, effective hydraulic conductivity tensor and effective solute macrodispersion tensor in a variety of situations [Bakr et al., 1978; Gelhar and Axness, 1983; Gelhar 1984, 1986, 1987a, and 1987b]. The "effective" transport properties were defined in connection with the "large scale" Darcy and Fickian laws, relating mean fluxes to mean gradients. Sudicky (1986) found that ensemble macrodispersivity derived using spectral analysis by Gelhar and Axness (1983) are similar to those obtained from a spatial moment analysis of concentration data at the Borden site. The leading terms of Dagan's (1989) asymptotic longitudinal macrodispersivity expression match the results derived by Gelhar and Axness (1983).

The results of spectral analysis are analytically derived and can be rapidly obtained. The spectral analysis of time or space series has the advantage that under some conditions, the spectral transform of a partial differential equation is a polynomial whose solution is found much easier than the solution to a partial differential equation in the real field domain [Harter, 1994]. However, the performance of a spectral method is limited by the stationarity and infinite domain hypotheses and by small variability of the stochastic process required for the small perturbation assumption [Gelhar, 1984; Dagan, 1982a, 1982b; McLaughlin and Wood, 1988a, 1988b].

More recent developments in Eulerian perturbation techniques relax some of these limiting assumptions. Graham and McLaughlin's (1989a, 1989b; 1991) moment method and Li and McLaughlin's (1991, 1995) non-stationary spectral method can perform Eulerian stochastic analyses for non-stationary fields using numerical methods. However, they are still restricted to a small variability of the stochastic processes, and suffer from high computation time and memory requirements in multi-dimensional cases. Deng et al.'s (1993) stochastic fast Fourier transform method is a computationally efficient method for computing the ensemble mean and effective

flow and transport properties for non-stationary fields. Recently this method was extended to estimate the second-order log-fluctuating conductivity variance corrections to the head and velocity covariance functions by Deng and Cushman (1995) for a log-normal, stationary hydraulic conductivity field. Kapoor and Gelhar (1994a, 1994b) extended the infinite domain spectral analysis to take account of higher-order perturbation products, but their method is still based on the controversial assumption that the mean concentration gradient is constant in space and time.

Eulerian-Lagrangian Techniques

Neuman (1993) presented a unified Eulerian-Lagrangian theory for the transport of a conservative solute in a space-time non-stationary random velocity field conditioned on hydraulic data. The theory gives an exact, closed-form transport equation in terms of two conditional Lagrangian velocity moments and the conditional Lagrangian cross-covariance between velocity and its forcing terms. Neuman (1993) proposed three approximate methods to solve the Eulerian-Lagrangian equation. For the prediction of early time concentration due to an instantaneous point source, an analytical solution modified slightly from that of Batchelor (1952) is recommended. For intermediate time, Neuman proposed a weak approximation which improves with conditioning, which requires only Eulerian input moments and yields explicit expressions for the second conditional moments of the concentration. For late time, Neuman advocated a combined weak and pseudo-Fickian approximation similar to Corrsin's conjecture.

Zhang and Neuman (1995a) proposed a combined analytical-numerical approach to the Eulerian-Lagrangian transport theory [Neuman, 1993] for a nonreactive solute transport problem under a special case of steady-state flow in a mildly fluctuating, statistically homogeneous, log-normal hydraulic conductivity field. At early dimensionless travel distance (*i.e.*, less than half a log transmissivity correlation scale), the approach adopted an extended Batchelor's analytical solution (1952) to

calculate the concentration moments. At the intermediate dimensionless travel distance (greater than half of the log transmissivity correlation scale), a pseudo-Fickian numerical solution method was used. One- and two-dimensional unconditional examples were studied to compare the concentration covariance based on the Eulerian-Lagrangian theory to that obtained from Dagan's closed-form formula for variance [Dagan, 1987, 1989]. Zhang and Neuman (1995a) found that their results tend to approach the lower bounds of that predicted by Dagan's formula. These pseudo-Fickian lower bounds, however, compared amenably to those obtained by Graham and McLaughlin (1989a, 1989b). The authors indicated that the reliance of this method on an analytical solution at early time has a computational advantage over Neuman's conditional Lagrangian method [Neuman, 1993] in that it avoids the need for Monte Carlo simulations of velocity fields and particle motions.

1.4 Scope for the Dissertation

Most previous stochastic analyses of flow and solute transport in saturated porous media are based on the assumptions of steady flow and/or stationary random field conditions. These studies have mainly focused on the the effects of randomly heterogeneous hydraulic conductivity fields on predictions of flow [Mizell et al., 1982; Bakr et al., 1978; Dagan, 1982a, 1982b, 1989; Rubin and Dagan, 1987a, 1987b, 1992; Dagan and Rubin, 1988; McLaughlin and Wood, 1988a, 1988b; Li and McLaughlin, 1991, 1995] and solute transport [Gelhar et al., 1979; Gelhar and Axness, 1983; Dagan, 1984, 1989; Graham and McLaughlin, 1989a, 1989b, 1991; Dagan et al., 1992; Cvetkovic and Dagan, 1994; Zhang and Neuman, 1995a, 1995b, 1995c, 1995d] in porous media. Some studies focused on trying to identify large-scale, spatially-averaged, effective macrodispersion parameters to describe the influence of physical aquifer heterogeneities on subsurface transport of nonreactive species, while other

studies tried to evaluate the uncertainty of mass transport predictions based on models which used effective macrodispersive parameters [Gelhar et al., 1981; Gelhar and Gutjhar, 1982; Dagan, 1987; Black and Freyberg, 1987; Graham and McLaughlin, 1989a, 1989b; Kapoor and Gelhar, 1994a, 1994b]. Recently the coupled effects of spatially variable hydraulic conductivity and aquifer sorption characteristics have been studied by Bellin et al. (1993, 1995), Tompson and Gelhar (1990), James et al. (1997), and Zhang (1997). However, little research has been reported which incorporates the effects of uncertain recharge, uncertain aquifer properties, and uncertain contaminant source characteristics on the prediction of flow and solute transport in porous media, especially for the transient flow case.

This dissertation will focus on stochastic analysis of flow and inert solute transport in heterogenous aquifers subject to steady random recharge, transient random recharge, and random contaminant source fields. Chapter 2 examines the impact of nonzero mean, steady-state spatially random recharge and spatially random transmissivity on the statistical moments of head, flow, and solute transport in a two dimensional aquifer system. A first-order Eulerian perturbation technique is used to generate a system of coupled flow and transport moment equations for this physical system [Graham and McLaughlin, 1989a; Graham and Tankersley, 1994]. Closed-form analytical solutions for the covariances and cross-covariances between head, velocity, log-transmissivity, and recharge are obtained using Fourier transform techniques. The resulting flow-related covariances and cross-covariances are incorporated into a numerical solution algorithm to investigate the coupled impacts of spatially random recharge and transmissivity on the evolution of the solute concentration field moments (i.e., the mean, variance, and macrodispersive flux).

Chapter 3 extends the studies of Chapter 2 into the new case of spatiotemporally random recharge and spatially random transmissivity. A series of semi-analytical solutions are derived for describing the velocity variances and covariances using the

first-order Eulerian perturbation approach and Fourier transform techniques. A new solution technique is developed for decoupling and solving the mean concentration and macrodispersion equations in the Laplace-Fourier domain using convolution theory. The transient velocity covariances are incorporated into a fast Fourier transform solution algorithm to investigate the new impacts of spatiotemporally random recharge and spatially random transmissivity on the evolution of the solute concentration moments.

Chapter 4 analyzes solute concentration moments resulting from an uncertain contaminant source distribution, spatio-temporally random recharge, and spatially random transimissivity. Comparisons are made to examine and distinguish between the ensemble plume spreading and prediction uncertainty contributions from random contaminant source and random velocity fields. Evaluation of a new term, the cross-correlation between random source and random concentration, is required to the compute the variance of concentration.

Chapter 5 presents the summary and conclusions of this dissertation.

CHAPTER 2
SPATIALLY RANDOM RECHARGE

2.1 Introduction

It is now progressively accepted in the literature that natural heterogeneity, including the spatial irregularity of physical properties such as hydraulic conductivity and storativity, and the temporal and spatial variations of recharge, contaminant sources and boundary conditions can be significant in natural aquifer systems. This natural heterogeneity causes uncertainty in flow field predictions, and further influences the accuracy with which solute transport can be predicted in groundwater systems. Describing the relationship among moments of uncertain inputs and resulting moments of flow and solute transport, constitutes the basis for the stochastic approach to subsurface hydrology.

Many researchers have shown the effects of randomly heterogeneous hydraulic conductivity fields on predictions of flow [Mizell et al., 1982; Bakr et al., 1978; Dagan, 1982a, 1982b, 1989; Rubin and Dagan, 1987a, 1987b, 1992; Dagan and Rubin, 1988; McLaughlin and Wood, 1988a, 1988b; Li and McLaughlin, 1991, 1995] and solute transport [Gelhar and Axness, 1983; Dagan, 1984, 1989; Graham and McLaughlin, 1989a, 1989b, 1991; Dagan et al., 1992; Cvetkovic and Dagan, 1994; Zhang and Neuman, 1995a, 1995b, 1995c, 1995d] in porous media. However, little research has been reported which incorporates both the effects of uncertain recharge and uncertain aquifer properties on the prediction of flow and solute transport.

Gomez-Hernandez and Gorelick (1989) examined the influence of spatially variable hydraulic conductivity, leakance and recharge on uniform effective (macroscale) groundwater flow parameters using a Monte-Carlo simulation approach. Nine

different cases were studied that separately examined the ability of assumed effective hydraulic conductivity, leakance and recharge parameters to simulate the mean steady-state hydraulic head behavior. Results indicate that the arithmetic mean of aerially distributed recharge produces small deviations from the expected head values.

Serrano (1992) examined the form of the advection-dispersion equation under constant recharge and its analytical solution in one-dimensional homogeneous media. Serrano found that under constant recharge the velocity varies with distance and recharge intensity, which generates an evolving dispersion coefficient that increases with distance. It was found that the recharge rate substantially affects the contaminant distribution even in homogeneous media.

Graham and Tankersley (1994) and Graham and Neff (1994) analyzed two-dimensional steady groundwater flow subject to spatially random recharge and transmissivity using a first-order perturbation method, and derived the closed-form solutions for the covariances and cross-covariances between the random head, transmissivity and recharge fields under the assumption of zero mean recharge. They showed that as the variance and correlation scale of the random recharge field increase, the head variance increases, the anisotropy of the head correlation function decreases, and the correlation between head and transmissivity decreases.

Rubin and Bellin (1994) investigated the statistical structure of the pore water velocity field in a uniformly recharged heterogeneous aquifer, and derived the spatial covariance of the velocity field, the solute particle displacement covariances and the macrodispersion coefficients using a Lagrangian approach. The results showed that positive uniform recharge increases the rate of longitudinal displacement and longitudinal spreading, but has a lesser effect on lateral spreading.

Rehfeldt and Gelhar (1992) examined the dispersion of a solute plume in three-dimensional, heterogeneous porous media subject to transient flow using an Eulerian first-order perturbation method. The transient flow was assumed to be composed

of a constant mean flow, a spatially random fluctuation due to the heterogeneous media, and a temporally random fluctuation due to uncertain boundary conditions. Asymptotic solutions of the unsteady flow and solute transport moment equations were used to estimate the macroscopic dispersive flux and to evaluate the resulting macrodispersivity tensor. A three-dimensional, statistically anisotropic stationary input covariance was assumed for the hydraulic conductivity field and a one-dimensional stationary input covariance was assumed to describe the temporal variability of the mean hydraulic gradient. The results from two special cases (variation in the magnitude, and variation in direction of the hydraulic gradient) of transient flow suggest that gradient magnitude variation produces a slightly larger longitudinal macrodispersivity than does the steady flow case, whereas gradient direction variation produces a significantly larger transverse macrodispersivity.

Dagan et al. (1996) investigated a similar problem to the one Rehfeldt and Gelhar (1992) studied. In this work the transient flow was caused by deterministic temporally-fluctuating boundary conditions which produced fluctuations in the magnitude and direction of the mean head gradient, and the transport analysis was based on a first-order Lagrangian approach. Dagan et al. showed that this type of unsteady flow strongly increases transverse spreading, but that the effects on longitudinal spreading were insignificant.

This work extends the previous work to examine the impact of nonzero mean, spatially random recharge and spatially random transmissivity on the predictions of flow and transport in a two dimensional aquifer system. A first-order perturbation technique is used to generate a system of coupled flow and transport moment equations for this physical system [Graham and McLaughlin, 1989a; Graham and Tankersley, 1994]. Closed form analytical solutions for the covariances and cross-covariances between head, velocity, log-transmissivity, and recharge are obtained using Fourier transform techniques. The resulting flow-related covariances and cross-covariances

are incorporated into a numerical solution algorithm to investigate the coupled impacts of spatially random recharge and transmissivity on the evolution of the solute concentration field moments (i.e. the mean, covariance and macrodispersive flux).

2.2 Derivation of the Unconditional Moment Equations

2.2.1 Head Field

The governing equation for hydraulic head distribution in a steady-state, two-dimensional aquifer system with spatially random transmissivity and recharge is:

$$\frac{\partial}{\partial x_i}\left[T(\mathbf{x})\frac{\partial H}{\partial x_i}\right] + R(\mathbf{x}) = 0 \tag{2.1}$$

where x_i are Cartesian coordinates in the horizontal plane (with indices i taking on values of 1 or 2), $T(\mathbf{x})$ is the transmissivity at vector location $\mathbf{x}$, $R(\mathbf{x})$ is the steady-state recharge at vector location $\mathbf{x}$ (positive for accretion) and $H(\mathbf{x})$ is the steady-state hydraulic head at vector location $\mathbf{x}$. Summation over repeated indices is assumed.

Letting $Y = lnT$, expanding the log transmissivity, recharge and head fields into the sums of potentially spatially-varying means and the corresponding small perturbations, neglecting higher order perturbation products, and taking the expected value, the following ensemble mean head equation is derived [Graham and Tankersley, 1994]:

$$\frac{\partial^2 \bar{H}}{\partial x_i^2} + \bar{R}e^{-\bar{Y}} = 0 \tag{2.2}$$

Subtracting the mean equation from the expanded equation to get the head perturbation $\delta H(\mathbf{x})$, post-multiplying by the perturbations of $\delta \mathrm{H}(\mathbf{x}')$, $\delta \mathrm{Y}(\mathbf{x}')$, and $\delta \mathrm{R}(\mathbf{x}')$ at vector location $\mathbf{x}'$, and taking expected values results in the following system of coupled nonstationary moment equations [Graham and Tankersley, 1994]:

$$\frac{\partial^2 P_{HR}(\mathbf{x},\mathbf{x}')}{\partial x_i^2} + \frac{\partial P_{YR}(\mathbf{x},\mathbf{x}')}{\partial x_i}\frac{\partial \bar{H}(\mathbf{x})}{\partial x_i} + e^{-\bar{Y}(\mathbf{x})}\left[-\bar{R}(\mathbf{x})P_{YR}(\mathbf{x},\mathbf{x}') + P_{RR}(\mathbf{x},\mathbf{x}')\right] = 0 \tag{2.3}$$

$$\frac{\partial^2 P_{HY}(\mathbf{x},\mathbf{x}')}{\partial x_i^2} + \frac{\partial P_{YY}(\mathbf{x},\mathbf{x}')}{\partial x_i}\frac{\partial \bar{H}(\mathbf{x})}{\partial x_i} + e^{-\bar{Y}(\mathbf{x})}\left[-\bar{R}(\mathbf{x})P_{YY}(\mathbf{x},\mathbf{x}') + P_{RY}(\mathbf{x},\mathbf{x}')\right] = 0 \tag{2.4}$$

$$\frac{\partial^2 P_{HH}(\mathbf{x},\mathbf{x}')}{\partial x_i^2} + \frac{\partial P_{YH}(\mathbf{x},\mathbf{x}')}{\partial x_i}\frac{\partial \bar{H}(\mathbf{x})}{\partial x_i} + e^{-\bar{Y}(\mathbf{x})}\left[-\bar{R}(\mathbf{x})P_{YH}(\mathbf{x},\mathbf{x}') + P_{RH}(\mathbf{x},\mathbf{x}')\right] = 0 \tag{2.5}$$

where arguments with overbars represent expected values, $P_{FG}(\mathbf{x},\mathbf{x}')$ is defined as $\overline{\delta F(\mathbf{x})\delta G(\mathbf{x}')}$, in which δF and δG are small perturbations of random variables F and G at vector locations $\mathbf{x}$ and $\mathbf{x}'$, respectively.

In the work of Graham and Tankersley (1994), equations (2.2) through (2.5) were solved for the stationary flow field that results when the mean recharge is assumed to be zero. In this work, a constant mean recharge value is assumed, which introduces a linearly trending ensemble mean head gradient and thus a linearly trending velocity flow field. This causes the head covariance and cross-covariances to be location dependent and therefore nonstationary. From equation (2.2), the general solution for the ensemble mean head gradient is :

$$J(x_1) = -\frac{\partial \bar{H}}{\partial x_1} = \bar{R}e^{-\bar{Y}}x_1 + J_0 \tag{2.6}$$

in which the coordinate system has been aligned with the mean flow direction x_1, J_0 is a constant reference gradient at location x_0, and the mean head gradient is location dependent.

2.2.2 Velocity Field

The pore velocity vector for two-dimensional flow is:

$$v_i(\mathbf{x}) = -\frac{T(\mathbf{x})}{bn}\frac{\partial H(\mathbf{x})}{\partial x_i}, \quad i = 1, 2 \tag{2.7}$$

in which $v_i(\mathbf{x})$ is the pore velocity at vector location $\mathbf{x}$, $T(\mathbf{x})$ is the transmissivity, b is the aquifer thickness, n is the porosity, and both the porosity and aquifer thickness are assumed constant.

Expanding random quantities into the sums of deterministic means and the corresponding small perturbations, approximating $e^{\bar{Y}+\delta Y}$ as $e^{\bar{Y}}(1+\delta Y)$, and taking the expected value leads to the following ensemble mean pore water velocity equations [Gelhar, 1993]:

$$\bar{v_1}(\mathbf{x}) = -\frac{e^{\bar{Y}}}{bn}\frac{\partial \bar{H}(\mathbf{x})}{\partial x_1}, \quad \bar{v_2}(\mathbf{x}) = 0 \tag{2.8}$$

where $\bar{v_1}(\mathbf{x})$ is the linearly trending pore water velocity in the mean flow direction, x_1.

Subtracting equation (2.8) from the expanded equation (2.7) and neglecting higher order perturbation products yields the velocity perturbation expression $\delta v_i(\mathbf{x})$ [Gelhar, 1993]. Post-multiplying this perturbation equation at the spatial location $\mathbf{x}$ by the perturbations of $\delta v_j(\mathbf{x}')$, $\delta \mathrm{Y}(\mathbf{x}')$ and $\delta \mathrm{H}(\mathbf{x}')$ at a different spatial location $\mathbf{x}'$, and taking the expected value yields a system of coupled equations which describes the unconditional non-stationary velocity covariance and cross-covariance equations:

$$
\begin{aligned}
P_{v_1 Y}(\mathbf{x},\mathbf{x}') &= -\frac{e^{\bar{Y}}}{bn}\left[P_{YY}(\mathbf{x},\mathbf{x}')\frac{\partial \bar{H}(\mathbf{x})}{\partial x_1} + \frac{\partial P_{HY}(\mathbf{x},\mathbf{x}')}{\partial x_1}\right] \\
P_{v_1 H}(\mathbf{x},\mathbf{x}') &= -\frac{e^{\bar{Y}}}{bn}\left[P_{YH}(\mathbf{x},\mathbf{x}')\frac{\partial \bar{H}(\mathbf{x})}{\partial x_1} + \frac{\partial P_{HH}(\mathbf{x},\mathbf{x}')}{\partial x_1}\right] \\
P_{v_1 v_1}(\mathbf{x},\mathbf{x}') &= -\frac{e^{\bar{Y}}}{bn}\left[P_{Yv_1}(\mathbf{x},\mathbf{x}')\frac{\partial \bar{H}(\mathbf{x})}{\partial x_1} + \frac{\partial P_{Hv_1}(\mathbf{x},\mathbf{x}')}{\partial x_1}\right] \\
P_{v_1 v_2}(\mathbf{x},\mathbf{x}') &= -\frac{e^{\bar{Y}}}{bn}\left[P_{Yv_2}(\mathbf{x},\mathbf{x}')\frac{\partial \bar{H}(\mathbf{x})}{\partial x_1} + \frac{\partial P_{Hv_2}(\mathbf{x},\mathbf{x}')}{\partial x_1}\right]
\end{aligned}
\tag{2.9}
$$

$$
\begin{aligned}
P_{v_2 Y}(\mathbf{x},\mathbf{x}') &= -\frac{e^{\bar{Y}}}{bn}\frac{\partial P_{HY}(\mathbf{x},\mathbf{x}')}{\partial x_2} \\
P_{v_2 H}(\mathbf{x},\mathbf{x}') &= -\frac{e^{\bar{Y}}}{bn}\frac{\partial P_{HH}(\mathbf{x},\mathbf{x}')}{\partial x_2} \\
P_{v_2 v_1}(\mathbf{x},\mathbf{x}') &= -\frac{e^{\bar{Y}}}{bn}\frac{\partial P_{Hv_1}(\mathbf{x},\mathbf{x}')}{\partial x_2} \\
P_{v_2 v_2}(\mathbf{x},\mathbf{x}') &= -\frac{e^{\bar{Y}}}{bn}\frac{\partial P_{Hv_2}(\mathbf{x},\mathbf{x}')}{\partial x_2}
\end{aligned}
\tag{2.10}
$$

2.2.3 Concentration Field

The governing equation for the transport of a conservative solute in a two-dimensional flow field is [Bear, 1979]:

$$
\begin{aligned}
\frac{\partial c}{\partial t} + \frac{\partial (v_i\, c)}{\partial x_i} - \frac{\partial}{\partial x_i}\left[D_{ij}\frac{\partial c}{\partial x_j}\right] &= 0 \quad \mathbf{x} \in D \\
c &= c_b \quad \mathbf{x} \in \partial D \\
c &= c_0 \quad \mathbf{x} \in D \quad \mathrm{t} = \mathrm{t}_0
\end{aligned}
\tag{2.11}
$$

in which the concentration c is assumed to be a nonstationary random function of the location $\mathbf{x}$ (with coordinates x_i) and time t, repeated indices are assumed to be summed from 1 to 2; c_b and c_0 are boundary and initial conditions, respectively, which are assumed to be known.

The dispersion tensor D_{ij} is assumed to be a deterministic constant which accounts for pore-scale dispersion effects [Bear, 1979]:

$$D_{ij} = \alpha_T \, \bar{v} \, \delta_{ij} + (\alpha_L - \alpha_T) \frac{\bar{v}_i \, \bar{v}_j}{\bar{v}} \tag{2.12}$$

where α_L and α_T are the longitudinal and transverse local dispersivities, $\bar{v}$ is the magnitude of the mean velocity vector and δ_{ij} is one if $i = j$ and zero otherwise. Molecular diffusion is neglected.

Following the perturbation procedure discussed above, Graham and McLaughlin (1989a) derived the following set of coupled partial differential equations which approximately describe the propagation of the mean concentration, the velocity-concentration cross covariance, and the concentration covariance through a random velocity field with known mean velocity and velocity covariances $P_{v_i v_j}(\mathbf{x}', \mathbf{x})$.

$$\begin{gathered}
\frac{\partial \bar{c}}{\partial t} + \frac{\partial \bar{v}_i \, \bar{c}}{\partial x_i} - \frac{\partial}{\partial x_i}\left[D_{ij} \frac{\partial \bar{c}}{\partial x_j}\right] + \frac{\partial J_{D_i}}{\partial x_i} = 0 \quad \mathbf{x} \in D \\
c = c_b \quad \mathbf{x} \in \partial D \\
c = c_0 \quad \mathbf{x} \in D \quad t = t_0 \\
J_{D_i} = P_{v_i c}(\mathbf{x}, \mathbf{x}, t)
\end{gathered} \tag{2.13}$$

$$\begin{gathered}
\frac{\partial P_{v_i c}(\mathbf{x}', \mathbf{x}, t)}{\partial t} + \frac{\partial \bar{v}_j \, P_{v_i c}(\mathbf{x}', \mathbf{x}, t)}{\partial x_j} - \frac{\partial}{\partial x_j}\left[D_{jk} \frac{\partial P_{v_i c}(\mathbf{x}', \mathbf{x}, t)}{\partial x_k}\right] \\
+ \frac{\partial P_{v_i v_j}(\mathbf{x}', \mathbf{x}) \bar{c}(\mathbf{x}, t)}{\partial x_j} \approx 0 \quad \mathbf{x}, \mathbf{x}' \in D \\
P_{v_i c}(\mathbf{x}', \mathbf{x}, t) = 0 \quad \mathbf{x} \in \partial D \quad \mathbf{x}' \in D \\
P_{v_i c}(\mathbf{x}', \mathbf{x}, t) = 0 \quad \mathbf{x}, \mathbf{x}' \in D \quad t = t_0
\end{gathered} \tag{2.14}$$

$$\frac{\partial P_{cc}(\mathbf{x}',\mathbf{x},t)}{\partial t}+\frac{\partial \bar{v}_i(\mathbf{x})\,P_{cc}(\mathbf{x}',\mathbf{x},t)}{\partial x_i}+\frac{\partial \bar{v}_i(\mathbf{x}')\,P_{cc}(\mathbf{x},\mathbf{x}',t)}{\partial x_i'}$$
$$-\frac{\partial}{\partial x_i}\left[D_{ij}\frac{\partial P_{cc}(\mathbf{x}',\mathbf{x},t)}{\partial x_j}\right]-\frac{\partial}{\partial x_i'}\left[D_{ij}\frac{\partial P_{cc}(\mathbf{x},\mathbf{x}',t)}{\partial x_j'}\right]$$
$$+\frac{\partial P_{cv_i}(\mathbf{x}',\mathbf{x},t)\bar{c}(\mathbf{x},t)}{\partial x_i}+\frac{\partial P_{cv_i}(\mathbf{x},\mathbf{x}',t)\bar{c}(\mathbf{x}',t)}{\partial x_i'}\approx 0 \quad \mathbf{x},\mathbf{x}'\in D \tag{2.15}$$
$$P_{cc}(\mathbf{x}',\mathbf{x},t)=0 \quad \mathbf{x}\in\partial D \quad \mathbf{x}'\in D$$
$$P_{cc}(\mathbf{x},\mathbf{x}',t)=0 \quad \mathbf{x}'\in\partial D \quad \mathbf{x}\in D$$
$$P_{cc}(\mathbf{x}',\mathbf{x},t)=0 \quad \mathbf{x},\mathbf{x}'\in D \quad t=t_0$$

Incorporating equations (2.8) for the mean velocity, (2.9), and (2.10) for the velocity covariances into equations (2.13) through (2.15) gives a system of equations which describes the propagation of a conservative solute through a heterogeneous aquifer subject to spatially variable recharge with a nonzero constant mean. In this work, spectral transform techniques are used to obtain analytical solutions to the head and velocity covariance and cross-covariance equations. A Galerkin finite element algorithm is then used to solve the concentration related moment equations.

2.3 Solution of the Unconditional Moment Equations

2.3.1 Head and Pore Water Velocity Moment Equations

For the convenience of deriving closed form solutions for the head and pore water velocity covariance and cross-covariance equations, the flow domain is assumed to be infinite. This is reasonable if the domain is sufficiently large compared to the head correlation scale [Graham and Tankersley, 1994; Rubin and Dagan, 1987a; Dagan, 1989]. The log-transmissivity and recharge are assumed to be uncorrelated stationary random fields [Graham and Tankersley, 1994] with the following hole-type covariance structures [Mizell et al., 1982]:

$$
\begin{aligned}
P_{YY}(\xi) &= \sigma_Y^2 \left[(1 + \frac{1}{8}\alpha_Y^2\xi^2)\alpha_Y\xi K_1(\alpha_Y\xi) - \alpha_Y^2\xi^2 K_0(\alpha_Y\xi) \right] \\
P_{RR}(\xi) &= \sigma_R^2 \left[(1 + \frac{1}{8}\alpha_R^2\xi^2)\alpha_R\xi K_1(\alpha_R\xi) - \alpha_R^2\xi^2 K_0(\alpha_R\xi) \right] \\
P_{YR}(\xi) &= 0 \\
\alpha_Y &= \frac{3\pi}{16\lambda_Y} \\
\alpha_R &= \frac{3\pi}{16\lambda_R}
\end{aligned}
\tag{2.16}
$$

where ξ=**x**-**x**′ is the two-dimensional separation vector between **x** and **x**′, in which x_1 is aligned with the direction of the mean hydraulic gradient; $K_n(z)$ is the modified Bessel function of order n; σ_Y^2 and λ_Y are the variance and correlation scale of the log transmissivity field and σ_R^2 and λ_R are the variance and correlation scale of the recharge field.

The spectra corresponding to these covariance functions are:

$$
S_{YY}(\mathbf{k}) = \frac{3\sigma_Y^2\alpha_Y^2 k^4}{\pi(k^2+\alpha_Y^2)^4}; \quad S_{RR}(\mathbf{k}) = \frac{3\sigma_R^2\alpha_R^2 k^4}{\pi(k^2+\alpha_R^2)^4}; \quad S_{YR}(\mathbf{k}) = 0 \tag{2.17}
$$

in which **k** is a two-dimensional wave number vector, k^2=k_1^2+k_2^2.

Plugging the recharge covariance function (2.16) into (2.3) and noting that $P_{YR}(\xi) = 0$ due to the assumption that Y and R are uncorrelated, equation (2.3) can be solved using Fourier transform techniques [Graham and Tankersley, 1994]:

$$
P_{HR}(\mathbf{x},\mathbf{x}') = \frac{e^{-\bar{Y}}\sigma_R^2}{48\alpha_R^2}\left[24\alpha_R\xi K_1(\alpha_R\xi) + 12\alpha_R^2\xi^2 K_0(\alpha_Y\xi)\right] \tag{2.18}
$$

with zero lag cross-covariance:

$$
P_{HR}(\mathbf{x},\mathbf{x}) = \frac{e^{-\bar{Y}}\sigma_R^2}{2\alpha_R^2} \tag{2.19}
$$

Plugging the log transmissivity covariance function (2.16) and the mean head gradient (2.6) into equation (2.4), and solving using a Fourier transform technique yields the following new solution for the head-log transmissivity cross-covariance, detailed derivation is given in Appendix A:

$$P_{HY}(\mathbf{x},\mathbf{x}') = 6\sigma_Y^2\alpha_Y^2(\bar{R}e^{-\bar{Y}}x_1' + J_0)\left[\frac{\xi_1\xi K_1(\alpha_Y\xi)}{8\alpha_Y} - \frac{\xi_1\xi^2 K_2(\alpha_Y\xi)}{48}\right]$$
$$+6\bar{R}e^{-\bar{Y}}\sigma_Y^2\alpha_Y^2\left[\frac{\xi^3 K_3(\alpha_Y\xi)}{48\alpha_Y} - \frac{\xi^2 K_2(\alpha_Y\xi)}{12\alpha_Y^2} + \frac{\xi_1^2\xi K_1(\alpha_Y\xi)}{12\alpha_Y} - \frac{\xi_1^2\xi^2 K_2(\alpha_Y\xi)}{48}\right] \quad (2.20)$$

in which ξ_1=x_1-x_1', and ξ^2=x_1^2+x_2^2; and the zero-lag cross-covariance is $P_{HY}(\mathbf{x},\mathbf{x}) = 0$.

Note that due to the assumption that the log-transmissivity and recharge fields are uncorrelated, the head-recharge cross covariance is independent of the mean recharge and the mean head gradient. The cross-covariance between head and log transmissivity, however, depends on the mean head gradient, which for nonzero mean recharge is a linear function of position, making the head-log tansmissivity covariance function nonstationary. Inspection of (2.20) indicates that the cross-covariance between head and log transmissivity increases linearly with distance along the mean flow direction, and is symmetric with respect to the mean flow direction, similar to results found by Rubin and Bellin (1994). This phenomenon reflects the fact that the mean head gradient establishes a preferential flow direction which influences the random head perturbations. This leads to the increasing cross-covariances between head and log transmissivity along the preferential flow direction, and a symmetrical distribution perpendicular to this direction.

Using the solutions for P_{HY} (2.20), and P_{HR} (2.18) and the mean head gradient (2.6), and solving (2.5) using Fourier transform techniques yields the head covariance function (see Appendix A):

$$
\begin{aligned}
P_{HH}(\mathbf{x},\mathbf{x}') =& \sigma_Y^2(\bar{R}e^{-\bar{Y}}x_1 + J_0)(\bar{R}e^{-\bar{Y}}x_1' + J_0)\left[\frac{\xi^2 K_2(\alpha_Y\xi)}{8} - \frac{\alpha_Y\xi_1^2\xi K_1(\alpha_Y\xi)}{8}\right] \\
&+\bar{R}^2e^{-2\bar{Y}}\sigma_Y^2\left[\frac{576(6\xi_1^2\xi_2^2 - \xi_1^4 - \xi_2^4)}{\xi^8\alpha_Y^8} - \frac{12(\xi_1^2 - \xi_2^2)}{\xi^4\alpha_Y^6} + \frac{(\xi_1^4 - \xi_1^2\xi_2^2)K_2(\alpha_Y\xi)}{8}\right. \\
&+\frac{(3\xi_1^4 - 8\xi_1^2\xi_2^2 + \xi_2^4)K_3(\alpha_Y\xi)}{8\alpha_Y\xi} + \frac{(2\xi_1^4 - 9\xi_1^2\xi_2^2 + \xi_2^4)K_4(\alpha_Y\xi)}{2\alpha_Y^2\xi^2} \\
&\left.+\frac{3(\xi_1^4 - 6\xi_1^2\xi_2^2 + \xi_2^4)K_5(\alpha_Y\xi)}{2\alpha_Y^3\xi^3}\right] \\
&+\frac{\sigma_R^2e^{-2\bar{Y}}\xi^3K_3(\alpha_R\xi)}{8\alpha_R}
\end{aligned}
\tag{2.21}
$$

and its variance expression:

$$
P_{HH}(\mathbf{x},\mathbf{x}) = \frac{\sigma_Y^2(\bar{R}e^{-\bar{Y}}x_1 + J_0)^2}{4\alpha_Y^2} + \frac{\bar{R}^2e^{-2\bar{Y}}\sigma_Y^2}{2\alpha_Y^4} + \frac{\sigma_R^2e^{-2\bar{Y}}}{\alpha_R^4} \tag{2.22}
$$

Figures 2.1 and 2.2 show the effects of deterministic mean recharge and uncertain recharge on the head correlation function (i.e., equation (2.21) normalized by equation (2.22). Case 1 considers only an uncertain log-transmissivity field [i.e., results of Mizell, 1982]; Cases 2 and 3 superimpose a positive and a negative deterministic recharge, respectively, on the uncertain log-transmissivity field considered in Case 1; Case 4 further adds an uncertain recharge field to Case 2; and Case 5 considers only an uncertain recharge field. The parameter values used for each case are summarized in Table 2.1. The results suggest that 1) although introduction of mean recharge (either positive or negative) increases the head variance, it does not change the head correlation function (head covariance normalized by head standard deviations at points x and x') significantly either in the mean flow direction or the lateral direction; 2) introduction of spatially random recharge increases the head correlation function both in the mean flow and lateral directions; 3) the head correlation functions resulting from both random fields are bounded by the head correlation functions

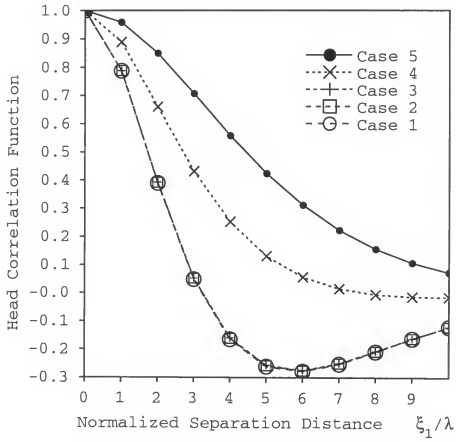

Figure 2.1: The head correlation function vs normalized separation distance in the direction of mean flow (Note: Curves for Cases 2 and 3 coincide with the curve of Case 1)

which result when each random field is considered separately; and 4) as the recharge variance increases, the head correlation structure tends to become isotropic, since the assumed recharge covariance function is isotropic.

Plugging the expressions (2.18) through (2.21) into equations (2.9) and (2.10), taking derivatives where necessary, and regrouping terms leads to the following velocity covariance equations required as input in the solute transport moment equations:

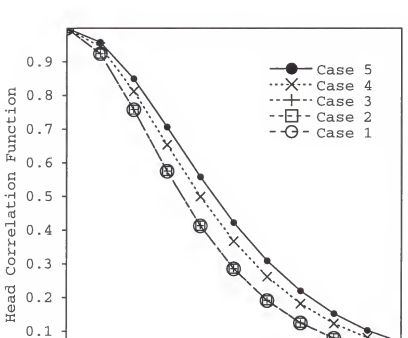

Figure 2.2: The head correlation function vs normalized separation distance transverse to the direction of mean flow(Note: Curves for Cases 2 and 3 coincide with the curve of Case 1)

$$
\begin{aligned}
P_{v_1v_1}(\mathbf{x},\mathbf{x}') = \frac{6\,e^{2\bar{Y}}\sigma_Y^2\alpha_Y^2}{b^2n^2}\Bigg[& (\bar{R}e^{-\bar{Y}}x_1 + J_0)(\bar{R}e^{-\bar{Y}}x_1' + J_0) \\
& \left[\frac{11\xi K_1(\alpha_Y\xi)}{48\alpha_Y} - \frac{(7\xi_1^2+4\xi_2^2)K_0(\alpha_Y\xi)}{24} + \frac{\alpha_Y(\xi_1^4+\xi^4)K_1(\alpha_Y\xi)}{48\xi}\right] \\
& - \left[(\bar{R}e^{-\bar{Y}}x_1 + J_0)^2 + (\bar{R}e^{-\bar{Y}}x_1' + J_0)^2\right] \\
& \left[\frac{\xi K_1(\alpha_Y\xi)}{8\alpha_Y} - \frac{\xi_1^2 K_0(\alpha_Y\xi)}{8} - \frac{\xi^2 K_2(\alpha_Y\xi)}{48} - \frac{\alpha_Y\xi_1^2\xi K_1(\alpha_Y\xi)}{48}\right] \\
& - \bar{R}^2 e^{-2\bar{Y}}[B + B_0K_0(\alpha_Y\xi) + B_1K_1(\alpha_Y\xi) + B_2K_2(\alpha_Y\xi) + B_3K_3(\alpha_Y\xi) \\
& + B_4K_4(\alpha_Y\xi) + B_5K_5(\alpha_Y\xi)]\Bigg] + \frac{\sigma_R^2[\xi^2K_2(\alpha_R\xi) - \alpha_R\xi_1^2\xi K_1(\alpha_R\xi)]}{8b^2n^2}
\end{aligned}
\tag{2.23}
$$

and its variance expression:

$$P_{v_1v_1}(\mathbf{x},\mathbf{x}) = \frac{e^{2\bar{Y}}}{b^2n^2}\left[\frac{3\sigma_Y^2(\bar{R}e^{-\bar{Y}}x_1+J_0)^2}{8}+\frac{\bar{R}^2e^{-2\bar{Y}}\sigma_Y^2}{8\alpha_Y^2}+\frac{\sigma_R^2e^{-2\bar{Y}}}{4\alpha_R^2}\right]$$

$$\begin{aligned}P_{v_2v_2}(\mathbf{x},\mathbf{x}') =& \frac{6\,e^{2\bar{Y}}\sigma_Y^2\alpha_Y^2}{b^2n^2}\Bigg[(\bar{R}e^{-\bar{Y}}x_1+J_0)(\bar{R}e^{-\bar{Y}}x_1'+J_0)\\ &\left[\frac{\xi K_1(\alpha_Y\xi)}{48\alpha_Y}-\frac{\xi^2K_0(\alpha_Y\xi)}{48}+\frac{\alpha_Y\xi_1^2\xi_2^2K_1(\alpha_Y\xi)}{48\xi}\right]\\ &-\bar{R}^2e^{-2\bar{Y}}[C+C_0K_0(\alpha_Y\xi)+C_1K_1(\alpha_Y\xi)+C_2K_2(\alpha_Y\xi)\\ &+C_3K_3(\alpha_Y\xi)+C_4K_4(\alpha_Y\xi)+C_5K_5(\alpha_Y\xi)]\Bigg]\\ &+\frac{\sigma_R^2}{8b^2n^2}\left[\xi^2K_2(\alpha_R\xi)-\alpha_R\xi_2^2\xi K_1(\alpha_R\xi)\right]\end{aligned} \tag{2.24}$$

and its variance expression:

$$P_{v_2v_2}(\mathbf{x},\mathbf{x}) = \frac{e^{2\bar{Y}}}{b^2n^2}\left[\frac{\sigma_Y^2(\bar{R}e^{-\bar{Y}}x_1+J_0)^2}{8}+\frac{\bar{R}^2e^{-2\bar{Y}}\sigma_Y^2}{8\alpha_Y^2}+\frac{\sigma_R^2e^{-2\bar{Y}}}{4\alpha_R^2}\right]$$

$$\begin{aligned}P_{v_1v_2}(\mathbf{x},\mathbf{x}') =& \frac{6\,e^{2\bar{Y}}\sigma_Y^2\alpha_Y^2}{b^2n^2}\Bigg[(\bar{R}e^{-\bar{Y}}x_1+J_0)^2\left[\frac{\xi_1\xi_2K_0(\alpha_Y\xi)}{16}-\frac{\alpha_Y\xi_1\xi_2^3K_1(\alpha_Y\xi)}{48\xi}\right]\\ &+\bar{R}e^{-\bar{Y}}(\bar{R}e^{-\bar{Y}}x_1+J_0)\\ &\left[\frac{\alpha_Y\xi_1^2\xi_2^3K_1(\alpha_Y\xi)}{48\xi}+\frac{\xi_2\xi K_1(\alpha_Y\xi)}{16\alpha_Y}-\frac{(3\,\xi_1^2\xi_2+\xi_2^3)K_1(\alpha_Y\xi)}{48}\right]\\ &-\bar{R}^2e^{-2\bar{Y}}[D+D_0K_0(\alpha_Y\xi)+D_1K_1(\alpha_Y\xi)+D_2K_2(\alpha_Y\xi)\\ &+D_3K_3(\alpha_Y\xi)+D_4K_4(\alpha_Y\xi)+D_5K_5(\alpha_Y\xi)]\Bigg]\\ &-\frac{\sigma_R^2\alpha_R\xi_1\xi_2\xi K_1(\alpha_R\xi)}{8b^2n^2}\end{aligned} \tag{2.25}$$

and its variance expression:

$$P_{v_1v_2}(\mathbf{x},\mathbf{x}) = 0$$

in which:

$$
\begin{aligned}
B = -C &= \frac{12(6\xi_1^2\xi_2^2 - \xi_1^4 - \xi_2^4)}{\xi^8\alpha_Y^8} + \frac{1920(\xi_2^6 - \xi_1^6 - 15\xi_1^2\xi_2^4 + 15\xi_1^4\xi_2^2)}{\xi^{12}\alpha_Y^{10}} \\
B_0 &= \frac{(7\xi_1^6 + 8\xi_1^4\xi_2^2 + 3\xi_1^2\xi_2^4)}{48\xi^2} \\
B_1 &= \frac{(3\xi_1^6 + 7\xi_1^2\xi_2^4)}{24\alpha_Y\xi^3} + \frac{\alpha_Y\xi_1^4\xi}{48} \\
B_2 &= \frac{(4\xi_1^6 - \xi_2^6 - 39\xi_1^4\xi_2^2 + 36\xi_1^2\xi_2^4)}{48\alpha_Y^2\xi^4} \\
B_3 = -C_3 &= \frac{(3\xi_1^6 - 2\xi_2^6 - 40\xi_1^4\xi_2^2 + 35\xi_1^2\xi_2^4)}{4\alpha_Y^3\xi^5} \\
B_4 = -C_4 &= \frac{(11\xi_1^6 - 9\xi_2^6 - 155\xi_1^4\xi_2^2 + 145\xi_1^2\xi_2^4)}{4\alpha_Y^4\xi^6} \\
B_5 = -C_5 &= \frac{5(\xi_1^6 - \xi_2^6 - 15\xi_1^4\xi_2^2 + 15\xi_1^2\xi_2^4)}{48\alpha_Y^5\xi^7} \\
C_0 &= \frac{(\xi_1^4\xi_2^2 - \xi_1^2\xi_2^4)}{48} \\
C_1 &= \frac{(\xi_2^6 - \xi_1^6 + 11\xi_1^4\xi_2^2 - 7\xi_1^2\xi_2^4)}{48\alpha_Y\xi^3} \\
C_2 &= \frac{(3\xi_2^6 - 7\xi_1^6 + 81\xi_1^4\xi_2^2 - 69\xi_1^2\xi_2^4)}{48\alpha_Y^2\xi^4} \\
D &= \frac{48(\xi_1\xi_2^3 - \xi_1^3\xi_2)}{\xi^8\alpha_Y^8} + \frac{3840(10\xi_1^3\xi_2^3 - 3\xi_1\xi_2^5 - 3\xi_1^5\xi_2)}{\xi^{12}\alpha_Y^{10}} \\
D_0 &= -\frac{\xi_1^3\xi_2^3}{24\xi^2} \\
D_1 &= \frac{(8\xi_1\xi_2^5 + 13\xi_1^5\xi_2 - 19\xi_1^3\xi_2^3)}{96\alpha_Y\xi^3} \\
D_2 &= \frac{(6\xi_1\xi_2^5 + 9\xi_1^5\xi_2 - 25\xi_1^3\xi_2^3)}{12\alpha_Y^2\xi^4} \\
D_3 &= \frac{(13\xi_1\xi_2^5 + 17\xi_1^5\xi_2 - 50\xi_1^3\xi_2^3)}{4\alpha_Y^3\xi^5} \\
D_4 &= \frac{(14\xi_1\xi_2^5 + 16\xi_1^5\xi_2 - 50\xi_1^3\xi_2^3)}{\alpha_Y^4\xi^6} \\
D_5 &= \frac{10(3\xi_1\xi_2^5 + 3\xi_1^5\xi_2 - 10\xi_1^3\xi_2^3)}{\alpha_Y^5\xi^7}
\end{aligned}
\tag{2.26}
$$

Inspecting the velocity covariance equations shows that the first part of each velocity auto-covariance function is stationary and anisotropic, independent of the

mean recharge and the mean head gradient, and proportional to the recharge variance. The second part is nonstationary due to its dependence on the mean hydraulic gradient at $\mathbf{x}$ and $\mathbf{x}'$, anisotropic, and proportional to the log-transmissivity variance. The linear additive relationship between contributions of uncertain recharge and of uncertain log-transmissivity variance reflects the assumption that the transmissivity and recharge fields are uncorrelated. Note that if σ_R^2 and $\bar{\mathrm{R}}$ are taken to be zero, equations (2.23) to (2.25) collapse to those used by Graham and McLaughlin (1989a). If σ_R^2 is taken to be zero, but $\bar{\mathrm{R}}$ is nonzero, equations (2.23) to (2.25) are similar to those found by Rubin and Bellin (1994).

Figures 2.3 and 2.4 show the effects of deterministic recharge and uncertain recharge on the x_1-velocity correlation function and the x_2-velocity correlation function in the direction of mean flow, respectively, for the same five cases discussed previously. Also plotted in these figures are the velocity covariance functions derived by Rubin and Bellin (1994) using an isotropic negative exponential log-transmissivity covariance function with deterministic recharge. Cases 1 through 3 coincide with the deterministic recharge cases considered by Rubin and Bellin (1994). Both the velocity covariances derived here, and Rubin and Bellin's results, show that although introduction of deterministic recharge (either positive or negative) systematically increases the velocity covariance (see equations (2.23) and (2.25)). Both our results and Rubin and Bellin's results also show that positive mean recharge slightly increases the x_1-velocity correlation function and slightly decreases the x_2-velocity correlation function in the mean flow direction, while negative mean recharge slightly decreases the x_1-velocity correlation function and slightly increases the x_2-velocity correlation function slightly in the mean flow direction. The close agreement of the results derived here with those derived by Rubin and Bellin (1994) indicates that the form of the underlying log-transmissivity covariance function is not important when evaluating the ensemble moments of the resulting velocity field. This is in spite of the fact that

use of the exponential log-transmissivity covariance in two-dimensional analyses leads to unbounded head variances, a problem circumvented by using the hole covariance function adopted here.

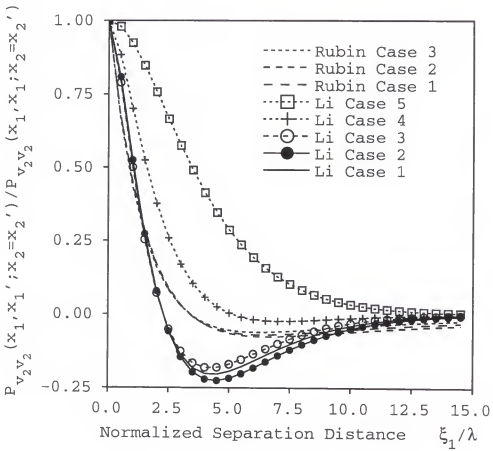

Figure 2.3: Comparison of x_1-velocity correlation functions (equation (2.9)) to x_1-velocity correlation functions derived by Rubin and Bellin (1994) in the direction of mean flow for Cases 1 through 4.

Results for Cases 4 and 5 suggest that introduction of spatially random recharge further increases the velocity covariance, decreases the x_1-velocity correlation function in the mean flow direction, but increases the x_2 velocity correlation in the mean flow direction. As the recharge variance increases, and the first term in the velocity

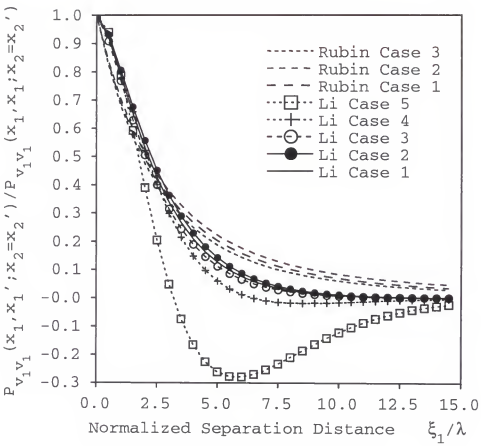

Figure 2.4: Comparison of x_2-velocity correlation functions (equation (2.9)) to x_2-velocity correlation functions derived by Rubin and Bellin (1994) in the direction of mean flow for Cases 1 through 4.

covariance functions begins to dominate, the magnitude of the x_2-velocity correlation approaches the magnitude of the x_1-velocity correlation. For the case of random recharge only (i.e. deterministic transmissivity) the magnitude of the x_2-velocity correlation exceeds the magnitude of the x_1-velocity correlation in the direction of mean flow.

2.3.2 Concentration Plume Moments

The velocity covariance functions (equations (2.23) through (2.25)) were incorporated into a Galerkin finite element algorithm to obtain numerical solutions for the ensemble mean (equation (2.13)) and covariance (equation (2.15)) of the solute concentration field, and the cross-covariance between the velocity and concentration fields (equation (2.14)). The moment equations were discretized using a standard Galerkin finite element procedure, then decomposed into a mathematically equivalent square-root form, and solved using a dual-grid to reduce computer storage and run times [Graham and McLaughlin, 1991].

For illustrative purposes, a conservative planar source (4 m by 4m) was assumed to be instantaneously released into a 20 m by 60 m domain at time zero. Its location, initial release time, and initial release concentration were all considered to be known perfectly. The initial concentration in the domain was assumed to be zero except in the source area. The boundaries were assumed to be located far enough from the solute source so that homogeneous Dirichlet boundary conditions apply on all sides of the domain. Table 2.1 lists the values for the input parameters used in this example problem. The values for the statistics of the log-transmissivity field and the hydraulic gradient are taken from the Borden field experiment [Mackay et al., 1986; Sudicky, 1986]. The statistics of the log-transmissivity field were determined by Dagan (1989) by vertical averaging of the three-dimensional log-conductivity field over the vertical correlation length. This methodology was proposed by Dagan (1989) due to the very limited vertical extent and vertical spreading of the plume, and was adopted by Freyberg (1986), Sposito and Barry (1987), Barry et al. (1988) and Graham and McLaughlin (1991) in subsequent analyses of the Borden experiment. The statistics for recharge field are somewhat arbitrarily determined, but were selected to roughly conform, where applicable, to values used in Rubin and Bellin (1994).

Table 2.1: Input parameters for different simulation cases.

Parameter	Case 1	Case 2	Case 3	Case 4	Case 5
K_G (m/d)	6.18	6.18	6.18	6.18	6.18
σ_Y^2	0.29	0.29	0.29	0.29	0.0
R (m/d)	0.0	0.003	-0.003	0.003	0.003
σ_R^2 (m^2/d^2)	0.0	0.0	0.0	0.0006	0.0006
Common parameters in all Cases	λ_Y =2.8 m*; α_L =0.05 m; n =0.33; b=10m λ_R =2.8 m; α_T =0.05 m; J_0 =0.0056; c_0 = 337 mg/l Total simulation time =276 days; Time step =5 days Domain size =20m by 60m Mean grid $\Delta x = \Delta y = 1m$; Covariance grid $\Delta x = \Delta y = 2m$				

*To obtain an equivalent log transmissivity correlation length for comparison with results from Rubin and Bellin (1994), the exponential correlation parameter was taken to be 1.4 times the hole-function correlation parameter (i.e. $\lambda_e = 1.4\lambda$), as recommended by Mizell et al., 1982.

Case 1 is considered as the base case for comparison and contrast with the other cases because it considers only uncertainty in the transmissivity field (i.e., mean recharge and recharge variance are zero). This case has been quite extensively studied and reported in the literature [Dagan, 1989; Graham and McLaughlin, 1989a; Zhang and Neuman, 1995a]. Cases 2 and 3 introduce a deterministic positive and negative constant recharge, respectively. These cases investigate the evolution of the ensemble mean, variance, and macrodispersive flux of a solute plume released into a random transmissivity field subject to spatially uniform recharge (i.e., the case studied by Rubin and Bellin (1994)). Case 4 investigates the new scenario of evolution of a solute plume released into a random transmissivity field subject to a randomly variable recharge field. Table 2.1 summarizes the parameter values used for each case.

Figure 2.5 presents the mean concentration simulation results for Cases 1 through 4 at 225 days after solute release. The plume shape for Case 1 is consistent with previous results by Graham and McLaughlin (1991) and Zhang and Neuman (1995a). Introduction of the deterministic positive recharge term in Case 2 enhances

the longitudinal spreading of plume in the mean flow direction. Similarly, the deterministic negative recharge term in Case 3 contracts the mean concentration plume, producing less longitudinal spread than the base case. This phenomenon is due to the existence of a mean velocity gradient along the mean flow direction caused by the addition(or removal) of water through recharge (or discharge). In the positive recharge case the presence of the positive velocity gradient increases the range of pore water velocities experienced by the mean solute plume, both because of the differential mean velocity experienced by the plume and the fact that the mean plume experiences a larger volume of the heterogeneous transmissivity field. Thus the spreading of the ensemble mean plume is enhanced in the longitudinal direction. In the negative recharge case (i.e., groundwater discharge due to evaporation or upward leakage through a confining layer), the negative velocity gradient implies a reduction in mean velocity compared with the base case. Thus the ensemble mean plume experiences a smaller volume of the heterogeneous transmissivity field and experiences less ensemble spreading. The constant recharge term (either positive or negative) affects both the location of the center of mass of the plume and the spread around this center of mass. The introduction of positive (or negative) recharge increases (or decreases) the mean velocity, thus increasing (or decreasing) the rate at which the center of mass moves in the domain and increasing (or decreasing) the longitudinal spread around the center of mass.

The shape of the mean concentration plume in Case 4 suggests that introduction of the recharge uncertainty slightly enhances longitudinal spreading and significantly enhances lateral spreading of the ensemble mean plume. Introduction of the recharge variability increases the magnitude of the velocity covariance, which in turn increases the spreading of the mean plume. The higher the recharge uncertainty (σ_R^2), the larger the x_2-velocity covariances tend to become relative to the x_1-velocity

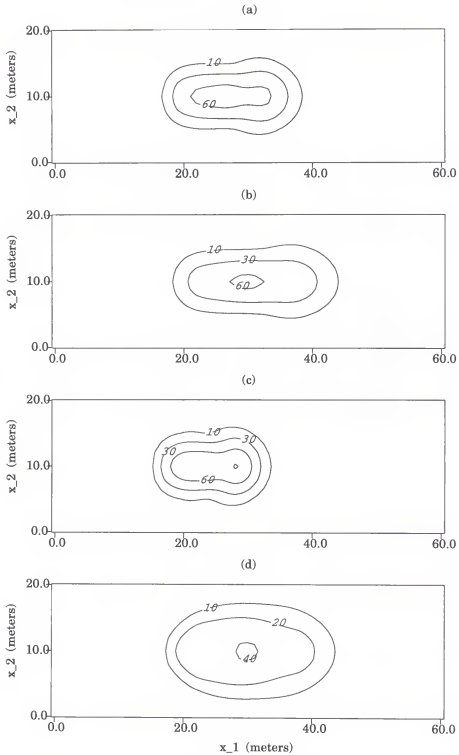

Figure 2.5: Mean concentration at 225 days after release, (a) for Case 1, (b) for Case 2, (c) for Case 3, (d) for Case 4.

covariances in the mean flow direction (see Figures 2.3 and 2.4), thus leading to the more isotropic macroscopic mean plume spreading.

It is important to note that plumes presented in Figure 2.5 represent the ensemble mean conditions. The ensemble mean concentration plume shape is not necessarily a reflection of the shape of any single replicate concentration plume, particularly when concentration standard deviations are high. Figures 2.6 and 2.7 present concentration plumes for two different transmissivity realizations for each of the four recharge cases generated using parameters in Table 1. The dashed line in these figures represents the respective ensemble mean 30 mg/l concentration contour for each single realization plume. Inspecting Figures 2.6 and 2.7 suggests that single replicate concentration plumes tends to have much higher peak concentrations, less spreading, and more tendency to deviate from the mean flow direction than the ensemble mean plumes. This is particularly apparent for Case 4 where the single replicate plumes are substantially narrower than the ensemble mean. The spreading in the ensemble mean plumes is thus caused by averaging over the ensemble of more narrow single replicate plumes with variable trajectories.

Figure 2.8 shows the concentration standard deviation 225 days after solute release for Cases 1 through 4. The plot for Case 1 reveals that low variance and thus low prediction uncertainty occurs at ensemble mean plume center of mass. Maximum uncertainty occurs near the leading and trailing inflection points of the ensemble mean plume, where mean concentration gradients are large. Introduction of constant positive mean recharge in Case 2 elongates the standard deviation plume along the mean flow direction and reduces peak uncertainty. Negative mean recharge, on the other hand, contracts the standard deviation plume and increases peak uncertainty. Thus, for the range of parameter values investigated here, the incorporation of deterministic recharge affects the plume prediction uncertainty primarily through its effect on the position and areal distribution of the mean plume, rather than its effect on the

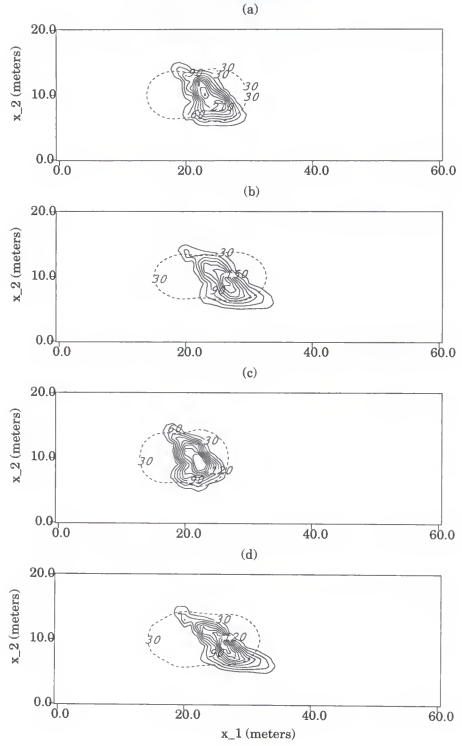

Figure 2.6: Concentration plume for single replicate at 225 days after release, (a) for Case 1, (b) for Case 2, (c) for Case 3, (d) for Case 4.

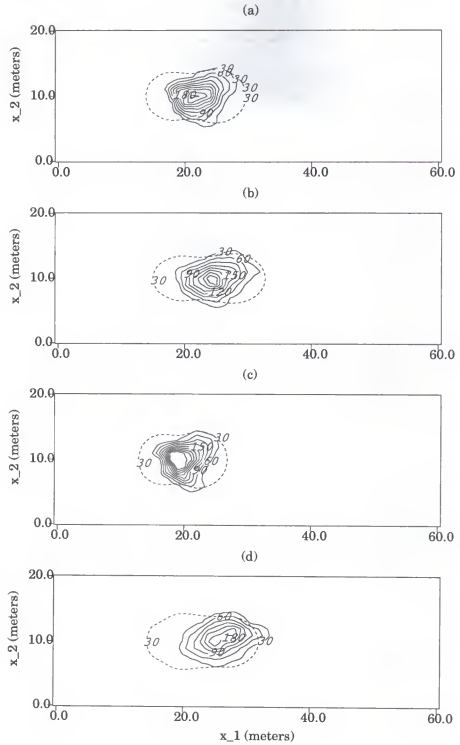

Figure 2.7: Concentration plume for single replicate at 225 days after release, (a) for Case 1, (b) for Case 2, (c) for Case 3, (d) for Case 4.

magnitude of the velocity covariance. Figure 2.8 suggests that for the deterministic recharge (i.e. nonuniform mean flow) case it is possible that the evolution of the concentration standard deviation plume could be approximately predicted from the uniform flow result using the nonlinear travel-time transformation proposed by Rubin and Bellin (1994) for the displacement covariance in non-uniform mean flows.

Case 4 shows that considering uncertain spatial variability in the recharge field increases the extent of the ensemble concentration standard deviation plume, particularly in the transverse direction. The peak concentration uncertainty for Case 4 is approximately the same as for Case 2. However, since the mean concentration for Case 4 is generally lower for than for Case 2, the coefficient of variation is higher, particularly near the center of mass. As the uncertainty (standard deviation) of the recharge increases, the shape of both the mean concentration plume and the concentration standard deviation plume become isotropic. This is due to the assumption of isotropy in the recharge field, the assumption that the log-transmissivity and recharge fields are independent, and the increasing equivalence of the x_1- and x_2-velocity covariances in the direction of flow as the variance of recharge increases.

Case 4 shows that considering uncertain spatial variability in the recharge field increases the ensemble concentration standard deviation. As the uncertainty (standard deviation) of the recharge increases, the shape of both the mean concentration plume and the concentration standard deviation plume become isotropic. This is due to the assumption of isotropy in the recharge field, the assumption that the log-transmissivity and recharge fields are independent, and the increasing equivalence of the velocity covariances in the direction of flow as the variance of recharge increases. From equation (2.3) for the cross-covariance between head and recharge, it is evident that assuming the recharge and log transmissivity fields are uncorrelated (i.e. $P_{YR}(\xi)=0$) causes the head-recharge cross-covariance to be independent of the head gradient. This results in a term in the velocity covariance equation which is isotropic

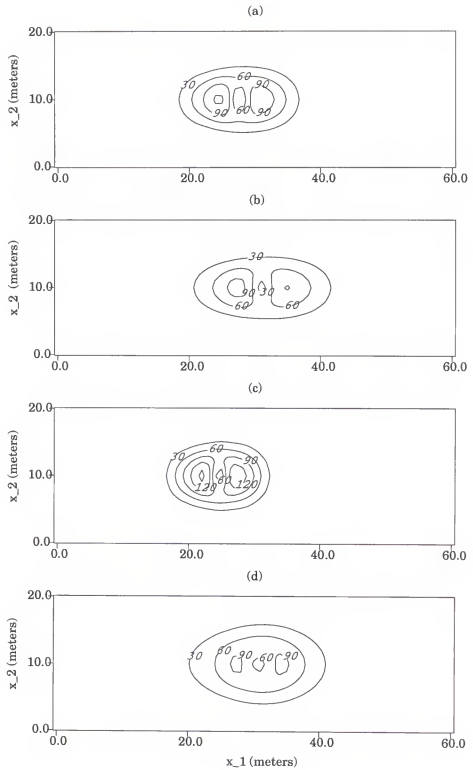

Figure 2.8: Concentration standard deviation at 225 days after release, (a) for Case 1, (b) for Case 2, (c) for Case 3, (d) for Case 4.

and independent of the mean head gradient. Therefore, as uncertainty in recharge increases, the isotropic portion of the velocity covariance becomes dominant in affecting the shape of the standard deviation plume.

Figure 2.9 presents the evolution of the normalized spatial moments of the ensemble mean plume for each of the 4 cases, and confirms the effects of recharge on the mean plume behavior discussed above. Figure 2.9a presents the evolution of the normalized first moment of the ensemble mean plume. This figure shows that both nonzero mean recharge and recharge uncertainty affect the evolution of the mean plume center of mass. A positive mean recharge (Case 2) increases both the mean velocity along the mean flow direction, and the longitudinal spreading on the leading edge of the plume, which increases the rate of movement of the center of mass through the domain compared with Case 1. A negative mean recharge (Case 3) decreases the rate of movement of the center of mass for similar reasons. Interestingly, the evolution of the center of mass in Case 4 (uncertain positive mean recharge) is slightly slower than in Case 2. This may be due to the fact that randomness of recharge increases lateral spreading of the center of mass, and thus at any given time more of the plume experiences the lower upstream mean velocities than in the deterministic recharge scenario. In a non-uniform flow field the macrodispersive flux is not symmetric and thus can affect the location of the center of mass.

Figure 2.9b shows the second centralized moment in the x_1-direction for the four cases, and confirms the results discussed above. That is, introduction of deterministic recharge affects the longitudinal mean plume spreading, with positive recharge enhancing the longitudinal spreading and negative recharge reducing the longitudinal spreading as found by Rubin and Bellin (1994). Since local dispersion was neglected in Rubin and Bellin (1994), and an initial point source condition was assumed, the longitudinal spreading determined here will be slightly larger than the longitudinal displacement covariance predicted using the methodology developed in

that study. In the absence of recharge variation, our results for longitudinal spreading will match closely with the results of Rubin and Bellin (1994), due to the close agreement between the two sets of velocity covariance functions shown in Figures 2.3 and 2.4. The agreement between ensemble-mean plume spreading predicted by the non-local Eulerian method used here, and the Lagrangian method used by Rubin and Bellin (1994) has been previously demonstrated by Graham and McLaughlin (1989a) and Dagan (1990) for the divergence-free (i.e., zero recharge) case. The temporal evolution of Case 4 in Figure 2.9b indicates that spatial variability in a nonzero mean recharge field will further enhance longitudinal spreading.

Figure 2.9c shows the evolution of the second centralized moments in the x_2-direction. This figure confirms that ensemble mean transverse spreading is moderately affect by a constant (nonzero) recharge term, with positive recharge leading to more transverse spreading, and negative recharge leading to less transverse spreading. However, transverse mean plume spreading increases significantly when uncertain spatial variability in recharge is considered. This is similar to results by Rehfeldt and Gelhar (1992) and Dagan et al. (1996) which showed that transient flow fields which enhance transverse velocities tend to increase transverse macrodispersion.

Previous work [Gelhar and Axness, 1983; Dagan, 1984; Graham and McLaughlin, 1989a] showed that higher lnK correlation scales produced more dispersed mean plumes as well as higher concentration standard deviations throughout the domain. The work reported here shows that increasing recharge correlation scales will also produce more dispersed mean plumes as well as higher concentration standard deviations. This is a result of the fact that increasing the correlation scale of uncertain recharge increases the flow field variability. This causes the trajectories of different single replicate plumes to be more different from one another which increases spreading of the ensemble mean plume and increases concentration prediction uncertainties in the absence of site-specific measurements. It should be noted, however, that as the

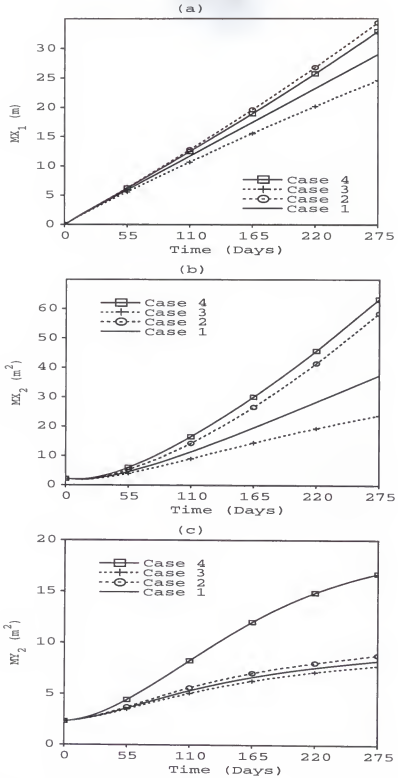

Figure 2.9: a. Normalized first moment, MX_1, vs time (days); b. Second centralized moment, MX_2, vs time (days); c. Second centralized moment, MY_2, vs time (days).

correlation scales of underlying log transmissivity and recharge random fields increase, the correlation scale of the concentration field will also increase. Thus site-specific measurements of any of these more spatially correlated random fields will have an impact over a longer distances and thus conditional uncertainties are likely to be lower than for random fields with less spatial correlation.

2.3.3 Analysis of Higher-Order Concentration Covariance Approximations

The concentration covariance equation (2.15) is a first-order approximate equation which neglects terms which involve three-way products of small perturbations. The exact equation for the concentration covariance is:

$$\begin{aligned}
&\frac{\partial P_{cc}(\mathbf{x}',\mathbf{x},t)}{\partial t} + \frac{\partial \overline{v_i}(\mathbf{x})\, P_{cc}(\mathbf{x}',\mathbf{x},t)}{\partial x_i} + \frac{\partial \overline{v_i}(\mathbf{x}')\, P_{cc}(\mathbf{x},\mathbf{x}',t)}{\partial x_i'} \\
&\quad - \frac{\partial}{\partial x_i}\left[D_{ij}\frac{\partial P_{cc}(\mathbf{x}',\mathbf{x},t)}{\partial x_j}\right] - \frac{\partial}{\partial x_i'}\left[D_{ij}\frac{\partial P_{cc}(\mathbf{x},\mathbf{x}',t)}{\partial x_j'}\right] \\
&\quad + \frac{\partial P_{cv_i}(\mathbf{x}',\mathbf{x},t)\overline{c(\mathbf{x},t)}}{\partial x_i} + \frac{\partial P_{cv_i}(\mathbf{x},\mathbf{x}',t)\overline{c(\mathbf{x}',t)}}{\partial x_i'} \\
&+ \frac{\partial P_{ccv_i}(\mathbf{x}',\mathbf{x},\mathbf{x},t)}{\partial x_i} + \frac{\partial P_{ccv_i}(\mathbf{x},\mathbf{x}',\mathbf{x}',t)}{\partial x_i'} \quad = 0 \;\; \mathbf{x},\mathbf{x}' \in D
\end{aligned} \tag{2.27}$$

where the last two terms in the equation are the divergence of the expected value of the three-way product of a concentration perturbation and a velocity perturbation at the same spatial location (e.g., x) at time t, and a concentration perturbation at a different spatial location (e.g., x') at the same time. Kapoor and Gelhar (1994a) and Dagan and Neuman (1991) argue that dropping these terms in the concentration covariance equation is unwarranted because they involve the derivatives of small concentration perturbations, which may not be small even if the perturbations themselves are small. Kapoor and Gelhar (1994a) show that these new terms create a macrodispersive transport mechanism for the concentration covariance, but do not cause any global dissipation or production of concentration variance. Kapoor and Gelhar (1994a) claim that there is little merit in dropping these terms and still retaining the transport terms

due to local dispersion as done in this study, and by Graham and McLaughlin (1989a, 1989b, 1991).

In a divergence-free velocity field (i.e., analogous to our Case 1), equation (2.27) reduces to the following exact concentration variance equation:

$$\begin{aligned} &\frac{\partial \sigma_c^2}{\partial t} + \overline{v_i}\frac{\partial \sigma_c^2}{\partial x_i} - \frac{\partial}{\partial x_i}\left[D_{ij}\frac{\partial \sigma_c^2}{\partial x_j}\right] + \frac{\partial P_{ccv_i}(\mathbf{x},\mathbf{x},\mathbf{x},t)}{\partial x_i} \\ &= -2J_{D_i}\frac{\partial c(\mathbf{x},t)}{\partial x_i} - 2D_{ij}\overline{\frac{\partial \delta c(x,t)}{\partial x_i}\frac{\partial \delta c(x,t)}{\partial x_j}} \quad \mathbf{x} \in D \end{aligned} \tag{2.28}$$

Under the assumptions that the mean concentration gradient varies slowly over time and space, and that local dispersion can be neglected in evaluating the macrodispersive flux of the concentration variance, Kapoor and Gelhar (1994a) derive the following approximate asymptotic Fickian relationship for the concentration variance macrodispersive term (the last term on the left-hand-side of equation (2.28):

$$P_{ccv_i}(\mathbf{x},\mathbf{x},\mathbf{x},t) \approx -\overline{v}A_{ij}\left[\frac{\partial P_{cc}(\mathbf{x},\mathbf{x},t)}{\partial x_j}\right] = -\overline{v}A_{ij}\left[\frac{\partial \sigma^2{}_c(\mathbf{x},t)}{\partial x_j}\right] \tag{2.29}$$

where A_{ij} is the same asymptotic macrodispersion tensor found for the mean concentration field. The assumption that the mean concentration gradient varies slowly implies a large, smooth, mean concentration plume that has traveled a sufficient distance to sample the entire range of heterogeneity of the velocity field.

The finite element solution of equation (2.15) includes the full non-stationary effects of concentration variance dissipation by local dispersion represented by the last term on the right-hand side of equation (2.28). Kapoor and Gelhar (1994a) assume that the concentration covariance function is locally stationary, and propose that the concentration variance dissipation term can be approximated as:

$$2D_{ij}\overline{\frac{\partial \delta c(x,t)}{\partial x_i}\frac{\partial \delta c(x,t)}{\partial x_j}} = \chi\sigma_c^2 \approx \frac{2D_{ij}}{\Delta_i^c \Delta_i^c}\sigma_c^2 \tag{2.30}$$

where Δ_i^c is the concentration microscale (the spatial scale that characterizes the derivatives of the concentration perturbation field). Kapoor and Gelhar (1994a) develop approximate expressions for a spatially constant concentration microscale that assume that the local dispersivity is much smaller than the lnK microscale. This assumption requires an lnK spectrum which yields a finite lnK microscale; a property is not met by the commonly assumed exponential spectrum, or the *WhittleB* spectrum assumed here. Therefore Kapoor and Gelhar's approximation for the variance dissipation coefficient cannot be evaluated for our example.

To evaluate the impact of neglecting the higher-order macrodispersive flux term on the magnitude and distribution of the concentration variance plume equation (2.28) was evaluated for Case 1 (the only divergence-free velocity case considered here) using the Kapoor and Gelhar approximation for macrodispersive flux (equation (2.29)). Figure 10 shows a comparison of the concentration standard deviation for Case 1 calculated using 1) the finite element solution of equation (2.15) (which includes both the local spreading and dissipation effects of local dispersion, but neglects macrodispersive spreading of the concentration variance plume); 2) a fast Fourier transform solution of equation (2.28) neglecting both the macrodispersion and the dissipation of the concentration variance (i.e., the last term on the left-hand side and the last term on the right-hand side of equation (2.28); and c) a fast Fourier transform solution of equation (2.28) using the Kapoor and Gelhar approximation for macrodispersive flux (equation (2.29)), but again neglecting the concentration variance dissipation term.

A comparison of Figures 10a and 10b shows the importance of the variance dissipation term which is included in Figure 10a but neglected in Figure 10b. For the parameters investigated here it is evident that the variance dissipation term is spatially variable, and acts to lower the concentration variance primarily in the region near the center of mass. Thus, as asserted by Kapoor and Gelhar (1994a), without

the variance dissipation term the magnitude of the concentration variance is over-predicted near the center of mass. It is not clear, however, that an approximate spatially-constant variance dissipation term, as proposed by Kapoor and Gelhar, will accurately simulate the variance dissipation effect observed in Figure 2.10a.

A comparison of Figure 2.10a and 2.10c shows the effect of the higher-order macrodispersion term on the distribution of the concentration standard deviation. As expected, the concentration standard deviation plume calculated using the Kapoor and Gelhar approximation for macrodispersion is significantly more spread in the longitudinal direction. Furthermore, as predicted by Kapoor and Gelhar (1994a), the macrodispersive flux eliminates the bimodality of the concentration standard deviation plume when the local dispersive effect on variance dissipation is neglected. It should be noted however that the effect of variance macrodispersion is exaggerated in Figure 10c, because the large-time asymptotic macrodispersion has been used from time zero in the simulation. It is likely that including both the effects of local- and an evolving macro-dispersion on the concentration variance would produce a plume that is a composite between the two plumes shown in Figures 2.10a and 2.10c. That is, the plume would be slightly more spread in the longitudinal direction than the first-order plume but would be bimodal (like the first-order plume). Unfortunately it is numerically difficult to include both the effects of local and an evolving macro-dispersion on the concentration standard deviation using either the finite element or the fast Fourier transform methods.

2.4 Summary

This work examines the evolution of the unconditional ensemble moments for a concentration plume resulting from an instantaneous planar source in a two-dimensional spatially random transmissivity field subject to spatially variable recharge and nonuniform (i.e., linear trending) velocity. Under the assumptions of steady flow

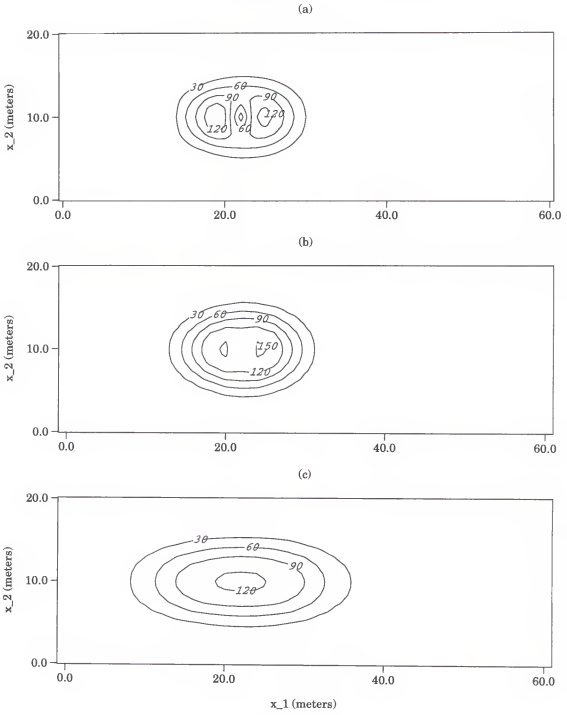

Figure 2.10: Comparison of the higher-order estimate of concentration standard deviation (equation (2.30)) and the first order estimate of concentration standard deviation (equation (2.15)) for Case 1 at 170 days.

in an infinite domain and no correlation between the log-transmissivity and recharge fields, a set of closed-form solutions were derived for the first-order approximate unconditional head covariance, head-log transmissivity cross-covariance, head-recharge cross-covariance, velocity covariance, velocity- head cross-covariance, and velocity-log-transmissivity cross-covariance using Fourier transform techniques. Hole-type covariance functions [Graham and McLaughlin, 1989a; Mizell et al., 1982] were selected for the input log-transmissivity and recharge random fields in order to obtain finite closed-form solutions for all the flow-related covariances. Assumption of more simple exponential input covariance structures in two-dimensional analyses has been shown to lead to unbounded head covariances [Dagan, 1989]. However, it should be noted that even for exponential log-transmissivity covariance functions the resulting head variogram is finite, and thus the velocity covariances can be defined [Rubin and Bellin, 1994]. The agreement of the velocity covariances presented here with those derived by Rubin and Bellin (1994) indicates that the form of the underlying covariance function is not important when evaluating the ensemble moments of the resulting velocity and concentration fields.

Introduction of a constant mean recharge term into the steady-state infinite domain flow problem caused the head and velocity fields to become nonstationary, i.e., the mean and covariance functions become dependent on location. The covariances for head and velocity show a quadratic dependence on location, while the cross-covariances for head-log-transmissivity and velocity-log-transmissivity exhibit a linear dependence on location. Under the assumption of no correlation between the recharge and transmissivity fields, the flow field covariance and cross-covariance functions are simply linear additions of components due to the random recharge and random transmissivity fields.

The unconditional velocity moment equations were incorporated into a system of solute transport moment equations, which were solved using a Galerkin finite

element algorithm. The following conclusions are made based on the results of this work.

1) Introduction of deterministic recharge (either positive or negative) does not change the head correlation or the velocity correlation function significantly either in the mean flow direction or the lateral direction.

2) With the same input covariance structure for log transmissivity and recharge fields, the head correlation function which includes random recharge is correlated over longer distances than the head correlation function resulting from only random log-transmissivity. The head correlation function resulting from impacts of both random fields are bounded by the head correlation functions resulting from each random field separately.

3) Introduction of deterministic recharge produces a mean velocity gradient which significantly affects the spreading of the plume in the longitudinal direction. A positive recharge increases the velocity along the mean flow direction, and enhances the plume spreading in the longitudinal direction. A negative recharge slows the movement of the mean plume and reduces the longitudinal spreading.

4) Introduction of spatially variable, uncertain recharge enhances the spreading of plume, particularly in the lateral direction. As the recharge variance increases, the plume tends to spread isotropically. The increase in transverse spreading slows the movement of the center of mass of the mean plume in the positive recharge case because less solute mass experiences the higher downstream velocities.

5) Uncertainty in the spatial distribution of recharge also increases the extent of the ensemble standard deviation plume, particularly in the lateral direction, and increases the coefficient of variation of solute concentration. The uncertainty in the prediction of solute transport increases with increasing recharge variance and spatial correlation scale. Higher recharge correlation scales increase both the ensemble

plume spreading and the ensemble plume variance in the absence of site-specific measurements, similar to the effect that log-transmissivity correlation scale has on the ensemble plume behavior.

6) Spatial variability in recharge increases the head, velocity and concentration field variances. Thus, neglecting the effect of spatial variability in the recharge field can lead to under-estimation of head, velocity, and concentration prediction uncertainties.

7) The first-order finite element concentration covariance solution presented here neglects higher-order terms in the concentration covariance equation which result in increased spreading of the concentration covariance in the longitudinal direction. However the asymptotic macrodispersion expressions proposed by Kapoor and Gelhar (1994a) are likely to over-predict spreading, particularly at early times. New closure terms and solution techniques which can appropriately deal with both the effects of local and evolving macrodispersion on the concentration standard deviation are required to accurately assess the important of these higher-order terms.

CHAPTER 3
TRANSIENT RANDOM RECHARGE

3.1 Introduction

The stochastic approach to contaminant transport in the saturated zone has been studied by a number of researchers in recent years [Gelhar et al., 1979; Matheron and de Marsily, 1980; Gelhar and Axness, 1983; Guven et al., 1984; Dagan 1984, 1987; Neuman et al., 1987; Black and Freyberg, 1987; Graham and McLaughlin, 1989a, 1989b; Neuman and Zhang, 1990; Zhang and Neuman, 1990; Dagan et al., 1992; Cvetkovic et al., 1992]. The early studies focused on trying to identify large-scale, spatially-averaged, effective macrodispersion parameters to describe the influence of hydraulic conductivity heterogeneity on subsurface transport of nonreactive species. The goal of these studies was generally to replace the laboratory-scale dispersivity in the classical model for advective/dispersive transport with a field-scale macrodispersion coefficient derived based on spatial variations in the hydraulic conductivity field. Subsequent studies [Gelhar et al., 1981; Gelhar and Gutjhar, 1982; Dagan, 1987, 1989; Black and Freyberg, 1987; Graham and McLaughlin, 1989a, 1989b, 1991; Dagan and Cvetkovic et al., 1992; Cvetkovic and Dagan, 1994; Li and McLaughlin, 1991, 1995; Neuman and Zhang, 1995a, 1995b, 1995c, 1995d] have tried to evaluate the uncertainty of mass transport predictions based on models which used effective macrodispersive parameters. Recently the coupled effects of spatially variable hydraulic conductivity and aquifer sorption characteristics have been studied by Bellin et al. (1993, 1995), Tompson and Gelhar (1990), James et al. (1997), and Zhang

(1997). However, little research has been reported which incorporates both the effects of spatially variable recharge and aquifer properties on the prediction of flow and solute transport, especially for the case of transient recharge.

Hydraulic conductivity heterogeneity generates variability in hydraulic head and pore water velocity and thus results in solute transport prediction uncertainty. Temporal and spatial fluctuations in recharge or discharge impact the magnitude and direction of the head gradient and thus increase the variability in pore water velocity resulting in increased solute transport prediction uncertainty.

Li and Graham (1998) examined the impact of steady-state spatially random recharge on the predictions of flow and transport in a two dimensional aquifer. They derived closed-form expressions for the unconditional, nonstationary auto-covariances for head and velocity, and the cross-covariances between velocity, head, recharge, and log-transmissivity based on a system of coupled first-order partial differential moment equations. These equations were then used to solve approximate unconditional moment equations for a concentration plume in a two-dimensional spatially random transmissivity field subject to spatially random recharge and nonuniform (linear trending) velocity using a finite element algorithm. The results showed that a constant positive mean recharge yields a mean velocity gradient which enhances the ensemble mean plume spreading in the longitudinal direction similar to results found by Rubin and Bellin (1994). Spatial variability in recharge was found to further enhance the spreading of the ensemble mean plume, especially in the lateral direction. The uncertainty in the prediction of solute transport was found to increase with increasing recharge variance and spatial correlation scale.

This chapter generalizes the previous work by Li and Graham (1998) (reported in Chapter 2) to examine the impact of temporally and spatially random recharge and spatially random transmissivity on the predictions of flow and transport in a two dimensional aquifer system. Semi-analytical solutions for the velocity covariances

resulting from a zero mean recharge and a constant mean recharge are obtained using a Fourier transform technique, assuming no correlation between the log-transmissivity field and the recharge field.

Concentration moments are generally transient and non-stationary due to the effects of finite initial source configurations, and the resulting equivalence between the size of the plume and the scale of the medium heterogeneity. Evaluating non-stationary concentration moments requires numeral solutions [Graham and McLaughlin, 1989a, 1989b, 1991; Li and McLaughlin, 1991, 1995; Neuman and Zhang, 1995a; Li and Graham, 1998] since analytical solutions are typically limited to stationary processes [Bakr et al., 1978; Gelhar and Axness, 1983; Gelhar, 1986]. Available approaches to analyze nonstationary concentration moments are computationally demanding when applied to problems of realistic size, thus their applications are often limited to steady-state velocity fields [Graham and McLaughlin, 1989a, 1989b, 1991; Li and McLaughlin, 1991, 1995; Neuman and Zhang, 1995a; Li and Graham, 1998]. In the transient velocity case, concentration moments are affected by space and time varying velocity moments, thus evaluating concentration moments results in much higher computation and storage requirements than for the steady state velocity case. Therefore, computational efficiency for evaluating concentration moments becomes one of the major concerns when considering transient flow.

Graham and McLaughlin [1989a, 1989b] derived a system of first-order ensemble concentration moment equations in a two-dimensional recharge free steady-state flow system and solved the equations using a Galerkin finite element algorithm. The advantage of this approach is that it estimates all first and second concentration moments, which include the mean concentration, the macrodispersive flux, as well as the cross-covariance between velocity and concentration and the concentration covariance. However, computation of these moments using this method requires on the order of N^2 operations and N^2 storage for N discretized nodes of the problem

domain, even for computing only the ensemble mean concentration. Therefore, this approach is computationally limited when applied to higher dimension problems.

Li and McLaughlin (1991, 1995) introduced a nonstationary spectral method for solving stochastic groundwater flow and transport problem, which combines the classical Fourier transform concepts with numerical solution techniques. The nonstationary spectra are expressed in terms of an unknown transfer function which depends on space, time, and wave number. The transfer function is found by solving a linearized deterministic partial differential equation which has the same form as the original stochastic flow or transport equation. Like the above-mentioned finite element method [Graham and McLaughlin, 1989a, 1989b, 1991], the nonstationary spectral method is able to evaluate all first and second concentration moments but it takes about same order of operations as the finite element method, though it may require less storage.

Deng et al. (1993) derived analytical expressions for the ensemble mean concentration and macrodispersive flux terms in the Fourier transform domain, where the coupled equations of mean concentration and macrodispersive flux become decoupled. The decoupled mean concentration and macrodispersive equations can be evaluated by numerical techniques such as fast Fourier transform or numerical inverse Laplace transform. Since the numerical fast Fourier transform involves only $N\,log_2 N$ order of operations for N discrete points of problem concerned, it dramatically reduces the computational demand compared to the finite element method or the nonstationary spectral method for the same size problem. The method is able to deal with nonstationary solute transport in multi-dimensional domains. However, Deng et al. (1993) do not develop the method for evaluating the covariance of concentration, which is essential for uncertainty analysis of solute transport.

In this chapter, the mean concentration, macrodispersive flux, and variance equations for heterogenous aquifers subject to spatially and temporally variable recharge

fields are derived using the first-order perturbation approach. Following Deng et al. (1993), the solutions for the mean concentration and macrodispersive flux are decoupled analytically in the Fourier domain and solved using a fast Fourier transform algorithm. The concentration variance is also approximated using a fast Fourier transform algorithm by neglecting the effects of the variance dissipation term [Kapoor and Gelhar, 1994a; Li and Graham, 1998]. The resulting concentration variance is compared to results obtained by a finite element method and a direct integration method, which include the effects of the variance dissipation term.

3.2 Unconditional Flow-related Moment Equations

3.2.1 Head Field

The governing equation for hydraulic head distribution in a transient two-dimensional aquifer system with spatially random transmissivity and spatiotemporally random recharge is:

$$\frac{\partial}{\partial x_i}\left[T(\mathbf{x})\frac{\partial H}{\partial x_i}\right] + R(\mathbf{x},t) = S_y\frac{\partial H}{\partial t} \tag{3.1}$$

where $\mathbf{x} = (x_1, x_2)$ is a vector point in the horizontal plane, $T(\mathbf{x})$ is the transmissivity at location $\mathbf{x}$, $R(\mathbf{x},t)$ is the transient recharge at time t and location $\mathbf{x}$ (positive for accretion), $H(\mathbf{x},t)$ is the transient hydraulic head at time t and location $\mathbf{x}$, and S_y is specific yield, representing the volume of water produced per unit area per unit decline in head, treated here as a known constant. Summation over repeated indices is assumed.

Letting $Y = lnT$, expanding the log-transmissivity, recharge, and head fields into the sums of potentially spatially-varying means and the corresponding small perturbations ($H = \bar{H} + \delta H$, $Y = \bar{Y} + \delta Y$, and $R = \bar{R} + \delta R$), neglecting higher order perturbation products, and taking the expected value, the following ensemble mean head equation is derived:

$$\frac{\partial^2 \bar{H}}{\partial x_i^2} + e^{-\bar{Y}} \bar{R} = S_y e^{-\bar{Y}} \frac{\partial \bar{H}}{\partial t} \tag{3.2}$$

in which $\bar{Y}$ is assumed to be spatially constant.

If the mean recharge is time invariant, the resulting mean head field will be time-invariant resulting in the following ensemble mean head gradient equation:

$$J(x_1) = -\frac{\partial \bar{H}}{\partial x_1} = \bar{R} e^{-\bar{Y}} x_1 + J_0 \tag{3.3}$$

Subtracting the mean head equation (3.2) from the expanded head equation (3.1) gives the head perturbation $\delta H(\mathbf{x}, t)$ equation. Post-multiplying the head perturbation equation by the perturbations of $\delta H(\mathbf{x}', t')$, $\delta Y(\mathbf{x}')$, and $\delta R(\mathbf{x}', t')$ at vector location $\mathbf{x}'$ and time t', and taking the expected values gives the following system of coupled non-stationary transient head moment equations:

$$\begin{aligned} &\frac{\partial^2 P_{HR}(\mathbf{x}, t, \mathbf{x}', t')}{\partial x_i^2} + \frac{\partial P_{YR}(\mathbf{x}, \mathbf{x}', t')}{\partial x_i} \frac{\partial \bar{H}(\mathbf{x}, t)}{\partial x_i} \\ &+ e^{-\bar{Y}} \Big[- \bar{R} P_{YR}(\mathbf{x}, \mathbf{x}', t') + P_{RR}(\mathbf{x}, t, \mathbf{x}', t') \Big] = S_y e^{-\bar{Y}} \frac{\partial P_{HR}(\mathbf{x}, t, \mathbf{x}', t')}{\partial t} \end{aligned} \tag{3.4}$$

$$\begin{aligned} &\frac{\partial^2 P_{HY}(\mathbf{x}, t, \mathbf{x}')}{\partial x_i^2} + \frac{\partial P_{YY}(\mathbf{x}, \mathbf{x}')}{\partial x_i} \frac{\partial \bar{H}(\mathbf{x}, t)}{\partial x_i} \\ &+ e^{-\bar{Y}} \Big[- \bar{R} P_{YY}(\mathbf{x}, \mathbf{x}') + P_{RY}(\mathbf{x}, t, \mathbf{x}') \Big] = S_y e^{-\bar{Y}} \frac{\partial P_{HY}(\mathbf{x}, t, \mathbf{x}')}{\partial t} \end{aligned} \tag{3.5}$$

$$\begin{aligned} &\frac{\partial^2 P_{HH}(\mathbf{x}, t, \mathbf{x}', t')}{\partial x_i^2} + \frac{\partial P_{YH}(\mathbf{x}, \mathbf{x}', t')}{\partial x_i} \frac{\partial \bar{H}(\mathbf{x}, t)}{\partial x_i} \\ &+ e^{-\bar{Y}} \Big[- \bar{R} P_{YH}(\mathbf{x}, \mathbf{x}', t') + P_{RH}(\mathbf{x}, t, \mathbf{x}', t') \Big] = S_y e^{-\bar{Y}} \frac{\partial P_{HH}(\mathbf{x}, t, \mathbf{x}', t')}{\partial t} \end{aligned} \tag{3.6}$$

where arguments with overbar represent expected values, $P_{FG}(\mathbf{x}, t, \mathbf{x}', t')$ is defined as $\overline{\delta F(\mathbf{x}, t)\delta G(\mathbf{x}', t')}$, in which δF and δG are small perturbations of random variables F and G at vector locations and times $\mathbf{x}$, t and $\mathbf{x}'$, t' respectively. Equations (3.3) to (3.6) extend the previous work of Li and Graham (1998) which was based on a steady-state head assumption. Equations (3.3) to (3.6) describe the first and second moments for the spatiotemporally random head field resulting from spatiotemporally random recharge and spatially random transmissivity fields.

3.2.2 Velocity Field

The pore water velocity vector for two-dimensional transient flow is:

$$v_i(\mathbf{x}, t) = -\frac{T(\mathbf{x})}{bn}\frac{\partial H(\mathbf{x}, t)}{\partial x_i}, \quad i = 1, 2 \tag{3.7}$$

in which $v_i(\mathbf{x}, t)$ is the pore velocity at vector location $\mathbf{x}$ and time t, $T(\mathbf{x})$ is the transmissivity, b is the aquifer thickness, n is the porosity. Here both the porosity and aquifer thickness are assumed to be known constants.

Expanding random quantities in equation (3.7) into the sums of deterministic means and corresponding perturbations around these means, approximating $e^{\bar{Y}+\delta Y}$ as $e^{\bar{Y}}(1+\delta \mathrm{Y})$, and taking the expected value leads to the following ensemble mean pore water velocity equations [Gelhar, 1993]:

$$\bar{v}_1(\mathbf{x}) = -\frac{e^{\bar{Y}}}{bn}\frac{\partial \bar{H}(\mathbf{x}, t)}{\partial x_1}, \quad \bar{v}_2(\mathbf{x}) = 0 \tag{3.8}$$

where $v_1(\mathbf{x})$ is the mean pore water velocity which for convenience is aligned with the x_1 direction.

Subtracting equations (3.8) from the expanded equations (3.7) and neglecting higher order perturbation products yields the velocity perturbation expression $\delta v_i(\mathbf{x}, t)$ [Gelhar, 1993]. Post-multiplying this perturbation equation at the spatial

location $\mathbf{x}$ and time t by the perturbations of $\delta v_j(\mathbf{x}', t')$, $\delta Y(\mathbf{x}')$ and $\delta H(\mathbf{x}', t')$ at a different spatial location $\mathbf{x}'$ and time t', and taking the expected value yields a system of coupled equations which describes the unconditional transient non-stationary velocity covariance and cross-covariance equations:

$$\begin{aligned}
P_{v_1 Y}(\mathbf{x}, \mathbf{x}', t) &= -\frac{e^{\bar{Y}}}{bn}\left[P_{YY}(\mathbf{x}, \mathbf{x}')\frac{\partial \bar{H}(\mathbf{x}, t)}{\partial x_1} + \frac{\partial P_{HY}(\mathbf{x}, \mathbf{x}', t)}{\partial x_1}\right] \\
P_{v_1 H}(\mathbf{x}, \mathbf{x}', t, t') &= -\frac{e^{\bar{Y}}}{bn}\left[P_{YH}(\mathbf{x}, \mathbf{x}', t')\frac{\partial \bar{H}(\mathbf{x}, t)}{\partial x_1} + \frac{\partial P_{HH}(\mathbf{x}, \mathbf{x}', t, t')}{\partial x_1}\right] \\
P_{v_1 v_1}(\mathbf{x}, \mathbf{x}', t, t') &= -\frac{e^{\bar{Y}}}{bn}\left[P_{Y v_1}(\mathbf{x}, \mathbf{x}', t')\frac{\partial \bar{H}(\mathbf{x}, t)}{\partial x_1} + \frac{\partial P_{H v_1}(\mathbf{x}, \mathbf{x}', t, t')}{\partial x_1}\right] \\
P_{v_1 v_2}(\mathbf{x}, \mathbf{x}', t, t') &= -\frac{e^{\bar{Y}}}{bn}\left[P_{Y v_2}(\mathbf{x}, \mathbf{x}', t')\frac{\partial \bar{H}(\mathbf{x}, t)}{\partial x_1} + \frac{\partial P_{H v_2}(\mathbf{x}, \mathbf{x}', t, t')}{\partial x_1}\right]
\end{aligned} \tag{3.9}$$

$$\begin{aligned}
P_{v_2 Y}(\mathbf{x}, \mathbf{x}', t) &= -\frac{e^{\bar{Y}}}{bn}\frac{\partial P_{HY}(\mathbf{x}, \mathbf{x}', t)}{\partial x_2} \\
P_{v_2 H}(\mathbf{x}, \mathbf{x}', t, t') &= -\frac{e^{\bar{Y}}}{bn}\frac{\partial P_{HH}(\mathbf{x}, \mathbf{x}', t, t')}{\partial x_2} \\
P_{v_2 v_1}(\mathbf{x}, \mathbf{x}', t, t') &= -\frac{e^{\bar{Y}}}{bn}\frac{\partial P_{H v_1}(\mathbf{x}, \mathbf{x}', t, t')}{\partial x_2} \\
P_{v_2 v_2}(\mathbf{x}, \mathbf{x}', t, t') &= -\frac{e^{\bar{Y}}}{bn}\frac{\partial P_{H v_2}(\mathbf{x}, \mathbf{x}', t, t')}{\partial x_2}
\end{aligned} \tag{3.10}$$

It should be noted that equations (3.9) and (3.10) have similar structure to those derived by Li and Graham (1998), however, they are driven by spatiotemporal covariance equations due to the transient head field.

3.3 Solutions for Unconditional Flow-related Moment Expressions

Graham and Tankersley (1994) derived the head covariance expressions for a stationary flow field resulting from spatially variable recharge and transmissivity fields, assuming the mean recharge was zero. Li and Graham (1998) found closed-form solutions for the non-stationary head and velocity covariances resulting from spatially variable recharge and transmissivity fields assuming a constant mean recharge. Assuming that the log-transmissivity and recharge fields were uncorrelated, Li and

Graham (1998) showed that the derived head-recharge cross-covariance was independent of both the mean recharge and the mean head gradient, and head and velocity covariances were composed of the linear addition of terms resulting from recharge and log-transmissivity covariances. This suggests that the superposition principle for solutions of linear equations [Berg and McGregor, 1966] can be applied in solving the head and velocity moment equations.

For the convenience of deriving closed-form solutions for the velocity covariance, the flow domain is assumed to be infinite in space (i.e., far from any boundaries) and time (i.e., far from any fixed initial condition). This is reasonable if the domain is sufficiently large compared to the head correlation scale [Graham and Tankersley, 1994; Rubin and Dagan, 1987a; Dagan, 1989] and sufficient time has elapsed since any known initial head condition. The log-transmissivity is assumed to have a $WhittleB$ spectrum in space [Li and Graham, 1998] and a delta function spectrum in time, since it is time invariant (see equation (3.11)). The spatiotemporal recharge spectrum is assumed to be the product of a $WhittleB$ spectrum in space and an exponential spectrum in time (see equation (3.12)). The log-transmissivity and recharge fields are assumed to be uncorrelated (see equation (3.13)).

$$S_{YY}(\mathbf{k},\omega) = \sigma_Y^2 \frac{3\alpha_Y^2 k^4}{\pi(k^2+\alpha_Y^2)^4}\delta(\omega), \quad \alpha_Y = \frac{3\pi}{16\lambda_Y} \tag{3.11}$$

$$S_{RR}(\mathbf{k},\omega) = \sigma_R^2 \frac{3I_t\alpha_R^2 k^4}{\pi^2(k^2+\alpha_R^2)^4(1+I_t^2\omega^2)}, \quad \alpha_R = \frac{3\pi}{16\lambda_R} \tag{3.12}$$

$$S_{YR}(\mathbf{k},\omega) = 0 \tag{3.13}$$

In the above equations $\delta(\omega)$ is the Dirac delta function; $\mathbf{k}$ is a two-dimensional wave number vector, $k^2 = k_1^2 + k_2^2$, with k_1 aligned with the direction of the mean hydraulic gradient; ω is a frequency number; σ_Y^2 and λ_Y are the variance and spatial

correlation scale of the log-transmissivity field; and σ_R^2, λ_R, and I_t are the variance, spatial, and temporal correlation scales of the recharge field respectively.

3.3.1 Solutions of Head-log Transmissivity and Head-Recharge Cross-Covariances

We start with solving the governing equation (3.5). Since P_{YR} has been assumed to be zero, the driving force for equation (3.5) ($\bar{R}P_{YY}(\xi)$) is time invariant and a solution far from the initial time condition is sought, the solution of equation (3.5) with mean head gradient (3.3) is time invariant and thus identical to the corresponding one in previous work [Li and Graham, 1998]:

$$P_{HY}(\mathbf{x},\mathbf{x}') = 6\sigma_Y^2\alpha_Y^2(\bar{R}e^{-\bar{Y}}x_1' + J_0)\left[\frac{\xi_1\xi K_1(\alpha_Y\xi)}{8\alpha_Y} - \frac{\xi_1\xi^2 K_2(\alpha_Y\xi)}{48}\right]$$
$$+6\bar{R}e^{-\bar{Y}}\sigma_Y^2\alpha_Y^2\left[\frac{\xi^3 K_3(\alpha_Y\xi)}{48\alpha_Y} - \frac{\xi^2 K_2(\alpha_Y\xi)}{12\alpha_Y^2} + \frac{\xi_1^2\xi K_1(\alpha_Y\xi)}{12\alpha_Y} - \frac{\xi_1^2\xi^2 K_2(\alpha_Y\xi)}{48}\right] \quad (3.14)$$

in which ξ_1=x_1-x_1', and ξ^2=ξ_1^2+ξ_2^2; and the zero-lag cross-covariance is $P_{HY}(\mathbf{x},\mathbf{x}) = 0$.

Plugging the mean head gradient equation (3.3) into equation (3.4), applying equation (3.12), and solving using Fourier transform techniques gives the following new solution for the head-recharge cross-covariance resulting from a spatiotemporally random recharge field. Its detailed derivations are shown in Appendix B.

$$P_{HR}(\mathbf{x},\mathbf{x}',\tau) = \frac{6\sigma_R^2\alpha_R^2 e^{-|\tau'|}}{e^{\bar{Y}}}\left[\frac{S_y'^2 K_0(\sqrt{S_y'}\xi)}{(\alpha_R^2 - S_y')^4} - \frac{S_y'^2 K_0(\alpha_R\xi)}{(\alpha_R^2 - S_y')^4} - \frac{S_y'^2\alpha_R\xi K_1(\alpha_R\xi)}{2\alpha_R^2(\alpha_R^2 - S_y')^3}\right.$$
$$\left. + \frac{(-2S_y' + \alpha_R^2)\xi^2 K_2(\alpha_R\xi)}{8(\alpha_R^2 - S_y')^2} - \frac{\alpha_R\xi^3 K_3(\alpha_R\xi)}{48(\alpha_R^2 - S_y')}\right] \quad (3.15)$$

In equation (3.15) τ' is defined as $\frac{\tau}{I_t}$, τ is separation time lag $t - t'$; S_y' is defined as $\frac{S_y e^{-\bar{Y}}}{I_t}$; ξ=**x**-**x**′ is the two-dimensional separation vector between **x** and **x**′, in which x_1 is aligned with the direction of the mean hydraulic gradient; $K_n(z)$ is the

modified Bessel function of order n. The zero-lag cross-covariance between head and recharge is:

$$P_{HR}(\mathbf{x},\mathbf{x},0) = \sigma_R^2 e^{-\bar{Y}}\left[\frac{(\alpha_R^6 - 6\alpha_R^4 S_y' + 3\alpha_R^2 S_y'^2 + 2S_y'^3 + 6\alpha_R^2 S_y'^2 \ln(\frac{\alpha_R^2}{S_y'})}{2(S_y' - \alpha_R^2)^4}\right] \quad (3.16)$$

Equation (3.15) suggests that the head-recharge covariance is stationary, and is not influenced by the mean recharge. Its temporal correlation structure exhibits an exponential decrease as time lag increases.

3.3.2 Solutions of Head Covariances

Equation (3.6) is a linear equation with two driving force terms P_{YH} and P_{RH}, which are evaluated in the preceding section. According to the superposition principle for solutions of linear equations [Berg and McGregor, 1966], the solution of P_{HH} can be decomposed into two major terms $P_{HH}^{(1)}$ and $P_{HH}^{(2)}$, resulting from P_{YH} and P_{RH}, respectively. These terms are governed by the following equations:

$$S_y e^{-\bar{Y}} \frac{\partial P_{HH}^{(1)}(\mathbf{x},t,\mathbf{x}',t')}{\partial t} - \frac{\partial^2 P_{HH}^{(1)}(\mathbf{x},t,\mathbf{x}',t')}{\partial x_i^2} = -\bar{R}e^{-\bar{Y}} P_{YH}(\mathbf{x},t,\mathbf{x}',t') - (\bar{R}e^{-\bar{Y}} x_1 + J_0)\frac{\partial P_{YH}(\mathbf{x},t,\mathbf{x}',t')}{\partial x_1} \quad (3.17)$$

$$S_y e^{-\bar{Y}} \frac{\partial P_{HH}^{(2)}(\mathbf{x},t,\mathbf{x}',t')}{\partial t} - \frac{\partial^2 P_{HH}^{(2)}(\mathbf{x},t,\mathbf{x}',t')}{\partial x_i^2} = e^{-\bar{Y}} P_{RH}(\mathbf{x},t,\mathbf{x}',t') \quad (3.18)$$

Solving these two equations (for details see Appendix B) gives the transient head covariance resulting from spatiotemporally variable, constant mean, recharge:

$$
\begin{aligned}
P_{HH}(\mathbf{x},\mathbf{x}',\tau) =& P_{HH}^{(1)} + P_{HH}^{(2)} \\
=& \sigma_Y^2(\bar{R}e^{-\bar{Y}}x_1 + J_0)(\bar{R}e^{-\bar{Y}}x_1' + J_0)\left[\frac{\xi^2 K_2(\alpha_Y\xi)}{8} - \frac{\alpha_Y\xi_1^2\xi K_1(\alpha_Y\xi)}{8}\right] \\
&+\bar{R}^2e^{-2\bar{Y}}\sigma_Y^2\left[\frac{576(6\xi_1^2\xi_2^2 - \xi_1^4 - \xi_2^4)}{\xi^8\alpha_Y^8} - \frac{12(\xi_1^2 - \xi_2^2)}{\xi^4\alpha_Y^6}\right. \\
&+\frac{(\xi_1^4 - \xi_1^2\xi_2^2)K_2(\alpha_Y\xi)}{8} + \frac{(3\xi_1^4 - 8\xi_1^2\xi_2^2 + \xi_2^4)K_3(\alpha_Y\xi)}{8\alpha_Y\xi} \\
&+\frac{(2\xi_1^4 - 9\xi_1^2\xi_2^2 + \xi_2^4)K_4(\alpha_Y\xi)}{2\alpha_Y^2\xi^2} \\
&\left.+\frac{3(\xi_1^4 - 6\xi_1^2\xi_2^2 + \xi_2^4)K_5(\alpha_Y\xi)}{2\alpha_Y^3\xi^3}\right] \\
&+6\sigma_R^2\alpha_R^2e^{-2\bar{Y}}\int_0^\infty \frac{k^3J_0(k\xi)(k^2e^{-|\tau'|} - S_y'e^{-k^2|\frac{\tau'}{S_y'}|})}{(k^2+\alpha_R^2)^4(k^4 - S_y'^2)}dk
\end{aligned}
\tag{3.19}
$$

The head variance is:

$$
\begin{aligned}
P_{HH}(\mathbf{x},\mathbf{x},0) =& \frac{\sigma_Y^2(\bar{R}e^{-\bar{Y}}x_1 + J_0)^2}{4\alpha_Y^2} + \frac{\bar{R}^2e^{-2\bar{Y}}\sigma_Y^2}{2\alpha_Y^4} \\
&+\sigma_R^2e^{-2\bar{Y}}\left[\frac{2\alpha_R^6 + 3\alpha_R^4S_y' - 6\alpha_R^2S_y'^2 + S_y'^3 - 6\alpha_R^4S_y'\ln(\frac{\alpha_R^2}{S_y'})}{2\alpha_R^2(\alpha_R^2 - S_y')^4}\right]
\end{aligned}
\tag{3.20}
$$

For zero spatial separation distance the head covariance becomes:

$$
\begin{aligned}
P_{HH}(\mathbf{x},\mathbf{x},\tau) =& \frac{\sigma_Y^2(\bar{R}e^{-\bar{Y}}x_1 + J_0)^2}{4\alpha_Y^2} + \frac{\bar{R}^2e^{-2\bar{Y}}\sigma_Y^2}{2\alpha_Y^4} \\
&+6\sigma_R^2\alpha_R^2e^{-2\bar{Y}}\int_0^\infty \frac{k^3(k^2e^{-|\tau'|} - S_y'e^{-k^2|\frac{\tau'}{S_y'}|})}{(k^2+\alpha_R^2)^4(k^4 - S_y'^2)}dk
\end{aligned}
\tag{3.21}
$$

For zero temporal separation distance the head covariance becomes:

$$
\begin{aligned}
P_{HH}(\mathbf{x},\mathbf{x}',0) =& \sigma_Y^2(\bar{R}e^{-\hat{Y}}x_1 + J_0)(\bar{R}e^{-\hat{Y}}x_1' + J_0)\left[\frac{\xi^2 K_2(\alpha_Y\xi)}{8} - \frac{\alpha_Y\xi_1^2\xi K_1(\alpha_Y\xi)}{8}\right] \\
&+\bar{R}^2 e^{-2\hat{Y}}\sigma_Y^2\left[\frac{576(6\xi_1^2\xi_2^2 - \xi_1^4 - \xi_2^4)}{\xi^8\alpha_Y^8} - \frac{12(\xi_1^2 - \xi_2^2)}{\xi^4\alpha_Y^6}\right. \\
&+\frac{(\xi_1^4 - \xi_1^2\xi_2^2)K_2(\alpha_Y\xi)}{8} + \frac{(3\xi_1^4 - 8\xi_1^2\xi_2^2 + \xi_2^4)K_3(\alpha_Y\xi)}{8\alpha_Y\xi} \\
&\left.+\frac{(2\xi_1^4 - 9\xi_1^2\xi_2^2 + \xi_2^4)K_4(\alpha_Y\xi)}{2\alpha_Y^2\xi^2} + \frac{3(\xi_1^4 - 6\xi_1^2\xi_2^2 + \xi_2^4)K_5(\alpha_Y\xi)}{2\alpha_Y^3\xi^3}\right] \qquad (3.22) \\
&+\frac{6\sigma_R^2\alpha_R^2}{e^{2\hat{Y}}}\left[\frac{s_y'\left[K_0(\alpha_R\xi) - K_0(\sqrt{s_y'}\xi)\right]}{(\alpha_R^2 - s_y')^4} + \frac{s_y'\xi K_1(\alpha_R\xi)}{2\alpha_R(\alpha_R^2 - s_y')^3}\right. \\
&\left.+\frac{s_y'\xi^2 K_2(\alpha_R\xi)}{8\alpha_R^2(\alpha_R^2 - s_y')^2} + \frac{\xi^3 K_3(\alpha_R\xi)}{48\alpha_R(\alpha_R^2 - s_y')}\right]
\end{aligned}
$$

Inspecting equations (3.19) and (2.21) indicates that head covariance in both steady and transient states are composed of the sum of terms proportional to the recharge variance and log-transmissivity variance. Furthermore the part of covariance related to log-transmissivity variance is identical in both cases. In steady state recharge case the head covariance is time invariant, however for the transient case the portion of the head covariance related to recharge variance is stationary and decreases as time lag increases (see figure 3.1). The lower bound in Figure 3.1 is the head correlation function for the limiting case of infinite time lag corresponding to steady state recharge. The parameter values used in figures 3.1 to 3.4 are given in Table 3.1.

Figure 3.2 presents the sensitivity of the head correlation structure to the temporal correlation scale parameter. This figure suggests that increasing the recharge temporal correlation scale increases the head correlation function. As the temporal correlation scale approaches infinity, the head correlation function resulting from spatiotemporal recharge approaches the one resulting from steady-state spatially variable recharge. It should be pointed out that this result also applies to the head variance.

Table 3.1: Input parameters for head and velocity correlation function

Parameter	Value
Mean log-transmissivity $\bar{Y}$	61.8
Variance of transmissivity σ_Y^2	0.29
Correlation length of transmissivity λ_Y	2.8 m
Mean recharge $\bar{R}$	0.0 m/day
Variance of recharge σ_R^2	0.0003 m^2/day^2
Correlation length of recharge λ_R	2.8 m
Temporal correlation scale of recharge I_t	4 days
Aquifer storativity s_y	0.15
Mean hydraulic head gradient J_0	0.0056

That is, increasing the temporal correlation scale of transient random recharge increases the head variance, as shown in figure 3.3. Figure 3.4 illustrates the effect of the aquifer storativity on the head correlation structure for a transient recharge field with a temporal correlation scale of 4 days. Figure 3.4.(a) suggests that the sensitivity to this parameter is not significant when both transmissivity and recharge are random. The sensitivity of the head covariance to this parameter is futher investigated by choosing the recharge field as the only input random filed (or setting σ_Y^2=0). Figure 3.4.(b) indicates that increasing the aquifer storativity will reduce the head correlation function slightly when recharge is the only random field. This can be explained by the fact that increasing the aquifer storativity reduces the head rise or drop for the same change in stored water volume. Thus there is more damping of head fluctuations which reduces the head persistence and results in the smaller head spatial correlation.

3.3.3 Solutions of the Velocity Covariance

Solving equations (3.9) and (3.10) using Fourier transform techniques gives the following expressions for transient velocity covariances and variances with a constant mean recharge $\bar{R}$ (for details see Appendix B):

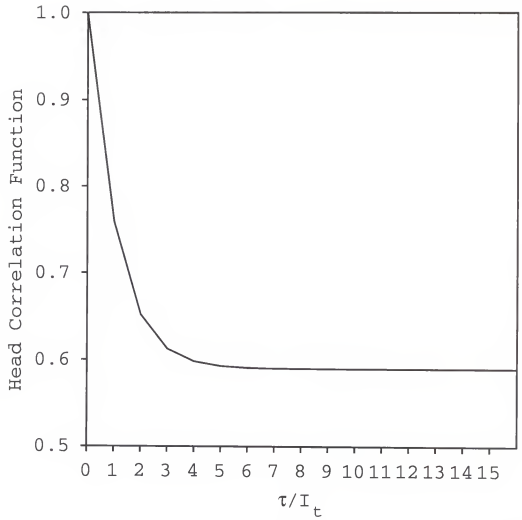

Figure 3.1: The head correlation function $P_{HH}(0,0,\tau)/\sigma_H^2$ vs normalized time lag resulting from the spatiotemporally random recharge field

$$
\begin{aligned}
P_{v_1v_1}(\mathbf{x},\mathbf{x}',\tau) &= P^{(1)}_{v_1v_1} - \frac{6\sigma_R^2\alpha_R^2}{(bn)^2}\frac{d^2}{d\xi_1^2}f(\xi,\tau) \\
P_{v_2v_2}(\mathbf{x},\mathbf{x}',\tau) &= P^{(1)}_{v_2v_2} - \frac{6\sigma_R^2\alpha_R^2}{(bn)^2}\frac{d^2}{d\xi_2^2}f(\xi,\tau) \\
P_{v_1v_2}(\mathbf{x},\mathbf{x}',\tau) &= P^{(1)}_{v_1v_2} - \frac{6\sigma_R^2\alpha_R^2}{(bn)^2}\frac{d^2}{d\xi_2 d\xi_1}f(\xi,\tau) \\
f(\xi,\tau) &= \int_0^\infty \frac{k^3 J_0(k\xi)(k^2e^{-|\tau'|} - S_y' e^{-k^2|\frac{\tau'}{S_y'}|})}{(k^2+\alpha_R^2)^4(k^4 - S_y'^2)}dk
\end{aligned}
\tag{3.23}
$$

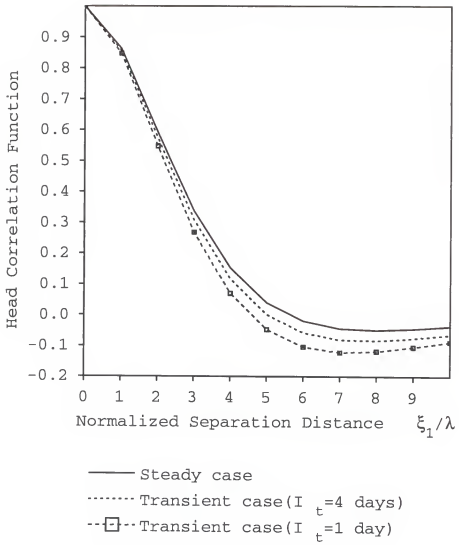

Figure 3.2: The head correlation function $P_{HH}(\xi_1, 0, 0)/\sigma_H^2$ vs normalized separation distance resulting from different recharge fields, in which s_y =0.15

in which $P^{(1)}_{v_i v_j}$ are identical to the first parts of equations (2.23) to (2.26), i.e., the components of velocity covariance driven by log-transmissivity fluctuations, and $\tau = t - t'$.

The corresponding variances are:

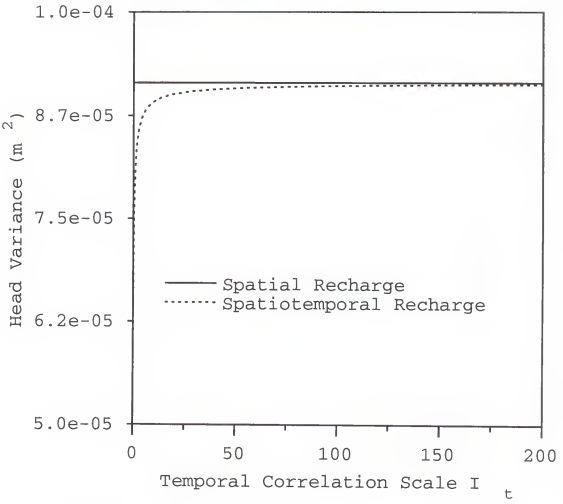

Figure 3.3: The head variance σ_H^2 vs the temporal correlation scale; $\bar{R}$=0.

$$P_{v_1v_1}(\mathbf{x},\mathbf{x},0) = \frac{e^{2\bar{Y}}}{b^2n^2}\left[\frac{3\sigma_Y^2(\bar{R}e^{-\bar{Y}}x_1+J_0)^2}{8}+\frac{\bar{R}^2e^{-2\bar{Y}}\sigma_Y^2}{8\alpha_Y^2}\right]+A$$

$$P_{v_2v_2}(\mathbf{x},\mathbf{x},0) = \frac{e^{2\bar{Y}}}{b^2n^2}\left[\frac{\sigma_Y^2(\bar{R}e^{-\bar{Y}}x_1+J_0)^2}{8}+\frac{\bar{R}^2e^{-2\bar{Y}}\sigma_Y^2}{8\alpha_Y^2}\right]+A$$

$$A = \frac{\sigma_R^2}{(bn)^2}\left[\frac{\alpha_R^6-6\alpha^4S_y'+3\alpha_R^2S_y'^2+2S_y'^3+6\alpha_R^2S_y'^2\ln(\frac{\alpha_R^2}{S_y'})}{4(\alpha_R^2-S_y')^4}\right] \quad (3.24)$$

$$P_{v_1v_2}(\mathbf{x},\mathbf{x},0) = 0$$

in which the terms driven by the transmissivity variance are the same as those proportional to σ_Y^2 in the velocity variance expressions in Chapter 2.

For zero spatial separation distance the velocity covariance become:

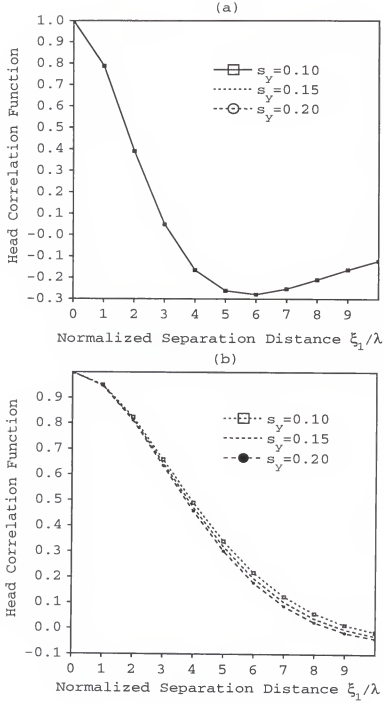

Figure 3.4: The head correlation function $P_{HH}(\xi_1, 0, \tau)/\sigma_H^2$ vs normalized time lag subject to different aquifer storativities; (a), σ_Y^2=0.29; (b), σ_Y^2=0.

$$
\begin{aligned}
P_{v_1v_1}(\mathbf{x},\mathbf{x},\tau) =& \frac{e^{2\hat{Y}}}{b^2n^2}\left[\frac{3\sigma_Y^2(\bar{R}e^{-\hat{Y}}x_1+J_0)^2}{8}+\frac{\bar{R}^2e^{-2\hat{Y}}\sigma_Y^2}{8\alpha_Y^2}\right]+f_1(\tau)\\
P_{v_2v_2}(\mathbf{x},\mathbf{x},\tau) =& \frac{e^{2\hat{Y}}}{b^2n^2}\left[\frac{\sigma_Y^2(\bar{R}e^{-\hat{Y}}x_1+J_0)^2}{8}+\frac{\bar{R}^2e^{-2\hat{Y}}\sigma_Y^2}{8\alpha_Y^2}\right]+f_1(\tau)\\
P_{v_1v_2}(\mathbf{x},\mathbf{x},\tau) =& 0\\
f_1(\tau) =& \frac{3\sigma_R^2\alpha_R^2}{2(bn\bar{S_y'})^2}\int_0^\infty \frac{k^2(ke^{-|\tau'|}-e^{-k|\tau'|})}{(k+\frac{\alpha_R^2}{S_y'})^4(k^2-1)}dk
\end{aligned}
\tag{3.25}
$$

For zero temporal separation distance the velocity covariance become:

$$
\begin{aligned}
P_{v_1v_1}(\mathbf{x},\mathbf{x}',0) =& P_{v_1v_1}^{(1)}\\
&-\frac{6\sigma_R^2\alpha_R^2}{(bn)^2}\left[\frac{-\xi^2K_2(\alpha_R\xi)+\alpha_R\xi_1^2\xi K_1(\alpha_R\xi)}{48(\alpha_R^2-S_y')}\right.\\
&\quad+\frac{S_y'}{(\alpha_R^2-S_y')^2}\frac{[-\xi K_1(\alpha_R\xi)+\alpha_R\xi_1^2K_0(\alpha_R\xi)]}{8\alpha_R}\\
&\quad+\frac{S_y'}{2(\alpha_R^2-S_y')^3}\left[-K_0(\alpha_R\xi)+\frac{\alpha_R\xi_1^2K_1(\alpha_R\xi)}{\xi}\right]\\
&\quad+\frac{S_y'}{(\alpha_R^2-S_y')^4}[\frac{\xi_1^2[\alpha_R^2K_0(\alpha_R\xi)-S_y'K_0(\sqrt{S_y'}\xi)]}{\xi^2}\\
&\quad\left.+\frac{(\xi_1^2-\xi_2^2)[\alpha_RK_1(\alpha_R\xi)-\sqrt{S_y'}K_1(\sqrt{S_y'}\xi)]}{\xi^3}]\right]
\end{aligned}
\tag{3.26}
$$

$$
\begin{aligned}
P_{v_2v_2}(\mathbf{x},\mathbf{x}',0) =& P_{v_2v_2}^{(1)}\\
&-\frac{6\sigma_R^2\alpha_R^2}{(bn)^2}\left[\frac{-\xi^2K_2(\alpha_R\xi)+\alpha_R\xi_2^2\xi K_1(\alpha_R\xi)}{48(\alpha_R^2-S_y')}\right.\\
&\quad+\frac{S_y'}{(\alpha_R^2-S_y')^2}\frac{[-\xi K_1(\alpha_R\xi)+\alpha_R\xi_2^2K_0(\alpha_R\xi)]}{8\alpha_R}\\
&\quad+\frac{S_y'}{2(\alpha_R^2-S_y')^3}\left[-K_0(\alpha_R\xi)+\frac{\alpha_R\xi_2^2K_1(\alpha_R\xi)}{\xi}\right]\\
&\quad+\frac{S_y'}{(\alpha_R^2-S_y')^4}[\frac{\xi_2^2[\alpha_R^2K_0(\alpha_R\xi)-S_y'K_0(\sqrt{S_y'}\xi)]}{\xi^2}\\
&\quad\left.+\frac{(\xi_2^2-\xi_1^2)[\alpha_RK_1(\alpha_R\xi)-\sqrt{S_y'}K_1(\sqrt{S_y'}\xi)]}{\xi^3}]\right]
\end{aligned}
\tag{3.27}
$$

$$
\begin{aligned}
P_{v_2v_1}(\mathbf{x},\mathbf{x}',0) = & P^{(1)}_{v_1v_2} \\
& - \frac{6\sigma_R^2\alpha_R^2}{(bn)^2}\Bigg[\frac{\alpha_R\xi_1\xi_2\xi K_1(\alpha_R\xi)}{48(\alpha_R^2 - S'_y)} + \frac{S'_y}{(\alpha_R^2 - S'_y)^2}\frac{\xi_1\xi_2 K_0(\alpha_R\xi)}{8} \\
& \quad + \frac{S'_y}{2(\alpha_R^2 - S'_y)^3}\frac{\alpha_R\xi_1\xi_2 K_1(\alpha_R\xi)}{\xi} \\
& \quad + \frac{S'_y}{(\alpha_R^2 - S'_y)^4}\Big[\frac{\xi_1\xi_2[\alpha_R^2 K_0(\alpha_R\xi) - S'_y K_0(\sqrt{S'_y}\xi)]}{\xi^2} \\
& \quad + \frac{2\xi_1\xi_2[\alpha_R K_1(\alpha_R\xi) - \sqrt{S'_y}K_1(\sqrt{S'_y}\xi)]}{\xi^3}\Big]\Bigg]
\end{aligned}
\tag{3.28}
$$

Figures 3.5 and 3.6 (The parameter values used in figures 3.5 to 3.8 are listed in Table 3.1) show the velocity covariance versus normalized spatial and temporal separation lag respectively and suggest that spatiotemporal velocity covariance is bounded above by the temporally uniform (i.e., steady-state) spatially random velocity covariance, and bounded below by the spatially uniform but temporally random velocity covariance (which is equivalent to the deterministic recharge case). These figures suggest that increasing the temporal recharge correlation scale increases the velocity covariance function. As the temporal correlation scale approaches infinity, the velocity correlation function resulting from spatiotemporal recharge approaches that resulting from spatially variable steady state recharge.

When the temporal correlation scale of the random recharge field approaches infinity, the spatiotemporal random recharge spectrum becomes:

$$
S_{RR}(\mathbf{k},\omega) = \sigma_R^2\frac{3\alpha_R^2 k^4\delta(\omega)}{\pi(k^2+\alpha_R^2)^4} \tag{3.29}
$$

where $\delta(\omega)$ represents the spectrum of a time-invariant random field (i.e., a random field with infinite temporal correlation length, or a random constant) [Rehfeldt and Gelhar, 1992]. According to the superposition principle [Berg and McGregor, 1966] the velocity covariance expressions which result from this recharge spectrum (3.29) and the transmissivity spectrum will be:

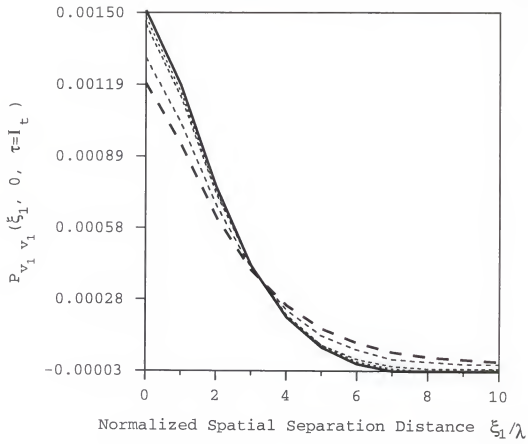

Figure 3.5: The velocity covariance vs normalized spatial separation distance subject to different temporal correlation scales; $I_t = \infty$ in Temporally uniform, spatially random R.

$$
\begin{aligned}
P_{v_i v_j}(\xi,\tau) &= P^{(1)}_{v_i v_j}(\xi) + \mathcal{F}^{-1}\left[\frac{k_i k_j S_{RR}}{(bn)^2(k^4 + S_y^2 e^{-2\tilde{Y}}\omega^2)}\right] \\
&= P^{(1)}_{v_i v_j}(\xi) + \mathcal{F}^{-1}\left[\frac{k_i k_j \sigma_R^2 3\alpha_R^2 k^4 \delta(\omega)}{(bn)^2(k^4 + S_y^2 e^{-2\tilde{Y}}\omega^2)\pi(k^2+\alpha_R^2)^4}\right] \\
&= P^{(1)}_{v_i v_j}(\xi) + \mathcal{F}^{-1}\left[\frac{3\sigma_R^2\alpha_R^2 k_i k_j}{(bn)^2\pi(k^2+\alpha_R^2)^4}\right] = P^{(1)}_{v_i v_j}(\xi) + P^{(2)}_{v_i v_j}(\xi)
\end{aligned}
\tag{3.30}
$$

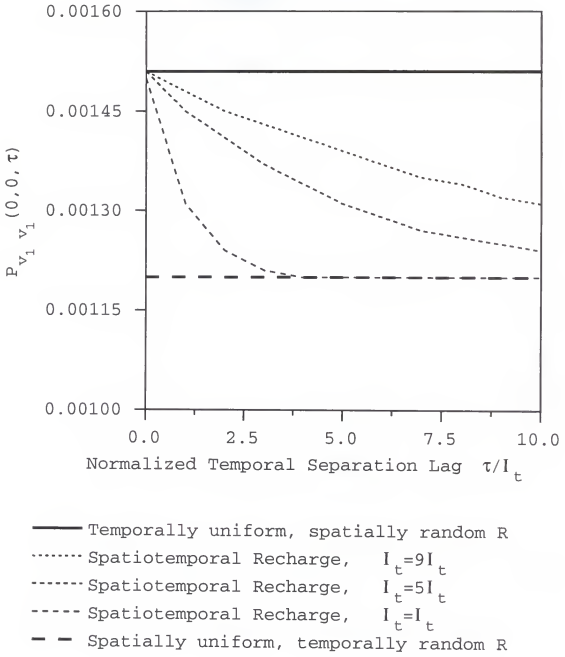

Figure 3.6: The velocity covariance vs normalized temporal separation lag subject to different temporal correlation scales; $I_t = \infty$ in Temporally uniform, spatially random R.

which are identical to equations (2.23) to (2.26) for the steady-state recharge case.

Similarly, as the spatial correlation scale of the random recharge field approaches infinity, the spatiotemporal random recharge has the following spectrum:

$$S_{RR}(\mathbf{k},\omega) = \sigma_R^2 \frac{I_t \delta(\mathbf{k})}{\pi(1 + I_t^2\omega^2)} \tag{3.31}$$

Again, according to the superposition principle for solutions of linear equations [Berg and McGregor, 1966], the velocity covariance resulting from a temporally random but spatially uniform recharge field will be:

$$\begin{aligned} P_{v_i v_j}(\xi,\tau) &= P^{(1)}_{v_i v_j}(\xi) + \mathcal{F}^{-1}\left[\frac{k_i k_j S_{RR}}{(bn)^2(k^4 + S_y^2 e^{-2\hat{Y}}\omega^2)}\right] \\ &= P^{(1)}_{v_i v_j}(\xi) + \mathcal{F}^{-1}\left[\frac{k_i k_j \sigma_R^2 I_t \delta(\mathbf{k})}{(bn)^2(k^4 + S_y^2 e^{-2\hat{Y}}\omega^2)\pi(1 + I_t^2\omega^2)}\right] \\ &= P^{(1)}_{v_i v_j}(\xi) \end{aligned} \tag{3.32}$$

in which $P^{(1)}_{v_i v_j}$ represents the part of velocity covariance contributed from the spatially random log-transmissivity field, and $\mathcal{F}^{-1}$ is the inverse Fourier transform operator. Thus as the spatial correlation scale of recharge approaches infinity the velocity covariance approaches that of the deterministic recharge case. This result can be explained by the fact that temporally variable and spatially uniform recharge does not affect the head perturbation gradient, which is the driving force for the velocity perturbation. Therefore, spatially uniform, temporally variable recharge does not increase the uncertainty of the random velocity field. The velocity covariance expressions for the spatially uniform, temporally random recharge case are thus identical to those derived for the deterministic recharge and spatially variable log-transmissivity field, i.e., the equations derived by Graham and McLaughlin (1989a) for the random zero-mean recharge case, or the equations derived by Li and Graham (1998) or Rubin and Bellin (1994) for the deterministic non-zero recharge.

Equation (3.24) and figure 3.7 show that as the temporal recharge correlation scale increases the spatiotemporal velocity variance increases. As the temporal

recharge correlation scale approaches infinity the spatiotemporal velocity variance approaches the spatially variable steady state velocity variance.

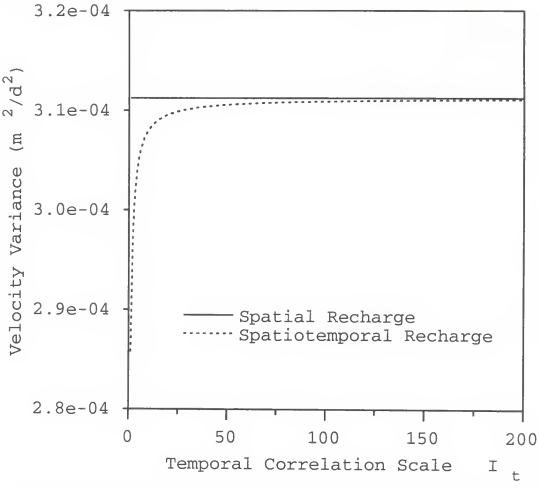

Figure 3.7: The velocity variance $\sigma^2_{v_1}$ vs the temporal correlation scale; $\bar{R}$=0.

Figure 3.8 illustrates the effect of the sensitivity of the transient velocity covariance to aquifer storativity. This figure reveals that changing aquifer storativity does not significantly impact the velocity covariance in saturated porous media. Therefore, the effect of aquifer storativity on solute transport moments will also be negligible.

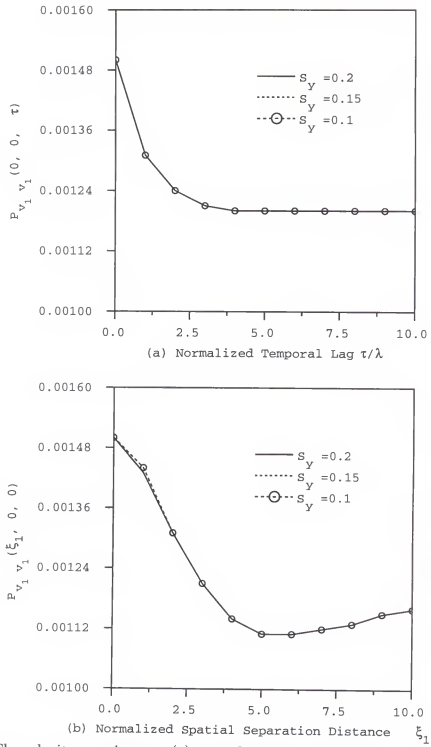

Figure 3.8: The velocity covariance vs (a) normalized temporal lag and (b) normalized spatial separation distance subject to different aquifer storativities; $\bar{R}$=0.

3.4 Moment Equations for Solute Transport

3.4.1 Governing Equations

The governing equation for the transport of a conservative solute in a two-dimensional transient flow field is the same as equation (2.11):

$$\begin{aligned} \frac{\partial c}{\partial t} + \frac{\partial (v_i\, c)}{\partial x_i} - \frac{\partial}{\partial x_i}\left[D_{ij} \frac{\partial c}{\partial x_j} \right] = 0 \quad & \mathbf{x} \in D \\ c = c_b \quad & \mathbf{x} \in \partial D \\ c = \phi(\mathbf{x}) \quad & \mathbf{x} \in D \quad t = t_0 \end{aligned} \tag{3.33}$$

in which it should be noted that the velocity field v_i is a spatiotemporally random field rather than spatially random field in the previous work [Li and Graham, 1998], $\phi(\mathbf{x})$ is the initial condition, which can be a random field, but is assumed to be known perfectly in this chapter. The concentration c is assumed to be a non-stationary random function of the location $\mathbf{x}$ (with coordinates x_i) and time t, repeated indices are assumed to be summed from 1 to 2; c_b are boundary conditions, which are assumed to be known perfectly.

The dispersion tensor D_{ij} is assumed to be a deterministic constant which accounts for pore-scale dispersion effects [Bear, 1979]:

$$D_{ij} = \alpha_T\, \bar{v}\, \delta_{ij} + (\alpha_L - \alpha_T) \frac{\bar{v}_i\, \bar{v}_j}{\bar{v}} \tag{3.34}$$

where α_L and α_T are the longitudinal and transverse local dispersivities, $\bar{v}$ is the magnitude of the mean velocity vector and δ_{ij} is one if $i = j$ and zero otherwise. Molecular diffusion is neglected.

3.4.2 Concentration Moment Equations Under Transient Velocity Field

For simplicity in the following we will assume that the mean recharge is zero and thus there is uniform mean flow. This is justified because the primary purpose of

this section is to investigate the impact of transient recharge on solute transport in heterogeneous media. Li and Graham (1998) demonstrated that under the assumption of no correlation between the log-transimissivity and recharge fields, the flow field covariance and cross-covariance functions are simply linear additions of components due to the random recharge and the random transmissivity fields. A non-zero mean recharge produces a mean velocity gradient along the mean flow direction. The magnitude of velocity gradient affects only the part of velocity covariance proportional to the variance of the log-transmissivity field, and primarily affects mean plume spreading in the longitudinal direction. This work will focus on the effect of uncertainty in the spatiotemporal distribution of recharge on the ensemble plume moments. Since uncertainty in the spatiotemporal distribution of recharge is independent of the magnitude of mean recharge and only affects the portion of the velocity covariance proportional to the recharge variance, the mean recharge will be assumed to equal zero for convenience. The effects of deterministic non-uniform mean flow on the concentration field moments were studied extensively for the steady state recharge case in Chapter 2 and Rubin et al. (1994). These results extend directly to the transient recharge case. Rubin and Bellin (1994) proposed an approximate method to evaluate particle displacement moments for non-uniform flow from those of uniform flow using a time transformation. This methodology will be investigated here to estimate concentration field moments for non-uniform flows from those of uniform flows.

Using the same first-order perturbation method used by Graham and McLaughlin (1989a) and Li and Graham (1998) the following set of coupled partial differential equations were derived which approximately describe the propagation of the concentration perturbation, the mean concentration, the velocity-concentration cross covariance, and the concentration covariance through a transient random velocity field with known mean velocity $\bar{v}_i$ and velocity covariances $P_{v_i v_j}(\mathbf{x}', \mathbf{x}, t', t)$:

$$\frac{\partial \delta c}{\partial t} + \bar{v}_1 \frac{\partial \delta c}{\partial x_1} - D_i \frac{\partial^2 \delta c}{\partial x_i{}^2} + \frac{\partial [\delta c \delta v_i - J_{D_i}]}{\partial x_i} + \frac{\partial \delta v_i \bar{c}}{\partial x_i} = 0 \quad \mathbf{x} \in D$$
$$\delta c(\mathbf{x}, t_0) = 0 \quad \mathbf{x} \in D \tag{3.35}$$
$$\delta c(\mathbf{x}, t) = 0 \quad \mathbf{x} \in \partial D$$

$$\frac{\partial \bar{c}}{\partial t} + \frac{\partial \bar{v}_i \bar{c}}{\partial x_i} - \frac{\partial}{\partial x_i}\left[D_{ij} \frac{\partial \bar{c}}{\partial x_j}\right] + \frac{\partial J_{D_i}}{\partial x_i} = 0 \quad \mathbf{x} \in D$$
$$\bar{c} = c_b \quad \mathbf{x} \in \partial D \tag{3.36}$$
$$\bar{c} = \bar{\phi}(\mathbf{x}) \quad \mathbf{x} \in D \quad t = t_0$$
$$J_{D_i} = P_{v_i c}(\mathbf{x}, \mathbf{x}, t)$$

$$\frac{\partial P_{v_i c}(\mathbf{x}', \mathbf{x}, t', t)}{\partial t} + \frac{\partial \bar{v}_j P_{v_i c}(\mathbf{x}', \mathbf{x}, t', t)}{\partial x_j} - \frac{\partial}{\partial x_j}\left[D_{jk} \frac{\partial P_{v_i c}(\mathbf{x}', \mathbf{x}, t', t)}{\partial x_k}\right]$$
$$+ \frac{\partial P_{v_i v_j}(\mathbf{x}', \mathbf{x}, t', t) \bar{c}(\mathbf{x}, t)}{\partial x_j} \approx 0 \quad \mathbf{x}, \mathbf{x}' \in D \tag{3.37}$$
$$P_{v_i c}(\mathbf{x}', \mathbf{x}, t', t) = 0 \quad \mathbf{x} \in \partial D \quad \mathbf{x}' \in D$$
$$P_{v_i c}(\mathbf{x}', \mathbf{x}, t', t) = 0 \quad \mathbf{x}, \mathbf{x}' \in D \quad t = t_0$$

$$\frac{\partial P_{cc}(\mathbf{x}', \mathbf{x}, t', t)}{\partial t} + \frac{\partial \bar{v}_i P_{cc}(\mathbf{x}', \mathbf{x}, t', t)}{\partial x_i} - \frac{\partial}{\partial x_i}\left[D_{ij} \frac{\partial P_{cc}(\mathbf{x}', \mathbf{x}, t', t)}{\partial x_j}\right]$$
$$+ \frac{\partial P_{cv_i}(\mathbf{x}', \mathbf{x}, t', t) \bar{c}(\mathbf{x}, t)}{\partial x_i} \approx 0 \quad \mathbf{x}, \mathbf{x}' \in D \tag{3.38}$$
$$P_{cc}(\mathbf{x}', \mathbf{x}, t', t) = 0 \quad \mathbf{x} \in \partial D \quad \mathbf{x}' \in D$$
$$P_{cc}(\mathbf{x}', \mathbf{x}, t', t) = 0 \quad \mathbf{x}, \mathbf{x}' \in D \quad t = t_0$$

in which mean velocity vector $\bar{v}_i$ is constant due to the assumption of $\bar{R} = 0$.

It is possible to solve these moment equations using numerical methods such as the finite element method [Graham and McLaughlin, 1989a; Li and Graham, 1998;] or

the non-stationary spectral method [Li and McLaughlin, 1991, 1995]. However, applying these two methods into this transient case is computationally difficult since equations (3.36) to (3.38) actually involve a six-dimensional domain because the second-order moments are a function of two 2-dimensional space coordinates $\mathbf{x}$ and $\mathbf{x}'$, and two time coordinates t and t'. Solving these equation therefore requires huge computer memory to store the second order moments and takes tremendous computation time. To reduce these computational requirements simplified analytic expressions for the mean concentration, macrodispersive flux, and concentration variance are derived here. The new expressions are a function of only two space coordinates and one time coordinate and can be efficiently evaluated using a fast Fourier transform algorithm.

3.4.3 Integration Expressions

Nonhomogeneous partial differential equations such as the perturbation equation (3.35) and mean equation (3.36) with specified initial conditions can be solved using a general integration expression by the momentum method [Arfken, 1966], which is similar to the Green's function method. Using this method equations (3.35) and (3.36) can be rewritten as following integration expressions (for details see Appendix C). Here two dimensional forms are used simply for the convenience of comparing the results between this approach and the previous work [Li and Graham, 1998].

$$\begin{aligned}\delta c(\mathbf{x},t) = -\int_0^t \int_{-\infty}^{\infty}\int_{-\infty}^{\infty} & \frac{1}{4\pi\sqrt{D_1 D_2}(t-t')} \\ & \left[\frac{\partial[\delta c(\mathbf{x}',t')\delta v_i(\mathbf{x}',t') - J_{D_i}(\mathbf{x}',t')]}{\partial x_i'} + \frac{\partial \delta v_i(\mathbf{x}',t')\bar{c}(\mathbf{x}',t')}{\partial x_i'}\right] \\ & \exp\left[-\frac{(x_1 - x_1' - \bar{v}_1(t-t'))^2}{4D_1(t-t')} - \frac{(x_2-x_2')^2}{4D_2(t-t')}\right] d\mathbf{x}'dt'\end{aligned} \tag{3.39}$$

$$\bar{c}(\mathbf{x},t) = \int_{-\infty}^{\infty}\int_{-\infty}^{\infty} \frac{\bar{\phi}(x_1',x_2')}{4\pi t\sqrt{D_1D_2}} \exp\left[-\frac{(x_1-x_1'-\bar{v}_1 t)^2}{4D_1 t} - \frac{(x_2-x_2')^2}{4D_2 t}\right] d\mathbf{x}' - \int_0^t \int_{-\infty}^{\infty}\int_{-\infty}^{\infty} \frac{\partial J_{D_i}(\mathbf{x}',t')}{\partial x_i'} \frac{1}{4\pi\sqrt{D_1D_2}(t-t')} \exp\left[-\frac{(x_1-x_1'-\bar{v}_1(t-t'))^2}{4D_1(t-t')} - \frac{(x_2-x_2')^2}{4D_2(t-t')}\right] d\mathbf{x}'dt' \tag{3.40}$$

in which $\bar{\phi}(x_1', x_2')$ is the known mean initial source concentration distribution.

Multiplying equation (3.39) by perturbation $\delta v_j(\mathbf{x},t)$ at the same vector location $\mathbf{x}$ and time t (which can be moved into the integral because the integration domain is $\mathbf{x}'$ and time t') and taking the expected value, leads to the following integration expression for macrodispersive flux.

$$J_{D_j}(\mathbf{x},t) = -\int_0^t \int_{-\infty}^{\infty}\int_{-\infty}^{\infty} \frac{1}{4\pi\sqrt{D_1D_2}(t-t')} \left[\frac{\partial \overline{\delta v_j(\mathbf{x},t)\delta c(\mathbf{x}',t')}\delta v_i(\mathbf{x}',t')}{\partial x_i'} + \frac{\partial P_{v_jv_i}(\mathbf{x},t,\mathbf{x}',t')\bar{c}(\mathbf{x}',t')}{\partial x_i'}\right] \exp\left[-\frac{(x_1-x_1'-\bar{v}_1(t-t'))^2}{4D_1(t-t')} - \frac{(x_2-x_2')^2}{4D_2(t-t')}\right] d\mathbf{x}'dt' \tag{3.41}$$

Equation (3.41) is the exact equation for the propagation of macrodispersive flux through a spatially and temporally random velocity field with constant mean velocity $\bar{v}_i$ and velocity covariances $P_{v_jv_i}(\mathbf{x},\mathbf{x}',t,t')$. The third-order forcing term $\overline{\delta v_j(\mathbf{x},t)\delta c(\mathbf{x}',t')\delta v_i(\mathbf{x}',t')}$ is often neglected for mildly heterogeneous velocity field [Deng et al., 1993; Kapoor and Gelhar, 1994a] using the plausible argument that it is higher order in velocity perturbations compared to the macrodispersive flux term in equation (3.41) and therefore will be small for small input log-transmissivity variance.

Since the random velocity field is a known stationary field, the velocity covariance matrix $P_{v_jv_i}(\mathbf{x}',\mathbf{x},t',t)$=$P_{v_jv_i}(x_1'-x_1, x_2'-x_2, t'-t)$. Thus after dropping $\overline{\delta v_j(\mathbf{x},t)\delta c(\mathbf{x}',t')\delta v_i(\mathbf{x}',t')}$ equation (3.41) can be approximated by:

$$J_{D_j(\mathbf{x},t)} \approx -\int_0^t \int_{-\infty}^{\infty}\int_{\infty}^{\infty} \frac{1}{4\pi\sqrt{D_1 D_2}(t-t')}$$
$$\left[\left[\frac{\partial P_{v_j v_1}(\mathbf{x}-\mathbf{x}',t-t')}{\partial x_1'} + \frac{\partial P_{v_j v_2}(\mathbf{x}-\mathbf{x}',t-t')}{\partial x_2'}\right]\bar{c}(\mathbf{x}',t')\right.$$
$$\left. + P_{v_j v_1}(\mathbf{x}-\mathbf{x}',t-t')\frac{\partial \bar{c}(\mathbf{x}',t')}{\partial x_1'} + P_{v_j v_2}(\mathbf{x}-\mathbf{x}',t-t')\frac{\partial \bar{c}(\mathbf{x}',t')}{\partial x_2'}\right] \quad (3.42)$$
$$\exp\left[-\frac{(x_1-x_1'-\bar{v}_1(t-t'))^2}{4D_1(t-t')} - \frac{(x_2-x_2')^2}{4D_2(t-t')}\right] d\mathbf{x}'dt'$$

in which it should be noted that $\frac{\partial P_{v_j v_i}(\mathbf{x}-\mathbf{x}',t-t')}{\partial x_i'} \neq 0$ because the recharge perturbation does not equal zero. Ensemble mean concentration equation (3.40) and macrodispersive flux equation (3.42) are coupled equations, which can be decoupled in the Laplace-Fourier transform domain and evaluated by fast Fourier transform technique following the work of Deng et al. (1993).

Multiplying equation (3.35) by $\delta c(\mathbf{x},t)$ at the same vector location $\mathbf{x}$ and time t and taking the expected value yields concentration variance equation [Kapoor and Gelhar, 1994a]:

$$\frac{\partial \sigma_c^2(\mathbf{x},t)}{\partial t} + \bar{v}_1\frac{\partial \sigma_c^2(\mathbf{x},t)}{\partial x_1} - D_i\frac{\partial^2 \sigma_c^2(\mathbf{x},t)}{\partial {x_i}^2} + 2D_i\overline{\frac{\partial \delta c(\mathbf{x},t)}{\partial x_i}\frac{\partial \delta c(\mathbf{x},t)}{\partial x_i}} + 2\delta c\overline{\frac{\partial \delta c \delta v_i}{\partial x_i}}$$
$$= -2J_{D_i}(\mathbf{x},t)\frac{\partial \bar{c}(\mathbf{x},t)}{\partial x_i} - 2\bar{c}(\mathbf{x},t)\overline{\delta c(\mathbf{x},t)\frac{\partial \delta v_i(\mathbf{x},t)}{\partial x_i}} \quad \mathbf{x}\in D$$
$$\sigma_c^2(\mathbf{x},t_0) = 0 \quad \mathbf{x}\in D \quad (3.43)$$
$$\sigma_c^2(\mathbf{x},t) = 0 \quad \mathbf{x}\in \partial D$$

in which the overbar represents the expectation operator. Similarly, the variance of concentration can be rewritten using a general integration expression by the momentum method [Arfken, 1966] as follows:

$$\sigma_c^2(\mathbf{x},t) = -\int_0^t \int_{-\infty}^{\infty}\int_{-\infty}^{\infty} \frac{1}{2\pi\sqrt{D_1 D_2}(t-t')}$$
$$\left[D_i \overline{\frac{\partial\delta c(\mathbf{x}',t')}{\partial x_i'}\frac{\partial\delta c(\mathbf{x}',t')}{\partial x_i'}} + J_{D_i}(\mathbf{x}',t')\frac{\partial\bar{c}(\mathbf{x}',t')}{\partial x_i'} \right.$$
$$\left. + \bar{c}(\mathbf{x}',t')\overline{\delta c(\mathbf{x}',t')\frac{\partial\delta v_i(\mathbf{x}',t')}{\partial x_i'}} + \overline{\delta c(\mathbf{x}',t')\frac{\partial\delta c(\mathbf{x}',t')\delta v_i(\mathbf{x}',t')}{\partial x_i'}} \right] \quad (3.44)$$
$$\exp\left[-\frac{(x_1 - x_1' - \bar{v}_1(t-t'))^2}{4D_1(t-t')} - \frac{(x_2 - x_2')^2}{4D_2(t-t')} \right] d\mathbf{x}'dt'$$

This equation describes the propagation of concentration variance exactly. Again, note that the term $\overline{\delta c(\mathbf{x}',t')\frac{\partial\delta v_i(\mathbf{x}',t')}{\partial x_i'}}$ is not zero because the recharge perturbation is not zero. This term can be evaluated in the same manner as $J_{D_i}(\mathbf{x},t)$ using the following expression:

$$\overline{\frac{\partial\delta v_i(\mathbf{x},t)}{\partial x_i}\delta c(\mathbf{x},t)} = -\int_0^t \int_{-\infty}^{\infty}\int_{-\infty}^{\infty} \frac{1}{4\pi\sqrt{D_1 D_2}(t-t')}$$
$$\left[\left[\frac{\partial P_{v_1v_1}(\mathbf{x}-\mathbf{x}',t-t')}{\partial x_1} + \frac{\partial P_{v_2v_1}(\mathbf{x}-\mathbf{x}',t-t')}{\partial x_2} \right] \frac{\partial\bar{c}(\mathbf{x}',t')}{\partial x_1'} \right.$$
$$+ \left[\frac{\partial P_{v_1v_2}(\mathbf{x}-\mathbf{x}',t-t')}{\partial x_1} + \frac{\partial P_{v_2v_2}(\mathbf{x}-\mathbf{x}',t-t')}{\partial x_2} \right] \frac{\partial\bar{c}(\mathbf{x}',t')}{\partial x_2'}$$
$$+ \left[\frac{\partial^2 P_{v_1v_1}(\mathbf{x}-\mathbf{x}',t-t')}{\partial x_1\partial x_1'} + \frac{\partial^2 P_{v_2v_1}(\mathbf{x}-\mathbf{x}',t-t')}{\partial x_2\partial x_1'} \right. \quad (3.45)$$
$$\left. \left. + \frac{\partial^2 P_{v_1v_2}(\mathbf{x}-\mathbf{x}',t-t')}{\partial x_1\partial x_2'} + \frac{\partial^2 P_{v_2v_2}(\mathbf{x}-\mathbf{x}',t-t')}{\partial x_2\partial x_2'} \right] \bar{c}(\mathbf{x}',t') \right]$$
$$\exp\left[-\frac{(x_1 - x_1' - \bar{v}_1(t-t'))^2}{4D_1(t-t')} - \frac{(x_2 - x_2')^2}{4D_2(t-t')} \right] d\mathbf{x}'dt'$$

Kapoor and Gelhar (1994a) assumed that the mean concentration gradient $\frac{\partial\bar{c}(\mathbf{x},t)}{\partial x_i}$ is a constant in space and time, and approximated the triple-product transport term $\overline{\delta c(\mathbf{x}',t')\frac{\partial\delta c(\mathbf{x}',t')\delta v_i(\mathbf{x}',t')}{\partial x_i'}}$ in equation (3.44) as:

$$\overline{c'^2 v_i'} = -vA_{ij}\frac{\partial\sigma_c^2}{\partial x_j} \quad (3.46)$$

in which A_{ij} is the constant macrodispersivity tensor. Equation (3.46) is asymptotically valid in the region of smooth concentration gradients field, at large times,

where the steady-state concentration field is established. Its early time application to the non-stationary concentration field however could overestimate the spreading of concentration variance plume. Therefore, this triple-product term is dropped in this work as it has been in previous work [Graham and McLaughlin, 1989a; Li and McLaughlin, 1995; Li and Graham, 1998].

The term $D_i \overline{\frac{\partial \delta c(\mathbf{x}',t')}{\partial x_i'} \frac{\partial \delta c(\mathbf{x}',t')}{\partial x_i'}}$ in equation (3.44) is referred to as the variance dissipation term by Kapoor and Gelhar (1994a). Assuming that the local dispersivity is much smaller than the lnK microscale, Kapoor and Gelhar [1994a, 1994b] suggested that the variance dissipation term is proportional to the concentration variance by a decay coefficient, or concentration microscale, which can be approximated by the lnK microscale. However, their assumption requires a lnK spectrum which yields a finite lnK microscale; a property is not met by the commonly assumed exponential spectrum, or $WhittleB$ spectrum assumed here. Therefore Kapoor and Gelhar's approximation for the variance dissipation coefficient cannot be evaluated for our example.

If the variance dissipation term can be dropped in equation (3.44) the concentration variance can be efficiently evaluated using a fast Fourier transform algorithm. To evaluate the impact of neglecting the concentration variance dissipation term on the magnitude and distribution of the concentration variance plume, an alternative direct integration method for evaluating concentration plume variance is derived by squaring the equation (3.39) and taking expected values:

$$\sigma_c^2(\mathbf{x},t) = \int_0^t \int_{-\infty}^{\infty}\int_{-\infty}^{\infty}\int_0^t \int_{-\infty}^{\infty}\int_{-\infty}^{\infty} \frac{1}{(4\pi\sqrt{D_1D_2})^2(t-t')(t-t'')}$$
$$\frac{\partial^2}{\partial x_i' \partial x_j''}\Bigg[\overline{\delta c \delta c \delta v_i \delta v_j}(\mathbf{x}',\mathbf{x}'',t',t'') - J_{D_i}(\mathbf{x}',t')J_{D_j}(\mathbf{x}'',t'')$$
$$+2\overline{\delta c \delta v_i \delta v_j}(\mathbf{x}',\mathbf{x}'',t',t'')\,\bar{c}(\mathbf{x}',t') + P_{v_iv_j}(\mathbf{x}',\mathbf{x}'',t',t'')\bar{c}(\mathbf{x}',t')\bar{c}(\mathbf{x}'',t'')\Bigg] \quad (3.47)$$
$$\exp\Bigg[-\frac{(x_1-x_1'-\bar{v}_1(t-t'))^2}{4D_1(t-t')} - \frac{(x_2-x_2')^2}{4D_2(t-t')}$$
$$-\frac{(x_1-x_1''-\bar{v}_1(t-t''))^2}{4D_1(t-t'')} - \frac{(x_2-x_2'')^2}{4D_2(t-t'')}\Bigg]d\mathbf{x}'d\mathbf{x}''dt'dt''$$

Equations (3.38), (3.44), and (3.47) are alternative formulations for solving the concentration plume variance. The computational demands are tremendously different for these three expressions. Equation (3.38) requires a six-dimensional finite difference or finite element solution, equation (3.47) involves a six-dimensional integration, however equation (3.44) involves only a three-dimensional integration. Equation (3.44) can be solved using the fast Fourier transform technique if the triple-product term and variance dissipation term are dropped. Equation (3.47) can be evaluated by direct numerical integration if the terms containing three-way and four-way products are dropped. Similarly, equation (3.38) can be solved by the finite element method if the terms containing three-way and four-way products are dropped. In the following sections the concentration variance will be evaluated to first-order using both these expressions, and the accuracy and efficiency of the methods will be compared.

3.5 Solutions in Laplace-Fourier Domain

3.5.1 Mean Concentration and Macrodispersive Flux Solutions

The ensemble mean concentration expression in the Laplace-Fourier domain can be derived either by taking the Laplace transform and then the double Fourier transform to the partial differential equation (3.36), or applying convolution theory and the Laplace-Fourier transform pairs in Appendix D to the integration equation

(3.40). Assuming the initial source distribution is a deterministic homogeneous planar source of length (2L) and width (2M) (a case which has been extensively studied in the literature [Graham and McLaughlin, 1989a, 1989b, 1991; Deng et al., 1993]) the ensemble mean concentration expression in the Laplace-Fourier domain is:

$$\begin{aligned}\tilde{c}(\mathbf{k},s) =& \frac{\sin(2\pi Lk_1)\,\sin(2\pi Mk_2)}{\pi^2 k_1 k_2}\frac{C_0}{(4\pi^2 D_i k_i^2 - 2\pi i v_1 k_1 + s)} \\ &+ \frac{2\pi i k_i \tilde{J}_{D_i}(\mathbf{k},s)}{(4\pi^2 D_i k_i^2 - 2\pi i v_1 k_1 + s)}\end{aligned} \tag{3.48}$$

where tilde represents a variable in the Laplace-Fourier domain, i.e., $\tilde{c}(\mathbf{k},s)$ is the mean concentration and $\tilde{J}_{D_i}(\mathbf{k},s)$ is the macrodispersive flux in the Laplace-Fourier domain, and C_0 is the known initial concentration.

Taking Laplace and double Fourier transforms of equation (3.42), and making use of the Laplace and Fourier convolution theory (Appendix D) yields:

$$\begin{aligned}\tilde{J}_{D_1}(\mathbf{k},s) \approx \tilde{c}(\mathbf{k},s)\Big[&2\pi i k_1 g_{11}(\mathbf{k},s) + 2\pi i k_2 g_{12}(\mathbf{k},s) \\ &- g_{10}(\mathbf{k},s)\Big] \\ \tilde{J}_{D_2}(\mathbf{k},s) \approx \tilde{c}(\mathbf{k},s)\Big[&2\pi i k_1 g_{21}(\mathbf{k},s) + 2\pi i k_2 g_{22}(\mathbf{k},s) \\ &- g_{20}(\mathbf{k},s)\Big]\end{aligned} \tag{3.49}$$

in which:

$$\begin{aligned} g_{i0}(\mathbf{k},s) =& \mathcal{L}.\mathcal{F}\left[\frac{\left[\frac{\partial P_{v_i v_1}(\mathbf{x},t)}{\partial x_1} + \frac{\partial P_{v_i v_2}(\mathbf{x},t)}{\partial x_2}\right]}{4\pi t\sqrt{D_1 D_2}}\exp\left[-\frac{(x_1-\bar{v}_1 t)^2}{4D_1 t} - \frac{x_2^2}{4D_2 t}\right]\right] \\ & i = 1,2 \\ g_{ij}(\mathbf{k},s) =& \mathcal{L}.\mathcal{F}\left[\frac{P_{v_i v_j}(\mathbf{x},t)}{4\pi t\sqrt{D_1 D_2}}\exp\left[-\frac{(x_1-\bar{v}_1 t)^2}{4D_1 t} - \frac{x_2^2}{4D_2 t}\right]\right] \\ & i = 1,2; \quad j = 1,2 \end{aligned} \tag{3.50}$$

where $\mathcal{L}.\mathcal{F}$ represents the forward Laplace and double Fourier transform operator (see Appendix D); and $g_{i0}(\mathbf{k},s)$, $g_{ij}(\mathbf{k},s)$ can be numerically integrated by fast Fourier transform algorithm.

Substituting equation (3.49) into equation (3.48) and rearranging terms leads to the following set of ensemble mean concentration and macrodispersive flux expressions:

$$\bar{c}(\mathbf{x},t) \approx \mathcal{L}.\mathcal{F}^{-1}\left[\frac{C_0 \sin(2\pi Lk_1)\sin(2\pi Mk_2)}{\pi^2 k_1 k_2\left[s - 2\pi i k_1 \bar{v}_1 + 4\pi^2 k_i^2 D_i + 4\pi^2 k_{ij}^2 g_{ij}(\mathbf{k},s) + 2\pi i k_i g_{i0}(\mathbf{k},s)\right]}\right] \quad (3.51)$$

$$\bar{J}_{D_1}(\mathbf{x},t) \approx \mathcal{L}.\mathcal{F}^{-1}\left[\frac{C_0 \sin(2\pi Lk_1)\sin(2\pi Mk_2)[2\pi i[k_1 g_{11}(\mathbf{k},s) + k_2 g_{12}(\mathbf{k},s)] - g_{10}(\mathbf{k},s)]}{\pi^2 k_1 k_2\left[s - 2\pi i k_1 \bar{v}_1 + 4\pi^2 k_i^2 D_i + 4\pi^2 k_{ij}^2 g_{ij}(\mathbf{k},s) + 2\pi i k_i g_{i0}(\mathbf{k},s)\right]}\right]$$

$$\bar{J}_{D_2}(\mathbf{x},t) \approx \mathcal{L}.\mathcal{F}^{-1}\left[\frac{C_0 \sin(2\pi Lk_1)\sin(2\pi Mk_2)[2\pi i[k_1 g_{21}(\mathbf{k},s) + k_2 g_{22}(\mathbf{k},s)] - g_{20}(\mathbf{k},s)]}{\pi^2 k_1 k_2\left[s - 2\pi i k_1 \bar{v}_1 + 4\pi^2 k_i^2 D_i + 4\pi^2 k_{ij}^2 g_{ij}(\mathbf{k},s) + 2\pi i k_i g_{i0}(\mathbf{k},s)\right]}\right] \quad (3.52)$$

in which $\mathcal{L}.\mathcal{F}^{-1}$ represents the inverse Laplace and double Fourier transform operator (see Appendix D).

Equations (3.51) and (3.52) indicate that the ensemble mean concentration and macrodispersive flux equations can be decoupled in three-dimensional Laplace-Fourier domain, which tremendously reduces the computational requirements compared to the finite element method [Graham and McLaughlin, 1989a, 1989b, 1991; Li and Graham, 1998] and the non-stationary spectral method [Li and McLaughlin, 1991, 1995]. Inspecting equation (3.51) suggests that the term $g_{ij}(\mathbf{k},s)$, which appears in the equation in the same way as the local dispersion tensor D_i, serves as the spatiotemporally variable macrodispersion tensor. The term $g_{i0}(\mathbf{k},s)$ in equation (3.51) , which appears in the same way as the mean velocity term, may impact the displacement of the center of mass when the divergence of velocity is not zero, a phenomenon discussed in Chapter 2 and by Li and Graham (1998). It should be noted that the ensemble mean concentration equation (3.51) is identical to equation (20) of Deng et al. (1993), when uncertain recharge is neglected in the expression for $P_{v_i v_j}$.

3.5.2 Concentration Variance Solution

Dropping the variance dissipation term from equation (3.44) an approximate expression for the concentration variance is:

$$\sigma_c^2(\mathbf{x},t) = -\int_0^t \int_{-\infty}^{\infty}\int_{-\infty}^{\infty} \frac{1}{2\pi\sqrt{D_1 D_2}(t-t')} \left[J_{D_i}(\mathbf{x}',t')\frac{\partial \bar{c}(\mathbf{x}',t')}{\partial x_i'} + \bar{c}(\mathbf{x}',t')\overline{\frac{\partial \delta v_i(\mathbf{x}',t')}{\partial x_i'}} \right] \exp\left[-\frac{(x_1 - x_1' - \bar{v}_1(t-t'))^2}{4D_1(t-t')} - \frac{(x_2 - x_2')^2}{4D_2(t-t')} \right] d\mathbf{x}'dt' \tag{3.53}$$

Performing the forward and then the inverse Laplace-Fourier transforms described previously for the mean and macrodispersive flux equations on equation (3.53) gives:

$$\sigma_c^2(\mathbf{x},t) \approx \mathcal{F}\,\mathcal{L}^{-1}\left[\frac{\mathcal{F}\,\mathcal{L}\left[-2\, J_{D_i}(\mathbf{x},t)\frac{\partial \bar{c}(\mathbf{x},t)}{\partial x_i} \right]}{(s - 2\pi i \bar{v}_1 k_1 + 4\pi^2 D_i k_i^2} \right] + \mathcal{F}\,\mathcal{L}^{-1}\left[\frac{\mathcal{F}\,\mathcal{L}\left[-2\bar{c}(\mathbf{x},t)\,\overline{\delta c(\mathbf{x},t)\frac{\partial \delta v_i(\mathbf{x},t)}{\partial x_i}} \right]}{(s - 2\pi i \bar{v}_1 k_1 + 4\pi^2 D_i k_i^2)} \right] \tag{3.54}$$

in which the term $\overline{\frac{\partial \delta v_i(\mathbf{x},t)}{\partial x_i}\delta c(\mathbf{x},t)}$ is evaluated in the Laplace-Fourier domain as:

$$\overline{\frac{\partial \delta v_i(\mathbf{x},t))}{\partial x_i}\delta c(\mathbf{x},t)} = \mathcal{L}.\mathcal{F}^{-1}\Big[\bar{c}(\mathbf{k},s)\Big[2\pi i k_1 g_{10}(\mathbf{k},s) + 2\pi i k_2 g_{20}(\mathbf{k},s) + g_{30}(\mathbf{k},s) \Big] \Big] \tag{3.55}$$

where $g_{10}(\mathbf{k},s)$ and $g_{20}(\mathbf{k},s)$ are the same as those in the macrodispersive flux expressions, and $g_{30}(\mathbf{k},s)$ is:

$$g_{30}(\mathbf{k},s) = \mathcal{L}.\mathcal{F}\left[\left[\frac{\partial^2 P_{v_1v_1}(\mathbf{x},t)}{\partial {x_1}^2} + \frac{\partial^2 P_{v_1v_2}(\mathbf{x},t)}{\partial x_1 \partial x_2} + \frac{\partial^2 P_{v_2v_1}(\mathbf{x},t)}{\partial x_1 \partial x_2} + \frac{\partial^2 P_{v_2v_2}(\mathbf{x},t)}{\partial {x_2}^2}\right]\right.$$
$$\left.\frac{1}{4\pi t\sqrt{D_1 D_2}} \exp\left[-\frac{(x_1 - \bar{v}_1 t)^2}{4D_1 t} - \frac{x_2^2}{4D_2 t}\right]\right] \tag{3.56}$$

3.5.3 Fast Fourier Transform Algorithm

A multi-dimensional fast Fourier transform routine from Press et al. (1992) was used for both the Laplace and Fourier transforms required in all of the above moment expressions. Generally, the time dependent part of these equations can be recovered from the solution in the Laplace-Fourier domain by a numerical inverse Laplace transform algorithm such as the one by DeHoog et al. (1982). However, numerical Laplace transforms are typically more computationally demanding than numerical fast Fourier transforms. Therefore, in this study, a fast Fourier transform algorithm was used to deal with both the temporal and spatial transformations.

3.6 Comparisons of Standard Deviation Computations

As indicated in section 3.4.3 an alternative form of the first-order concentration variance equation after dropping higher-order perturbation products from equation (3.47) is:

$$\sigma_c^2(\mathbf{x},t) = \int_0^t \int_{-\infty}^{\infty}\int_{-\infty}^{\infty} \int_0^t \int_{-\infty}^{\infty}\int_{-\infty}^{\infty} \frac{1}{(4\pi\sqrt{D_1 D_2})^2 (t-t')(t-t'')}$$
$$\frac{\partial^2}{\partial x_i' \partial x_j''}\left[P_{v_i v_j}(\mathbf{x}', \mathbf{x}'', t', t'')\bar{c}(\mathbf{x}', t')\bar{c}(\mathbf{x}'', t'')\right]$$
$$\exp\left[-\frac{(x_1 - x_1' - \bar{v}_1(t-t'))^2}{4D_1(t-t')} - \frac{(x_2 - x_2')^2}{4D_2(t-t')}\right. \tag{3.57}$$
$$\left. - \frac{(x_1 - x_1'' - \bar{v}_1(t-t''))^2}{4D_1(t-t'')} - \frac{(x_2 - x_2'')^2}{4D_2(t-t'')}\right] d\mathbf{x}' d\mathbf{x}'' dt' dt''$$

Equation (3.57) is equivalent to the moment equation for concentration covariance used by the finite element method [Graham and McLaughlin, 1989a; Li and Graham,

1998], and it is able to evaluate the concentration variance under the transient velocity state (i.e., Cases 2, 3, 4, and 5 in this study). This equation can be evaluated by direct numerical integration. The method is simple and straightforward, however, it is highly computationally demanding, because it requires a six-dimensional integration over two-spatial dimensional transient problems, i.e., c(x_1, x_2, t). The computational requirement is on the order of the finite element method used by Graham and McLaughlin (1989a) and Li and Graham (1998) and can be solved using similar square root decomposition methods. However since evaluation of equation (3.57) does not require storage of the second moments of $P_{v_i c}(\mathbf{x}, \mathbf{x}', t, t')$ which are required by the finite element method and the non-spectral method, this method takes less computer memory than the finite element and non-spectral methods. It should be noted that although equation (3.57) does not give the full covariance of concentration (it provides only the diagonal terms, i.e., variance), the covariance of concentration can be constructed by multiplying concentration perturbation equation (3.35) with a concentration perturbation at another vector location and time, taking expected values, and then evaluating by direct numerical integration.

Figure 3.9 presents the concentration standard deviations by three computational methods (i.e., direct integration, finite element [for methodology see Graham and McLaughlin (1989a) or Li and Graham (1998)], and fast fourier transform methods) at 85 days after the release of planar source in a heterogeneous aquifer without random recharge. The aquifer parameters used to generate this figure are listed in the Case 1 of Table 3.2. None of the three methods require the concentration field to be stationary. Figure 3.9 shows the general agreement of the standard deviation plume predicted by the three computational methods. The results from direct integration (equation (3.57)) and fast Fourier transform (equation (3.54)) methods are more symmetric around the center of mass than the results of the finite element solution (Li and Graham, 1998). Since the velocity field used in this case is a stationary random

field, the ensemble mean concentration and concentration standard deviation are expected to be symmetric around the center of mass. Therefore, the results by direct integration and the fast Fourier transform are apparently more accurate and realistic than the results of the finite element solution, which shows a slight asymmetry in the x_1 direction, most likely due to numerical errors. The results from the fast Fourier transform are slightly higher than the results obtained by the other two methods, especially near the center of mass. This indicates that dropping the variance dissipation term can overestimate the uncertainty of concentration around the center of mass. However, Figure 3.9 confirms that the fast Fourier transform approach can provide a fairly accurate upper bound on the concentration standard deviation away from the center of mass.

As mentioned previously, the direct integration method and the finite element method [Graham and McLaughlin, 1989a, 1989b, 1991] are very computationally demanding. It can be roughly estimated that computing the concentration variance generally needs at least $4*N^2$ order operations for N discrete nodes for a two-dimensional problem. The numerical fast Fourier transform involves only on the order of $4*N\,log_2 N$ of operations for N nodes. The CPU Time used for this simple two-dimensional steady-state velocity problem over a Sun Ultra workstation is about 18 minutes for the fast Fourier transform approximation versus about 6 hours using the finite element method and several days for the numeral integration method. Considering that more nodes are required in the computation of concentration standard deviation resulting from a temporally and spatially variable velocity field, the fast Fourier transform method was selected for use in this work. It should be noted that applying the fast Fourier transform to examine the prediction uncertainty does not give full covariance of concentration. To overcome this problem, other methods such as the direct integration method, which may require large computational time, must be used.

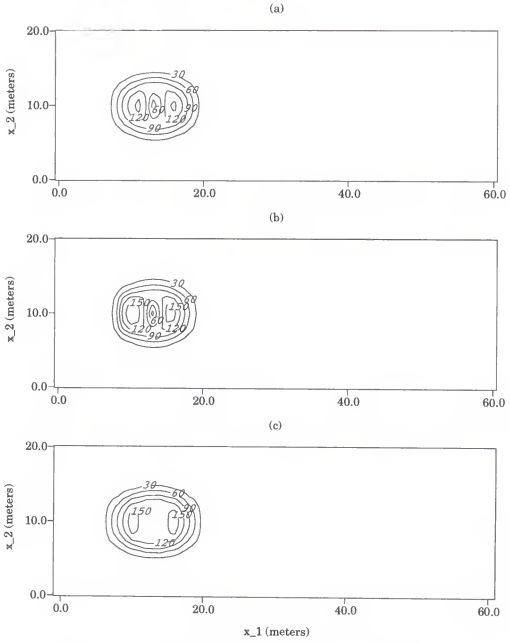

Figure 3.9: Standard deviation at 85 days after release for case 1: (a), the integration method; (b), the finite element method; (c), the fast Fourier transform method

3.7 Example Problems

3.7.1 Problem Description

For illustrative purposes, a conservative planar source is assumed to be instantaneously released into a 20 m by 60 m domain at time zero. Its location, initial

release time, and initial release concentration are all considered to be known perfectly. The initial concentration in the domain is assumed to be zero except in the source area. The boundaries are assumed to be located far enough from the solute source so that homogeneous Dirichlet boundary conditions apply on all sides of the domain. Table 3.2 lists the values for the input parameters used in this example problem. The values for the statistics of the log-transmissivity field and the hydraulic gradient are roughly based on the Borden field data [Sudicky, 1986; Graham and McLaughlin, 1991; Li and Graham, 1998]. The statistics for recharge field are somewhat arbitrarily determined, but were selected to roughly conform, where applicable, to values used in Rubin and Bellin (1994) and Li and Graham (1998).

Table 3.2: Input parameters for different simulation cases.

Parameter	Case 1	Case 2	Case 3	Case 4	Case 5
K_G (m/d)	6.18	6.18	6.18	6.18	6.18
σ_Y^2	0.29	0.29	0.29	0.29	0.0
I_t (days)	0.0	4.0	40.0	∞	∞
σ_R^2 (m^2/d^2)	0.0	0.0003	0.0003	0.0003	0.0003
Common parameters in all Cases	λ_Y =2.8 m; α_L =0.05 m; n =0.33; b=10m λ_R =2.8 m; α_T =0.05 m; J_0 =0.0056; c_0 = 337 mg/l Total simulation time =1024 days; Time step =1 day Domain size =20m by 60m Solution grid discretization $\Delta x = \Delta y = 0.5m$ No. of simulation nodes=128(N_{x_1}) by 32(N_{x_2}) by 2048(N_t)				

Case 1 is considered as the base case for comparison and contrast with the other cases because it considers the transmissivity field as the only random field (i.e., the recharge variance is zero). This case has been quite extensively studied and reported in the literature [Dagan, 1989; Graham and McLaughlin, 1989a; Zhang and Neuman, 1995a; Li and Graham, 1998]. Case 4 considers the spatially variable transmissivity and steady state spatially variable recharge as input random fields. This is the case previously studied by Li and Graham (1998) and reported in Chapter 2. As shown

in the preceding sections, Case 1 represents the special case of spatially uniform temporally random recharge, and Case 4 represents the special case of temporally uniform spatially random recharge. Cases 2 and 3 are used to investigate the effects of the recharge temporal correlation scale on the ensemble concentration moments. Case 5 investigates the evolution of a solute plume released into a steady state spatially variable recharge field with uniform transmissivity.

It should be noted that in the presence of recharge, the divergence of the velocity covariance does not equal zero as it does in the case of no recharge. The divergence of the velocity covariance in Cases 4 and 5 can be determined by differentiating the steady state random recharge velocity covariance in Cases 4 and 5 with respect to ξ_i giving the following closed-form solutions:

$$\begin{aligned}
\frac{\partial P_{v_1v_1}(\xi)}{\partial \xi_1} + \frac{\partial P_{v_2v_1}(\xi)}{\partial \xi_2} &= \frac{\sigma_R^2}{4b^2n^2\alpha_R^2}\left[-3\alpha_R^3\xi_1\xi K_1(\alpha_R\xi) + \frac{1}{2}\alpha_R^4\xi_1\xi^2 K_2(\alpha_R\xi)\right] \\
\frac{\partial P_{v_1v_2}(\xi)}{\partial \xi_1} + \frac{\partial P_{v_2v_2}(\xi)}{\partial \xi_2} &= \frac{\sigma_R^2}{4b^2n^2\alpha_R^2}\left[-3\alpha_R^3\xi_2\xi K_1(\alpha_R\xi) + \frac{1}{2}\alpha_R^4\xi_2\xi^2 K_2(\alpha_R\xi)\right]
\end{aligned} \tag{3.58}$$

Differentiating the above equations with respect to ξ_i leads to the following expressions, which are required to approximate the concentration variance using the fast Fourier transform algorithm:

$$\begin{aligned}
\frac{\partial^2 P_{v_1v_1}(\xi)}{\partial \xi_1^2} + \frac{\partial^2 P_{v_2v_1}(\xi)}{\partial \xi_1 \partial \xi_2} &= \frac{\sigma_R^2}{4b^2n^2}\left[\frac{\alpha_R^2}{2}[\xi^2 K_2(\alpha_R\xi) - \alpha_R\xi_1^2\xi K_1(\alpha_R\xi)]\right. \\
&\qquad \left. - 3\alpha_R[\xi K_1(\alpha_R\xi) - \alpha_R\xi_1^2 K_0(\alpha_R\xi)]\right] \\
\frac{\partial^2 P_{v_1v_2}(\xi)}{\partial \xi_1 \partial \xi_2} + \frac{\partial^2 P_{v_2v_2}(\xi)}{\partial \xi_2^2} &= \frac{\sigma_R^2}{4b^2n^2}\left[\frac{\alpha_R^2}{2}[\xi^2 K_2(\alpha_R\xi) - \alpha_R\xi_2^2\xi K_1(\alpha_R\xi)]\right. \\
&\qquad \left. - 3\alpha_R[\xi K_1(\alpha_R\xi) - \alpha_R\xi_2^2 K_0(\alpha_R\xi)]\right]
\end{aligned} \tag{3.59}$$

In Cases 2 and 3 the divergence of the velocity covariances must be numerically evaluated using the following expressions,

$$\begin{aligned}
\frac{\partial P_{v_1v_1}(\xi,\tau)}{\partial \xi_1} + \frac{\partial P_{v_1v_2}(\xi,\tau)}{\partial \xi_2} &= A\frac{d}{d\xi_1}\int_0^\infty \frac{k^5 J_0(k\xi)(k^2 e^{-|\tau'|} - S'_y e^{k^2|\frac{\tau'}{S'_y}|})}{(k^2+\alpha_R^2)^4(k^4 - S'^2_y)}dk \\
\frac{\partial P_{v_2v_1}(\xi,\tau)}{\partial \xi_1} + \frac{\partial P_{v_2v_2}(\xi,\tau)}{\partial \xi_2} &= A\frac{d}{d\xi_2}\int_0^\infty \frac{k^5 J_0(k\xi)(k^2 e^{-|\tau'|} - S'_y e^{k^2|\frac{\tau'}{S'_y}|})}{(k^2+\alpha_R^2)^4(k^4 - S'^2_y)}dk \\
A &= -\frac{6i\sigma_R^2\alpha_R^2}{(bn)^2} \\
\frac{dJ_0(k\xi)}{d\xi_1} &= -\frac{k\xi_1}{\xi}J_1(k\xi)
\end{aligned} \tag{3.60}$$

3.7.2 Concentration Plume Moments by Fast Fourier Transform

Figure 3.10 presents the simulation results of the mean concentration and concentration standard deviation for Cases 1 through 5 at 85 days after planar source release. The plume spreading shape and standard deviation plots for Case 1 are consistent with previous results by Graham and McLaughlin (1991), Deng et al (1993), Zhang and Neuman (1995a), and Li and Graham (1998). However they are more symmetric around the center of mass than the corresponding moments determined by the finite element method by Graham and McLaughlin (1991) and Li and Graham (1998). Since the velocity field used in this problem is a stationary random field, the ensemble mean concentration should be symmetric around the center of mass. Therefore, the results determined using fast Fourier transform technique seem more accurate than the results obtained by the finite element method. It merits attention that using the fast Fourier transform method reduces the simulation time significantly. For the simulations of the base case, it takes about 18 minutes for fast Fourier transform with 4193304 nodes versus about 6 hours for the finite element method with 96075 nodes.

Introduction of a spatiotemporally random recharge into Case 1 increases the velocity variance and covariance as shown in the preceding sections. However, the resulting effects on the concentration moments depend on the magnitude of the recharge

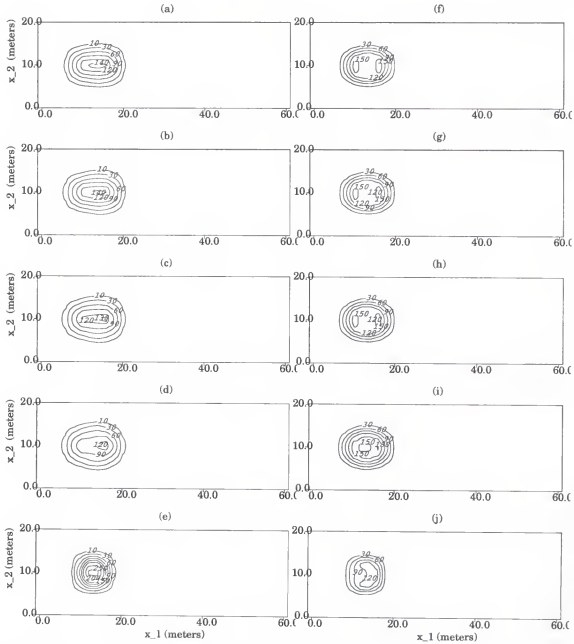

Figure 3.10: (a), (b), (c), (d), and (e) represent Mean Concentration of Cases 1, 2, 3, 4, and 5 respectively at 85 days after release; (f), (g), (h), (i), and (j) represent Concentration Standard Deviation of Cases 1, 2, 3, 4, and 5 respectively at 85 days after release

temporal correlation scale. Case 2 considers 4 days as the temporal correlation scale for the spatiotemporally random recharge. The resulting concentration and standard deviation plots shown in Figure 3.10.(b) and Figure 3.10.(g) do not show a

significant difference compared to Case 1, although the second normalized moment in the x_2 direction slightly increases compared to the base case (see Figure 3.13). As the temporal correlation scale increases to 40 days in case 3, the increased velocity variance and covariance enhance the spreading of concentration plume, particularly in the lateral direction. The concentration standard deviation is also slightly more spread compared to the base case; however the magnitude of the peak concentration standard deviation is about the same. As expected, when the recharge temporal correlation scale approaches infinity in Case 4, the velocity variance and covariance approach those resulting from the spatially variable steady state recharge field. In this case velocity variance and covariance reach their maximum values, and thus result in the maximum spreading of the concentration plume and the maximum values of concentration standard deviation.

Case 5 presents the mean concentration plume and concentration standard deviation for the random velocity field resulting from a deterministic transimissivity and a steady-state spatially random recharge field. In this case both the ensemble mean concentration plume and concentration variance spread more isotopically. This can be explained by the fact that the uncertainty of the velocity field resulting from only uncertain recharge is independent of mean head gradient. This is in contrast to the uncertain velocity field resulting from uncertain log-transmissivity which is dependent on the mean head gradient and thus leads to a strong anisotropic velocity covariances. Comparing the standard deviation plumes between Case 1 and Case 5 indicates that the log-transmissivity random field contributes more uncertainty for solute transport than the random recharge field does for this case. A more rigorous uncertainty contribution comparison should be made based on dimensionless parameters. However, this is difficult to implement in this study since the mean recharge is zero, which leads to an infinite coefficient of variation for random recharge. It should be noticed that the asymmetry of concentration standard deviation plume along the

x_1 direction is due to numerical errors which result from the asymmetry of the numbers of nodes used for performing numerical Fourier transforms along the x_1 direction since the plume is moving as time elapses.

Figures 3.11, 3.12 and 3.13 present the evolution of the normalized spatial moments of the ensemble mean plume for each of the cases, and confirm the effects of spatiotemporally random recharge on the mean plume behavior discussed above. Figure 3.11 presents the evolution of the normalized first moment of the ensemble mean plume. This figure shows that the evolution of the mean plume center of mass is approximately linear with a slope of $\bar{v} = \frac{T_G J}{bn}$ for all the cases. The slight deviation of the normalized first moment from the slope of $\frac{T_G J}{bn}$ after 150 days may be due to numerical errors, especially from the spatial unsymmetry of the simulated macrodispersive flux. Here we give a brief analytic analysis of the cause of these numerical errors. Rewriting the mean concentration equation (3.36) as:

$$\frac{\partial \bar{c}}{\partial t} + \bar{v}_1 \frac{\partial \bar{c}}{\partial x_1} - D_i \frac{\partial^2 \bar{c}}{\partial x_i^2} + \frac{\partial J_{D_i}}{\partial x_i} = c_0 \delta(t) H(x_1 - |L_1|) H(x_2 - |L_2|) \tag{3.61}$$

The n^{th} spatial moment of the mean concentration at a given temporal time t is:

$$m_n(t) = \int_{-\infty}^{\infty} \int_{-\infty}^{\infty} \bar{c}(\mathbf{x}, t) x_1^n dx_1 dx_2 \tag{3.62}$$

Taking double integration with respect to equation (3.61) reads:

$$m_0 = 4 L_1 L_2 c_0 \tag{3.63}$$

Multiplying equation (3.61) by x_1 and performing double integration of it with respect to x_1 and x_2 yields:

$$\frac{\partial m_1}{\partial t} - \bar{v}_1 m_0 - \int_{-\infty}^{\infty}\int_{-\infty}^{\infty} J_{D_1} dx_1 dx_2 = 0 \tag{3.64}$$

Equation (3.64) can be evaluated as:

$$m_1 = \bar{v}_1 m_0 t + \int_0^t \int_{-\infty}^{\infty}\int_{-\infty}^{\infty} J_{D_1} dx_1 dx_2 dt \tag{3.65}$$

Normalizing equation (3.65) by the total mass m_0 leads to the expression for the center of mass:

$$\mu_1 = \bar{v}_1 t + \frac{1}{m_0}\int_0^t \int_{-\infty}^{\infty}\int_{-\infty}^{\infty} J_{D_1} dx_1 dx_2 dt \tag{3.66}$$

in which J_{D_1} is:

$$J_{D_1}(\mathbf{x},t) = -\int_0^t \int_{-\infty}^{\infty}\int_{-\infty}^{\infty} \left[\frac{\partial P_{v_1 v_i}(\mathbf{x},t,\mathbf{x}',t')\bar{c}(\mathbf{x}',t')}{\partial x_i'}\right] \frac{1}{4\pi\sqrt{D_1 D_2}(t-t')} \exp\left[-\frac{(x_1 - x_1' - \bar{v}_1(t-t'))^2}{4D_1(t-t')} - \frac{(x_2 - x_2')^2}{4D_2(t-t')}\right] d\mathbf{x}' dt' \tag{3.67}$$

Equation (3.67) indicates that x_1 direction macrodispersive flux should be spatially symmetric since the mean concentration, velocity covariance, and the transfer function are spatially symmetric around the center of mass. Therefore, the second term in equation (3.66) should go to zero. The normalized first spatial moment of the mean concentration should equal the slope of $\bar{v}_1$. Deviations of the slope of the first spatial moment from this theoretical value are likely due to small numerical asymmetries in $J_{D_1}(\mathbf{x},t)$.

Figures 3.12 and 3.13 show the second centralized moments in the x_1 and x_2 directions respectively for all cases, and confirm the results discussed above. These figures show that introduction of spatially and temporally recharge affects both longitudinal and lateral mean plume spreading, with the steady-state random recharge

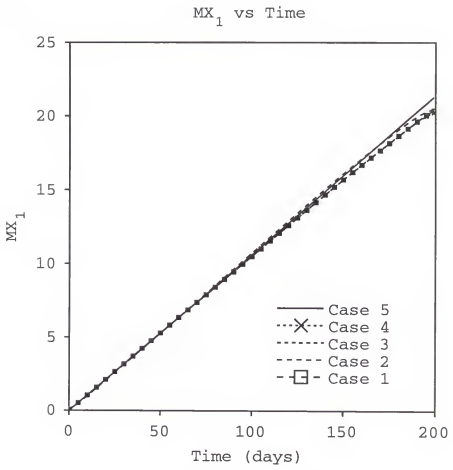

Figure 3.11: The first normalized moments at x_1 direction for each case

(Case 4) providing an upper bound and spatially uniform temporally random recharge (Case 1) providing a lower bound for both mean plume spreading and prediction uncertainty if transmissivity is a random field. Figure 3.12 indicates that the second centralized moment in Case 5 is much less than those in the other cases. This can be explained by the fact that Case 5 considers the steady-state spatially variable recharge as the only input random field and the velocity covariance resulting from random recharge is independent of the mean head gradient. Therefore the established preferential flow direction does not increase the head and velocity correlation structure in Case 5 and cause enhanced longitudinal spreading as it does in the other cases.

It should be recalled that the temporal correlation scale in Cases 4 and 5 approaches infinity while the temporal correlation scale in Cases 2 and 3 have finite values. This leads to a larger second centralized moment in the lateral direction in Case 5 than in Cases 2 and 3, shown in figure 3.13.

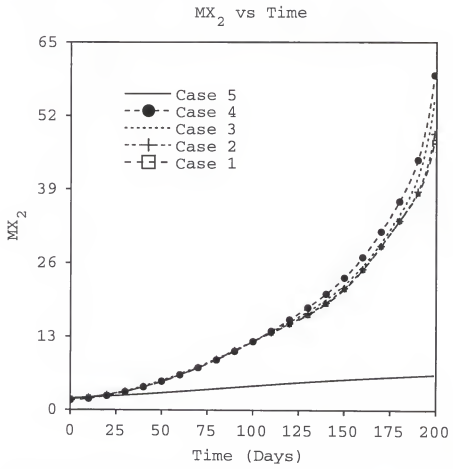

Figure 3.12: The second normalized moments at x_1 direction for each case

Comparing this study with the previous research by Li and Graham (1998) indicates that introduction of recharge (either spatially or spatiotemporally random recharge) will increase mean concentration spreading, especially in the lateral direction (shown in Figure 3.13). However, a spatiotemporally random recharge has a smaller effect on the mean concentration plume spreading than a steady state spatially random recharge does. This can be explained by considering that a steady state

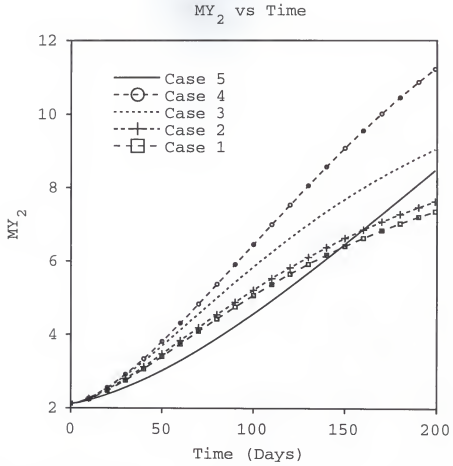

Figure 3.13: The second normalized moments at x_2 direction for each case

spatially random recharge is equivalent to an infinite temporal correlation scale, resulting in the maximum velocity variance and covariance compared to these resulting from a spatiotemporally random recharge. Thus using a spatially random but temporally uniform recharge to describe a spatiotemporally random recharge field could overestimate the ensemble spreading and prediction uncertainty.

This work shows that increasing the recharge variance while maintaining the same transmissivity variance will cause the plume to spread more isotropically. This is due to the fact that increasing the recharge variance increases the dominance of the isotropic portion of the velocity covariance resulting from recharge, which is independent of mean head gradient. It should be recalled that the solute concentration moments in this chapter are evaluated based on the assumption that the mean recharge

$\bar{R}$ is zero. According to the previous research result by Li and Graham (1998) (reported in Chapter 2), a non-zero mean recharge will produce a mean velocity gradient along the mean flow direction, which will primarily affect mean plume spreading in the longitudinal direction [Li and Graham, 1998; Rubin and Bellin, 1994]. These same effects will hold for the case of a spatiotemporally random recharge field with non-zero mean recharge.

Rubin and Bellin (1994) showed that the particle displacement variances at time t for non-uniform flow (i.e., non-zero mean recharge) can be approximated by the particle displacement variances obtained for uniform mean flow using the time transformation $\tau' = \frac{e^{\beta\tau}-1}{\beta}$, or:

$$X_{ii}(\tau) = X^u_{ii}(\frac{e^{\beta\tau}-1}{\beta}) \tag{3.68}$$

where $X_{ii}(\tau)$ are the particle displacement variances at time $\tau = \frac{t\bar{v}_1}{\lambda_Y}$; X^u_{ii} are the particle displacement variances applicable for the uniform flow case of $\beta = 0$; and β is defined as $\frac{\bar{R}\lambda_Y}{TJ_0}$. Thus Rubin and Bellin's (1994) result showed that the dominant effects of non-uniform flow on the particle displacement moments could be captured from the uniform flow moments evaluated at a later time for positive mean recharge, or an earlier time for negative mean recharge.

Using this same approximation the mean concentration and concentration variance for the non-uniform mean flow case may be approximated from the uniform mean flow case derived here using:

$$\bar{c}(\mathbf{x}, t) = \bar{c}^u(\mathbf{x}, \frac{\left[e^{\beta\tau}-1\right]}{\beta}\frac{\lambda_Y}{\bar{v}_1}) \tag{3.69}$$

$$\sigma^2_c(\mathbf{x}, t) = \sigma^{2u}_c(\mathbf{x}, \frac{\left[e^{\beta\tau}-1\right]}{\beta}\frac{\lambda_Y}{\bar{v}_1}) \tag{3.70}$$

Figure 3.14 shows the mean concentration and standard deviation plumes for Case 2 assuming a mean recharge of 0, +0.003 (which is equivalent to β=0.024), and -0.003 meter/day (β=-0.024), respectively. As demonstrated in Chapter 2 a positive mean recharge increases the mean travel distance and slightly enhances the mean concentration and standard deviation plumes spreading in the longitudinal direction. A negative mean recharge decreases the mean travel distance and slightly reduces spreading for both the mean and standard deviation plumes.

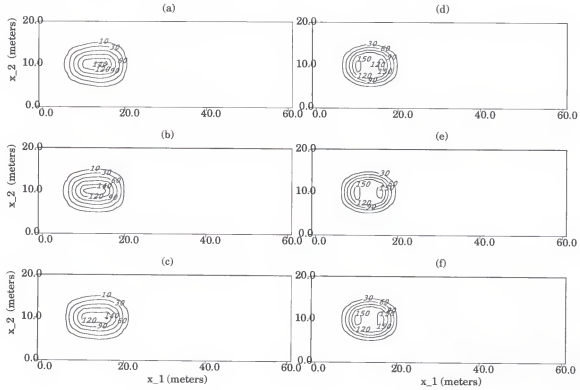

Figure 3.14: (a), (b), and (c) represent Mean Concentration of Case 2 with mean recharge $\bar{R}$ equals 0., -0.003, and 0.003, respectively; (d), (e), and (f) represent Concentration Standard Deviation of Case 2 with mean recharge $\bar{R}$ equals 0., -0.003, and 0.003 meter/day, respectively;

Rehfeldt and Gelhar (1992) examined the dispersion of a solute plume in heterogeneous aquifers subject to transient flow which was contributed from a spatially random hydraulic conductivity and a temporally random fluctuation due to uncertain boundary conditions. Dagan et al. (1996) investigated a similar problem, where the

transient flow was caused by deterministic temporally-fluctuating boundary conditions which produced fluctuations in the magnitude and direction of the mean head gradient. Zhang and Neuman (1996) developed low-order approximations for auto-covariances and cross covariances of velocity, head, and log-hydraulic conductivity under quasi-steady state flow, and then examined their effect on advective transport using a first-order Lagrangian approach. All these works indicated that unsteady flow strongly increases transverse spreading, but has insignificant effects on longitudinal direction. However, in all cases the transverse spreading was due to the changing of the mean head gradient. In this work transient flow was also found to increase transverse spreading significantly more than longitudinal spreading. However, in this work the mean head gradient is constant and the increased transverse spreading is caused by recharge fluctuations.

3.8 Summary

This work extends the previous work [Li and Graham, 1998] to a transient flow field and examines the evolution of the unconditional ensemble moments for a concentration plume resulting from an instantaneous planar source in a two-dimensional spatially random transmissivity field subject to a spatially and temporally random recharge field. Under the assumptions of transient flow in an infinite domain and no correlation between the log-transmissivity and recharge fields, a set of semi-analytical solutions were derived for velocity covariances using Fourier transform techniques.

The spatiotemporally random recharge causes randomness of velocity and concentration in both space and time. This significantly increases the computational and memory requirements for computing the ensemble mean concentration, macrodispersive fluxes, and concentration standard deviations if the finite element method [Graham, and MacLaughlin, 1989a; Li and Graham, 1998] or the non-stationary spectral method [Li and MacLaughlin, 1991, 1995] are applied. Following the work of Deng

et al. (1993), the ensemble mean concentration and macrodispersive flux equations were decoupled in the Fourier-Laplace space, then evaluated by a multi-dimensional fast Fourier transform routine, which significantly reduces the computational requirements. The first-order concentration standard deviation was computed exactly by a direct integration formulation and the finite element method, and approximated by a fast Fourier transform algorithm which requires that the variance dissipation terms generated by local dispersion be neglected.

Comparing this study with the previous research by Li and Graham (1998), we find following new conclusions:

1) Introduction of recharge (either spatially or spatiotemporally random recharge) increases the head and velocity variances and covariances, and thus enhances mean concentration spreading, especially in the lateral direction. The increased transverse spreading is due to the part of the velocity covariance contributed by the isotropic recharge covariance. This term enhances the isotropy of the velocity covariance which in turn enhances the isotropic spreading of the solute concentration plume.

2) Spatiotemporally random recharge causes less mean concentration plume spreading than steady state spatially random recharge. Therefore, using a spatially random but temporally uniform recharge to describe a spatiotemporally random recharge field could overestimate the spreading and prediction uncertainty of solute concentration. The effect of spatiotemporally random recharge is strongly impacted by the magnitude of the temporal correlation scale. As the temporal correlation scale approaches infinity, the spatiotemporally random recharge approaches the steady state spatially random recharge case. Therefore, the previous study by Li and Graham (1998) provides an upper bound on ensemble mean spreading and prediction uncertainty and is a special case of this work where the temporal correlation scale approaches infinity.

3) Another special case was examined by allowing the spatial correlation scale of the spatiotemporal recharge to approach infinity. When the spatial correlation scale of the spatiotemporal recharge approaches infinity the recharge uncertainty provides no contribution to velocity uncertainty under the assumption of no correlation between the log-transmissivity and recharge. Therefore temporally random spatially uniform recharge has no effect on the mean concentration plume spreading or prediction uncertainty and collapses to the case of deterministic recharge. This phenomenon can be explained by the fact that temporally variable but spatially uniform recharge does not change the head perturbation gradient, which is the driving force for uncertainty in the velocity field. Therefore, spatially uniform but temporally variable recharge will not impose any additional uncertainty on the random velocity field, or the resulting concentration field, and thus provides a lower bound for estimating ensemble mean spreading and prediction uncertainty.

4) Increasing the recharge variance increases the velocity uncertainty contribution from recharge, which enhances the ensemble mean concentration spreading, macrodispersive fluxes, and concentration standard deviations, and causes the concentration plume to spread more isotropically. Increasing the spatial or temporal recharge correlation scale also increases velocity uncertainty in the absence of site specific measurements of recharge.

5) Increasing the aquifer storativity reduces the head correlation function slightly, however it imposes insignificant effects on the velocity or plume concentration moments.

6) Using a fast Fourier transform algorithm to investigate the uncertainty of solute transport in heterogeneous media presents a significant computational advantage compared to the direct integration and finite element methods. However, the fast Fourier transform approximation overestimates the prediction uncertainty around the center of mass due to neglecting the variance dissipation term. Further work should

be done to evaluate the spatiotemporally variable variance dissipation term resulting from nonstationary fields. It should be noted that the fast Fourier transform technique developed here cannot be used to evaluate the full concentration covariance.

7) The solute-related moments in this work were evaluated assuming the mean recharge $\bar{R} = 0$. Incorporating the effects of $\bar{R} \neq 0$ into the solute transport analysis produces a mean velocity gradient along the mean flow direction which primarily affects mean plume spreading in the longitudinal direction [Li and Graham, 1998]. However, performing the rigorous analysis of effects of $\bar{R} \neq 0$ within the fast Fourier transform algorithm requires an analytic transfer function appropriate for the nonuniform velocity field resulting from the mean constant recharge. This may deserve some further efforts due to the computational efficiency of the fast Fourier transform approach. Rubin and Bellin (1994)'s time transformation approach, however, provides a simple, approximate relationship between concentration field moments with nonzero and zero mean recharge. The accuracy of this approximation for the transient flow case should be further investigated.

8) This work was based on the small perturbation assumption, which restricts the results to the input random fields with small variance. Further effort to evaluate higher order perturbation terms is required to relax the small input variance assumption.

CHAPTER 4
UNCERTAIN SOURCE CONDITIONS

4.1 Introduction

Results from studies of the uncertainty of solute transport predictions [Dagan, 1987; Black and Freyberg, 1987; Graham and McLaughlin, 1989a, 1989b] indicate that concentration prediction uncertainty can be very large, especially in the near source region. Field tracer investigations [Ellsworth et al., 1991a, 1991b; Freyberg, 1986; Garabedian, 1987, Garabedian et al., 1991; Killey and Moltyaner, 1988; Leblanc et al., 1991; Mackay et al., 1986] suggest that tracer concentration distribution immediately after injection is very complex and irregular due to the local aquifer heterogeneity. For example, local solute concentrations at the Borden test site one day after injection varied from background to injection levels over distances of 3-4 meters [Mackay et al., 1986; Freyberg, 1986]. Distributions of total mass in the source zone, mass release rate, and concentration in the source zone can also be spatially and temporally variable due to the presence of complex mixtures of constituents, physical heterogeneity of media properties, and complex chemical processes. The heterogeneity of contaminant sources can affect the accuracy of downstream concentration prediction through its variable loadings, uncertain location, size, shapes and other factors. However, little research has been reported in the literature concerning the effect of source uncertainties on the fate of solute transport at the field scale.

Reasons for contaminant source uncertainty in aquifers are numerous. Sources can be spatially and temporally variable in 1) physical size, shape, and location which can affect the plume configuration and arrival time to the compliance boundaries; 2) source concentration or mass loadings, which may or may not be correlated with

the local groundwater flow field; and 3) source constituents, which have different physical and chemical properties and thus impact the fate and transport of aqueous phase solutes. All these source-related uncertainties have the potential to impact the prediction uncertainty of solute transport either in homogeneous or heterogeneous media. How important the contribution from an uncertain source is compared to other uncertain fields such as transmissivity and recharge, and how source uncertainty interacts with other uncertain random fields, however, remain open questions.

Dagan et al. (1992) and Cvetkovic et al. (1992) derived approximate expressions for the expected value, variance of mass flux, and cumulative mass flux of solute moving from a buried source in the saturated zone past an arbitrary control plane. They found that for source sizes on the order of 20 hydraulic conductivity correlation scales the coefficient of variation of mass flux decreased considerably and the transport conditions were almost ergodic. However, the coupled effects of uncertainty arising from random variability in source morphology and aquifer characteristics were not explored. The contaminant source strength and distribution in these works were assumed by Dagan et al. (1992) and Cvetkovic et al. (1992) to be perfectly known.

Zhang and Neuman (1995d) examined the effects of uncertainties in the plume initial state and non-Gaussian groundwater velocities on ensemble plume spreading and concentration prediction uncertainty for instantaneous point and patch sources, assuming that the groundwater velocity and contaminant source were uncorrelated. They concluded that for the cases studied, source uncertainty increases the concentration prediction uncertainty, but has no effect on mean plume spreading.

Berglund (1997) used an analytical stochastic-advective framework to examine the coupled effects of uncertain advection and rate-limited mass transfer to the aqueous phase from residual DNAPL on ensemble mean solute flux in the saturated zone. The mass transfer coefficient and travel time were assumed to be potentially correlated random fields. Berglund's results emphasize the importance of the parameters

associated with the source zone; its length in the mean flow direction, the residual DNAPL saturation, and the mass transfer rate coefficient.

In this chapter, a continuous source is assumed to be located within a heterogeneous aquifer. The contaminant release rate in the source zone is assumed to be spatially variable and can be perfectly correlated and/or uncorrelated with the flow field. The purpose of this chapter is to:

1) investigate the relative contribution of source and groundwater velocity uncertainty to ensemble plume spreading and prediction uncertainty;

2) examine the effects of source size on ensemble concentration moments for the case in which the source size and location is assumed to be known perfectly, but the source loading is a random field; and

3) study the effect of correlation between the random velocity and source fields on ensemble plume spreading and prediction uncertainty.

4.2 Governing Equations

A subsurface contaminant source can be either a mobile or immobile phase (liquid, air, or solid) which releases contaminants into groundwater instantaneously or continuously. Examples include leaking underground storage tanks and pipelines, residual phase non aqueous phase liquids, hazardous waste sites, and surface spills or applications of potential contaminants. In this chapter we restrict our discussion to sources existing as an immobile phase (trapped NAPL; precipitated solids, etc.) in saturated porous media, which release solutes to the aqueous phase. We refer to the area in which solute is released as the "source zone", and the downstream region where solute advection, dispersion and reactions dominate as the "dissolved plume zone".

We assume that the following equation holds for solute transport resulting from an uncertain contaminant source within a two-dimensional flow field [Bear, 1979]:

$$\begin{aligned} \frac{\partial c}{\partial t} + \frac{\partial (v_i\, c)}{\partial x_i} - \frac{\partial}{\partial x_i}\left[D_{ij} \frac{\partial c}{\partial x_j} \right] - \phi = 0 \quad \mathbf{x} \in \mathrm{D} \\ c = 0 \quad \mathbf{x} \in \partial D \\ c = 0 \quad \mathbf{x} \in D \quad \mathrm{t} = \mathrm{t}_0 \end{aligned} \tag{4.1}$$

in which, the saturated water content θ_s is assumed to to spatially constant; v_i is the random pore water velocity, and ϕ ($[ML^{-3}T^{-1}]$) is the random mass release function in a source zone whose location, shape, and size are assumed to be known perfectly. The initial and boundary conditions for solute concentration (c) are set to zero for simplicity. It should be noted that the mass conservation law expressed in equation (4.1) applies throughout both the source and the plume zones. This indicates the continuity of concentration between source and transport zones, and acknowledges that the concentration in the source zone where ϕ is non-zero can be spatially and temporally variable.

As in the previous chapters, the dispersion tensor D_{ij} is assumed to be a deterministic constant which accounts for pore-scale dispersion effects [Bear, 1979]:

$$D_{ij} = \alpha_T\, \bar{v}\, \delta_{ij} + (\alpha_L - \alpha_T) \frac{\bar{v}_i\, \bar{v}_j}{\bar{v}} \tag{4.2}$$

where α_L and α_T are the longitudinal and transverse local dispersivities, $\bar{v}$ is the magnitude of the mean velocity vector and δ_{ij} is one if i=j and zero otherwise. Molecular diffusion is neglected.

If the mass release rate ϕ in equation (4.1) is treated as a random space function which occurs instantaneously as a delta function in time, the embedded source ϕ can be mathematically transformed into a spatially random initial condition representing the instantaneous injection of a contaminant source with uncertain strength. This is the case that was studied by Zhang and Neuman (1995d). In this chapter, we treat ϕ as an continuous source, which continuously releases contaminant to groundwater.

4.3 Ensemble Moment Equations

Following the procedure described in Chapters 2 and 3, the ensemble mean concentration equation in a two-dimensional transient flow field can be derived from equation (4.1):

$$\begin{aligned} &\frac{\partial \bar{c}}{\partial t} + \bar{v}_1 \frac{\partial \bar{c}}{\partial x_1} - D_i \frac{\partial^2 \bar{c}}{\partial x_i^2} + \frac{\partial J_{D_i}}{\partial x_i} - \bar{\phi} = 0 \quad \mathbf{x} \in \mathrm{D} \\ &\bar{c} = 0 \quad \mathbf{x} \in D \quad \mathrm{t} = \mathrm{t}_0 \\ &\bar{c} = 0 \quad \mathbf{x} \in \partial D \end{aligned} \tag{4.3}$$

in which J_{D_i} are the components of the macrodispersive flux, defined as $\overline{\delta c(\mathbf{x},t)\delta v_i(\mathbf{x},t)}$; $\bar{\phi}$ is the mean contaminant mass release rate; and mean velocity $\bar{v}_1$ is constant assuming that $\bar{R}$=0.

The first-order perturbation concentration equation can be written:

$$\begin{aligned} &\frac{\partial \delta c(\mathbf{x},t)}{\partial t} + \bar{v}_1 \frac{\partial \delta c(\mathbf{x},t)}{\partial x_1} - D_i \frac{\partial^2 \delta c(\mathbf{x},t)}{\partial {x_i}^2} + \frac{\partial \delta v_i(\mathbf{x},t)\bar{c}(\mathbf{x},t)}{\partial x_i} - \delta\phi \approx 0 \quad \mathbf{x} \in D \\ &\delta c = 0 \quad \mathbf{x} \in D \quad \mathrm{t} = \mathrm{t}_0 \\ &\delta c = 0 \quad \mathbf{x} \in \partial D \end{aligned} \tag{4.4}$$

Governing equations (4.3) and (4.4) for the ensemble mean concentration and first-order concentration perturbation can be solved using the momentum method described in Appendix C as follows:

$$\begin{aligned} \bar{c}(\mathbf{x},t) = \int_0^t \int_{-\infty}^{\infty} \int_{-\infty}^{\infty} &\left[\bar{\phi}(\mathbf{x}',t') - \frac{\partial J_{D_i}(\mathbf{x}',t')}{\partial x_i'} \right] \frac{1}{4\pi\sqrt{D_1 D_2}(t-t')} \\ &\exp\left[-\frac{(x_1 - x_1' - \bar{v}_1(t-t'))^2}{4D_1(t-t')} - \frac{(x_2 - x_2')^2}{4D_2(t-t')} \right] dx'dt' \end{aligned} \tag{4.5}$$

$$\begin{aligned} \delta c(\mathbf{x},t) = \int_0^t \int_{-\infty}^{\infty} \int_{-\infty}^{\infty} &\left[\delta\phi(\mathbf{x}',t') - \frac{\partial \delta v_i(\mathbf{x}',t')\bar{c}(\mathbf{x}',t')}{\partial x_i'} \right] \frac{1}{4\pi\sqrt{D_1 D_2}(t-t')} \\ &\exp\left[-\frac{(x_1 - x_1' - \bar{v}_1(t-t'))^2}{4D_1(t-t')} - \frac{(x_2 - x_2')^2}{4D_2(t-t')} \right] dx'dt' \end{aligned} \tag{4.6}$$

Assuming that the mean mass release rate $\bar{\phi}(\mathbf{x},t)$ in the source zone is a constant value in time $\bar{\phi}$ with known length $2L_1$ and width $2L_2$ or $\bar{\phi}(\mathbf{x},t) = \bar{\phi}H(L_1 - |x_1|)H(L_2 - |x_2|)$, equation (4.5) can be further simplified:

$$\begin{aligned}\bar{c}(\mathbf{x},t) =& \frac{\bar{\phi}}{4}\int_0^t \left[\mathrm{erf}(\frac{L_1 - x_1 + \bar{v}_1(t-t')}{2\sqrt{D_1(t-t')}}) - \mathrm{erf}(\frac{-L_1 - x_1 + \bar{v}_1(t-t')}{2\sqrt{D_1(t-t')}})\right] \\ & \left[\mathrm{erf}(\frac{L_2 - x_2}{2\sqrt{D_2(t-t')}}) - \mathrm{erf}(\frac{-L_2 - x_2}{2\sqrt{D_2(t-t')}})\right] dt' \\ & - \int_0^t \int_{-\infty}^{\infty}\int_{-\infty}^{\infty} \frac{\partial J_{D_i}(\mathbf{x}',t')}{\partial x_i'} \frac{1}{4\pi\sqrt{D_1 D_2}(t-t')} \\ & \exp\left[-\frac{(x_1 - x_1' - \bar{v}_1(t-t'))^2}{4D_1(t-t')} - \frac{(x_2 - x_2')^2}{4D_2(t-t')}\right] d\mathbf{x}'dt'\end{aligned} \tag{4.7}$$

in which the first term of equation (4.7) can be efficiently solved using numerical integration.

Solving equation (4.7) requires the explicit expressions or numerical values of $J_{D_i}(\mathbf{x}',t')$. Multiplying the concentration perturbation equation (4.6) by a velocity perturbation $\delta v_j(\mathbf{x},t)$ and taking the expected value leads to the following macrodispersive flux expressions:

$$\begin{aligned}J_{D_j}(\mathbf{x},t) = \int_0^t \int_{-\infty}^{\infty}\int_{-\infty}^{\infty} & \left[\overline{\delta v_j(\mathbf{x},t)\delta\phi(\mathbf{x}',t')} - P_{v_j v_i}(\mathbf{x},\mathbf{x}',t,t')\frac{\partial \bar{c}(\mathbf{x}',t')}{\partial x_i'}\right. \\ & \left. - \frac{\partial P_{v_j v_i}(\mathbf{x},\mathbf{x}',t,t')}{\partial x_i'}\bar{c}(\mathbf{x}',t')\right] \frac{1}{4\pi\sqrt{D_1 D_2}(t-t')} \\ & \exp\left[-\frac{(x_1 - x_1' - \bar{v}_1(t-t'))^2}{4D_1(t-t')} - \frac{(x_2 - x_2')^2}{4D_2(t-t')}\right] d\mathbf{x}'dt'\end{aligned} \tag{4.8}$$

Thus equations (4.7) and (4.8) are a set of coupled equations, which can be decoupled and solved in the Laplace and Fourier transform domain as we demonstrated in the previous chapter. Note that a new term, the cross-covariance between the random velocity and mass release rate fields, is introduced in equation (4.8). This suggests that, if correlated with the local velocity field, the random mass release rate

might affect the macrodispersive flux and thus impact the ensemble mean concentration plume. However, if the random velocity field is uncorrelated to the random mass release rate field, the equation for macrodispersive flux is identical to the deterministic source case. Thus a mass release rate that is uncorrelated with the local velocity field will have no impact on macrodispersive flux or ensemble mean plume spreading. It should be pointed out that terms $\frac{\partial P_{v_j v_i}(\mathbf{x},\mathbf{x}',t,t')}{\partial x_i'}\bar{c}(\mathbf{x}',t')$ in equation (4.8) and other equations presented later go to zero if the flow field is divergence free (i.e., no sources or sinks of water within the domain).

Multiplying equation (4.4) by $\delta c(\mathbf{x},t)$ and taking the expected values leads to:

$$\begin{aligned}
&\frac{\partial \sigma_c^2(\mathbf{x},t)}{\partial t} + \bar{v}_1 \frac{\partial \sigma_c^2(\mathbf{x},t)}{\partial x_1} - D_i \frac{\partial^2 \sigma_c^2(\mathbf{x},t)}{\partial {x_i}^2} + 2D_i \overline{\frac{\partial \delta c(\mathbf{x},t)}{\partial x_i} \frac{\partial \delta c(\mathbf{x},t)}{\partial x_i}} \\
&= -2J_{D_i}(\mathbf{x},t)\frac{\partial \bar{c}(\mathbf{x},t)}{\partial x_i} - 2\bar{c}(\mathbf{x},t)\overline{\delta c(\mathbf{x},t)\frac{\partial \delta v_i(\mathbf{x},t)}{\partial x_i}} + 2J_{\phi c}(\mathbf{x},t) \quad \mathbf{x} \in D \\
&\sigma_c^2(\mathbf{x},t_0) = 0 \quad \mathbf{x} \in D \\
&\sigma_c^2(\mathbf{x},t) = 0 \quad \mathbf{x} \in \partial D \\
&J_{\phi c}(\mathbf{x},t) = \overline{\delta\phi(\mathbf{x},t)\delta c(\mathbf{x},t)}
\end{aligned} \tag{4.9}$$

in which the overbar symbol represents the expected operator here and later.

Dropping the variance dissipation term from equation (4.9) and using the same momentum approach described in Appendix C, we get the following expression for concentration variance:

$$\begin{aligned}
\sigma_c^2(\mathbf{x},t) = -\int_0^t \int_{-\infty}^{\infty}\int_{-\infty}^{\infty} &\frac{1}{2\pi\sqrt{D_1 D_2}(t-t')} \\
&\left[\overline{\bar{c}(\mathbf{x}',t')\delta c(\mathbf{x}',t')\frac{\partial \delta v_i(\mathbf{x}',t')}{\partial x_i'}} + J_{D_i}(\mathbf{x}',t')\frac{\partial \bar{c}(\mathbf{x}',t')}{\partial x_i'} - J_{\phi c}(\mathbf{x}',t')\right] \\
&\exp\left[-\frac{(x_1 - x_1' - \bar{v}_1(t-t'))^2}{4D_1(t-t')} - \frac{(x_2 - x_2')^2}{4D_2(t-t')}\right] d\mathbf{x}' dt'
\end{aligned} \tag{4.10}$$

Comparing equation (4.10) to equation (3.53) for the deterministic source case, there is a new term, $J_{\phi c}(\mathbf{x}',t')$, which characterizes the correlation between random

concentration and contaminant release rate fields in the source zone. It should be noted that the linear addition principle applies to the computation on the right side of equations (4.10) and (4.11). This suggests that if random velocity and mass release rate fields are assumed to be uncorrelated, introduction of a random mass release rate will increase the concentration variance by simply adding a contribution due to the $J_{\phi c}(\mathbf{x}', t')$ term. However, if the random velocity and mass release rate fields are correlated, the randomness of the mass release rate affects the concentration variance not only through the new term of $J_{\phi c}(\mathbf{x}', t')$, but also through its impact on the ensemble mean concentration plume and the macrodisperive flux.

The new term can be evaluated multiplying equation (4.6) by $\delta\phi(\mathbf{x}, t)$ and taking the expected values:

$$J_{\phi c}(\mathbf{x}, t) = \int_0^t \int_{-\infty}^{\infty}\int_{-\infty}^{\infty} \left[P_{\phi\phi}(\mathbf{x}, \mathbf{x}', t, t') - P_{\phi v_i}(\mathbf{x}, \mathbf{x}', t, t') \frac{\partial \bar{c}(\mathbf{x}', t')}{\partial x_i'} - \frac{\partial P_{\phi v_i}(\mathbf{x}, \mathbf{x}', t, t')}{\partial x_i'} \bar{c}(\mathbf{x}', t') \right] \frac{1}{4\pi\sqrt{D_1 D_2}(t - t')} \exp\left[-\frac{(x_1 - x_1' - \bar{v}_1(t - t'))^2}{4D_1(t - t')} - \frac{(x_2 - x_2')^2}{4D_2(t - t')} \right] d\mathbf{x}' dt' \tag{4.11}$$

The remaining forcing term resulting from the recharge perturbation in equation (4.10) is:

$$\overline{\frac{\partial \delta v_j(\mathbf{x}, t)}{\partial x_j} \delta c(\mathbf{x}, t)} = \int_0^t \int_{-\infty}^{\infty}\int_{-\infty}^{\infty} \frac{1}{4\pi\sqrt{D_1 D_2}(t - t')} \left[\frac{\partial P_{v_j \phi}(\mathbf{x}, t, \mathbf{x}', t')}{\partial x_j} - \frac{\partial^2 P_{v_j v_i}(\mathbf{x}, t, \mathbf{x}', t') \bar{c}(\mathbf{x}', t')}{\partial x_j \partial x_i'} \right] \exp\left[-\frac{(x_1 - x_1' - \bar{v}_1(t - t'))^2}{4D_1(t - t')} - \frac{(x_2 - x_2')^2}{4D_2(t - t')} \right] d\mathbf{x}' dt' \tag{4.12}$$

Comparing equation (4.12) to equation (3.45) for the deterministic source case again shows that a new term, related to the correlation between the mass release rate and the local velocity field, affects the concentration variance. Note this term, $P_{v_j \phi}(\mathbf{x}, t, \mathbf{x}', t')$,

is only non-zero for $\mathbf{x}'$ in the source zone. Thus solving equations (4.8), (4.11), and (4.12) requires the specification of two extra relationships: (1) the autocovariance of the random mass release rate field $P_{\phi\phi}(\mathbf{x}, \mathbf{x}', t, t')$, and (2) the cross-covariance between random velocity field and random mass release rate in the source zone $P_{\phi v_i}(\mathbf{x}, \mathbf{x}', t, t')$.

Earlier research [e.g., Cvetkovic and Shapiro, 1990; Berglund, 1997] has suggested that strong correlation might exist between mass transfer parameters and hydraulic conductivity, groundwater velocity or travel time. However, there are no reports documenting the covariance between velocity and mass release rate at the field scale. Some laboratory work on the dissolution of Nonaqueous Phase Liquids (NAPL) in saturated porous media provide empirical relationships between velocity and mass transfer rate for NAPLs. For example, Imhoff et al. (1993) demonstrated that the mass transfer rate coefficient decreased with decreasing NAPL ganglion size and decreasing Darcy flux in an experimental study of dissolution of a NAPL in saturated porous media. Geller and Hunt (1993) showed a complex dependency of NAPL dissolution on flow velocity. This study indicated that higher flow rates would likely reconfigure ganglia into smaller sizes with higher interfacial areas leading to faster dissolution, but higher velocities would increase the length of the mass transfer zone. Berglund (1997) assumed that a dimensionless mass transfer coefficient k^* was perfectly correlated with the dimensionless travel time τ' (which is related to the Darcy flux) at the field scale. Similar assumptions have been applied to model the spatial correlation between the retardation factor and log hydraulic conductivity field [Roth and Jury, 1993; van der Zee and van Riemasdijk, 1987; Valocchi, 1989; Destouni and Cvetkovic, 1991; Bellin et al., 1993; James et al., 1997; Zhang, 1997].

The source strength function $\phi(\mathbf{x}, t)$ in equation (4.1) represents the mass released per unit volume of aquifer per unit time. In this work we assume that the source strength is a random function which can be proportional to the local velocity

field. That is, the random source strength is assumed to be positively correlated with random velocity field.

$$\phi(\mathbf{x},t) = \mathbf{v}(\mathbf{x},t)\cdot\mathbf{n}\, s_0 H(L_1-|x_1|)H(L_2-|x_2|) \tag{4.13}$$

in which s_0 ($[ML^{-4}]$) is a lumped constant which characterizes the mass available for release into the local pore water subject to the specific geometry of contaminant distribution in the source zone. This specific geometry may be further characterized as the specific mass transfer area, which represents the area of mass exposed to local pore water within the representative elementary volume. Note that $\mathbf{n}$ is a unit outward normal vector for the random source.

Equation (4.13) has the following mean and perturbation expressions:

$$\begin{aligned}\bar{\phi}(\mathbf{x},t) =& \bar{v}_1 s_0 H(L_1-|x_1|)H(L_2-|x_2|)\\ \delta\phi(\mathbf{x},t) =& (\delta v_1+\delta v_2)s_0 H(L_1-|x_1|)H(L_2-|x_2|)\end{aligned} \tag{4.14}$$

Thus, the cross-covariance expression between the random mass release rate and velocity fields and the covariance of random mass release rate for the perfectly correlated case are:

$$P_{v_j\phi}(\mathbf{x}',\mathbf{x},t',t) = s_0 P_{v_j v_i}(\mathbf{x}',\mathbf{x},t',t)H(L_1-|x_1|)H(L_2-|x_2|) \tag{4.15}$$

$$\begin{aligned}P_{\phi\phi}(\mathbf{x}',\mathbf{x},t',t) = s_0^2 P_{v_j v_i}(\mathbf{x}',\mathbf{x},t',t)&H(L_1-|x_1|)H(L_2-|x_2|)\\ &H(L_1-|x_1'|)H(L_2-|x_2'|)\end{aligned} \tag{4.16}$$

Substituting equations (4.15) and (4.16) into equations (4.8), (4.11), and (4.12) leads to:

$$
\begin{aligned}
J_{D_j}(\mathbf{x},t) = &-\int_0^t\int_{-\infty}^{\infty}\int_{-\infty}^{\infty}\frac{1}{4\pi\sqrt{D_1D_2}(t-t')}\\
&\left[P_{v_jv_i}(\mathbf{x},\mathbf{x}',t,t')\frac{\partial\bar{c}(\mathbf{x}',t')}{\partial x_i'}+\frac{\partial P_{v_jv_i}(\mathbf{x},\mathbf{x}',t,t')}{\partial x_i'}\bar{c}(\mathbf{x}',t')\right]\\
&\exp\left[-\frac{(x_1-x_1'-\bar{v}_1(t-t'))^2}{4D_1(t-t')}-\frac{(x_2-x_2')^2}{4D_2(t-t')}\right]d\mathbf{x}'dt'\\
&+I\int_0^t\int_{-L_1}^{L_1}\int_{-L_2}^{L_2}\frac{s_0P_{v_jv_i}(\mathbf{x},\mathbf{x}',t,t')}{4\pi\sqrt{D_1D_2}(t-t')}\\
&\exp\left[-\frac{(x_1-x_1'-\bar{v}_1(t-t'))^2}{4D_1(t-t')}-\frac{(x_2-x_2')^2}{4D_2(t-t')}\right]d\mathbf{x}'dt'
\end{aligned}
\tag{4.17}
$$

$$
\begin{aligned}
J_{\phi c}(\mathbf{x},t) =&H(L_1-|x_1|)H(L_2-|x_2|)\\
&\left[-I\int_0^t\int_{-\infty}^{\infty}\int_{-\infty}^{\infty}\frac{s_0}{4\pi\sqrt{D_1D_2}(t-t')}\right.\\
&\left[P_{v_jv_i}(\mathbf{x},\mathbf{x}',t,t')\frac{\partial\bar{c}(\mathbf{x}',t')}{\partial x_i'}+\frac{\partial P_{v_jv_i}(\mathbf{x},\mathbf{x}',t,t')}{\partial x_i'}\bar{c}(\mathbf{x}',t')\right]\\
&\exp\left[-\frac{(x_1-x_1'-\bar{v}_1(t-t'))^2}{4D_1(t-t')}-\frac{(x_2-x_2')^2}{4D_2(t-t')}\right]d\mathbf{x}'dt'\\
&+\int_0^t\int_{-L_1}^{L_1}\int_{-L_2}^{L_2}\frac{s_0^2P_{v_jv_i}(\mathbf{x},\mathbf{x}',t,t')}{4\pi\sqrt{D_1D_2}(t-t')}\\
&\left.\exp\left[-\frac{(x_1-x_1'-\bar{v}_1(t-t'))^2}{4D_1(t-t')}-\frac{(x_2-x_2')^2}{4D_2(t-t')}\right]d\mathbf{x}'dt'\right]
\end{aligned}
\tag{4.18}
$$

$$
\begin{aligned}
\overline{\frac{\partial\delta v_i(\mathbf{x},t)}{\partial x_i}\delta c(\mathbf{x},t)} = &-\int_0^t\int_{-\infty}^{\infty}\int_{-\infty}^{\infty}\frac{1}{4\pi\sqrt{D_1D_2}(t-t')}\\
&\left[\frac{\partial P_{v_iv_j}(\mathbf{x}-\mathbf{x}',t-t')}{\partial x_i}\frac{\partial\bar{c}(\mathbf{x}',t')}{\partial x_j'}\right.\\
&\left.+\bar{c}(\mathbf{x}',t')\frac{\partial^2P_{v_iv_j}(\mathbf{x}-\mathbf{x}',t-t')}{\partial x_i\partial x_j'}\right]\\
&\exp\left[-\frac{(x_1-x_1'-\bar{v}_1(t-t'))^2}{4D_1(t-t')}-\frac{(x_2-x_2')^2}{4D_2(t-t')}\right]d\mathbf{x}'dt'\\
&+I\int_0^t\int_{-L_1}^{L_1}\int_{-L_2}^{L_2}\frac{s_0}{4\pi\sqrt{D_1D_2}(t-t')}\frac{\partial P_{v_iv_j}(\mathbf{x}-\mathbf{x}',t-t')}{\partial x_i}\\
&\exp\left[-\frac{(x_1-x_1'-\bar{v}_1(t-t'))^2}{4D_1(t-t')}-\frac{(x_2-x_2')^2}{4D_2(t-t')}\right]d\mathbf{x}'dt'
\end{aligned}
\tag{4.19}
$$

in which repeated indices are assumed to be summed from i=1 to 2 and j=1 to 2; and I is an index value which takes on a value of 1 for perfectly correlated velocity and mass release rate and zero for uncorrelated velocity and mass release rate. Thus equations (4.7), (4.17), (4.19), (4.18), and (4.10) provide integration expressions for describing the expected mean, approximate macrodispersive flux, and approximate concentration standard deviation in transient flow fields, which can be solved using a fast Fourier transform algorithm.

The Heaviside function $H(L_1 - |x_1|)H(L_2 - |x_2|)$ in equation (4.18) limits the new term, $J_{\phi c}(\mathbf{x}, t)$, to be non-zero only in the source zone. Outside the source zone $J_{\phi c}(\mathbf{x}, t)$ equals zero since $\delta\phi(\mathbf{x})$ equals zero. This result suggests that the increased concentration prediction uncertainty due to introduction of the source uncertainty occurs primarily in the source zone. For the same reason, integration of the new terms related to the uncertain source in equation (4.17) and (4.19) are bounded by the source size (i.e., these terms are nonzero for $\mathbf{x}'$ in the source zone). This indicates that the source size has a major impact on the evaluation of terms of $J_{D_j}(\mathbf{x}, t)$ and $\overline{\frac{\partial \delta v_i(\mathbf{x},t)}{\partial x_i} \delta c(\mathbf{x}, t)}$. Again, if the flow is divergence-free, the terms $\overline{\frac{\partial \delta v_i(\mathbf{x},t)}{\partial x_i} \delta c(\mathbf{x}, t)}$ go to zero.

4.4 Cross-covariance between Source and Concentration

Multiplying concentration perturbation equation (4.6) with mass release rate perturbation at another location $\mathbf{x}^*$ and time t^* gives the following cross-covariance between uncertain mass release rate in the source zone and uncertain solute concentration at any point within the domain:

$$P_{\phi c}(\mathbf{x}^*, \mathbf{x}, t^*, t) = \int_0^t \int_{-\infty}^{\infty} \int_{-\infty}^{\infty} \frac{1}{4\pi\sqrt{D_1 D_2}(t-t')} \left[P_{\phi\phi}(\mathbf{x}^*, \mathbf{x}', t^*, t') - \frac{\partial P_{\phi v_i}(\mathbf{x}^*, \mathbf{x}', t^*, t')\bar{c}(\mathbf{x}', t')}{\partial x_i'} \right] \exp\left[-\frac{(x_1 - x_1' - \bar{v}_1(t-t'))^2}{4D_1(t-t')} - \frac{(x_2 - x_2')^2}{4D_2(t-t')} \right] d\mathbf{x}' dt' \tag{4.20}$$

Equation (4.20) may be useful in estimating the source strength using observations of aqueous phase concentrations downstream. It should be noted that $\mathbf{x}^*$ is restricted to any location in the source zone. Outside the source zone $\phi(\mathbf{x}^*)$ is assumed to be zero with certainty, thus $P_{\phi c}$ =0.

Substituting equations (4.15) and (4.16) into equation (4.20) leads to:

$$\begin{aligned} P_{\phi c}(\mathbf{x}^*, \mathbf{x}, t^*, t) =& H(L_1 - |x_1^*|)H(L_2 - |x_2^*|) \\ & \left[\int_0^t \int_{-L_1}^{L_1} \int_{-L_2}^{L_2} \frac{s_0^2 P_{v_j v_i}(\mathbf{x}^*, \mathbf{x}', t^*, t')}{4\pi\sqrt{D_1 D_2}(t-t')} \right. \\ & \exp\left[-\frac{(x_1 - x_1' - \bar{v}_1(t-t'))^2}{4D_1(t-t')} - \frac{(x_2 - x_2')^2}{4D_2(t-t')} \right] d\mathbf{x}' dt' \\ & - I \int_0^t \int_{-\infty}^{\infty} \int_{-\infty}^{\infty} \frac{s_0}{4\pi\sqrt{D_1 D_2}(t-t')} \\ & \left[P_{v_j v_i}(\mathbf{x}^*, \mathbf{x}', t^*, t') \frac{\partial \bar{c}(\mathbf{x}', t')}{\partial x_i'} + \frac{\partial P_{v_j v_i}(\mathbf{x}^*, \mathbf{x}', t^*, t')}{\partial x_i'} \bar{c}(\mathbf{x}', t') \right] \\ & \left. \exp\left[-\frac{(x_1 - x_1' - \bar{v}_1(t-t'))^2}{4D_1(t-t')} - \frac{(x_2 - x_2')^2}{4D_2(t-t')} \right] d\mathbf{x}' dt' \right] \end{aligned} \tag{4.21}$$

In cross-covariance equation (4.21), the Heaviside function $H(L_1 - |x_1^*|)H(L_2 - |x_2^*|)$ limits $\mathbf{x}^*$ to the source zone. As mentioned previously the cross-covariance between uncertain mass release rate and concentration will be zero if $\mathbf{x}^*$ is taken outside of the source zone because the uncertain mass release rate is zero beyond the source zone. Thus, equation (4.21) can be rewritten as:

$$
\begin{aligned}
P_{\phi c}(\mathbf{x}^*,\mathbf{x},t^*,t) = &\int_0^t \int_{-L_1}^{L_1} \int_{-L_2}^{L_2} \frac{s_0^2 P_{v_j v_i}(\mathbf{x}^*,\mathbf{x}',t^*,t')}{4\pi\sqrt{D_1 D_2}(t-t')} \\
&\exp\left[-\frac{(x_1-x_1'-\bar{v}_1(t-t'))^2}{4D_1(t-t')} - \frac{(x_2-x_2')^2}{4D_2(t-t')}\right] d\mathbf{x}' dt' \\
-I &\int_0^t \int_{-\infty}^{\infty} \int_{-\infty}^{\infty} \frac{s_0}{4\pi\sqrt{D_1 D_2}(t-t')} \\
&\left[P_{v_j v_i}(\mathbf{x}^*,\mathbf{x}',t^*,t')\frac{\partial \bar{c}(\mathbf{x}',t')}{\partial x_i'} + \frac{\partial P_{v_j v_i}(\mathbf{x}^*,\mathbf{x}',t^*,t')}{\partial x_i'}\bar{c}(\mathbf{x}',t')\right] \\
&\exp\left[-\frac{(x_1-x_1'-\bar{v}_1(t-t'))^2}{4D_1(t-t')} - \frac{(x_2-x_2')^2}{4D_2(t-t')}\right] d\mathbf{x}' dt' \\
&x_i^* \in [-L_i, L_i]
\end{aligned}
\tag{4.22}
$$

Holding $\mathbf{x}^*$ and t^* as specific location and time constants and taking forward and then inverse Laplace and double Fourier transforms of the right side of cross-covariance equation (4.22) yields:

$$
\begin{aligned}
P_{\phi c}(\mathbf{x}^*,\mathbf{x},t^*,t) = &\mathcal{L}\,\mathcal{F}^{-1}\left[\frac{[s_0^2 T_1(\mathbf{x}^*,\mathbf{k},t^*,s) - I s_0 T_2(\mathbf{x}^*,\mathbf{k},t^*,s)]}{(s - 2\pi i\bar{v}_1 k_1 + 4\pi^2 D_i k_i^2)}\right] \\
&x_i^* \in [-L_i, L_i]
\end{aligned}
\tag{4.23}
$$

in which $T_1(\mathbf{x}^*,\mathbf{k},t^*,s)$ and $T_2(\mathbf{x}^*,\mathbf{k},t^*,s)$ can be evaluated by:

$$
\begin{aligned}
T_1(\mathbf{x}^*,\mathbf{k},t^*,s) &= \int_0^\infty \int_{-L_1}^{L_1} \int_{-L_2}^{L_2} P_{v_i v_j}(\mathbf{x}^*,\mathbf{x},t^*,t) e^{-st} dt e^{2\pi i \mathbf{k}\mathbf{x}} d\mathbf{x} \\
T_2(\mathbf{x}^*,\mathbf{k},t^*,s) &= \int_0^\infty \int_{-\infty}^{\infty} \int_{-\infty}^{\infty} \left[P_{v_j v_i}(\mathbf{x}^*,\mathbf{x},t^*,t)\frac{\partial \bar{c}(\mathbf{x},t)}{\partial x_i}\right. \\
&\quad \left. + \frac{\partial P_{v_j v_i}(\mathbf{x}^*,\mathbf{x},t^*,t)}{\partial x_i}\bar{c}(\mathbf{x},t)\right] e^{-st} dt e^{2\pi i \mathbf{k}\mathbf{x}} d\mathbf{x}
\end{aligned}
\tag{4.24}
$$

4.5 Moment Solutions in Laplace-Fourier Domain

4.5.1 Mean Concentration and Macrodispersive Flux Solutions

Solute transport from a deterministic continuous patch source subject to a transient uncertain flow field is considered here and compared and contrasted to the case of solute transport from an uncertain continuous source in a transient uncertain

flow field. For convenience the mean flow field is assumed to be steady and uniform. Assuming that the source contaminant release rate is perfectly known equations (4.7), (4.17), (4.10), and (4.19) become:

$$\begin{aligned}\bar{c}(\mathbf{x},t) =& \frac{\bar{\phi}}{4}\int_0^t \left[\operatorname{erf}(\frac{L_1 - x_1 + \bar{v}_1(t-t')}{2\sqrt{D_1(t-t')}}) - \operatorname{erf}(\frac{-L_1 - x_1 + \bar{v}_1(t-t')}{2\sqrt{D_1(t-t')}})\right] \\ & \left[\operatorname{erf}(\frac{L_2 - x_2}{2\sqrt{D_2(t-t')}}) - \operatorname{erf}(\frac{-L_2 - x_2}{2\sqrt{D_2(t-t')}})\right] dt' \\ & - \int_0^t \int_{-\infty}^{\infty}\int_{-\infty}^{\infty} \overline{\frac{\partial J_{D_i}(\mathbf{x}',t')}{\partial x_i'}} \frac{1}{4\pi\sqrt{D_1 D_2}(t-t')} \\ & \exp\left[-\frac{(x_1 - x_1' - \bar{v}_1(t-t'))^2}{4D_1(t-t')} - \frac{(x_2 - x_2')^2}{4D_2(t-t')}\right] d\mathbf{x}' dt'\end{aligned} \tag{4.25}$$

$$\begin{aligned}J_{D_j}(\mathbf{x},t) =& -\int_0^t \int_{-\infty}^{\infty}\int_{-\infty}^{\infty} \frac{1}{4\pi\sqrt{D_1 D_2}(t-t')} \\ & \left[P_{v_j v_i}(\mathbf{x},\mathbf{x}',t,t')\frac{\partial \bar{c}(\mathbf{x}',t')}{\partial x_i'} + \bar{c}(\mathbf{x}',t')\frac{P_{v_j v_i}(\mathbf{x},\mathbf{x}',t,t')}{\partial x_i'}\right] \\ & \exp\left[-\frac{(x_1 - x_1' - \bar{v}_1(t-t'))^2}{4D_1(t-t')} - \frac{(x_2 - x_2')^2}{4D_2(t-t')}\right] d\mathbf{x}' dt'\end{aligned} \tag{4.26}$$

$$\begin{aligned}\sigma_c^2(\mathbf{x},t) =& -\int_0^t \int_{-\infty}^{\infty}\int_{-\infty}^{\infty} \frac{1}{2\pi\sqrt{D_1 D_2}(t-t')} \\ & \left[\bar{c}(\mathbf{x}',t')\overline{\delta c(\mathbf{x}',t')\frac{\partial \delta v_i(\mathbf{x}',t')}{\partial x_i'}} + J_{D_i}(\mathbf{x}',t')\frac{\partial \bar{c}(\mathbf{x}',t')}{\partial x_i'}\right] \\ & \exp\left[-\frac{(x_1 - x_1' - \bar{v}_1(t-t'))^2}{4D_1(t-t')} - \frac{(x_2 - x_2')^2}{4D_2(t-t')}\right] d\mathbf{x}' dt'\end{aligned} \tag{4.27}$$

$$\begin{aligned}\overline{\frac{\partial \delta v_i(\mathbf{x},t)}{\partial x_i}\delta c(\mathbf{x},t)} =& -\int_0^t \int_{-\infty}^{\infty}\int_{-\infty}^{\infty} \frac{1}{4\pi\sqrt{D_1 D_2}(t-t')} \\ & \left[\frac{\partial P_{v_i v_j}(\mathbf{x}-\mathbf{x}',t-t')}{\partial x_i}\frac{\partial \bar{c}(\mathbf{x}',t')}{\partial x_j'}\right. \\ & \left. + \bar{c}(\mathbf{x}',t')\frac{\partial^2 P_{v_i v_j}(\mathbf{x}-\mathbf{x}',t-t')}{\partial x_i \partial x_j'}\right] \\ & \exp\left[-\frac{(x_1 - x_1' - \bar{v}_1(t-t'))^2}{4D_1(t-t')} - \frac{(x_2 - x_2')^2}{4D_2(t-t')}\right] d\mathbf{x}' dt'\end{aligned} \tag{4.28}$$

Taking the Laplace transform and double Fourier transforms of the mean concentration equation (4.25) and the macrodispersive flux equation (4.26), and using the convolution theory of integral transform in Appendix D the following expressions for mean concentration and macrodispersive flux in the Laplace-Fourier domain are obtained:

$$\tilde{c}(\mathbf{k},s) = \mathcal{L}.\mathcal{F}\left[\bar{c}_1(\mathbf{x},t)\right] + \frac{2\pi i k_i \tilde{J}_{D_i}(\mathbf{k},s)}{[s - 2\pi i k_1 \bar{v}_1 + 4\pi^2 D_i k_i^2]} \tag{4.29}$$

$$\begin{aligned} \tilde{J}_{D_1}(\mathbf{k},s) &= \tilde{c}(\mathbf{k},s)\Big[2\pi i\left[k_1 g_{11}(\mathbf{k},s) + k_2 g_{12}(\mathbf{k},s)\right] - g_{10}(\mathbf{k},s)\Big] \\ \tilde{J}_{D_2}(\mathbf{k},s) &= \tilde{c}(\mathbf{k},s)\Big[2\pi i\left[k_1 g_{21}(\mathbf{k},s) + k_2 g_{22}(\mathbf{k},s)\right] - g_{20}(\mathbf{k},s)\Big] \end{aligned} \tag{4.30}$$

where the tilde symbol represents the transformed Laplace-Fourier variable; and $\bar{c}_1(\mathbf{x},t)$ is:

$$\begin{aligned} \bar{c}_1(\mathbf{x},t) = \frac{\bar{\phi}}{4}\int_0^t &\left[\operatorname{erf}\left(\frac{L_1 - x_1 + \bar{v}_1(t-t')}{2\sqrt{D_1(t-t')}}\right) - \operatorname{erf}\left(\frac{-L_1 - x_1 + \bar{v}_1(t-t')}{2\sqrt{D_1(t-t')}}\right)\right] \\ &\left[\operatorname{erf}\left(\frac{L_2 - x_2}{2\sqrt{D_2(t-t')}}\right) - \operatorname{erf}\left(\frac{-L_2 - x_2}{2\sqrt{D_2(t-t')}}\right)\right] dt' \end{aligned} \tag{4.31}$$

Inserting equation (4.30) into equation (4.29) and taking the inverse Laplace and Fourier transform, the following decoupled mean concentration and macrodispersive flux expressions are obtained:

$$\bar{c}(\mathbf{x},t) \approx \mathcal{L}.\mathcal{F}^{-1}\left[\mathcal{L}.\mathcal{F}\left[\bar{c}_1(\mathbf{x},t)\right]\left[1 + \frac{4\pi^2 k_{ij}^2 g_{ij}(\mathbf{k},s) + 2\pi i k_i g_{i0}(\mathbf{k},s)}{s - 2\pi i k_1 \bar{v}_1 + 4\pi^2 D_i k_i^2}\right]^{-1}\right] \tag{4.32}$$

$$\begin{aligned} J_{D_1}(\mathbf{x},t) &\approx \mathcal{L}.\mathcal{F}^{-1}\left[\tilde{c}(\mathbf{k},s)\Big[2\pi i\left[k_1 g_{11}(\mathbf{k},s) + k_2 g_{12}(\mathbf{k},s)\right] - g_{10}(\mathbf{k},s)\Big]\right] \\ J_{D_2}(\mathbf{x},t) &\approx \mathcal{L}.\mathcal{F}^{-1}\left[\tilde{c}(\mathbf{k},s)\Big[2\pi i\left[k_1 g_{21}(\mathbf{k},s) + k_2 g_{22}(\mathbf{k},s)\right] - g_{20}(\mathbf{k},s)\Big]\right] \end{aligned} \tag{4.33}$$

in which:

$$g_{i0}(\mathbf{k},s) = \mathcal{L}.\mathcal{F}\left[\frac{\left[\frac{\partial P_{v_1v_1}(\mathbf{x},t)}{\partial x_1}+\frac{\partial P_{v_1v_2}(\mathbf{x},t)}{\partial x_2}\right]}{4\pi t\sqrt{D_1D_2}}\exp\left[-\frac{(x_1-\bar{v}_1t)^2}{4D_1t}-\frac{x_2^2}{4D_2t}\right]\right]$$
$$g_{i,j}(\mathbf{k},s) = \mathcal{L}.\mathcal{F}\left[\frac{P_{v_iv_j}(\mathbf{x},t)}{4\pi t\sqrt{D_1D_2}}\exp\left[-\frac{(x_1-\bar{v}_1t)^2}{4D_1t}-\frac{x_2^2}{4D_2t}\right]\right] \tag{4.34}$$

where i equals 1 or 2, and repeated summation is not implied. The expressions $g_{i,0}(k_1,k_2,s)$, $g_{i,j}(k_1,k_2,s)$ can be numerically integrated by a fast Fourier transform algorithm.

Similarly, the equation (4.28) can be transformed using Laplace and Fourier transforms in the same manner as $J_{D_i}(\mathbf{x},t)$:

$$\overline{\frac{\partial\delta v_i(\mathbf{x},t))}{\partial x_i}\delta c(\mathbf{x},t)} \approx \mathcal{L}.\mathcal{F}^{-1}\Big[\bar{c}(\mathbf{k},s)\Big[2\pi i[k_1g_{10}(\mathbf{k},s)+k_2g_{20}(\mathbf{k},s)] +g_{30}(\mathbf{k},s)\Big]\Big] \tag{4.35}$$

in which g_{10} and g_{20} are same as those in the macrodispersive flux expressions. Since ξ=$\mathbf{x}-\mathbf{x}'$ is defined, $\frac{\partial^2 P_{v_iv_j}(\mathbf{x}-\mathbf{x}')}{\partial x_i\partial x_j} = \frac{\partial^2 P_{v_iv_j}(\xi)}{\partial\xi_i\partial\xi_j}$. The new term, g_{30}, can be evaluated by:

$$g_{30}(\mathbf{k},s) = \mathcal{L}.\mathcal{F}\left[\left[\frac{\partial^2 P_{v_1v_1}(\mathbf{x},t)}{\partial {x_1}^2}+\frac{\partial^2 P_{v_1v_2}(\mathbf{x},t)}{\partial x_1\partial x_2}+\frac{\partial^2 P_{v_2v_1}(\mathbf{x},t)}{\partial x_1\partial x_2}+\frac{\partial^2 P_{v_2v_2}(\mathbf{x},t)}{\partial {x_2}^2}\right]\right.$$
$$\left.\frac{1}{4\pi t\sqrt{D_1D_2}}\exp\left[-\frac{(x_1-\bar{v}_1t)^2}{4D_1t}-\frac{x_2^2}{4D_2t}\right]\right] \tag{4.36}$$

Performing the forward and then backward Laplace and Fourier transforms, the concentration variance in the Laplace-Fourier domain can be expressed:

$$\sigma_c^2(\mathbf{x},t) \approx \mathcal{L}\,\mathcal{F}^{-1}\left[\frac{\mathcal{L}\,\mathcal{F}\left[-2\,J_{D_i}(\mathbf{x},t)\frac{\partial\bar{c}}{\partial x_i}-2\bar{c}(\mathbf{x},t)\,\overline{\delta c(\mathbf{x},t)\frac{\partial\delta v_i(\mathbf{x},t)}{\partial x_i}}\right]}{(s-2\pi i\bar{v}_1k_1+4\pi^2D_ik_i^2)}\right] \tag{4.37}$$

which can be computed using the previously evaluated results for the mean concentration and macrodispersive flux.

Equations (4.32) to (4.37) provide expressions for the statistical moments of concentration subject to a known continuous patch source. Replacing this continuous patch source by an instantaneous patch source with a delta function as the temporal function gives the same solutions obtained using the known initial condition, which was derived in the previous chapter.

4.5.2 Uncertain Contaminant Source

Taking the Laplace transform and double Fourier transform of the mean concentration equation (4.7), macrodispersive flux equation (4.17), equation (4.18), equation (4.19), and concentration variance equation (4.10), using the convolution theory of integral transforms, and taking the advantage of the stationary velocity field, we obtain the following moment expressions for the case of random mass release rate and random velocity in the Laplace-Fourier domain:

$$\tilde{c}(\mathbf{k},s) = \mathcal{L}.\mathcal{F}\left[\bar{c}_1(\mathbf{x},t)\right] + \frac{2\pi i k_i \tilde{J}_{D_i}(\mathbf{k},s)}{\left[s - 2\pi i k_1 \bar{v}_1 + 4\pi^2 D_i k_i^2\right]} \tag{4.38}$$

$$\begin{aligned}
\tilde{J}_{D_1}(\mathbf{k},s) =& \tilde{c}(\mathbf{k},s)\Big[2\pi i\left[k_1 g_{11}(\mathbf{k},s) + k_2 g_{12}(\mathbf{k},s)\right] - g_{10}(\mathbf{k},s)\Big] \\
&+ I\left[g_{11}(\mathbf{k},s) + g_{12}(\mathbf{k},s)\right]\mathcal{L}.\mathcal{F}\left[\bar{c}_1(\mathbf{x},t)\right]\left[s - 2\pi i k_1 \bar{v}_1 + 4\pi^2 D_i k_i^2\right] \\
\tilde{J}_{D_2}(\mathbf{k},s) =& \tilde{c}(\mathbf{k},s)\Big[2\pi i\left[k_1 g_{21}(\mathbf{k},s) + k_2 g_{22}(\mathbf{k},s)\right] - g_{20}(\mathbf{k},s)\Big] \\
&+ I\left[g_{21}(\mathbf{k},s) + g_{22}(\mathbf{k},s)\right]\mathcal{L}.\mathcal{F}\left[\bar{c}_1(\mathbf{x},t)\right]\left[s - 2\pi i k_1 \bar{v}_1 + 4\pi^2 D_i k_i^2\right]
\end{aligned} \tag{4.39}$$

$$\begin{aligned}
\tilde{J}_{\phi c}(\mathbf{k},s) =& I\tilde{c}(\mathbf{k},s)\Big[2\pi i\left[k_1 h_1(\mathbf{k},s) + k_2 h_2(\mathbf{k},s)\right] - h_0(\mathbf{k},s)\Big] \\
&+ \left[h_1(\mathbf{k},s) + h_2(\mathbf{k},s)\right]\mathcal{L}.\mathcal{F}\left[\bar{c}_1(\mathbf{x},t)\right]\left[s - 2\pi i k_1 \bar{v}_1 + 4\pi^2 D_i k_i^2\right]
\end{aligned} \tag{4.40}$$

$$\mathcal{L}.\mathcal{F}\left[\overline{\frac{\partial \delta v_i(\mathbf{x},t))}{\partial x_i}\delta c(\mathbf{x},t)}\right] = \tilde{c}(\mathbf{k},s)\Big[2\pi i k_1 g_{10}(\mathbf{k},s) + 2\pi i k_2 g_{20}(\mathbf{k},s) + g_{30}(\mathbf{k},s)\Big] + I h_0(\mathbf{k},s) \tag{4.41}$$

$$\mathcal{L}\,\mathcal{F}\left[\sigma_c^2(\mathbf{x},t)\right] \approx 2\left[\frac{\mathcal{L}\,\mathcal{F}\left[-J_{D_i}(\mathbf{x},t)\frac{\partial \bar{c}}{\partial x_i} - \bar{c}(\mathbf{x},t)\overline{\delta c(\mathbf{x},t)\frac{\partial \delta v_i(\mathbf{x},t)}{\partial x_i}} + J_{\phi c}(\mathbf{x},t)\right]}{(s - 2\pi i \bar{v}_1 k_1 + 4\pi^2 D_i k_i^2)}\right] \tag{4.42}$$

Although the mean concentration equation (4.38) in the above Laplace-Fourier domain has the same form as the equation (4.29) for the deterministic source, it should be recalled that these two equations will yield different results due to the different coupled macrodispersive equations in the case of perfectly correlated velocity and mass release rate, i.e., $I = 1$. However when the index parameter, I, takes on the value zero, i.e., there is no correlation between velocity and mass release rate, the concentration plume will show identical spreading whether an uncertain source exists or not.

After decoupling the mean concentration and macrodispersive equations, performing the inverse Laplace and Fourier transforms, and rearranging terms where necessary, we obtain the following decoupled mean concentration, macrodispersive flux, and concentration variance expressions in the Laplace-Fourier domain for the uncertain source case:

$$\bar{c}(\mathbf{x},t) \approx \mathcal{L}.\mathcal{F}^{-1}\left[\frac{\mathcal{L}.\mathcal{F}\left[\bar{c}_1(\mathbf{x},t)\right]\left[1 + 2\pi i I\left[k_i g_{ij}(\mathbf{k},s)\right]\right]}{\left[1 + \frac{4\pi^2 k_{ij}^2 g_{ij}(\mathbf{k},s) + 2\pi i k_i g_{i0}(\mathbf{k},s)}{s - 2\pi i k_1 \bar{v}_1 + 4\pi^2 D_i k_i^2}\right]}\right] \tag{4.43}$$

$$J_{D_1}(\mathbf{x},t) \approx \mathcal{L}.\mathcal{F}^{-1}\Bigg[\tilde{c}(\mathbf{k},s)\Big[2\pi i\left[k_1 g_{11}(\mathbf{k},s)+k_2 g_{12}(\mathbf{k},s)\right]-g_{10}(\mathbf{k},s)\Big] + I\left[g_{11}(\mathbf{k},s)+g_{12}(\mathbf{k},s)\right] \mathcal{L}.\mathcal{F}\left[\bar{c}_1(\mathbf{x},t)\right]\left[s-2\pi i k_1\bar{v}_1+4\pi^2 D_i k_i^2\right]\Bigg]$$

$$J_{D_2}(\mathbf{x},t) \approx \mathcal{L}.\mathcal{F}^{-1}\Bigg[\tilde{c}(\mathbf{k},s)\Big[2\pi i\left[k_1 g_{21}(\mathbf{k},s)+k_2 g_{22}(\mathbf{k},s)\right]-g_{20}(\mathbf{k},s)\Big] + I\left[g_{21}(\mathbf{k},s)+g_{22}(\mathbf{k},s)\right] \mathcal{L}.\mathcal{F}\left[\bar{c}_1(\mathbf{x},t)\right]\left[s-2\pi i k_1\bar{v}_1+4\pi^2 D_i k_i^2\right]\Bigg] \tag{4.44}$$

$$J_{\phi c}(\mathbf{x},t) = \mathcal{L}\,\mathcal{F}^{-1}\Bigg[I\tilde{c}(\mathbf{k},s)\Big[2\pi i\left[k_1 h_1(\mathbf{k},s)+k_2 h_2(\mathbf{k},s)\right]-h_0(\mathbf{k},s)\Big] + \left[h_1(\mathbf{k},s)+h_2(\mathbf{k},s)\right] \mathcal{L}.\mathcal{F}\left[\bar{c}_1(\mathbf{x},t)\right]\left[s-2\pi i k_1\bar{v}_1+4\pi^2 D_i k_i^2\right]\Bigg] \tag{4.45}$$

$$\overline{\frac{\partial\delta v_i(\mathbf{x},t))}{\partial x_i}\delta c(\mathbf{x},t)} = \mathcal{L}.\mathcal{F}^{-1}\Bigg[\tilde{c}(\mathbf{k},s)\Big[2\pi i k_1 g_{10}(\mathbf{k},s)+2\pi i k_2 g_{20}(\mathbf{k},s) +g_{30}(\mathbf{k},s)\Big]+I h_0(\mathbf{k},s)\Bigg] \tag{4.46}$$

$$\sigma_c^2(\mathbf{x},t) \approx 2\mathcal{L}\,\mathcal{F}^{-1}\left[\frac{\mathcal{L}\,\mathcal{F}\left[-J_{D_i}(\mathbf{x},t)\frac{\partial\bar{c}}{\partial x_i}-\bar{c}(\mathbf{x},t)\overline{\delta c(\mathbf{x},t)\frac{\partial\delta v_i(\mathbf{x},t)}{\partial x_i}}+J_{\phi c}(\mathbf{x},t)\right]}{(s-2\pi i\bar{v}_1 k_1+4\pi^2 D_i k_i^2)}\right] \tag{4.47}$$

Note that the decoupling process does not apply to the equation (4.47), which must be evaluated after having results for mean concentration, macrodispersive flux, and the terms $J_{\phi c}$ and $\overline{\delta c(\mathbf{x},t)\frac{\partial\delta v_i(\mathbf{x},t)}{\partial x_i}}$. In the above equations g_{ij} and g_{i0} are the same as previously given. However, the new terms $h_0(\mathbf{k},s)$ and $h_i(\mathbf{k},s)$ are given by:

$$h_0(\mathbf{k},s) = \int_0^{\infty}\int_{-L_1}^{L_1}\int_{-L_2}^{L_2}\left[\frac{\partial P_{v_1v_1}(\mathbf{x},t)}{\partial x_1}+\frac{\partial P_{v_1v_2}(\mathbf{x},t)}{\partial x_2}\right.$$
$$\left.+\frac{\partial P_{v_2v_1}(\mathbf{x},t)}{\partial x_1}+\frac{\partial P_{v_2v_2}(\mathbf{x},t)}{\partial x_2}\right]$$
$$\frac{s_0}{4\pi\sqrt{D_1D_2}t}\exp\left[-\frac{(x_1-\bar{v}_1t)^2}{4D_1t}-\frac{x_2^2}{4D_2t}\right]e^{-st}dte^{2\pi i\mathbf{kx}}d\mathbf{x} \qquad (4.48)$$
$$h_i(\mathbf{k},s) = \int_0^{\infty}\int_{-L_1}^{L_1}\int_{-L_2}^{L_2}\left[P_{v_1v_i}(\mathbf{x},t)+P_{v_2v_i}(\mathbf{x},t)\right]$$
$$\frac{s_0}{4\pi\sqrt{D_1D_2}t}\exp\left[-\frac{(x_1-\bar{v}_1t)^2}{4D_1t}-\frac{x_2^2}{4D_2t}\right]e^{-st}dte^{2\pi i\mathbf{kx}}d\mathbf{x}$$

where i=1 or 2.

4.6 Example Problems

4.6.1 Problem Settings

In Chapters 2 and 3, we examined and contrasted the impacts of transient and steady uniform and non-uniform flow on statistical moments of solute transport in heterogeneous aquifers subject to random recharge field. In this chapter, we investigate the joint effects of a random contaminant source field and random groundwater velocity on the statistical moments of solute transport in a two-dimensional domain. For convenience, steady state divergence free flow (uniform mean flow) is assumed in this example. This is justified because the main purpose of this chapter is to distinguish between the uncertainty resulting from velocity uncertainty versus source uncertainty.

For illustrative purposes, a conservative planar source is assumed to be continuously released into a 20 m by 60 m domain. The source location, size, shape, and mean mass release rate are all considered to be known perfectly. The initial concentration is assumed to be zero throughout the domain. The boundaries are assumed to be located far enough from the solute source so that homogeneous Dirichlet boundary conditions apply on all sides of the domain. Table 4.1 lists the values for the

input parameters used in this example problem. The values for the statistics of the log-transmissivity field and the hydraulic gradient are taken from the Borden field experiment [Mackay et al., 1986; Sudicky, 1986]. The statistics of the log-transmissivity field were determined by Dagan (1989) by vertical averaging of the three-dimensional log-conductivity field over the vertical correlation length. This methodology was proposed by Dagan (1989) due to the very limited vertical extent and vertical spreading of the plume, and was adopted by Freyberg (1986), Sposito and Barry (1987), Barry et al. (1988) and Graham and McLaughlin (1991) in subsequent analyses of the Borden experiment. In all cases the multidimensional fast Fourier transform routine described in Chapter 3 was used to evaluate the concentration moments. Steady-state velocity covariance matrix without recharge derived in previous Chapters was used in this simulation.

Table 4.1: Input parameters for different simulation cases*

Parameter	Value
Mean log-transmissivity Y	61.8
Aquifer thickness b	10 m
Variance of transmissivity σ_Y^2	0.25
Correlation length of transmissivity λ_Y	2.8 m
Variance of mass release rate σ_ϕ^2	$s_0^2(\sigma_{v_1}^2 + \sigma_{v_2}^2)$
Correlation length of mass release rate λ_ϕ	2.8 m
Mass release rate constant s_0	8.425 g/m^4
Mean mass release rate $\bar{\phi}$	$\bar{v}_1 s_0$
Longitudinal dispersivity α_L	0.05 m
Transverse dispersivity α_T	0.05 m
Porosity n	0.33
Mean hydraulic head gradient J_0	0.0056
Total simulation time	200 days
Domain size	20 m * 60 m
Mean solution grid	0.5 m * 0.5 m
Source centroid location	4m, 10m
Time step	1 day
No. of simulation nodes	$128(N_{x_1})$*$32(N_{x_2})$*$2048(N_t)$

* $I(Index)$ takes on a value zero for Cases 1 and 2, and one for Case 3.

Case 1 is the deterministic source base case which considers the transmissivity field as the only random field. This case has been quite extensively studied and reported in the literature [Dagan, 1989; Rubin and Dagan, 1987a; Graham and McLaughlin, 1989a; Zhang and Neuman, 1995a, 1995d; Li and Graham, 1998]. An uncorrelated random mass release rate is introduced in Case 2 in addition to the random transmissivity field. A random mass release rate which is perfectly correlated with random velocity is considered in Case 3. Different combinations of source length (L_1) and width (L_2) are used in each case for studying the impacts of source size on ensemble concentration moments.

4.6.2 Concentration Plume Moments

Figures 4.1 - 4.3 present the simulation results of the mean concentration for Cases 1, 2, and 3 at 85 days after initial source release for different source sizes. Note that the mean plume for Case 2 is identical to Case 1 since the previous analysis shows that a mass release rate that is uncorrelated to the velocity field does not impact the ensemble mean concentration and macrodispersive flux. The Case 1 and Case 2 results are similar to those obtained in the case of the instantaneous uncertain source by Neuman and Zhang (1995d).

Comparison of figures 4.1, 4.2, and 4.3 shows that each of three cases produce very similar ensemble mean plumes. These results suggest that the correlated random mass release rate has little effect on the mean concentration plume spreading due to the small size of the uncertain source zone. Introduction of a correlated uncertain source generates a new term, the cross-covariance between the random velocity and mass release rate fields. However, the impact of this new term on the macrodispersive flux and thus the mean concentration is restricted by the source size because this new term is only non-zero for $\mathbf{x}'$ in the source zone (shown in equation (4.17)). This suggests that for small source zones the source uncertainty may be neglected in the

computation of the ensemble mean concentration in comparison with the velocity field uncertainty.

Inspecting figures 4.1, 4.2, and 4.3 suggests that the deterministic source size can have an important impact on the magnitude of the maximum mean concentration plume for the mass release mechanism studied here. Increasing the source length significantly increases the magnitude of the maximum mean concentration because more solute mass is introduced into the domain. However, this does not affect the rate of spreading (macrodispersion) significantly as indicated in figures 4.4 and 4.5.

Figures 4.4 and 4.5 plot the second normalized moments of the mean concentration plume at x_1 and x_2 directions for each case and each source size. These figures confirm that an uncertain source, either correlated or uncorrelated with the velocity field, has little impact on the rate of spreading in either the longitudinal or lateral directions. These figures also show that increasing the source size in the longitudinal direction increases the magnitude of the second moment in the longitudinal direction but does not affect the rate of spreading (i.e., the macrodispersivity in this direction). Similarly increasing the source size in the lateral direction increases the magnitude of the second moment in the transverse direction but does not affect the rate of spreading. Note that in Figure 4.4 the longitudinal second moment evolution for the 2*2 m and 2*4 m sources are coincident, whereas in Figure 4.5 the transverse second moment evoluation for the 2*2 m and 4*2 m sources are coincident.

Figures 4.6 - 4.8 show simulation results for concentration variances in Cases 1, 2, and 3 at 85 days after planar source release for different source sizes. It should be noted that concentration variance rather than concentration standard deviation is shown here because the linear addition principle can be applied on the former. Under the linear addition principle, total variance of concentration can be decomposed into the variances contributed from the uncertain source and velocity fields respectively. These figures suggest that introduction of an uncorrelated random source slightly

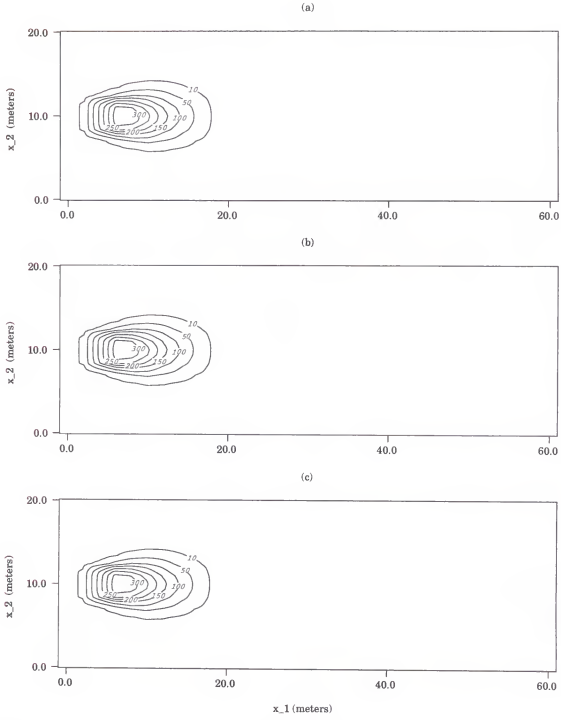

Figure 4.1: (a) Mean Concentration at 85 days after release for Case 1; (b) Mean Concentration at 85 days after release for Case 2; (c) Mean Concentration at 85 days after release for Case 3. Source size is 2.0 meters * 2.0 meters.

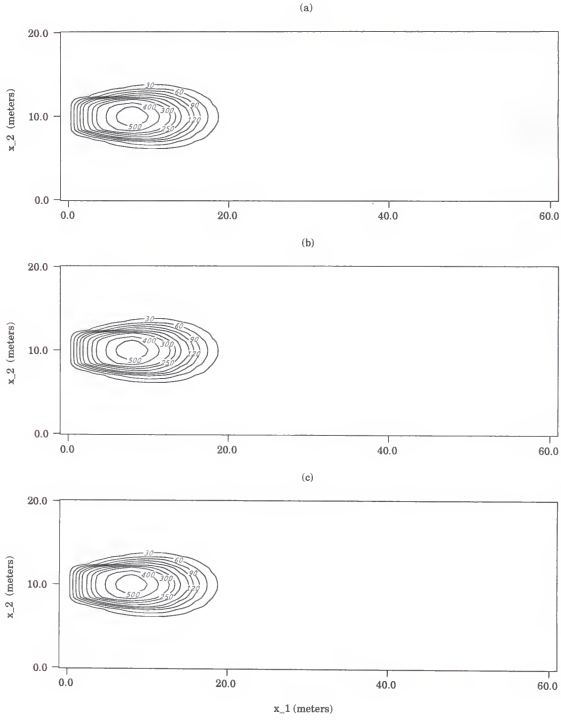

Figure 4.2: (a) Mean Concentration at 85 days after release for Case 1; (b) Mean Concentration at 85 days after release for Case 2; (c) Mean Concentration at 85 days after release for Case 3. Source size is 4.0 meters * 2.0 meters.

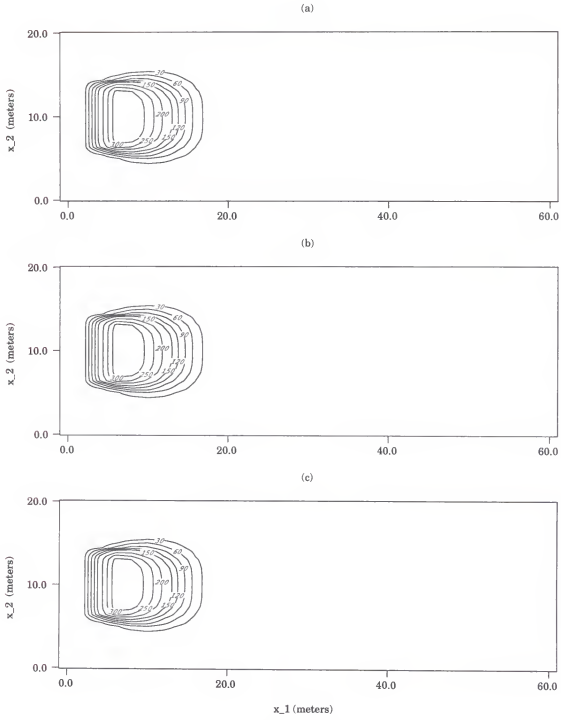

Figure 4.3: (a) Mean Concentration at 85 days after release for Case 1; (b) Mean Concentration at 85 days after release for Case 2; (c) Mean Concentration at 85 days after release for Case 3. Source size is 2.0 meters * 4.0 meters.

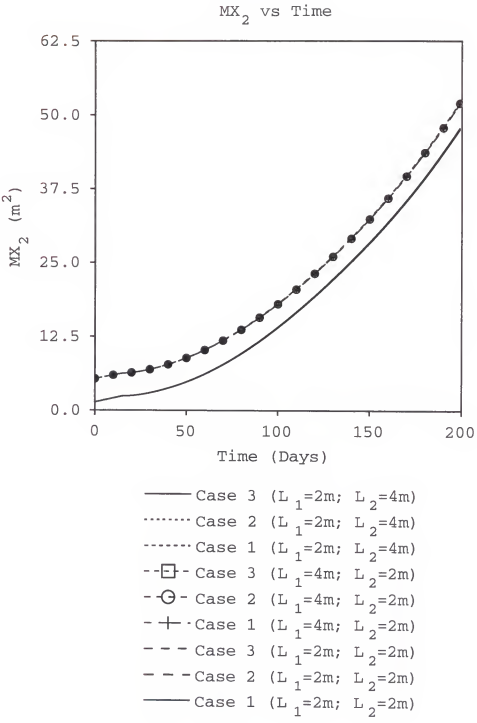

Figure 4.4: The second normalized moments at x_1 direction for each case.

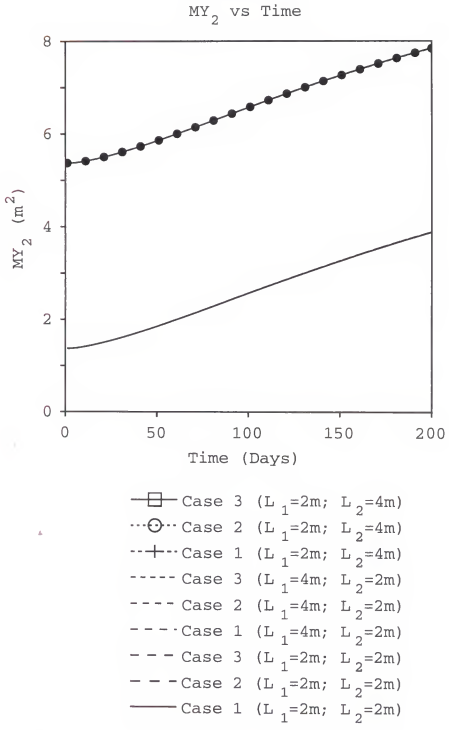

Figure 4.5: The second normalized moments at x_1 direction for each case.

increases the prediction uncertainty of concentration, while the correlated random source produces more prediction uncertainty than the uncorrelated uncertain source does. However, in either case (introduction of uncorrelated or correlated uncertain source) the impact on the magnitude of concentration variance compared to the uncertainty contribution from the random velocity field is not significant. The maximum region of increased concentration prediction uncertainties due to the random source occurs near the source zone. Comparing figures 4.6 and 4.7 suggests that the deterministic source size can have an important impact on the magnitude of the maximum concentration variance for the mass release mechanism studied here. In particular, increasing the source length significantly increases the magnitude of concentration variance while increasing the source width has little impact on the magnitude of concentration variance. This phenomenon is analogous to the observed increase in the magnitude of mean concentration with the increasing length of the uncertain source, i.e., increasing the extent of the source in the longitudinal direction increases the "mass of uncertainty" introduced into the domain.

To investigate the relative contribution of source and groundwater velocity uncertainty to solute transport prediction uncertainty, the total concentration variance can be decomposed into the sum of the concentration variances resulting from random velocity and source strength uncertainty. Figures 4.9 and 4.10 present concentration variances resulting from the different input random fields at 85 days after release for Cases 2 and 3, respectively. Inspecting figure 4.9 indicates that the relative contribution of uncertain source in the uncorrelated case is about 1 percent, while the relative contribution of uncertain source in the correlated case is less than 10 percent.

Figure 4.11 presents the cross-covariance between source strength at the specific point $\mathbf{x}^*$ at the center of the source zone ($\mathbf{x}^*$=(4,10)) and concentration at any point $\mathbf{x}$ throughout domain at 85 days after release for Cases 2 and 3. The plot for

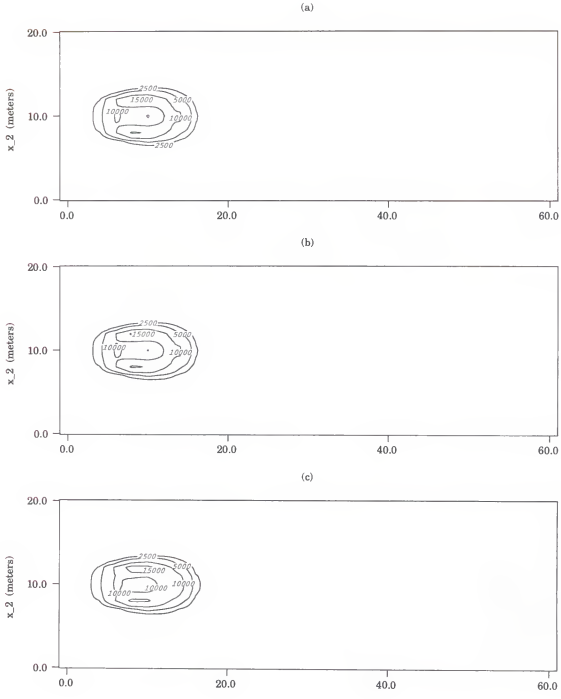

Figure 4.6: (a) Concentration variance at 85 days after release for Case 1; (b) Concentration variance at 85 days after release for Case 2; (c) Concentration Variance at 85 days after release for Case 3. Source size is 2.0 meters * 2.0 meters.

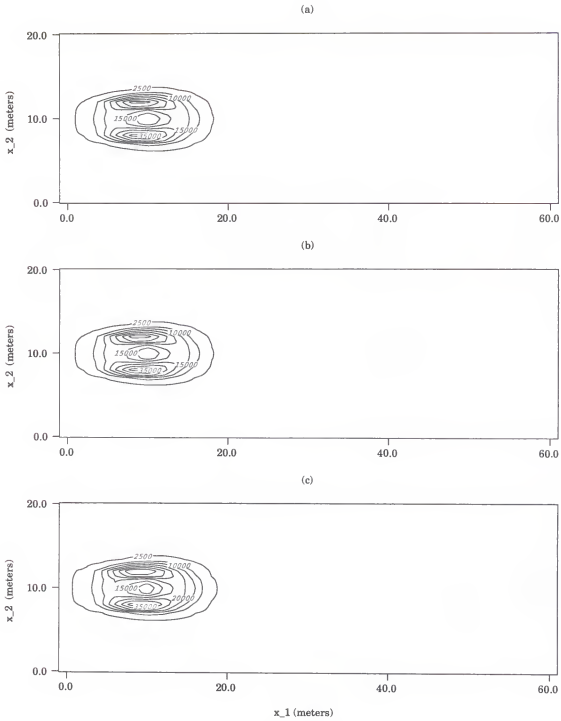

Figure 4.7: (a) Concentration variance at 85 days after release for Case 1; (b) Concentration variance at 85 days after release for Case 2; (c) Concentration Variance at 85 days after release for Case 3. Source size is 4.0 meters * 2.0 meters.

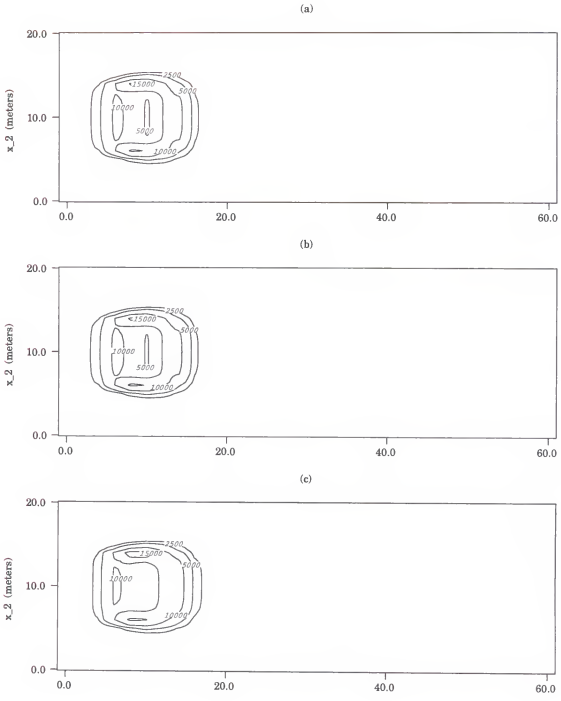

Figure 4.8: (a) Concentration variance at 85 days after release for Case 1; (b) Concentration variance at 85 days after release for Case 2; (c) Concentration Variance at 85 days after release for Case 3. Source size is 2.0 meters * 4.0 meters.

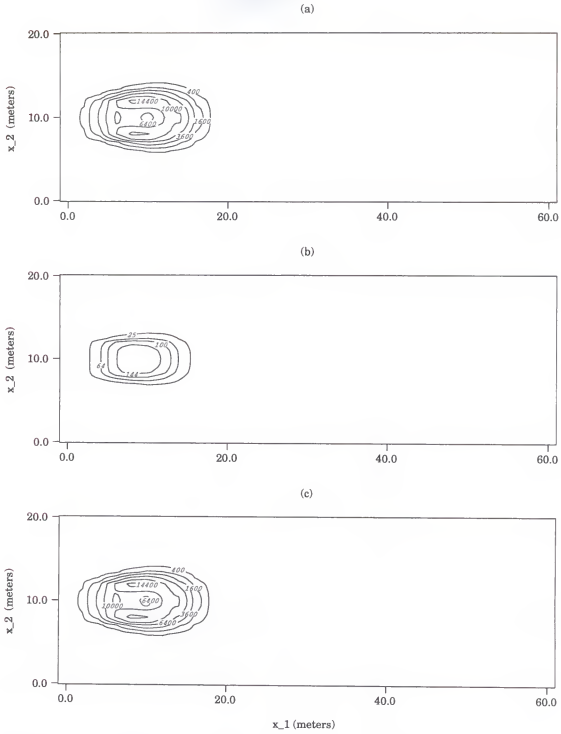

Figure 4.9: (a) Concentration variance resulting from the random velocity field at 85 days after release for Case 2; (b) Concentration variance resulting from the random contaminant source field at 85 days after release for Case 2; (c) Total concentration Variance at 85 days after release for Case 2. Source size is 2.0 meters * 2.0 meters.

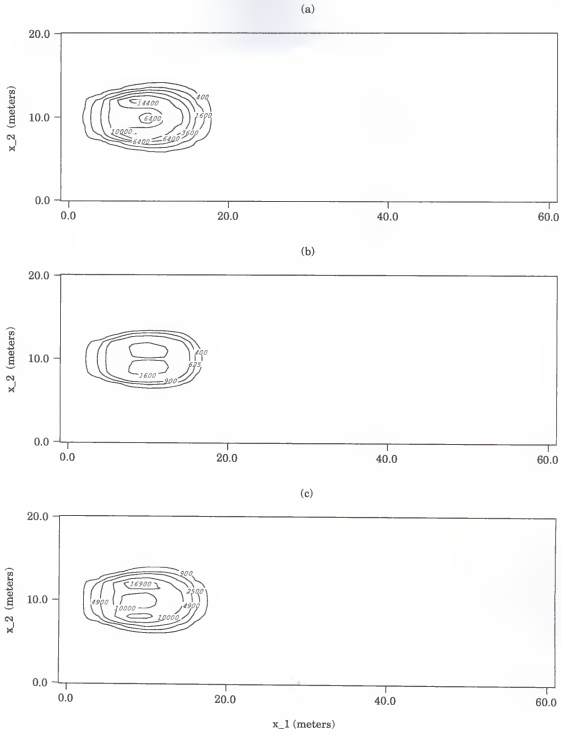

Figure 4.10: (a) Concentration variance resulting from the random velocity field at 85 days after release for Case 3; (b) Concentration variance resulting from the random contaminant source field at 85 days after release for Case 3; (c) Total concentration Variance at 85 days after release for Case 3. Source size is 2.0 meters * 2.0 meters.

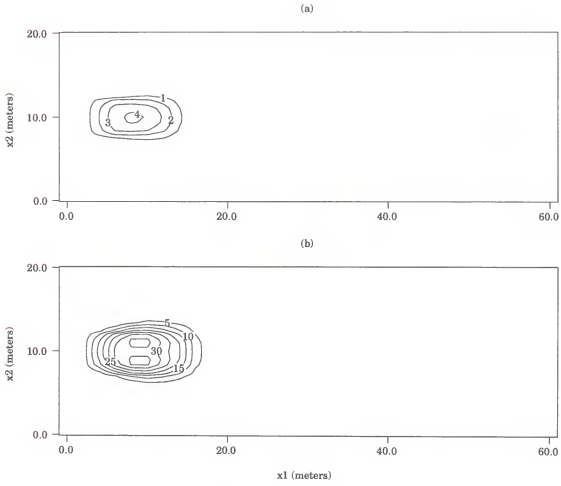

Figure 4.11: Cross-covariance between source strength in the source zone and concentration throughout the domain at 85 days after release for Cases 2 (a) and 3 (b); $\mathbf{x}^*$ =(4,10); Source size is 2.0 meters * 2.0 meters.

Case 2 (figure 4.11.(a)) shows that, for the source that is uncorrelated with velocity, correlation of the source with local concentrations are small in magnitude but are stronger along the mean flow direction than along the lateral direction, with the maximum covariance values near the point $\mathbf{x}^*$. The Case 3 results, for the source that is correlated with velocity, show larger magnitude and spatial extent of the correlation of source with local concentration. Figure 4.12 presents the cross-covariance between source strength at a point $\mathbf{x}^*$ located at the edge of the source zone ($\mathbf{x}^*$=(4,12)) and concentration at any point $\mathbf{x}$ throughout domain at 85 days after release for Cases

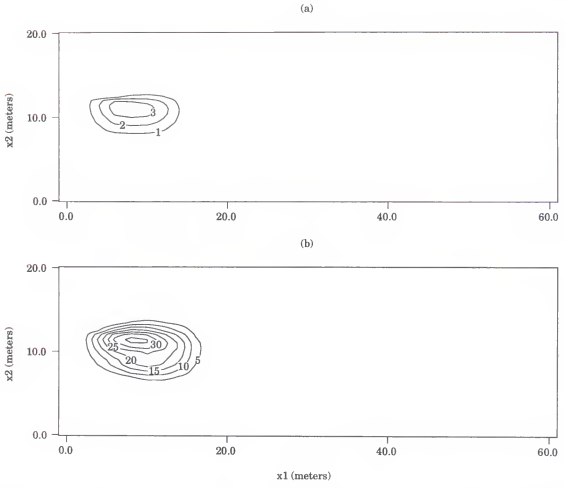

Figure 4.12: Cross-covariance between source strength in the source zone and concentration throughout the domain at 85 days after release for Cases 2 (a) and 3 (b); $\mathbf{x}^*$ =(4,12); Source size is 2.0 meters * 2.0 meters.

2 and 3. Comparing figures 4.11 and 4.12 shows that the cross-covariance plume $J_{\phi c}(\mathbf{x}^*, t^*, \mathbf{x}, t)$ is asymmetric around the center of mass, which reflects the fact that $\mathbf{x}^*$ is more correlated with local concentrations at points on the same side of the source zone than with the concentration at points on the other side of the source zone.

4.7 Summary

This chapter deals with stochastic analysis of solute transport in heterogeneous aquifers subject to a spatiotemporally random source field. The continuous

mass-release rate in the source zone is assumed to be a random field which is either perfectly correlated or uncorrelated with the random velocity field. General solution expressions for statistical moments of concentration subject to the spatiotemporally variable velocity and spatiotemporally variable mass release rate fields are derived using Laplace-Fourier transform techniques, assuming that the mean mass release rate is temporally constant, and the mean velocity is spatially uniform. These equations are solved by a fast Fourier algorithm in the Laplace and Fourier domain.

As an illustrative example, the continuous mass-release rate in the source zone is assumed to be a spatially random field which is either perfectly correlated or uncorrelated with the spatially random steady state velocity field, assuming divergence free flow. The resulting steady-state unconditional velocity cross-covariance functions were incorporated into the fast Fourier transform algorithm to compute the concentration moments.

The following conclusions are made based on the simulation results.

1) Whether the random mass release rate is uncorrelated or perfectly correlated with velocity field, the random source causes little impact on the ensemble mean concentration plume spreading. This is similar to the result obtained by Zhang and Neuman (1995d) who analyzed concentration moments assuming a random initial condition which was uncorrelated with the local velocity field. This work extends Zhang and Neuman's result to a continuous source, and to the case in which the uncertain source is perfectly correlated with the velocity field.

2) The size of source zone has an important effect on the magnitude of the concentration moments for the mass release mechanism studied here. Increasing the length of source in the flow direction causes an increase in the magnitude of the mean and variance of concentrations as more solute mass and uncertainty are introduced into the domain. However, increasing source size (either in longitudinal

or lateral direction) does not affect the rate of spreading of the mean plume (i.e., the macrodispersivity in either the longitudinal or lateral direction).

3) A new term, the covariance between random mass release rate and concentration, is derived. This term characterizes the correlation between mass release rate in the source zone and concentration throughout the simulated region and serves to transfer the mass release rate uncertainty to the concentration prediction uncertainty. It is worthwhile to mention that the cross-covariance between uncertain mass release rate and concentration in domain can be used to optimally estimate or condition source strength if aqueous phase concentrations are available downstream of an uncertain source.

4) The correlated random mass release rate produces a higher concentration variance than the uncorrelated mass release rate does. However, the introduction of the random mass release rate does not significantly increase the uncertainty of concentration prediction for solute transport, particularly for the small sources. The maximum region of increased concentration prediction uncertainty due to the random source occurs near the source zone.

5) Characteristics for contaminant source uncertainty in aquifers can be numerous. This study focused on investigating the impacts of mass release rate uncertainty and the correlation between mass release and velocity fields on solute transport moments in aquifers. However, as this study showed, the source size has an important effect on plume configuration. The impacts of uncertainties of source size and location on plume moments deserves further investigation.

CHAPTER 5
SUMMARY AND CONCLUSIONS

5.1 Assumptions and Limitations

This dissertation focuses on stochastic analysis of flow and inert solute transport in two-dimensional heterogeneous aquifers subject to random recharge (steady and transient) and random contaminant source fields. The primary goal of this work is to integrate the natural variablity of transmissivity, recharge, and contaminant source into an advective-dispersive stochastic model to investigate the impacts of these random fields on the mean distributions and prediction errors for head, velocity, and solute concentration in saturated confined aquifers or unconfined aquifers. The resulting model should be applicable to many practical situations and provide a useful tool for understanding physical phenomena related to flow and solute transport at the field-scale, for intepreting the field data, and in selecting management options.

An Eulerian perturbation framework is utilized in this research, in which water flow is described by Darcy's law and solute transport is governed by the classical advection-dispersion equation. Transmissivity, spatially and spatio-temporally variable recharge, and contaminant mass release rate are assumed to be the input random fields with known mean values and auto-covariance structures. Decomposing all input random fields into mean values and small perturbations around the mean values allows the derivation of the resulting mean and perturbation equations for head, velocity, and concentration fields. Multiplying the first-order perturbation equations by the same or other perturbed variables at another independent location and time (used in the Chapter 2) or at the same location and time (in Chapters 3 and 4) generates second-order moment equations. These second-order moment equations in

conjunction with the mean-value equations, describe the mean head, velocity, and concentration behavior, and the propagation of prediction uncertainties throughout the spatial and temporal domain of concern.

The first-order approximation is applied throughout this work, based on the plausible argument that perturbation products are an order of magnitude smaller than the perturbations themselves and therefore can be neglected [Deng et al., 1993; Kapoor and Gelhar, 1994a]. The results of Ababou et al. (1988), who investigated the limitations of the small-perturbation on evaluating head-variance, show that the perturbation theroy is astoundingly robust and that the first-order approximation theory provides a reasonable estimate even for very heterogeneous media ($\sigma_Y \geq 2.3$). However, the results of this research are more applicable in mildly heterogeneous media ($\sigma_Y < 1$).

For the convenience of deriving closed-form solutions for the head and velocity covariance and cross-covariances, the flow domain is assumed to be infinite in space (i.e., far from any boundaries, in Chapters 2, 3, and 4) and time (i.e., far from any fixed initial condition, in Chapter 3). This is reasonable if the domain is sufficiently large compared to the head correlation scale [Graham and Tankersley, 1994; Rubin and Dagan, 1987a; Dagan, 1989] and sufficient time has elapsed since any known initial head condition. For the hole-type covariance used in this research, the boundary effects (or the effects of initial condition) can be neglected for head variance after a practical distance of around 10λ (log transmissivity correlation scale) from the boundary [Gelhar, 1993].

Under the assumption of no correlation between the log-transmissivity and recharge fields, Fourier transform techniques are used to derive a set of closed-form solutions for the first-order, approximate, unconditional head covariance, head-log transmissivity cross-covariance, head-recharge cross-covariance, velocity covariance, velocity-head cross-covariance, and velocity-log-transmissivity cross-covariance for

a two-dimensional spatially random transmissivity field subject to a steady-state spatially variable recharge and nonuniform (i.e., linear trending) velocity (Chapter 2). Further efforts were then made to find similar solutions for the transient non-uniform velocity field which results from spatially random transmissivity and spatio-temporally random recharge fields. A set of semi-analytical solutions were derived for the unconditional moments of head and velocity for the transient case using similar Fourier transform techniques (Chapter 3).

The assumption that transmissivity and recharge are uncorrelated should be applicable to confined aquifers or deeper unconfined aquifers. For the former case, the recharge infiltrating into confined aquifers is governed by the vertical head gradient across, and the hydraulic conductivity within, the upper confining unit. In many cases, the confining unit and the aquifer of interest can be expected to have uncorrelated properties. In the latter case, the correlation of recharge and soil properties is likely to be dampened as recharge travels through the unsaturated zone. Furthermore, equations 2.3 and 2.4 suggest that a perfectly positive correlation between the transmissivity and recharge fields reduces the cross-covariance between head and recharge and the cross-covariance between head and transimissivity. Thus, a perfectly positive correlation between transmissivity and recharge will reduce the head variance. Analogously, a perfectly negative correlation will increase head variance. In the case of positive correlation between transmissivity and recharge fields, high recharge areas will occur near high transmissivity areas, which will tend to produce smaller spatial head gradients and thus smaller head variances. In the case of negative correlation between transmissivity and recharge fields, however, high recharge areas will occur near low transmissivity areas which will tend to increase the spatial head gradient and thus increase the head variance. Quantifying the impacts of correlation between recharge and transimissivty on the head, velocity, and solute transport will require

specification of the mathematical relationship between transmissivity and recharge fields.

Hole-type covariance functions [Graham and McLaughlin, 1989a; Mizell, 1982] were selected for the input log-transmissivity and recharge random fields in order to obtain finite closed-form solutions for all the flow-related covariances. The assumption of a more simple exponential input covariance structure in two-dimensional analyses has been shown to result in unbounded head covariances [Dagan, 1989]. However, it should be noted that even for exponential log-transmissivity covariance functions the resulting head variogram is finite, and thus the velocity covariances can be defined [Rubin and Bellin, 1994]. The agreement of the velocity covariances presented in Chapter 2 with those derived by Rubin and Bellin (1994) indicates that the form of the underlying covariance function is not important when evaluating the ensemble moments of the resulting velocity and concentration fields.

Finally, this work is a two-dimensional analysis for flow and solute transport, in which Dupuit assumptions are implied when it is applied to unconfined aquifers, i.e., the flow is horizontal and vertical head gradient can be neglected. This assumption suggests that the results of this research may be applicable for shallow aquifers where groundwater flow can be approximated as horizontal flow.

5.2 Conclusions and Applications

5.2.1 Spatio-temporally Random Recharge

The following conclusions, which may have many potential practical applications, are reached from the steady-state and transient recharge analyses.

1) Steady-state head and velocity moments reveal that introduction of a constant mean recharge term into the steady-state infinite domain flow problem causes the head and velocity fields to become nonstationary, i.e., the mean and covariance functions become dependent on location. This result implies that ergodicity is not

valid for head and velocity fields subject to a constant mean recharge. Therefore, spatial measurements of head or velocity are insufficient to estimate the ensemble mean and/or covariance of head or velocity unless the spatial trend is known a prior and taken into account. It is necessary to utilize a stochastic model which can incorporate the nonstationary phenomenon to intepret field data or design sampling schemes in groundwater systems where the effects of recharge can not be neglected.

2) The head and velocity covariances and cross-covariances provide measures of correlation between two observations within one random field or between two random fields. Thus, covariances contain important information related to how far information from one observation may be extrapolated, which can provide guidance in designing sampling schemes. Cross-covariances can be used to condition the predictions of one random field using the observations of another related random field. The cross-covariance for head-log-transmissivity may be particularly valuable in determining the dense or sparse sampling schemes for transmissivity or head observations. This is significant since the cost associated with obtaining head is generally lower than that associated with obtaining saturated hydraulic conductivity or transmissivity data.

3) Introduction of deterministic recharge produces a mean velocity gradient which significantly affects the spreading of the plume in the longitudinal direction. A positive recharge increases the velocity along the mean flow direction, and enhances the plume spreading in the longitudinal direction. A negative recharge slows the movement of the mean plume and reduces the longitudinal spreading. Introduction of spatially or spatio-temporally variable recharge enhances the spreading of plume, particularly in the lateral direction. This result provides an explanation for the larger transverse macrodispersivity observed at the field-scale when hydraulic conductivity is assumed to be the only random field [Freyberg, 1986; Leblanc et al., 1991]. Although it has been shown that the heterogeneity of hydraulic conductivity provides

a reasonable explanation for field-scale longitudinal macrodispersivity, it fails to explain the magnitude of macrodispersivity in the lateral direction. Understanding that uncertain recharge enhances head and velocity variation in the transverse direction and thus increases the lateral deviation of concentration plume from the mean flow direction helps to identify sampling locations where additional samples could be taken to improve the estimate of the extent of a contaminant plume.

4) Uncertainty in the spatial or spatio-temporal distribution of recharge also increases the extent of the ensemble standard deviation plume, particularly in the lateral direction, and increases the coefficient of variation of solute concentration. The uncertainty in the prediction of solute transport increases with increasing recharge variance and spatial and temporal correlation scale. Higher recharge correlation scales (either spatial or temporal) increase both the ensemble plume spreading and the ensemble plume variance in the absence of site-specific measurements, similar to the effect that log-transmissivity correlation scale has on the ensemble plume behavior. However, it should be noted that if site-specific measurements are available prediction uncertainty can be reduced considerably by conditioning with a random field with a larger correlation scale.

5) Comparing the head and velocity moments for steady and transient flow reveals that both the steady-state random recharge and the spatially uniform, temporally random recharge are special cases of the transient flow case. As the temporal recharge correlation scale in the transient case approaches infinity, the transient flow moments approach the steady-state flow moments. As the spatial recharge correlation scale in the transient case approaches infinity the transient flow moments approach the flow moments resulting from deterministic recharge. Thus, the steady-state random recharge case provides an upper bound, and spatially uniform transient recharge provides a lower bound on the flow-field uncertainty.

6) Spatio-temporally random recharge has a smaller effect on the mean concentration plume spreading and concentration prediction uncertainty than steady-state, spatially random recharge. The difference between the spatio-temporally and the spatially random recharge depends on the temporal correlation scale of the recharge field. Increasing the temporal correlation scale increases the velocity variance and covariance, thus increasing the solute concentration spreading and concentration prediction uncertainty. As the temporal correlation scale approaches infinity, the spatio-temporally random recharge case approaches the spatially random recharge case. This result may have two physical applications. For shallow unconfined aquifers, temporal recharge fluctuations may be attenuated little when travelling through the unsaturated zone. In this case, the spatiotemporally variable recharge will have a small temporal correlation scale, and may be approximated as the lower bound case (spatially uniform transient recharge) to simplify the analysis. The other case is related to deeper unconfined aquifers, where recharge variation may be significantly dampered by the overlying porous medium, and thus may have a large temporal correlation scale. Therefore, the spatio-temporally variable recharge will have a large impact on solute transport, and may be approximated as the upper bound case (steady-state spatially random recharge). For the example studied here, the magnitude of difference between these lower and upper bounds is approximately 40 percent for the head variance.

5.2.2 Spatio-temporally Random Contaminant Source

The study of the analysis of uncertain contaminant sources suggests:

1) Whether the uncertain mass release rate is correlated or uncorrelated with the velocity field, the uncertain source produces little impact on the ensemble mean concentration plume spreading. This confirms a similar result obtained by Zhang and Neuman (1995d) for the case where the initial concentration and velocity fields were considered to be uncorrelated random fields. This can be explained by the fact that

the mean concentration plume spreading is controlled by the local dispersion and macrodispersion. When the uncertain source is uncorrelated with the velocity field, the source uncertainty does not impact the macrodispersion or the mean concentration plume spreading. When the uncertain source is correlated with random velocity field, it impacts the macrodispersion slightly around the source zone, but has little impact on the macrodispersive flux away from the source zone.

2) The size of source zone has an important effect on the concentration variance for the mass release mechanism studied here. Increasing the source length increases the magnitude of concentration variance, however, increasing the source width has little impact on the magnitude of concentration variance. However, increasing source size (either in longitudinal or lateral direction) does not affect the rate of spreading (i.e., the macrodispersivity in either the longitudinal or the lateral direction).

3) The cross-covariance between random mass release rate and solute concentration was derived to characterize the correlation between these variables. This term serves to transfer the mass release rate uncertainty to the concentration prediction uncertainty, and depends on the correlation between the source and the local velocity field. The cross-covariance between uncertain mass release rate and concentration at any other place or time in the domain may be useful for field applications where it is desirable to estimate source strength from downstream aqueous phase contaminant concentrations. This is particularly important for characterizing the spatial distribution of existing contaminant source zones which may be necessary for designing remediation strategies or for assessing public health risks from groundwater contamination.

4) The introduction of an uncertain source (or random mass release rate) does not significantly increase the uncertainty of concentration prediction for solute transport, particularly for small sources. An uncertain source slightly increases concentration prediction uncertainty near the source zone. This increase is more pronounced

for sources that are correlated with the local velocity fields than for uncorrelated source fields.

5.3 Suggestions for Future Research

Using the fast Fourier transform algorithm to investigate the uncertainty of solute transport in heterogeneous media is computationally more efficient than other techniques such as direct integration and finite element methods. However, the fast Fourier transform approach overestimates the prediction uncertainty around the center of mass because the variance dissipation term is neglected. Therefore further research needs to be done to efficiently evaluate the spatio-temporally variable variance dissipation term resulting from nonstationary concentration fields. Since the fast Fourier transform approach cannot evaluate the full covariance of concentration, more work should be done to develop a general scheme to evaluate the full second moments.

The solute-related moments in the transient flow regime were evaluated assuming zero mean recharge ($\bar{R} = 0$). Incorporating the effects of $\bar{R} \neq 0$ into the solute transport analysis produces a mean velocity gradient along the mean flow direction which primarily affects mean plume spreading in the longitudinal direction [Li and Graham, 1998]. However, performing a rigorous analysis of the effects of $\bar{R} \neq 0$ within the fast Fourier transform algorithm requires an analytic expression for the transfer function appropriate for the non-uniform velocity field which results from the mean constant recharge. This may deserve further effort due to the computational efficiency of the fast Fourier transform method. Rubin and Bellin (1994)'s time transformation approach, however, provides a simple, approximate relationship between concentration field moments with non-zero and zero mean recharge for the steady state flow case. The accuracy of this approximation for the transient flow case should be investigated.

Causes of contaminant source uncertainty in aquifers can be numerous. This study focused only on investigating the impacts of uncertain mass release rate on solute transport moments in aquifers. The impacts of uncertainties of source size and location on plume moments deserve further investigation. Finally, this work was based on the small perturbation assumption, which restricts this method to input random fields with small variance. Further effort is required to evaluate higher-order approximations to both the flow and transport moment equations in order to relax this assumption.

APPENDIX A
DERIVATION FOR THE HEAD-RELATED STATISTICS

A.1 Fourier Transform

The following Fourier Transform is used in deriving the head-log transmissivity cross-covariance, head covariance, head-velocity cross-covariance, and velocity cross-covariance and others in Chapters 2 and 3.

The Fourier transform equations for a n-dimensionally spatial function $f(\mathbf{x})$ can be expressed as:

$$\begin{aligned} F(\mathbf{k}) &= \frac{1}{(2\pi)^n} \int_{-\infty}^{\infty} f(\mathbf{x}) e^{-i\mathbf{k}\mathbf{x}} d\mathbf{x} = \mathcal{F}[f(\mathbf{x})] \\ f(\mathbf{x}) &= \int_{-\infty}^{\infty} F(\mathbf{k}) e^{i\mathbf{k}\mathbf{x}} d\mathbf{k} = \mathcal{F}^{-1}[F(\mathbf{k})] \end{aligned} \tag{A.1}$$

in which $\mathcal{F}$ and $\mathcal{F}^{-1}$ represent forward and inverse Fourier transform operators; $\mathbf{k}$ and $\mathbf{x}$ are n-dimensional wave and location vectors, respectively.

A.2 Basic Equations

In deriving the head-log transmissivity cross-covariance, following relationships about Bessel functions $J_m(x)$ and modified Bessel functions $K_n(x)$ are repeatedly used, in which m and n represent integer orders for corresponding Bessel functions [Mizell et al., 1982; Abramowitz and Stegun, 1970, pp. 376, 484, 488]:

$$\int_0^{2\pi} e^{ik\xi\cos\theta} d\theta = 2\pi J_0(k\xi) \tag{A.2}$$

$$\frac{dJ_0(x)}{dx} = -J_1(x) \tag{A.3}$$

$$\int_0^\infty J_0(k\xi)d\xi = \frac{1}{k} \tag{A.4}$$

$$\int_0^\infty \frac{k^{m+1}J_m(k\xi)dk}{(k^2+\alpha^2)^{n+1}} = \frac{\xi^n\alpha^{m-n}K_{n-m}(\alpha\xi)}{n!2^n} \tag{A.5}$$

$$\alpha\xi K_{n+1}(\alpha\xi) = 2nK_n(\alpha\xi) + \alpha\xi K_{n-1}(\alpha\xi) \tag{A.6}$$

$$\frac{dx^nK_n(x)}{dx} = -x^nK_{n-1}(x) \tag{A.7}$$

$$\int_0^\xi xK_0(\alpha x)dx = \frac{1}{\alpha^2} - \frac{\xi}{\alpha}K_1(\alpha\xi) \tag{A.8}$$

$$\int_{-\infty}^{\infty}\int_{-\infty}^{\infty} e^{i(k_1\xi_1+k_2\xi_2)}g(k)dk_1dk_2 = 2\pi\int_0^\infty kJ_0(k\xi)g(k)dk \tag{A.9}$$

where $k^2 = k_1^2 + k_2^2$ and $\xi^2 = \xi_1^2 + \xi_2^2$.

A.3 P_{HY} derivation

Letting $\xi_1 = x_1 - x_1'$ and $\xi_2 = x_2 - x_2'$ and substituting equation (2.6) into equation (2.4) leads to:

$$\frac{\partial^2 P_{HY}(\xi, x_1', x_2')}{\partial\xi_i^2} - (\bar{R}e^{-\bar{Y}}x_1 + J_0)\frac{\partial P_{YY}(\xi)}{\partial\xi_1} - \bar{R}e^{-\bar{Y}}P_{YY}(\xi) = 0 \tag{A.10}$$

in which ξ_i represents the separate distance in the i direction, and the recharge and log-transmissivity are assumed to be uncorrelated.

Using equations (A.6)-(A.7) and differentiating P_{YY} in equation (2.16) with respect to ξ_1 yields:

$$\frac{\partial P_{YY}(\xi)}{\partial \xi_1} = \sigma_Y^2 \left[-3\alpha_Y^2 \xi_1 K_0(\alpha_Y \xi) + \frac{3}{2}\alpha_Y^3 \xi_1 \xi K_1(\alpha_Y \xi) - \frac{\alpha_Y^4 \xi_1 \xi^2 K_2(\alpha_Y \xi)}{8} \right] \tag{A.11}$$

Therefore:

$$\begin{aligned}
&(\bar{R}e^{-\bar{Y}} x_1 + J_0) \frac{\partial P_{YY}(\xi)}{\partial \xi_1} \\
&\quad = (\bar{R}e^{-\bar{Y}} \xi_1 + \bar{R}e^{-\bar{Y}} x_1' + J_0) \frac{\partial P_{YY}(\xi)}{\partial \xi_1} \\
&\quad = \bar{R}e^{-\bar{Y}} \sigma_Y^2 \\
&\qquad \left[-3\alpha_Y^2 \xi_1^2 K_0(\alpha_Y \xi) + \frac{3}{2}\alpha_Y^3 \xi_1^2 \xi K_1(\alpha_Y \xi) - \frac{\alpha_Y^4 \xi_1^2 \xi^2 K_2(\alpha_Y \xi)}{8} \right] \\
&\quad + (\bar{R}e^{-\bar{Y}} x_1' + J_0) \sigma_Y^2 \\
&\qquad \left[-3\alpha_Y^2 \xi_1 K_0(\alpha_Y \xi) + \frac{3}{2}\alpha_Y^3 \xi_1 \xi K_1(\alpha_Y \xi) - \frac{\alpha_Y^4 \xi_1 \xi^2 K_2(\alpha_Y \xi)}{8} \right]
\end{aligned} \tag{A.12}$$

Performing the Fourier transform of equation (A.10) with respect to ξ_1 and ξ_2, we have:

$$S_{HY}(\mathbf{k}, x_1', x_2') = -\frac{\mathcal{F}\left[(\bar{R}e^{-\bar{Y}} \xi_1 + \bar{R}e^{-\bar{Y}} x_1' + J_0) \frac{\partial P_{YY}(\xi)}{\partial \xi_1} + \bar{R}e^{-\bar{Y}} P_{YY}(\xi) \right]}{k^2} \tag{A.13}$$

Using equations (A.9) and (A.5), we can evaluate:

$$\begin{aligned}
&\mathcal{F}\Big[(\bar{R}e^{-\bar{Y}} \xi_1 + \bar{R}e^{-\bar{Y}} x_1' + J_0) \frac{\partial P_{YY}(\xi)}{\partial \xi_1} \Big] \\
&= \bar{R}e^{-\bar{Y}} \sigma_Y^2 \mathcal{F}\Big[-3\alpha_Y^2 \xi_1^2 K_0(\alpha_Y \xi) + \frac{3}{2}\alpha_Y^3 \xi_1^2 \xi K_1(\alpha_Y \xi) - \frac{1}{8}\alpha_Y^4 \xi_1^2 \xi^2 K_2(\alpha_Y \xi) \Big] \\
&+ (\bar{R}e^{-\bar{Y}} x_1' + J_0) \sigma_Y^2 \\
&\mathcal{F}\Big[-3\alpha_Y^2 \xi_1 K_0(\alpha_Y \xi) + \frac{3}{2}\alpha_Y^3 \xi_1 \xi K_1(\alpha_Y \xi) - \frac{1}{8}\alpha_Y^4 \xi_1 \xi^2 K_2(\alpha_Y \xi) \Big] \\
&= \frac{\bar{R}e^{-\bar{Y}} \sigma_Y^2 \alpha_Y^2}{2\pi} \left[\frac{24 k_1^2 k^2 (k^2 - \alpha_Y^2)}{(k^2 + \alpha_Y^2)^5} - \frac{6k^4}{(k^2 + \alpha_Y^2)^4} \right] \\
&+ \frac{(\bar{R}e^{-\bar{Y}} x_1' + J_0) \sigma_Y^2 \alpha_Y^2}{2\pi} \left[\frac{6ik_1 k^4}{(k^2 + \alpha_Y^2)^4} \right]
\end{aligned} \tag{A.14}$$

Similarly, we have:

$$\mathcal{F}\left[\bar{R}e^{-\bar{Y}}P_{YY}(\xi)\right] = \bar{R}e^{-\bar{Y}}\frac{6\sigma_Y^2\alpha_Y^2}{2\pi}\left[\frac{k^4}{(k^2+\alpha_Y^2)^4}\right] \tag{A.15}$$

Substituting equations (A.14) and equations (A.15) into equation (A.13) yields:

$$\begin{aligned}
S_{HY}(\mathbf{k}, x_1', x_2') =& -\frac{\mathcal{F}\left[(\bar{R}e^{-\bar{Y}}\xi_1 + \bar{R}e^{-\bar{Y}}x_1' + J_0)\frac{\partial P_{YY}(\xi)}{\partial \xi_1} + \bar{R}e^{-\bar{Y}}P_{YY}(\xi)\right]}{k^2} \\
=& -\frac{\bar{R}e^{-\bar{Y}}\sigma_Y^2\alpha_Y^2}{2\pi}\left[\frac{24k_1^2(k^2-\alpha_Y^2)}{(k^2+\alpha_Y^2)^5} - \frac{6k^2}{(k^2+\alpha_Y^2)^4}\right] \\
& -\frac{(\bar{R}e^{-\bar{Y}}x_1' + J_0)\sigma_Y^2\alpha_Y^2}{2\pi}\left[\frac{6ik_1k^2}{(k^2+\alpha_Y^2)^4}\right] \\
& -\bar{R}e^{-\bar{Y}}\frac{\sigma_Y^2\alpha_Y^2}{2\pi}\left[\frac{6k^2}{(k^2+\alpha_Y^2)^4}\right] \\
=& -\frac{\bar{R}e^{-\bar{Y}}\sigma_Y^2\alpha_Y^2}{2\pi}\left[\frac{24k_1^2(k^2-\alpha_Y^2)}{(k^2+\alpha_Y^2)^5}\right] \\
& -\frac{(\bar{R}e^{-\bar{Y}}x_1' + J_0)\sigma_Y^2\alpha_Y^2}{2\pi}\left[\frac{6ik_1k^2}{(k^2+\alpha_Y^2)^4}\right]
\end{aligned} \tag{A.16}$$

Performing the inverse Fourier transform, we have:

$$\begin{aligned}
P_{HY}(\xi, x_1', x_2') =& -\frac{\bar{R}e^{-\bar{Y}}\sigma_Y^2\alpha_Y^2}{2\pi}\mathcal{F}^{-1}\left[\frac{24k_1^2(k^2-\alpha_Y^2)}{(k^2+\alpha_Y^2)^5}\right] \\
& -\frac{(\bar{R}e^{-\bar{Y}}x_1' + J_0)\sigma_Y^2\alpha_Y^2}{2\pi}\mathcal{F}^{-1}\left[\frac{6ik_1k^2}{(k^2+\alpha_Y^2)^4}\right] \\
=& 6\sigma_Y^2\alpha_Y^2(\bar{R}e^{-\bar{Y}}x_1' + J_0)\left[\frac{\xi_1\xi K_1(\alpha_Y\xi)}{8\alpha_Y} - \frac{\xi_1\xi^2K_2(\alpha_Y\xi)}{48}\right] \\
& +6\bar{R}e^{-\bar{Y}}\sigma_Y^2\alpha_Y^2\Big[\frac{\xi^3K_3(\alpha_Y\xi)}{48\alpha_Y} - \frac{\xi^2K_2(\alpha_Y\xi)}{12\alpha_Y^2} \\
& +\frac{\xi_1^2\xi K_1(\alpha_Y\xi)}{12\alpha_Y} - \frac{\xi_1^2\xi^2K_2(\alpha_Y\xi)}{48}\Big]
\end{aligned} \tag{A.17}$$

A.4 P_{HH} derivation

Applying $\xi_1 = x_1 - x_1'$, $\xi_2 = x_2 - x_2'$ and inserting equation (2.6) into equation (2.5) gives:

$$\frac{\partial^2 P_{HH}(\xi,x_1',x_2')}{\partial \xi_i^2} - (\bar{R}e^{-\bar{Y}}x_1 + J_0)\frac{\partial P_{YH}(\xi,x_1',x_2')}{\partial \xi_1} - \bar{R}e^{-\bar{Y}}P_{YH}(\xi,x_1',x_2') + e^{-\bar{Y}}P_{RH}(\xi) = 0 \quad \text{(A.18)}$$

in which same notations and assumptions are implied as the derivation of P_{HY}.

Performing the Fourier transform of equation (A.18) with respect to ξ_1 and ξ_2, we have:

$$\begin{aligned} S_{HH}(\mathbf{k},x_1',x_2') = &-\frac{\mathcal{F}\left[(\bar{R}e^{-\bar{Y}}\xi_1 + \bar{R}e^{-\bar{Y}}x_1' + J_0)\frac{\partial P_{YH}(\xi,x_1',x_2')}{\partial \xi_1}\right]}{k^2} \\ &-\frac{\mathcal{F}\left[\bar{R}e^{-\bar{Y}}P_{YH}(\xi,x_1',x_2')\right]}{k^2} \\ &+\frac{\mathcal{F}\left[e^{-\bar{Y}}P_{RH}(\xi)\right]}{k^2} \end{aligned} \quad \text{(A.19)}$$

Graham and Tankersley (1994) derived

$$P_{HR}(\xi) = P_{RH}(\xi) = 6\sigma_R^2 e^{-\bar{Y}}\left[\frac{\xi^2 K_2(\alpha_R\xi)}{8} - \frac{\alpha_R\xi^3 K_3(\alpha_R\xi)}{48}\right] \quad \text{(A.20)}$$

Therefore:

$$\frac{\mathcal{F}\left[e^{-\bar{Y}}P_{RH}(\xi)\right]}{k^2} = \frac{6\sigma_R^2\alpha_R^2 e^{-2\bar{Y}}}{2\pi(k^2+\alpha_R^2)^4} \quad \text{(A.21)}$$

It should be noted that $P_{YH}(\xi,x_1',x_2') \neq P_{HY}(\xi,x_1',x_2')$. However, $P_{YH}(\xi,x_1',x_2')$ can be derived from $P_{HY}(\xi,x_1',x_2')$ since $P_{YH}(\xi,x_1',x_2')$=$P_{YH}(-\xi,x_1,x_2)$. Using equation (A.17), we obtain:

$$\begin{aligned} P_{YH}(\xi,x_1',x_2') =& 6\sigma_Y^2\alpha_Y^2(\bar{R}e^{-\bar{Y}}x_1' + J_0)\left[\frac{\xi_1\xi^2 K_2(\alpha_Y\xi)}{48} - \frac{\xi_1\xi K_1(\alpha_Y\xi)}{8\alpha_Y}\right] \\ &+6\bar{R}e^{-\bar{Y}}\sigma_Y^2\alpha_Y^2\left[\frac{\xi^3 K_3(\alpha_Y\xi)}{48\alpha_Y} - \frac{\xi^2 K_2(\alpha_Y\xi)}{12\alpha_Y^2} - \frac{\xi_1^2\xi K_1(\alpha_Y\xi)}{24\alpha_Y}\right] \end{aligned} \quad \text{(A.22)}$$

Applying Fourier transform to equation (A.22) leads to:

$$
\begin{aligned}
S_{YH}(\mathbf{k}, x_1', x_2') = &-\frac{6\bar{R}e^{-\bar{Y}}\sigma_Y^2\alpha_Y^2}{2\pi}\left[\frac{(k^2-2k_1^2)}{(k^2+\alpha_Y^2)^4}\right] \\
&+\frac{(\bar{R}e^{-\bar{Y}}x_1'+J_0)\sigma_Y^2\alpha_Y^2}{2\pi}\left[\frac{6ik_1k^2}{(k^2+\alpha_Y^2)^4}\right]
\end{aligned} \tag{A.23}
$$

Differentiating equation (A.22) yields:

$$
\begin{aligned}
\frac{\partial P_{YH}(\xi, x_1', x_2')}{\partial \xi_1} = &\, 6\sigma_Y^2\alpha_Y^2(\bar{R}e^{-\bar{Y}}x_1'+J_0) \\
&\left[\frac{\xi^2K_2(\alpha_Y\xi)}{48}-\frac{\alpha_Y\xi_1^2\xi K_1(\alpha_Y\xi)}{48}+\frac{\xi K_1(\alpha_Y\xi)}{8\alpha_Y}-\frac{\xi_1^2K_0(\alpha_Y\xi)}{8}\right] \\
&+6\bar{R}e^{-\bar{Y}}\sigma_Y^2\alpha_Y^2 \\
&\left[\frac{\xi_1\xi K_1(\alpha_Y\xi)}{8\alpha_Y}-\frac{\xi_1^3K_0(\alpha_Y\xi)}{12}+\frac{\alpha_Y\xi_1^3\xi K_1(\alpha_Y\xi)}{48}-\frac{\xi_1\xi^2K_2(\alpha_Y\xi)}{24}\right]
\end{aligned} \tag{A.24}
$$

Multiplying equation (A.24) by $(\bar{R}e^{-\bar{Y}}\xi_1+\bar{R}e^{-\bar{Y}}x_1'+J_0)$ gives:

$$
\begin{aligned}
&(\bar{R}e^{-\bar{Y}}\xi_1+\bar{R}e^{-\bar{Y}}x_1'+J_0)\frac{P_{YH}(\xi, x_1', x_2')}{\partial\xi_1} \\
&=6\bar{R}^2e^{-2\bar{Y}}\sigma_Y^2\alpha_Y^2\left[\frac{\xi_1^4K_0(\alpha_Y\xi)}{24}-\frac{\xi_1^2\xi^2K_2(\alpha_Y\xi)}{48}\right] \\
&\quad+6\sigma_Y^2\alpha_Y^2\bar{R}e^{-\bar{Y}}(\bar{R}e^{-\bar{Y}}x_1'+J_0) \\
&\quad\left[\frac{\xi_1^3K_0(\alpha_Y\xi)}{6}-\frac{\alpha_Y\xi_1^3\xi K_1(\alpha_Y\xi)}{48}-\frac{\xi_1\xi K_1(\alpha_Y\xi)}{8\alpha_Y}\right] \\
&\quad+6\sigma_Y^2\alpha_Y^2(\bar{R}e^{-\bar{Y}}x_1'+J_0)^2 \\
&\quad\left[\frac{\xi^2K_2(\alpha_Y\xi)}{48}-\frac{\alpha_Y\xi_1^2\xi K_1(\alpha_Y\xi)}{48}-\frac{\xi K_1(\alpha_Y\xi)}{8\alpha_Y}+\frac{\xi_1^2K_0(\alpha_Y\xi)}{8}\right]
\end{aligned} \tag{A.25}
$$

Applying the Fourier transform to equation (A.25) leads to:

$$
\begin{aligned}
&\mathcal{F}\left[-(\bar{R}e^{-\bar{Y}}\xi_1+\bar{R}e^{-\bar{Y}}x_1'+J_0)\frac{P_{YH}(\xi, x_1', x_2')}{\partial\xi_1}\right] \\
&=\frac{6\bar{R}^2e^{-2\bar{Y}}\sigma_Y^2\alpha_Y^2}{2\pi}\left[\frac{12k_1^2}{(k^2+\alpha_Y^2)^4}-\frac{16k_1^4}{(k^2+\alpha_Y^2)^5}-\frac{k^2}{(k^2+\alpha_Y^2)^4}-\frac{8\alpha_Y^2k_1^2}{(k^2+\alpha_Y^2)^5}\right] \\
&+\frac{6\sigma_Y^2\alpha_Y^2\bar{R}e^{-\bar{Y}}(\bar{R}e^{-\bar{Y}}x_1'+J_0)}{2\pi}\left[\frac{3ik_1k^2}{(k^2+\alpha_Y^2)^4}-\frac{8ik_1^3k^2}{(k^2+\alpha_Y^2)^5}\right] \\
&+\frac{6\sigma_Y^2\alpha_Y^2(\bar{R}e^{-\bar{Y}}x_1'+J_0)^2}{2\pi}\frac{k_1^2k^2}{(k^2+\alpha_Y^2)^4}
\end{aligned} \tag{A.26}
$$

Plugging equations (A.21), (A.23), and (A.26) into equation (A.19) gives:

$$\begin{aligned}
S_{HH}(\mathbf{k}, x_1', x_2') =& \frac{6\sigma_R^2\alpha_R^2 e^{-2\hat{Y}}}{2\pi(k^2+\alpha_R^2)^4} \\
&+ \frac{6\bar{R}^2 e^{-2\hat{Y}}\sigma_Y^2\alpha_Y^2}{2\pi k^2}\left[\frac{10k_1^2}{(k^2+\alpha_Y^2)^4} - \frac{16k_1^4}{(k^2+\alpha_Y^2)^5} - \frac{8\alpha_Y^2 k_1^2}{(k^2+\alpha_Y^2)^5}\right] \\
&+ \frac{6\sigma_Y^2\alpha_Y^2\bar{R}e^{-\hat{Y}}(\bar{R}e^{-\hat{Y}}x_1' + J_0)}{2\pi}\left[\frac{2ik_1}{(k^2+\alpha_Y^2)^4} - \frac{8ik_1^3}{(k^2+\alpha_Y^2)^5}\right] \\
&+ \frac{6\sigma_Y^2\alpha_Y^2(\bar{R}e^{-\hat{Y}}x_1' + J_0)^2}{2\pi}\frac{k_1^2}{(k^2+\alpha_Y^2)^4}
\end{aligned} \tag{A.27}$$

Taking the inverse Fourier transform of equation (A.27) and regrouping the terms where necessary, we have:

$$\begin{aligned}
P_{HH}(\mathbf{x}, \mathbf{x}') =& \sigma_Y^2(\bar{R}e^{-\hat{Y}}x_1 + J_0)(\bar{R}e^{-\hat{Y}}x_1' + J_0)\left[\frac{\xi^2 K_2(\alpha_Y\xi)}{8} - \frac{\alpha_Y\xi_1^2\xi K_1(\alpha_Y\xi)}{8}\right] \\
&+ \bar{R}^2 e^{-2\hat{Y}}\sigma_Y^2\left[\frac{576(6\xi_1^2\xi_2^2 - \xi_1^4 - \xi_2^4)}{\xi^8\alpha_Y^8} - \frac{12(\xi_1^2 - \xi_2^2)}{\xi^4\alpha_Y^6} + \frac{(\xi_1^4 - \xi_1^2\xi_2^2)K_2(\alpha_Y\xi)}{8}\right. \\
&+ \frac{(3\xi_1^4 - 8\xi_1^2\xi_2^2 + \xi_2^4)K_3(\alpha_Y\xi)}{8\alpha_Y\xi} + \frac{(2\xi_1^4 - 9\xi_1^2\xi_2^2 + \xi_2^4)K_4(\alpha_Y\xi)}{2\alpha_Y^2\xi^2} \\
&\left.+ \frac{3(\xi_1^4 - 6\xi_1^2\xi_2^2 + \xi_2^4)K_5(\alpha_Y\xi)}{2\alpha_Y^3\xi^3}\right] \\
&+ \frac{\sigma_R^2 e^{-2\hat{Y}}\xi^3 K_3(\alpha_R\xi)}{8\alpha_R}
\end{aligned} \tag{A.28}$$

and its variance expression:

$$P_{HH}(\mathbf{x}, \mathbf{x}) = \frac{\sigma_Y^2(\bar{R}e^{-\hat{Y}}x_1 + J_0)^2}{4\alpha_Y^2} + \frac{\bar{R}^2 e^{-2\hat{Y}}\sigma_Y^2}{2\alpha_Y^4} + \frac{\sigma_R^2 e^{-2\hat{Y}}}{\alpha_R^4} \tag{A.29}$$

A.5 Derivation for $P_{v_i v_j}$

Differentiating equations (A.17) and (A.28) with respect to x_1 and x_2, plugging the results into equations (2.9) and (2.10), and regrouping terms gives the following velocity covariance $P_{v_i v_j}(\xi, x_1', x_2')$ solutions:

$$
\begin{aligned}
P_{v_1v_1}(\mathbf{x},\mathbf{x}') =& \frac{6\, e^{2\bar{Y}}\sigma_Y^2\alpha_Y^2}{b^2n^2}\Bigg[(\bar{R}e^{-\bar{Y}}x_1+J_0)(\bar{R}e^{-\bar{Y}}x_1'+J_0)\\
&\left[\frac{11\xi K_1(\alpha_Y\xi)}{48\alpha_Y}-\frac{(7\,\xi_1^2+4\,\xi_2^2)K_0(\alpha_Y\xi)}{24}+\frac{\alpha_Y(\xi_1^4+\xi^4)K_1(\alpha_Y\xi)}{48\,\xi}\right]\\
&-\left[(\bar{R}e^{-\bar{Y}}x_1+J_0)^2+(\bar{R}e^{-\bar{Y}}x_1'+J_0)^2\right]\\
&\left[\frac{\xi K_1(\alpha_Y\xi)}{8\alpha_Y}-\frac{\xi_1^2K_0(\alpha_Y\xi)}{8}-\frac{\xi^2K_2(\alpha_Y\xi)}{48}-\frac{\alpha_Y\xi_1^2\xi K_1(\alpha_Y\xi)}{48}\right]\\
&-\bar{R}^2e^{-2\bar{Y}}[B+B_0K_0(\alpha_Y\xi)+B_1K_1(\alpha_Y\xi)+B_2K_2(\alpha_Y\xi)\\
&+B_3K_3(\alpha_Y\xi)+B_4K_4(\alpha_Y\xi)+B_5K_5(\alpha_Y\xi)]\Bigg]\\
&+\frac{\sigma_R^2}{8b^2n^2}\left[\xi^2K_2(\alpha_R\xi)-\alpha_R\xi_1^2\xi K_1(\alpha_R\xi)\right]
\end{aligned}
\tag{A.30}
$$

and its variance expression:

$$
P_{v_1v_1}(\mathbf{x},\mathbf{x}) = \frac{e^{2\bar{Y}}}{b^2n^2}\left[\frac{3\sigma_Y^2(\bar{R}e^{-\bar{Y}}x_1+J_0)^2}{8}+\frac{\bar{R}^2e^{-2\bar{Y}}\sigma_Y^2}{8\alpha_Y^2}+\frac{\sigma_R^2e^{-2\bar{Y}}}{4\alpha_R^2}\right]
$$

$$
\begin{aligned}
P_{v_2v_2}(\mathbf{x},\mathbf{x}') =& \frac{6\, e^{2\bar{Y}}\sigma_Y^2\alpha_Y^2}{b^2n^2}\Bigg[(\bar{R}e^{-\bar{Y}}x_1+J_0)(\bar{R}e^{-\bar{Y}}x_1'+J_0)\\
&\left[\frac{\xi K_1(\alpha_Y\xi)}{48\alpha_Y}-\frac{\xi^2K_0(\alpha_Y\xi)}{48}+\frac{\alpha_Y\xi_1^2\xi_2^2K_1(\alpha_Y\xi)}{48\,\xi}\right]\\
&-\bar{R}^2e^{-2\bar{Y}}[C+C_0K_0(\alpha_Y\xi)+C_1K_1(\alpha_Y\xi)+C_2K_2(\alpha_Y\xi)\\
&+C_3K_3(\alpha_Y\xi)+C_4K_4(\alpha_Y\xi)+C_5K_5(\alpha_Y\xi)]\Bigg]\\
&+\frac{\sigma_R^2}{8b^2n^2}\left[\xi^2K_2(\alpha_R\xi)-\alpha_R\xi_2^2\xi K_1(\alpha_R\xi)\right]
\end{aligned}
\tag{A.31}
$$

and its variance expression:

$$
P_{v_2v_2}(\mathbf{x},\mathbf{x}) = \frac{e^{2\bar{Y}}}{b^2n^2}\left[\frac{\sigma_Y^2(\bar{R}e^{-\bar{Y}}x_1+J_0)^2}{8}+\frac{\bar{R}^2e^{-2\bar{Y}}\sigma_Y^2}{8\alpha_Y^2}+\frac{\sigma_R^2e^{-2\bar{Y}}}{4\alpha_R^2}\right]
$$

$$
\begin{aligned}
P_{v_1 v_2}(\mathbf{x}, \mathbf{x}') = & \frac{6\epsilon^{2\bar{Y}}\sigma_Y^2\alpha_Y^2}{b^2 n^2}\left[(\bar{R}e^{-\bar{Y}}x_1 + J_0)^2\left[\frac{\xi_1\xi_2 K_0(\alpha_Y\xi)}{16} - \frac{\alpha_Y\xi_1\xi_2^3 K_1(\alpha_Y\xi)}{48\xi}\right]\right. \\
& + \bar{R}e^{-\bar{Y}}(\bar{R}e^{-\bar{Y}}x_1 + J_0) \\
& \left[\frac{\alpha_Y\xi_1^2\xi_2^3 K_1(\alpha_Y\xi)}{48\xi} + \frac{\xi_2\xi K_1(\alpha_Y\xi)}{16\alpha_Y} - \frac{(3\,\xi_1^2\xi_2 + \xi_2^3)K_1(\alpha_Y\xi)}{48}\right] \\
& - \bar{R}^2 e^{-2\bar{Y}}[D + D_0 K_0(\alpha_Y\xi) + D_1 K_1(\alpha_Y\xi) + D_2 K_2(\alpha_Y\xi) \\
& \left. + D_3 K_3(\alpha_Y\xi) + D_4 K_4(\alpha_Y\xi) + D_5 K_5(\alpha_Y\xi)]\right] \\
& - \frac{\sigma_R^2\alpha_R\xi_1\xi_2\xi K_1(\alpha_R\xi)}{8b^2 n^2}
\end{aligned}
\tag{A.32}
$$

and its variance expression:

$$P_{v_1 v_2}(\mathbf{x}, \mathbf{x}) = 0$$

in which:

$$
\begin{aligned}
B &= -C = \frac{12(6\xi_1^2\xi_2^2 - \xi_1^4 - \xi_2^4)}{\xi^8\alpha_Y^8} + \frac{1920(\xi_2^6 - \xi_1^6 - 15\xi_1^2\xi_2^4 + 15\xi_1^4\xi_2^2)}{\xi^{12}\alpha_Y^{10}} \\
B_0 &= \frac{(7\xi_1^6 + 8\xi_1^4\xi_2^2 + 3\xi_1^2\xi_2^4)}{48\xi^2} \\
B_1 &= \frac{(3\xi_1^6 + 7\xi_1^2\xi_2^4)}{24\alpha_Y\xi^3} + \frac{\alpha_Y\xi_1^4\xi}{48} \\
B_2 &= \frac{(4\xi_1^6 - \xi_2^6 - 39\xi_1^4\xi_2^2 + 36\xi_1^2\xi_2^4)}{48\alpha_Y^2\xi^4} \\
B_3 &= -C_3 = \frac{(3\xi_1^6 - 2\xi_2^6 - 40\xi_1^4\xi_2^2 + 35\xi_1^2\xi_2^4)}{4\alpha_Y^3\xi^5} \\
B_4 &= -C_4 = \frac{(11\xi_1^6 - 9\xi_2^6 - 155\xi_1^4\xi_2^2 + 145\xi_1^2\xi_2^4)}{4\alpha_Y^4\xi^6} \\
B_5 &= -C_5 = \frac{5(\xi_1^6 - \xi_2^6 - 15\xi_1^4\xi_2^2 + 15\xi_1^2\xi_2^4)}{48\alpha_Y^5\xi^7} \\
C_0 &= \frac{(\xi_1^4\xi_2^2 - \xi_1^2\xi_2^4)}{48} \\
C_1 &= \frac{(\xi_2^6 - \xi_1^6 + 11\xi_1^4\xi_2^2 - 7\xi_1^2\xi_2^4)}{48\alpha_Y\xi^3} \\
C_2 &= \frac{(3\xi_2^6 - 7\xi_1^6 + 81\xi_1^4\xi_2^2 - 69\xi_1^2\xi_2^4)}{48\alpha_Y^2\xi^4} \\
D &= \frac{48(\xi_1\xi_2^3 - \xi_1^3\xi_2)}{\xi^8\alpha_Y^8} + \frac{3840(10\xi_1^3\xi_2^3 - 3\xi_1\xi_2^5 - 3\xi_1^5\xi_2)}{\xi^{12}\alpha_Y^{10}} \\
D_0 &= -\frac{\xi_1^3\xi_2^3}{24\xi^2} \\
D_1 &= \frac{(8\xi_1\xi_2^5 + 13\xi_1^5\xi_2 - 19\xi_1^3\xi_2^3)}{96\alpha_Y\xi^3} \\
D_2 &= \frac{(6\xi_1\xi_2^5 + 9\xi_1^5\xi_2 - 25\xi_1^3\xi_2^3)}{12\alpha_Y^2\xi^4} \\
D_3 &= \frac{(13\xi_1\xi_2^5 + 17\xi_1^5\xi_2 - 50\xi_1^3\xi_2^3)}{4\alpha_Y^3\xi^5} \\
D_4 &= \frac{(14\xi_1\xi_2^5 + 16\xi_1^5\xi_2 - 50\xi_1^3\xi_2^3)}{\alpha_Y^4\xi^6} \\
D_5 &= \frac{10(3\xi_1\xi_2^5 + 3\xi_1^5\xi_2 - 10\xi_1^3\xi_2^3)}{\alpha_Y^5\xi^7}
\end{aligned}
\tag{A.33}
$$

APPENDIX B
DERIVATION FOR THE TRANSIENT HEAD-COVARIANCE

B.1 P_{HY} derivation

Letting $\xi_1 = x_1 - x_1'$, $\xi_2 = x_2 - x_2'$, and $\tau = t - t'$, substituting equation (2.6) into equation (3.5) leads to:

$$\frac{\partial^2 P_{HY}(\xi,\tau,x_1',x_2',t')}{\partial \xi_i^2} - (\bar{R}e^{-\bar{Y}}x_1 + J_0)\frac{\partial P_{YY}(\xi,\tau)}{\partial \xi_1} - \bar{R}e^{-\bar{Y}}P_{YY}(\xi,\tau) = S_y e^{-\bar{Y}}\frac{\partial P_{HY}(\xi,\tau,x_1',x_2',t')}{\partial \tau} \quad \text{(B.1)}$$

in which ξ_i represents the separate distance in the i direction; the recharge and log-transmissivity fields have been assumed to be uncorrelated.

Performing the Fourier transform on equation (B.1) with respect to ξ_1, ξ_2, and τ we have:

$$S_{HY}(\mathbf{k},\omega,\mathbf{x}',t') = -\frac{\mathcal{F}\left[(\bar{R}e^{-\bar{Y}}\xi_1 + \bar{R}e^{-\bar{Y}}x_1' + J_0)\frac{\partial P_{YY}(\xi,\tau)}{\partial \xi_1} + \bar{R}e^{-\bar{Y}}P_{YY}(\xi,\tau)\right]}{k^2 + S_y e^{-\bar{Y}} i\omega} \quad \text{(B.2)}$$

Since P_{YY} is time invariant, its spectrum shown in equation (3.11) is a *Whittle B* spectrum in space [Li and Graham, 1998] multiplied by a delta function spectrum in time. Therefore performing the inverse Fourier transform of equation (B.2) with respect to τ and applying the integration property of delta function, we derive the exactly same spectrum solution of S_{HY} as (A.13). Therefore, we have the identical solution of cross-covariance of head-log transmissivity as equation (A.17):

$$
\begin{aligned}
P_{HY}(\xi, x_1', x_2') =& 6\sigma_Y^2\alpha_Y^2(\bar{R}e^{-\hat{Y}}x_1' + J_0)\left[\frac{\xi_1\xi K_1(\alpha_Y\xi)}{8\alpha_Y} - \frac{\xi_1\xi^2 K_2(\alpha_Y\xi)}{48}\right] \\
&+6\bar{R}e^{-\hat{Y}}\sigma_Y^2\alpha_Y^2\Big[\frac{\xi^3 K_3(\alpha_Y\xi)}{48\alpha_Y} - \frac{\xi^2 K_2(\alpha_Y\xi)}{12\alpha_Y^2} \\
&+\frac{\xi_1^2\xi K_1(\alpha_Y\xi)}{12\alpha_Y} - \frac{\xi_1^2\xi^2 K_2(\alpha_Y\xi)}{48}\Big]
\end{aligned} \tag{B.3}
$$

B.2 P_{HR} derivation

Substituting equation (2.6) into equation (3.4), and letting $\xi_1 = x_1 - x_1'$, $\xi_2 = x_2 - x_2'$, and $\tau = t - t'$ leads to:

$$
\frac{\partial^2 P_{HR}(\xi, \tau, \mathbf{x}', t')}{\partial \xi_i^2} + e^{-\hat{Y}}P_{RR}(\xi, \tau) = S_y e^{-\hat{Y}}\frac{\partial P_{HR}(\xi, \tau, \mathbf{x}', t')}{\partial \tau} \tag{B.4}
$$

Performing the Fourier transform on equation (B.4) with respect to ξ_1, ξ_2, and τ, we have:

$$
\begin{aligned}
S_{HR}(\mathbf{k}, \omega, \mathbf{x}', t') =& e^{-\hat{Y}}\frac{\mathcal{F}\left[P_{RR}(\xi, \tau)\right]}{k^2 + S_y e^{-\hat{Y}} i\omega} = e^{-\hat{Y}}\frac{S_{RR}(\mathbf{k}, \omega)}{k^2 + S_y e^{-\hat{Y}} i\omega} \\
=& e^{-\hat{Y}}\frac{S_{RR}(\mathbf{k}, \omega)\left[k^2 - iS_y e^{-\hat{Y}}\omega\right]}{k^4 + S_y^2 e^{-2\hat{Y}}\omega^2}
\end{aligned} \tag{B.5}
$$

which suggests that the cross-covariance for transient head-recharge is a stationary process, unaffected by the mean recharge $\bar{R}$.

Plugging the recharge spectrum (3.12) into equation (B.5) and applying the inverse Fourier transform to equation (B.5) gives:

$$
\begin{aligned}
P_{HR}(\mathbf{x},\tau) =& \frac{3\sigma_R^2\alpha_R^2 e^{-\bar{Y}}}{\pi^2}\int_{-\infty}^{\infty}\int_{-\infty}^{\infty}\int_{-\infty}^{\infty}\frac{(k^6 I_t - iS_y e^{-\bar{Y}}\omega k^4 I_t)e^{i(\mathbf{kx}+\omega\tau)}d\mathbf{k}d\omega}{(k^4+S_y^2 e^{-2\bar{Y}}\omega^2)(k^2+\alpha_R^2)^4(1+I_t^2\omega^2)} \\
=& \frac{3\sigma_R^2\alpha_R^2}{e^{\bar{Y}}\pi^2}\int_{-\infty}^{\infty}\int_{-\infty}^{\infty}\int_{-\infty}^{\infty}\frac{k^6 I_t e^{i(\mathbf{kx}+\omega\tau)}d\mathbf{k}d\omega}{(k^4+S_y^2 e^{-2\bar{Y}}\omega^2)(k^2+\alpha_R^2)^4(1+I_t^2\omega^2)} \\
&-\frac{3\sigma_R^2\alpha_R^2 S_y}{e^{2\bar{Y}}\pi^2}\frac{d}{d\tau}\int_{-\infty}^{\infty}\int_{-\infty}^{\infty}\int_{-\infty}^{\infty}\frac{k^4 I_t e^{i(\mathbf{kx}+\omega\tau)}d\mathbf{k}d\omega}{(k^4+S_y^2 e^{-2\bar{Y}}\omega^2)(k^2+\alpha_R^2)^4(1+I_t^2\omega^2)} \qquad \text{(B.6)} \\
=& \frac{3\sigma_R^2\alpha_R^2}{e^{\bar{Y}}\pi^2}\int_{-\infty}^{\infty}\int_{-\infty}^{\infty}\frac{k^6}{(k^2+\alpha_R^2)^4}\int_{-\infty}^{\infty}\frac{I_t e^{i(\mathbf{kx}+\omega\tau)}}{(k^4+S_y^2 e^{-2\bar{Y}}\omega^2)(1+I_t^2\omega^2)}d\omega d\mathbf{k} \\
&-\frac{3\sigma_R^2\alpha_R^2 S_y}{e^{2\bar{Y}}\pi^2}\frac{d}{d\tau}\int_{-\infty}^{\infty}\int_{-\infty}^{\infty}\frac{k^4}{(k^2+\alpha_R^2)^4}\int_{-\infty}^{\infty}\frac{I_t e^{i(\mathbf{kx}+\omega\tau)}}{(k^4+S_y^2 e^{-2\bar{Y}}\omega^2)(1+I_t^2\omega^2)}d\omega d\mathbf{k}
\end{aligned}
$$

in which

$$
\int_{-\infty}^{\infty}\frac{I_t e^{i\omega\tau}}{(k^4+S_y^2 e^{-2\bar{Y}}\omega^2)(1+I_t^2\omega^2)}d\omega = \frac{\pi}{(\frac{S_y^2 e^{-2\bar{Y}}}{I_t^2}-k^4)}\left[\frac{\frac{S_y e^{-\bar{Y}}}{I_t}}{k^2 e^{k^2|\frac{\tau}{S_y e^{-\bar{Y}}}|}}-\frac{1}{e^{|\frac{\tau}{I_t}|}}\right] \qquad \text{(B.7)}
$$

which was evaluated by Mathematica [Wolfram, 1991].

Letting $\tau' = \frac{\tau}{I_t}$ and $S_y' = \frac{S_y e^{-\bar{Y}}}{I_t}$,applying equation (B.7) to equation (B.6), and using (A.9) gives:

$$
\begin{aligned}
P_{HR}(\mathbf{x},\tau) =& \frac{3\sigma_R^2\alpha_R^2}{e^{\hat{Y}}\pi^2}\int_{-\infty}^{\infty}\int_{-\infty}^{\infty}\frac{k^6}{(k^2+\alpha_R^2)^4}\frac{\pi\left[k^2e^{-|\tau'|}-S_y'e^{-k^2|\frac{\tau'}{S_y'}|}\right]}{k^2(k^4-S_y'^2)}e^{i\mathbf{kx}}d\mathbf{k} \\
&-\frac{3\sigma_R^2\alpha_R^2S_y}{e^{2\hat{Y}}\pi^2}\frac{d}{d\tau}\int_{-\infty}^{\infty}\int_{-\infty}^{\infty}\frac{k^4}{(k^2+\alpha_R^2)^4}\frac{\pi\left[k^2e^{-|\tau'|}-S_y'e^{-k^2|\frac{\tau'}{S_y'}|}\right]}{k^2(k^4-S_y'^2)}e^{i\mathbf{kx}}d\mathbf{k} \\
=&\frac{3\sigma_R^2\alpha_R^2}{e^{\hat{Y}}\pi}\int_{-\infty}^{\infty}\int_{-\infty}^{\infty}\frac{k^4}{(k^2+\alpha_R^2)^4}\frac{\left[k^2e^{-|\tau'|}-S_y'e^{-k^2|\frac{\tau'}{S_y'}|}\right]}{(k^4-S_y'^2)}e^{i\mathbf{kx}}d\mathbf{k} \\
&-\frac{3\sigma_R^2\alpha_R^2S_y}{e^{2\hat{Y}}\pi}\frac{d}{d\tau}\int_{-\infty}^{\infty}\int_{-\infty}^{\infty}\frac{k^2}{(k^2+\alpha_R^2)^4}\frac{\left[k^2e^{-|\tau'|}-S_y'e^{-k^2|\frac{\tau'}{S_y'}|}\right]}{(k^4-S_y'^2)}e^{i\mathbf{kx}}d\mathbf{k} \qquad \text{(B.8)} \\
=&\frac{6\sigma_R^2\alpha_R^2}{e^{\hat{Y}}}\left[\int_0^{\infty}\frac{k^5J_0(k\xi)(k^2e^{-|\tau'|}-S_y'e^{-k^2|\frac{\tau'}{S_y'}|})}{(k^2+\alpha_R^2)^4(k^4-S_y'^2)}dk\right] \\
&-\frac{6\sigma_R^2\alpha_R^2S_y'}{e^{\hat{Y}}}\frac{d}{d\tau'}\left[\int_0^{\infty}\frac{k^3J_0(k\xi)(k^2e^{-|\tau'|}-S_y'e^{-k^2|\frac{\tau'}{S_y'}|})}{(k^2+\alpha_R^2)^4(k^4-S_y'^2)}dk\right] \\
=&\frac{6\sigma_R^2\alpha_R^2e^{-|\tau'|}}{e^{\hat{Y}}}\left[\int_0^{\infty}\frac{k^5J_0(k\xi)}{(k^2+\alpha_R^2)^4(k^2+S_y')}dk\right]
\end{aligned}
$$

Equation (B.8) was evaluated by Mathematica [Wolfram, 1991] to get:

$$
\begin{aligned}
P_{HR}(\mathbf{x},\tau) = \frac{6\sigma_R^2\alpha_R^2e^{-|\tau'|}}{e^{\hat{Y}}}&\left[\frac{S_y'^2K_0(\sqrt{S_y'}\xi)}{(\alpha_R^2-S_y')^4}-\frac{S_y'^2K_0(\alpha_R\xi)}{(\alpha_R^2-S_y')^4}-\frac{S_y'^2\alpha_R\xi K_1(\alpha_R\xi)}{2\alpha_R^2(\alpha_R^2-S_y')^3}\right. \\
&\left.+\frac{(-2S_y'+\alpha_R^2)\xi^2K_2(\alpha_R\xi)}{8(\alpha_R^2-S_y')^2}-\frac{\alpha_R\xi^3K_3(\alpha_R\xi)}{48(\alpha_R^2-S_y')}\right] \qquad \text{(B.9)}
\end{aligned}
$$

Correspondingly, the cross-covariance of head-recharge with zero separation distance and time lag can be evaluated by setting separation distance and time lag as zero, or,

$$
\begin{aligned}
P_{HR}(0,0) =& \frac{3\sigma_R^2\alpha_R^2 e^{-\bar{Y}}}{\pi^2}\int_{-\infty}^{\infty}\int_{-\infty}^{\infty}\int_{-\infty}^{\infty}\frac{(k^6 I_t - iS_y e^{-\bar{Y}}\omega k^4 I_t)d\mathbf{k}d\omega}{(k^4+S_y^2 e^{-2\bar{Y}}\omega^2)(k^2+\alpha_R^2)^4(1+I_t^2\omega^2)} \\
=& \frac{3\sigma_R^2\alpha_R^2 e^{-\bar{Y}} I_t}{\pi^2}\int_{-\infty}^{\infty}\int_{-\infty}^{\infty}\int_{-\infty}^{\infty}\frac{k^6 d\mathbf{k}d\omega}{(k^4+S_y^2 e^{-2\bar{Y}}\omega^2)(k^2+\alpha_R^2)^4(1+I_t^2\omega^2)} \\
=& \frac{3\sigma_R^2\alpha_R^2 e^{-\bar{Y}}}{\pi}\int_{-\infty}^{\infty}\int_{-\infty}^{\infty}\frac{k^4 d\mathbf{k}}{(k^2+\alpha_R^2)^4(k^2+S_y')} \qquad \text{(B.10)} \\
=& \sigma_R^2 e^{-\bar{Y}}\left[\frac{(\alpha_R^6 - 6\alpha_R^4 S_y' + 3\alpha_R^2 {S_y'}^2 + 2{S_y'}^3 + 6\alpha_R^2 {S_y'}^2\ln(\frac{\alpha_R^2}{S_y'})}{2(S_y'-\alpha_R^2)^4}\right]
\end{aligned}
$$

B.3 P_{HH} derivation

Letting $\xi_1 = x_1 - x_1'$, $\xi_2 = x_2 - x_2'$, and $\tau = t - t'$, substituting equation (2.6) into equation (3.6) leads to:

$$
\begin{aligned}
\frac{\partial^2 P_{HH}(\xi,\tau,x_1',x_2',t')}{\partial\xi_i^2} - (\bar{R}e^{-\bar{Y}}x_1 + J_0)\frac{\partial P_{YH}(\xi,x_1',x_2')}{\partial\xi_1} - \bar{R}e^{-\bar{Y}}P_{YH}(\xi,x_1',x_2') \\
+ e^{-\bar{Y}}P_{RH}(\xi,\tau) = S_y e^{-\bar{Y}}\frac{\partial P_{HH}(\xi,\tau,\mathbf{x}',t')}{\partial\tau} \qquad \text{(B.11)}
\end{aligned}
$$

Equation (B.11) is a linear equation with two driving force terms P_{YH} and P_{RH}. Therefore by the principle of superposition, the solution of P_{HH} must be composed of two major terms $P_{HH}^{(1)}$ and $P_{HH}^{(2)}$, resulting from P_{YH} and P_{RH} respectively and which satisfy the following equations:

$$
\begin{aligned}
\frac{\partial^2 P_{HH}^{(1)}(\xi,\tau,x_1',x_2',t')}{\partial\xi_i^2} - (\bar{R}e^{-\bar{Y}}x_1 + J_0)\frac{\partial P_{YH}(\xi,x_1',x_2')}{\partial\xi_1} - \bar{R}e^{-\bar{Y}}P_{YH}(\xi,x_1',x_2') \\
= S_y e^{-\bar{Y}}\frac{\partial P_{HH}^{(1)}(\xi,\tau,\mathbf{x}',t')}{\partial\tau} \qquad \text{(B.12)}
\end{aligned}
$$

$$
\frac{\partial^2 P_{HH}^{(2)}(\xi,\tau,x_1',x_2',t')}{\partial\xi_i^2} + e^{-\bar{Y}}P_{RH}(\xi,\tau) = S_y e^{-\bar{Y}}\frac{\partial P_{HH}^{(2)}(\xi,\tau,\mathbf{x}',t')}{\partial\tau} \qquad \text{(B.13)}
$$

Equation (B.12) is a steady state equation since the driving force P_{YH} is time invariant and a solution far from the initial condition is sought. Thus the solution

$P_{HH}^{(1)}$ is identical to the first part of the solution (A.28) under the steady state random recharge.

Thus, the key step for the new solution of equation (3.6) under transient conditions is to seek the second part of P_{HH}, or $P_{HH}^{(2)}$ in equation (B.13). Performing the Fourier transform on equation (B.13) with respect to ξ_1, ξ_2, and τ, we have:

$$\begin{aligned} S_{HH}^{(2)}(\mathbf{k},\tau) =& e^{-\bar{Y}} \frac{\mathcal{F}\left[P_{RH}(\xi,\tau)\right]}{k^2 + S_y e^{-\bar{Y}} i\omega} = e^{-\bar{Y}} \frac{S_{RH}(\mathbf{k},\omega)}{k^2 + S_y e^{-\bar{Y}} i\omega} \\ =& e^{-\bar{Y}} \frac{S_{HR}^*(\mathbf{k},\omega)\left[k^2 - iS_y e^{-\bar{Y}}\omega\right]}{k^4 + S_y^2 e^{-2\bar{Y}}\omega^2} \\ =& e^{-2\bar{Y}} \frac{S_{RR}(\mathbf{k},\omega)}{k^4 + S_y^2 e^{-2\bar{Y}}\omega^2} \end{aligned} \tag{B.14}$$

in which due to S_{HR}^* is the complex conjugate of the Fourier transform S_{HR}. Since S_{HR} is a stationary process:

$$S_{RH}(\mathbf{k},\omega) = S_{HR}^*(\mathbf{k},\omega) = e^{-\bar{Y}} \frac{S_{RR}(\mathbf{k},\omega)\left[k^2 + iS_y e^{-\bar{Y}}\omega\right]}{k^4 + S_y^2 e^{-2\bar{Y}}\omega^2} \tag{B.15}$$

Taking the inverse Fourier transform of equation (B.14) and regrouping terms we have:

$$P_{HH}^{(2)}(\xi,\tau) = 6\sigma_R^2\alpha_R^2 e^{-2\bar{Y}} \int_0^\infty \frac{k^3 J_0(k\xi)(k^2 e^{-|r'|} - S_y' e^{-k^2|\frac{\tau'}{S_y'}|})}{(k^2+\alpha_R^2)^4(k^4 - S_y'^2)} dk \tag{B.16}$$

Thus the complete solution for equation (B.11) is:

$$
\begin{aligned}
P_{HH}(\mathbf{x},\mathbf{x}',\tau) =& \sigma_Y^2(\bar{R}e^{-\bar{Y}}x_1 + J_0)(\bar{R}e^{-\bar{Y}}x_1' + J_0)'\left[\frac{\xi^2 K_2(\alpha_Y\xi)}{8} - \frac{\alpha_Y\xi_1^2\xi K_1(\alpha_Y\xi)}{8}\right] \\
&+\bar{R}^2 e^{-2\bar{Y}}\sigma_Y^2\left[\frac{576(6\xi_1^2\xi_2^2 - \xi_1^4 - \xi_2^4)}{\xi^8\alpha_Y^8} - \frac{12(\xi_1^2 - \xi_2^2)}{\xi^4\alpha_Y^6}\right. \\
&+\frac{(\xi_1^4 - \xi_1^2\xi_2^2)K_2(\alpha_Y\xi)}{8} + \frac{(3\xi_1^4 - 8\xi_1^2\xi_2^2 + \xi_2^4)K_3(\alpha_Y\xi)}{8\alpha_Y\xi} \\
&\left.+\frac{(2\xi_1^4 - 9\xi_1^2\xi_2^2 + \xi_2^4)K_4(\alpha_Y\xi)}{2\alpha_Y^2\xi^2} + \frac{3(\xi_1^4 - 6\xi_1^2\xi_2^2 + \xi_2^4)K_5(\alpha_Y\xi)}{2\alpha_Y^3\xi^3}\right] \\
&+6\sigma_R^2\alpha_R^2 e^{-2\bar{Y}}\int_0^\infty \frac{k^3 J_0(k\xi)(k^2 e^{-|\tau'|} - S_y' e^{-k^2\left|\frac{\tau'}{S_y'}\right|})}{(k^2+\alpha_R^2)^4(k^4 - S_y'^2)}dk
\end{aligned} \tag{B.17}
$$

The head variance corresponding to equation (B.14) can be derived by inverse Fourier transforming equation (B.14) with the separation distance and time set equal to zero, or:

$$
\begin{aligned}
P_{HH}^{(2)}(0,0) =& \int_{-\infty}^{\infty}\int_{-\infty}^{\infty}\int_{-\infty}^{\infty} e^{-2\bar{Y}}\frac{S_{RR}(\mathbf{k}\omega)}{k^4 + S_y^2 e^{-2\bar{Y}}\omega^2}d\mathbf{k}d\omega \\
=& \int_{-\infty}^{\infty}\int_{-\infty}^{\infty}\int_{-\infty}^{\infty}\frac{3\sigma_R^2\alpha_R^2 k^4 I_t e^{-2\bar{Y}}}{\pi^2(k^2+\alpha_R^2)^4(k^4 + s_y^2 e^{-2\bar{Y}}\omega^2)(1 + I_t^2\omega^2)}d\mathbf{k}d\omega \\
=& \frac{3\sigma_R^2\alpha_R^2 e^{-2\bar{Y}}}{\pi}\int_{-\infty}^{\infty}\int_{-\infty}^{\infty}\frac{k^2}{(k^2+\alpha_R^2)^4(k^2+S_y')}dk_1dk_2 \\
=& \frac{3\sigma_R^2\alpha_R^2 e^{-2\bar{Y}}}{\pi}\int_{-\infty}^{\infty}\int_{-\infty}^{\infty}\frac{1}{(k^2+\alpha_R^2)^3(k^2+S_y')}dk_1dk_2 \\
&-\frac{3\sigma_R^2\alpha_R^2 e^{-2\bar{Y}}}{\pi}\int_{-\infty}^{\infty}\int_{-\infty}^{\infty}\frac{\alpha_R^2}{(k^2+\alpha_R^2)^4(k^2+S_y')}dk_1dk_2 \\
=& \frac{3\sigma_R^2\alpha_R^2 e^{-2\bar{Y}}}{\pi}\left[\frac{\pi(-3\alpha_R^2 + s_y')}{4\alpha_R^4(-\alpha_R^2 + s_y')^2}\right. \\
&-\frac{\pi\left[3\alpha_R^4 - 4\alpha_R^2 s_y' + s_y'^2 - 4\alpha_R^4\ln(\frac{\alpha_R^2}{S_y'})\right]}{4\alpha_R^4(\alpha_R^2 - s_y')^3} - \frac{\pi(11\alpha_R^4 - 7\alpha_R^2 s_y' + 2s_y'^2)}{12\alpha_R^4(-\alpha_R^2 + s_y')^3} \\
&\left.+\frac{\pi\left[11\alpha_R^6 - 18\alpha_R^4 s_y' + 9\alpha_R^2 s_y'^2 - 2s_y'^3 - 12\alpha_R^6\ln(\frac{\alpha_R^2}{S_y'})\right]}{12\alpha_R^4(\alpha_R^2 - s_y')^4}\right] \\
=& \sigma_R^2 e^{-2\bar{Y}}\left[\frac{2\alpha_R^6 + 3\alpha^4 S_y' - 6\alpha_R^2 S_y'^2 + S_y'^3 - 6\alpha_R^4 S_y'\ln(\frac{\alpha_R^2}{S_y'})}{2\alpha_R^2(\alpha_R^2 - S_y')^4}\right]
\end{aligned} \tag{B.18}
$$

in which the integration was evaluated using Mathematica [Wolfram, 1991].

Therefore, the complete solution of head variance for equation (B.11) is:

$$\begin{aligned} P_{HH}(\mathbf{x},0) =& \frac{\sigma_Y^2(\bar{R}e^{-\hat{Y}}x_1 + J_0)^2}{4\alpha_Y^2} + \frac{\bar{R}^2 e^{-2\hat{Y}}\sigma_Y^2}{2\alpha_Y^4} \\ &+\sigma_R^2 e^{-2\hat{Y}}\left[\frac{2\alpha_R^6 + 3\alpha^4 S'_y - 6\alpha_R^2 S'^2_y + S'^3_y - 6\alpha_R^4 S'_y \ln(\frac{\alpha_R^2}{S'_y})}{2\alpha_R^2(\alpha_R^2 - S'_y)^4}\right] \end{aligned} \tag{B.19}$$

For zero temporal separation distance the head covariance can be derived by inverse Fourier transforming equation (B.14) with the separation time set equal to zero, or:

$$\begin{aligned} P_{HH}^{(2)}(\xi,0) =& \int_{-\infty}^{\infty}\int_{-\infty}^{\infty}\int_{-\infty}^{\infty} e^{-2\hat{Y}}\frac{S_{RR}(\mathbf{k},\omega)}{k^4 + S_y^2 e^{-2\hat{Y}}\omega^2} e^{i\mathbf{kx}} dk_1 dk_2 d\omega \\ =& \int_{-\infty}^{\infty}\int_{-\infty}^{\infty}\int_{-\infty}^{\infty} \frac{3\sigma_R^2\alpha_R^2 k^4 I_t e^{-2\hat{Y}} e^{i\mathbf{kx}}}{\pi^2(k^2+\alpha_R^2)^4(k^4 + s_y^2 e^{-2\hat{Y}}\omega^2)(1 + I_t^2\omega^2)} dk_1 dk_2 d\omega \\ =& \frac{3\sigma_R^2\alpha_R^2 e^{-2\hat{Y}}}{\pi}\int_{-\infty}^{\infty}\int_{-\infty}^{\infty} \frac{k^2}{(k^2+\alpha_R^2)^4(k^2+S'_y)} e^{i\mathbf{kx}} dk_1 dk_2 \\ =& \frac{6\sigma_R^2\alpha_R^2}{e^{2\hat{Y}}}\int_0^{\infty} \frac{k^3 J_0(k\xi)}{(k^2+\alpha_R^2)^4(k^2+S'_y)} dk \\ =& \frac{6\sigma_R^2\alpha_R^2}{e^{2\hat{Y}}}\left[\frac{s'_y\left[K_0(\alpha_R\xi) - K_0(\sqrt{s'_y}\xi)\right]}{(\alpha_R^2 - s'_y)^4} + \frac{s'_y\xi K_1(\alpha_R\xi)}{2\alpha_R(\alpha_R^2 - s'_y)^3}\right. \\ &\left. + \frac{s'_y\xi^2 K_2(\alpha_R\xi)}{8\alpha_R^2(\alpha_R^2 - s'_y)^2} + \frac{\xi^3 K_3(\alpha_R\xi)}{48\alpha_R(\alpha_R^2 - s'_y)}\right] \end{aligned} \tag{B.20}$$

Therefore, the complete solution of head covariance with zero temporal separation distance is:

$$
\begin{aligned}
P_{HH}(\mathbf{x},\mathbf{x}',0) =& \sigma_Y^2(\bar{R}e^{-\hat{Y}}x_1 + J_0)(\bar{R}e^{-\hat{Y}}x_1' + J_0)\left[\frac{\xi^2 K_2(\alpha_Y\xi)}{8} - \frac{\alpha_Y\xi_1^2\xi K_1(\alpha_Y\xi)}{8}\right] \\
&+\bar{R}^2e^{-2\hat{Y}}\sigma_Y^2\left[\frac{576(6\xi_1^2\xi_2^2 - \xi_1^4 - \xi_2^4)}{\xi^8\alpha_Y^8} - \frac{12(\xi_1^2 - \xi_2^2)}{\xi^4\alpha_Y^6}\right. \\
&+\frac{(\xi_1^4 - \xi_1^2\xi_2^2)K_2(\alpha_Y\xi)}{8} + \frac{(3\xi_1^4 - 8\xi_1^2\xi_2^2 + \xi_2^4)K_3(\alpha_Y\xi)}{8\alpha_Y\xi} \\
&\left.+\frac{(2\xi_1^4 - 9\xi_1^2\xi_2^2 + \xi_2^4)K_4(\alpha_Y\xi)}{2\alpha_Y^2\xi^2} + \frac{3(\xi_1^4 - 6\xi_1^2\xi_2^2 + \xi_2^4)K_5(\alpha_Y\xi)}{2\alpha_Y^3\xi^3}\right] \\
&+\frac{6\sigma_R^2\alpha_R^2}{e^{2\hat{Y}}}\left[\frac{s_y'\left[K_0(\alpha_R\xi) - K_0(\sqrt{s_y'}\xi)\right]}{(\alpha_R^2 - s_y')^4} + \frac{s_y'\xi K_1(\alpha_R\xi)}{2\alpha_R(\alpha_R^2 - s_y')^3}\right. \\
&\left.+\frac{s_y'\xi^2 K_2(\alpha_R\xi)}{8\alpha_R^2(\alpha_R^2 - s_y')^2} + \frac{\xi^3 K_3(\alpha_R\xi)}{48\alpha_R(\alpha_R^2 - s_y')}\right]
\end{aligned}
\tag{B.21}
$$

For zero spatial separation distance the head covariance can be derived by inverse Fourier transforming equation (B.14) with the separation distance set equal to zero, or:

$$
\begin{aligned}
P_{HH}^{(2)}(0,\tau) &= \int_{-\infty}^{\infty}\int_{-\infty}^{\infty}\int_{-\infty}^{\infty} e^{-2\hat{Y}}\frac{S_{RR}(\mathbf{k},\omega)}{k^4 + S_y'^2e^{-2\hat{Y}}\omega^2}e^{i\omega\tau}dk_1dk_2d\omega \\
&= \int_{-\infty}^{\infty}\int_{-\infty}^{\infty}\int_{-\infty}^{\infty}\frac{3\sigma_R^2\alpha_R^2k^4I_te^{-2\hat{Y}}e^{i\omega\tau}}{\pi^2(k^2+\alpha_R^2)^4(k^4 + s_y'^2e^{-2\hat{Y}}\omega^2)(1 + I_t^2\omega^2)}dk_1dk_2d\omega \\
&= 6\sigma_R^2\alpha_R^2e^{-2\hat{Y}}\int_0^{\infty}\frac{k^3(k^2e^{-|\tau'|} - S_y'e^{-k^2|\frac{\tau'}{S_y'}|})}{(k^2+\alpha_R^2)^4(k^4 - S_y'^2)}dk
\end{aligned}
\tag{B.22}
$$

Therefore, the complete solution of head covariance with zero spatial separation distance is:

$$
\begin{aligned}
P_{HH}(\mathbf{x},\tau) &= \frac{\sigma_Y^2(\bar{R}e^{-\hat{Y}}x_1 + J_0)^2}{4\alpha_Y^2} + \frac{\bar{R}^2e^{-2\hat{Y}}\sigma_Y^2}{2\alpha_Y^4} \\
&+6\sigma_R^2\alpha_R^2e^{-2\hat{Y}}\int_0^{\infty}\frac{k^3(k^2e^{-|\tau'|} - S_y'e^{-k^2|\frac{\tau'}{S_y'}|})}{(k^2+\alpha_R^2)^4(k^4 - S_y'^2)}dk
\end{aligned}
\tag{B.23}
$$

B.4 Derivation for $P_{v_iv_j}$

Since the equations for $P_{v_iv_j}$ are linear, their solutions should be composed of the superposition of two parts : $P^{(1)}_{v_iv_j}$ and $P^{(2)}_{v_iv_j}$, contributed from time-invariant P_{YY} and spatiotemporally variable P_{RR}, respectively. The solutions of $P^{(1)}_{v_iv_j}$ are identical to the first parts of solutions from (2.23) to (2.26). What we need to find is the solution of $P^{(2)}_{v_iv_j}$.

Again, performing the Fourier transform of equations (3.9) and (3.10) and applying the complex conjugate property for stationary processes, we have the following velocity spectra for $P^{(2)}_{v_iv_j}$,

$$\begin{aligned}
S^{(2)}_{v_1v_1}(\mathbf{k},\omega) =& \frac{1}{(bn)^2}\left[\frac{k_1^2 S_{RR}}{k^4 + S_y^2 e^{-2\hat{Y}}\omega^2}\right] \\
S^{(2)}_{v_2v_2}(\mathbf{k},\omega) =& \frac{1}{(bn)^2}\left[\frac{k_2^2 S_{RR}}{k^4 + S_y^2 e^{-2\hat{Y}}\omega^2}\right] \\
S^{(2)}_{v_1v_2}(\mathbf{k},\omega) =& S^{(2)}_{v_2v_1}(\mathbf{k},\omega) = \frac{1}{(bn)^2}\left[\frac{k_1k_2 S_{RR}}{k^4 + S_y^2 e^{-2\hat{Y}}\omega^2}\right]
\end{aligned} \tag{B.24}$$

Inverse Fourier transforming equation (B.24) leads to:

$$\begin{aligned}
P^{(2)}_{v_1v_1}(\xi,\tau) =& -\frac{6\sigma_R^2\alpha_R^2}{(bn)^2}\frac{d^2}{d\xi_1^2}\left[\int_0^\infty \frac{k^3 J_0(k\xi)(k^2 e^{-|\tau'|} - S'_y e^{-k^2|\frac{\tau'}{S'_y}|})}{(k^2+\alpha_R^2)^4(k^4 - S'^2_y)}dk\right] \\
P^{(2)}_{v_2v_2}(\xi,\tau) =& -\frac{6\sigma_R^2\alpha_R^2}{(bn)^2}\frac{d^2}{d\xi_2^2}\left[\int_0^\infty \frac{k^3 J_0(k\xi)(k^2 e^{-|\tau'|} - S'_y e^{-k^2|\frac{\tau'}{S'_y}|})}{(k^2+\alpha_R^2)^4(k^4 - S'^2_y)}dk\right] \\
P^{(2)}_{v_1v_2}(\xi,\tau) =& P^{(2)}_{v_2v_1}(\xi,\tau) = -\frac{6\sigma_R^2\alpha_R^2}{(bn)^2}\frac{d^2}{d\xi_1 d\xi_2}\left[\int_0^\infty \frac{k^3 J_0(k\xi)(k^2 e^{-|\tau'|} - S'_y e^{-k^2|\frac{\tau'}{S'_y}|})}{(k^2+\alpha_R^2)^4(k^4 - S'^2_y)}dk\right]
\end{aligned} \tag{B.25}$$

Therefore, the complete solutions for velocity covariance $P_{v_iv_j}$ are:

$$
\begin{aligned}
P_{v_1v_1}(\xi,\tau) =& P^{(1)}_{v_1v_1} - \frac{6\sigma_R^2\alpha_R^2}{(bn)^2}\frac{d^2}{d\xi_1^2}\left[\int_0^\infty \frac{k^3 J_0(k\xi)(k^2 e^{-|\tau'|} - S'_y e^{-k^2|\frac{\tau'}{S'_y}|})}{(k^2+\alpha_R^2)^4(k^4 - {S'_y}^2)}dk\right] \\
P_{v_2v_2}(\xi,\tau) =& P^{(1)}_{v_2v_2} - \frac{6\sigma_R^2\alpha_R^2}{(bn)^2}\frac{d^2}{d\xi_2^2}\left[\int_0^\infty \frac{k^3 J_0(k\xi)(k^2 e^{-|\tau'|} - S'_y e^{-k^2|\frac{\tau'}{S'_y}|})}{(k^2+\alpha_R^2)^4(k^4 - {S'_y}^2)}dk\right] \\
P_{v_1v_2}(\xi,\tau) =& P^{(1)}_{v_1v_2} - \frac{6\sigma_R^2\alpha_R^2}{(bn)^2}\frac{d^2}{d\xi_1 d\xi_2}\left[\int_0^\infty \frac{k^3 J_0(k\xi)(k^2 e^{-|\tau'|} - S'_y e^{-k^2|\frac{\tau'}{S'_y}|})}{(k^2+\alpha_R^2)^4(k^4 - {S'_y}^2)}dk\right]
\end{aligned}
\tag{B.26}
$$

in which $P^{(1)}_{v_iv_j}$ are identical to the first parts of solutions (2.23) to (2.26).

As in the derivation of the head variance, we use Mathematica [Wolfram, 1991] to derive the velocity variance corresponding to equation (B.24), then add the contribution to the velocity variance resulting from log-transmissivity field [Li and Graham, 1998], to get:

$$
\begin{aligned}
P_{v_1v_1}(\mathbf{x},0) =& \frac{e^{2\bar{Y}}}{b^2n^2}\left[\frac{3\sigma_Y^2(\bar{R}e^{-\bar{Y}}x_1 + J_0)^2}{8} + \frac{\bar{R}^2 e^{-2\bar{Y}}\sigma_Y^2}{8\alpha_Y^2}\right] \\
&+ \frac{\sigma_R^2}{(bn)^2}\left[\frac{\alpha_R^6 - 6\alpha^4 S'_y + 3\alpha_R^2 {S'_y}^2 + 2{S'_y}^3 + 6\alpha_R^2 {S'_y}^2\ln(\frac{\alpha_R^2}{S'_y})}{4(\alpha_R^2 - S'_y)^4}\right] \\
P_{v_2v_2}(\mathbf{x},0) =& \frac{e^{2\bar{Y}}}{b^2n^2}\left[\frac{\sigma_Y^2(\bar{R}e^{-\bar{Y}}x_1 + J_0)^2}{8} + \frac{\bar{R}^2 e^{-2\bar{Y}}\sigma_Y^2}{8\alpha_Y^2}\right] \\
&+ \frac{\sigma_R^2}{(bn)^2}\left[\frac{\alpha_R^6 - 6\alpha^4 S'_y + 3\alpha_R^2 {S'_y}^2 + 2{S'_y}^3 + 6\alpha_R^2 {S'_y}^2\ln(\frac{\alpha_R^2}{S'_y})}{4(\alpha_R^2 - S'_y)^4}\right] \\
P_{v_1v_2}(\mathbf{x},0) =& 0
\end{aligned}
\tag{B.27}
$$

The velocity covariance of zero spatial separation distance can be derived by setting the spatial separation distance to zero in equation (B.26):

$$
\begin{aligned}
P_{v_1v_1}(\mathbf{x},\tau) =& \frac{e^{2\bar{Y}}}{b^2n^2}\left[\frac{3\sigma_Y^2(\bar{R}e^{-\bar{Y}}x_1+J_0)^2}{8}+\frac{\bar{R}^2e^{-2\bar{Y}}\sigma_Y^2}{8\alpha_Y^2}\right]+f_1(\tau)\\
P_{v_2v_2}(\mathbf{x},\tau) =& \frac{e^{2\bar{Y}}}{b^2n^2}\left[\frac{\sigma_Y^2(\bar{R}e^{-\bar{Y}}x_1+J_0)^2}{8}+\frac{\bar{R}^2e^{-2\bar{Y}}\sigma_Y^2}{8\alpha_Y^2}\right]+f_1(\tau)\\
P_{v_1v_2}(\mathbf{x},\tau) =& 0\\
f_1(\tau) =& \frac{3\sigma_R^2\alpha_R^2}{2(bnS_y')^2}\int_0^\infty \frac{k^2(ke^{-|\tau'|}-e^{-k|\tau'|})}{(k+\frac{\alpha_R^2}{S_y'})^4(k^2-1)}dk
\end{aligned}
\tag{B.28}
$$

The velocity covariance of zero temporal separation distance can be derived by setting the temporal separation distance to zero in equation (B.26):

$$
\begin{aligned}
P_{v_1v_1}(\mathbf{x},\mathbf{x}',0) =& P_{v_1v_1}^{(1)}\\
&-\frac{6\sigma_R^2\alpha_R^2}{(bn)^2}\left[\frac{-\xi^2K_2(\alpha_R\xi)+\alpha_R\xi_1^2\xi K_1(\alpha_R\xi)}{48(\alpha_R^2-S_y')}\right.\\
&+\frac{S_y'}{(\alpha_R^2-S_y')^2}\frac{[-\xi K_1(\alpha_R\xi)+\alpha_R\xi_1^2K_0(\alpha_R\xi)]}{8\alpha_R}\\
&+\frac{S_y'}{2(\alpha_R^2-S_y')^3}\left[-K_0(\alpha_R\xi)+\frac{\alpha_R\xi_1^2K_1(\alpha_R\xi)}{\xi}\right]\\
&+\frac{S_y'}{(\alpha_R^2-S_y')^4}\left[\frac{\xi_1^2[\alpha_R^2K_0(\alpha_R\xi)-S_y'K_0(\sqrt{S_y'}\xi)]}{\xi^2}\right.\\
&\left.\left.+\frac{(\xi_1^2-\xi_2^2)[\alpha_RK_1(\alpha_R\xi)-\sqrt{S_y'}K_1(\sqrt{S_y'}\xi)]}{\xi^3}\right]\right]
\end{aligned}
\tag{B.29}
$$

$$
\begin{aligned}
P_{v_2v_2}(\mathbf{x},\mathbf{x}',0) =& P_{v_2v_2}^{(1)}\\
&-\frac{6\sigma_R^2\alpha_R^2}{(bn)^2}\left[\frac{-\xi^2K_2(\alpha_R\xi)+\alpha_R\xi_2^2\xi K_1(\alpha_R\xi)}{48(\alpha_R^2-S_y')}\right.\\
&+\frac{S_y'}{(\alpha_R^2-S_y')^2}\frac{[-\xi K_1(\alpha_R\xi)+\alpha_R\xi_2^2K_0(\alpha_R\xi)]}{8\alpha_R}\\
&+\frac{S_y'}{2(\alpha_R^2-S_y')^3}\left[-K_0(\alpha_R\xi)+\frac{\alpha_R\xi_2^2K_1(\alpha_R\xi)}{\xi}\right]\\
&+\frac{S_y'}{(\alpha_R^2-S_y')^4}\left[\frac{\xi_2^2[\alpha_R^2K_0(\alpha_R\xi)-S_y'K_0(\sqrt{S_y'}\xi)]}{\xi^2}\right.\\
&\left.\left.+\frac{(\xi_2^2-\xi_1^2)[\alpha_RK_1(\alpha_R\xi)-\sqrt{S_y'}K_1(\sqrt{S_y'}\xi)]}{\xi^3}\right]\right]
\end{aligned}
\tag{B.30}
$$

$$
\begin{aligned}
P_{v_2v_1}(\mathbf{x},\mathbf{x}',0) = P^{(1)}_{v_1v_2} \\
&- \frac{6\sigma_R^2\alpha_R^2}{(bn)^2}\Bigg[\frac{\alpha_R\xi_1\xi_2\xi K_1(\alpha_R\xi)}{48(\alpha_R^2-S'_y)} + \frac{S'_y}{(\alpha_R^2-S'_y)^2}\frac{\xi_1\xi_2 K_0(\alpha_R\xi)}{8} \\
&\quad + \frac{S'_y}{2(\alpha_R^2-S'_y)^3}\frac{\alpha_R\xi_1\xi_2 K_1(\alpha_R\xi)}{\xi} \\
&\quad + \frac{S'_y}{(\alpha_R^2-S'_y)^4}\Big[\frac{\xi_1\xi_2[\alpha_R^2 K_0(\alpha_R\xi) - S'_y K_0(\sqrt{S'_y}\xi)]}{\xi^2} \\
&\quad + \frac{2\xi_1\xi_2[\alpha_R K_1(\alpha_R\xi) - \sqrt{S'_y}K_1(\sqrt{S'_y}\xi)]}{\xi^3}\Big]\Bigg]
\end{aligned}
\tag{B.31}
$$

APPENDIX C
MOMENTUM METHOD

C.1 General Integration Expressions for Initial Condition

Consider a two-dimensional homogeneous transport problem with the following initial condition and boundary conditions:

$$\frac{\partial c}{\partial t} + \bar{v}_1 \frac{\partial c}{\partial x_1} - D_1 \frac{\partial^2 c}{\partial x_1^2} - D_2 \frac{\partial^2 c}{\partial x_2^2} = 0 \in D \tag{C.1}$$

$$c(t, \mathbf{x}) = 0 \quad \mathbf{x} \in \partial D \tag{C.2}$$

$$c(0, \mathbf{x}) = f(\mathbf{x}) \quad \mathbf{x} \in D \tag{C.3}$$

where D is a two-dimensional domain with boundary $\partial D = \partial D_1 \cup \partial D_2$; and $\mathbf{x} = (x_1, x_2)$ is a point in D; the boundary conditions are set to zero for the convenience of discussions; and $f(\mathbf{x})$ can be any continuously spatial function.

Performing the Laplace and Double Fourier transform of equations (C.1) - (C.3), using the derivative properties of Fourier transform in Appendix D, and rearranging terms leads to:

$$\tilde{c}(s, \mathbf{k}) = \frac{F(\mathbf{k})}{[s - 2\pi i \bar{v}_1 k_1 + 4\pi^2 D_1 k_1^2 + 4\pi^2 D_2 k_2^2]} \tag{C.4}$$

in which tilde represents the Laplace-Fourier domain; $F(\mathbf{k})$ is a double Fourier transform function, $\mathcal{F}[f(\mathbf{x})]$ for $f(\mathbf{x})$, as described in Appendix D.

Applying double Fourier transform convolution theory and using equation (D.9) leads the general solution of transport equation for $c(t, \mathbf{x})$ subject to the general initial condition:

$$c(x,t) = \int_{-\infty}^{\infty}\int_{-\infty}^{\infty} f(\mathbf{x}')\frac{1}{4\pi\sqrt{D_1 D_2}t}\exp\left[-\frac{(x_1 - x_1' - \bar{v}_1 t)^2}{4D_1 t} - \frac{(x_2 - x_2')^2}{4D_2 t}\right] d\mathbf{x}' \tag{C.5}$$

As an example, assuming that initial condition is a homogeneous patch source with concentration c_0 and length $2L_1$ and width $2L_2$, the equation (C.5) becomes:

$$\begin{aligned}\bar{c}(\mathbf{x},t) = \frac{c_0}{4}\Bigg\{&\operatorname{erf}\left[\frac{(x_1 + L_1 - \bar{v}_1 t)}{2\sqrt{D_1 t}}\right] + \operatorname{erf}\left[\frac{(-x_1 + L_1 + \bar{v}_1 t)}{2\sqrt{D_1 t}}\right]\Bigg\} \\ &\Bigg\{\operatorname{erf}\left[\frac{(x_2 + L_2)}{2\sqrt{D_2 t}}\right] + \operatorname{erf}\left[\frac{(-x_2 + L_2)}{2\sqrt{D_2 t}}\right]\Bigg\}\end{aligned} \tag{C.6}$$

C.2 General Integration Expressions for Non-homogeneous P.D.E.s

The momentum method is a general method for solving non-homogeneous partial differential equations, which is conceptually similar to the Green function method. A brief description is given here:

Rewriting equations (C.1)-(C.3) with a continuous forcing term $f(t,\mathbf{x})$ gives:

$$\frac{\partial c}{\partial t} + \bar{v}_1\frac{\partial c}{\partial x_1} - D_1\frac{\partial^2 c}{\partial x_1^2} - D_2\frac{\partial^2 c}{\partial x_2^2} = f(t,\mathbf{x}) \quad \mathbf{x} \in D \tag{C.7}$$

$$c(t,\mathbf{x}) = 0 \quad \mathbf{x} \in \partial D \tag{C.8}$$

$$c(0,\mathbf{x}) = 0 \quad \mathbf{x} \in D \tag{C.9}$$

The continuous forcing term $f(t,\mathbf{x})$ in equation (C.7) from time at 0 to time t can be viewed as the summation of numerous instantaneous forcing terms $f(\tau,\mathbf{x})\delta(t-\tau)d\tau$. Thus

$$f(t,\mathbf{x}) = \int_0^t f(\tau,\mathbf{x})\delta(t-\tau)d\tau \tag{C.10}$$

Equations (C.7) - (C.9) are linear equations, for which the principle of superposition can be applied. Since equation (C.10) is also linear, the solution of equation

(C.7) should be the summation of transport problem $g(x,t;\tau)d\tau$ caused by the instantaneous source $f(x,\tau)\delta(t-\tau)d\tau$, or:

$$c(t,\mathbf{x}) = \int_0^t g(t,\mathbf{x};\tau)d\tau \tag{C.11}$$

The solution for $g(t,\mathbf{x};\tau)$ satisfies:

$$\frac{\partial g}{\partial t} + \bar{v}_1\frac{\partial g}{\partial x_1} - D_1\frac{\partial^2 g}{\partial x_1^2} - D_2\frac{\partial^2 g}{\partial x_2^2} = f(t,\mathbf{x})\delta(t-\tau) \quad \mathbf{x}\in D \tag{C.12}$$

$$g(t,\mathbf{x}) = 0 \quad \mathbf{x}\in \partial D \tag{C.13}$$

$$g(0,\mathbf{x}) = 0 \quad \mathbf{x}\in D \tag{C.14}$$

The instantaneous source $f(x,\tau)$ will have no effect after $\tau+0$. Thus equations (C.12) - (C.14) can be written:

$$\frac{\partial g}{\partial t} + \bar{v}_1\frac{\partial g}{\partial x_1} - D_1\frac{\partial^2 g}{\partial x_1^2} - D_2\frac{\partial^2 g}{\partial x_2^2} = 0 \quad \mathbf{x}\in D \tag{C.15}$$

$$g(t,\mathbf{x}) = 0 \quad \mathbf{x}\in \partial D \tag{C.16}$$

$$g(\tau+0,\mathbf{x}) = f(\tau,\mathbf{x}) \quad \mathbf{x}\in D \tag{C.17}$$

The solution for equations (C.15) - (C.17) in an infinite domain can be derived following the previous procedure for the initial value problem, i.e.:

$$g(t,\mathbf{x};\tau) = \int_{-\infty}^{\infty}\int_{-\infty}^{\infty} f(\tau,\xi)\frac{1}{4\pi\sqrt{D_1D_2}(t-\tau)} \exp\left[-\frac{(x_1-\xi_1-\bar{v}_1(t-\tau))^2}{4D_1(t-\tau)} - \frac{(x_2-\xi_2)^2}{4D_2(t-\tau)}\right]d\xi \tag{C.18}$$

in which it should be noted that equation (C.5) is solved based on the initial time at $t=0$, while equation (C.18) is obtained with the initial time at $t=\tau+0$.

Therefore the general solution for the original problem (C.7) - (C.9) in an infinite domain is:

$$c(x,t) = \int_{\tau=0}^{t} \int_{\xi_1=-\infty}^{\infty} \int_{\xi_2=-\infty}^{\infty} f(\xi,\tau) \frac{1}{4\pi\sqrt{D_1 D_2}(t-\tau)} \exp\left[-\frac{(x_1-\xi_1-\bar{v}_1(t-\tau))^2}{4D_1(t-\tau)} - \frac{(x_2-\xi_2)^2}{4D_2(t-\tau)}\right] d\xi d\tau \quad \text{(C.19)}$$

It is worthwhile to mention that this method can be easily extended to the three-dimensional advective-dispersive or wave problem, and to non-homogeneous boundary conditions using boundary condition transform techniques.

APPENDIX D
LAPLACE AND FOURIER TRANSFORM

D.1 Definiation

The f-convention is used in the Fourier transform in Chapters 3 and 4 of this dissertation to be consistent with the code adopted from the numerical recipe [Press et al., 1992]. The double Fourier transform equations for a two-dimensionally spatial function $f(x_1, x_2)$ can be expressed as [Press et al., 1992]:

$$\begin{aligned} F(k_1, k_2) &= \int_{-\infty}^{\infty}\int_{-\infty}^{\infty} f(x_1, x_2) e^{2\pi i(k_1 x_1 + k_2 x_2)} dx_1 dx_2 = \mathcal{F}[f(x_1, x_2)] \\ f(x_1, x_2) &= \int_{-\infty}^{\infty}\int_{-\infty}^{\infty} F(k_1, k_2) e^{-2\pi i(k_1 x_1 + k_2 x_2)} dk_1 dk_2 = \mathcal{F}^{-1}[F(k_1, k_2)] \end{aligned} \quad \text{(D.1)}$$

in which $\mathcal{F}$ and $\mathcal{F}^{-1}$ represent the forward and inverse Fourier transform operators, respectively; $\mathbf{k}$ is a two-dimensional wave vector.

The Laplace transform of a temporal function $f(t)$ is defined:

$$\begin{aligned} F(s) &= \int_0^{\infty} f(t) e^{-st} dt = \mathcal{L}[f(t)] \\ f(t) &= \int_{\gamma - i\infty}^{\gamma + i\infty} F(s) e^{st} ds = \mathcal{L}^{-1}[F(s)] \end{aligned} \quad \text{(D.2)}$$

in which $\mathcal{L}$ and $\mathcal{L}^{-1}$ represent the forward and inverse Laplace transform operators, respectively; γ is such that the contour of integration is to the right of any singularities of $F(s)$ [De Hoog et al., 1982].

We define the Laplace-Fourier transform for a spatiotemporal function $f(\mathbf{x}, t)$ as:

$$\mathcal{L}\mathcal{F}\Big[f(\mathbf{x},t)\Big] = F(\mathbf{k},s) = \int_0^\infty \int_{-\infty}^\infty \int_{-\infty}^\infty f(\mathbf{x},t)e^{-st+2\pi i\mathbf{k}\mathbf{x}}d\mathbf{x}dt$$
$$\mathcal{L}\mathcal{F}^{-1}\Big[F(\mathbf{k},s)\Big] = f(\mathbf{x},t) = \int_{\gamma-i\infty}^{\gamma+i\infty} \int_{-\infty}^\infty \int_{-\infty}^\infty F(\mathbf{k},s)e^{st-2\pi i\mathbf{k}\mathbf{x}}d\mathbf{k}ds \qquad \text{(D.3)}$$

D.2 Two-Dimensional Convolution

The convolution theory of Laplace and Fourier transforms are heavily used in this dissertation, here we give a brief description.

The convolution theory for Laplace or one dimensional Fourier transforms can be referenced in any related textbook or mathematics handbook. With two function $f_1(t)$ [or $f_1(x)$] and $f_2(t)$ [or $f_2(x)$], and their corresponding Laplace or Fourier transform $F_1(s)$ [or $F_1(k)$] and $F_2(s)$ [or $F_2(k)$], the *convolution* of the two functions, denoted $f_1(t) \otimes f_2(t)$ [or $f_1(x) \otimes f_2(x)$], is defined by:

$$\mathcal{L}^{-1}\left[F_1(s)F_2(s)\right] = f_1(t) \otimes f_2(t) = \int_0^t f_1(\tau)f_2(t-\tau)d\tau \qquad \text{(D.4)}$$

$$\mathcal{F}^{-1}\left[F_1(k)F_2(k)\right] = f_1(x) \otimes f_2(x) = \int_{-\infty}^\infty f_1(x')f_2(x-x')dx' \qquad \text{(D.5)}$$

Since there are not many books which detail two-dimensional Fourier convolution theory, we present the following derivation for the readers' reference.

For any two functions $f_1(x_1,x_2)$ and $f_2(x_1,x_2)$, their *convolution* can be defined by

$$f_1(x_1,x_2) \otimes f_2(x_1,x_2) = \int_{-\infty}^\infty \int_{-\infty}^\infty f_1(x_1',x_2')f_2(x_1-x_1',x_2-x_2')dx_1'dx_2' \qquad \text{(D.6)}$$

Note that $f_1(x_1,x_2) \otimes f_2(x_1,x_2)$ is a function in a two-dimensional space domain, which can be donated by $f(x_1,x_2)$.

Performing the double Fourier transform with respect to equation (D.6) leads to:

$$\begin{aligned}
\mathcal{F}[f_1(x_1,x_2)\otimes f_2(x_1,x_2)] &= \int_{-\infty}^{\infty}\int_{-\infty}^{\infty}\int_{-\infty}^{\infty}\int_{-\infty}^{\infty} f_1(x_1',x_2')f_2(x_1-x_1',x_2-x_2') \\
&\quad dx_1'dx_2'e^{2\pi(k_1x_1+k_2x_2)}dx_1dx_2 \\
&= \int_{-\infty}^{\infty}\int_{-\infty}^{\infty} f_1(x_1',x_2')\int_{-\infty}^{\infty}\int_{-\infty}^{\infty} f_2(x_1-x_1',x_2-x_2') \\
&\quad e^{2\pi(k_1x_1+k_2x_2)}dx_1dx_2dx_1'dx_2' \\
&= \int_{-\infty}^{\infty}\int_{-\infty}^{\infty} f_1(x_1',x_2')\int_{-\infty}^{\infty}\int_{-\infty}^{\infty} f_2(\xi_1,\xi_2) \\
&\quad e^{2\pi(k_1\xi_1+k_2\xi_2)}d\xi_1d\xi_2e^{2\pi(k_1x_1'+k_2x_2')}dx_1'dx_2' \\
&= \int_{-\infty}^{\infty}\int_{-\infty}^{\infty} f_1(x_1',x_2')F_2(k_1,k_2)e^{2\pi(k_1x_1'+k_2x_2')}dx_1'dx_2' \\
&= F_2(k_1,k_2)\int_{-\infty}^{\infty}\int_{-\infty}^{\infty} f_1(x_1',x_2')e^{2\pi(k_1x_1'+k_2x_2')}dx_1'dx_2' \\
&= F_2(k_1,k_2)\,F_1(k_1,k_2)
\end{aligned} \tag{D.7}$$

in which $\xi_1 = x_1 - x_1'$ and $\xi_2 = x_2 - x_2'$.

D.3 Some Useful Laplace and Fourier Transform Pairs

The following two Laplace-Fourier transform pairs are often used in the derivation of this dissertation:

$$\mathcal{F}[H(L-|x_1|)H(M-|x_2|)] = \frac{\sin(2\pi Lk_1)\,\sin(2\pi Mk_2)}{\pi^2k_1k_2} \tag{D.8}$$

$$\begin{aligned}
&\mathcal{L}\mathcal{F}\left[\frac{C_0}{4\pi t\sqrt{D_1D_2}}\exp\left[-\frac{(x_1-\bar{v}_1t)^2}{4D_1t}-\frac{x_2^2}{4D_2t}\right]\right] \\
&\qquad = \frac{C_0}{(4\pi^2D_1k_1^2+4\pi^2D_2k_2^2-2\pi i\bar{v}_1k_1+s)}
\end{aligned} \tag{D.9}$$

Brigham (1988) presents the derivation for equation (D.8) on page 239. Here we derive the transform pair in equation (D.9).

Performing the inverse Laplace transform to the right side of equation (D.9) and using a Laplace transform table [Gradshteyn and Ryzhik, 1980] leads to:

$$\begin{aligned}&\mathcal{L}^{-1}\left[\frac{C_0}{(4\pi^2 D_1 k_1^2 + 4\pi^2 D_2 k_2^2 - 2\pi i \bar{v}_1 k_1 + s)}\right] \\ &= \exp\left[-(4\pi^2 D_1 k_1^2 + 4\pi^2 D_2 k_2^2 - 2\pi i \bar{v}_1 k_1)t\right]\end{aligned} \tag{D.10}$$

Applying the double inverse Fourier transform to equation (D.10) leads to:

$$\begin{aligned}&\mathcal{L}\mathcal{F}^{-1}\left[\frac{C_0}{(4\pi^2 D_1 k_1^2 + 4\pi^2 D_2 k_2^2 - 2\pi i \bar{v}_1 k_1 + s)}\right] \\ &= C_0 \int_{-\infty}^{\infty} \exp\left[-4\pi^2 D_1 t k_1^2 + 2\pi i \bar{v}_1 t k_1 t - 2\pi i x_1 k_1\right] dk_1 \\ &\qquad \int_{-\infty}^{\infty} \exp\left[-4\pi^2 D_2 t k_2^2 - 2\pi i x_2 k_2\right] dk_2\end{aligned} \tag{D.11}$$

in which the definite integrals can be evaluated as followings:

$$\begin{aligned}&\int_{-\infty}^{\infty} \exp\left[-4\pi^2 D_1 t k_1^2 + 2\pi i \bar{v}_1 t k_1 t - 2\pi i x_1 k_1\right] dk_1 \\ &= \int_{-\infty}^{\infty} \exp\left[-4\pi^2 D_1 t k_1^2 - 2\pi i (x_1 - \bar{v}_1 t) k_1\right] dk_1 \\ &= \int_{-\infty}^{\infty} \exp\left[-\left[2\pi\sqrt{D_1 t} k_1 + \frac{i(x_1 - \bar{v}_1 t)}{2\sqrt{D_1 t}}\right]^2 + \left[\frac{i(x_1 - \bar{v}_1 t)}{2\sqrt{D_1 t}}\right]^2\right] dk_1\end{aligned} \tag{D.12}$$

Substituting $u = 2\pi\sqrt{D_1 t} k_1 + \frac{i(x_1 - \bar{v}_1 t)}{2\sqrt{D_1 t}}$ into the above integral leads to:

$$\begin{aligned}&\int_{-\infty}^{\infty} \exp\left[-\left[2\pi\sqrt{D_1 t} k_1 + \frac{i(x_1 - \bar{v}_1 t)}{2\sqrt{D_1 t}}\right]^2 + \left[\frac{i(x_1 - \bar{v}_1 t)}{2\sqrt{D_1 t}}\right]^2\right] dk_1 \\ &= \frac{1}{2\pi\sqrt{D_1 t}} \exp\left[-\frac{(x_1 - \bar{v}_1 t)^2}{4 D_1 t}\right] \int_{-\infty}^{\infty} \exp\left[-u^2\right] du \\ &= \frac{1}{2\sqrt{\pi D_1 t}} \exp\left[-\frac{(x_1 - \bar{v}_1 t)^2}{4 D_1 t}\right]\end{aligned} \tag{D.13}$$

where $\int_{-\infty}^{\infty} \exp\left[-u^2\right] du = \sqrt{\pi}$ [p. 307 of Gradshteyn and Ryzhik, 1980].

Similarly, the integral in the x_2 direction can be evaluated:

$$\int_{-\infty}^{\infty} \exp\left[-4\pi^2 D_2 t k_2^2 - 2\pi i x_2 k_2\right] dk_2 = \frac{1}{2\sqrt{\pi D_2 t}} \exp\left[-\frac{x_2^2}{4D_2 t}\right] \tag{D.14}$$

Substituting equations (D.13) and (D.14) into equation (D.11) yields:

$$\begin{aligned} &\mathcal{L}\mathcal{F}^{-1}\left[\frac{C_0}{(4\pi^2 D_1 k_1^2 + 4\pi^2 D_2 k_2^2 - 2\pi i \bar{v}_1 k_1 + s)}\right] \\ =&\frac{C_0}{4\pi t\sqrt{D_1 D_2}} \exp\left[-\frac{(x_1 - \bar{v}_1 t)^2}{4D_1 t} - \frac{x_2^2}{4D_2 t}\right] \end{aligned} \tag{D.15}$$

which equals to equation (D.9).

D.4 Derivative Properties of Fourier Transform

Two useful derivative properties of f-conventional Fourier transform are derived following the conventional Fourier transform [Gradshteyn and Ryzhik, 1980]:

$$\begin{aligned} \int_{-\infty}^{\infty} \frac{\partial f(x)}{\partial x} e^{2\pi i k x} dx &= \int_{-\infty}^{\infty} e^{2\pi i k x} df(x) = -\int_{-\infty}^{\infty} f(x) 2\pi i k e^{2\pi i k x} dx \\ &= -2\pi i k F(k) \end{aligned} \tag{D.16}$$

$$\begin{aligned} \int_{-\infty}^{\infty} \frac{\partial^2 f(x)}{\partial x^2} e^{2\pi i k x} dx &= \int_{-\infty}^{\infty} e^{2\pi i k x} d\frac{\partial f(x)}{\partial x} = -\int_{-\infty}^{\infty} \frac{\partial f(x)}{\partial x} 2\pi i k e^{2\pi i k x} dx \\ &= -\int_{-\infty}^{\infty} 2\pi i k e^{2\pi i k x} df(x) = -4\pi^2 k^2 F(k) \end{aligned} \tag{D.17}$$

REFERENCES

Ababou, R., *Three-Dimensional Flow in Random Porous Media*, Ph.D Dissertation, Dep. Civ. Eng., Mass. Inst. of Technol., Cambridge, 1988.

Abramowitz, M. and I. A. Stegun, *Handbook of Mathematical Functions*, Dover Publishing Co., New York, 1970, pp.1046.

Ahlstrom, S., H.Foote, R. Arnett, C. Cole, and R. Serne, Multicomponent mass transport model: Theory and numerical implementation, *Rep. BNWL 2127*,, Battelle Pac, Northwest Lab., Richland, Wash., 1977.

Amoozegar-Fard, A., D. R. Nielsen and A.W. Warrick, Soil solute concentration distribution for spatially varying pore water velocities and apparent diffusion coefficients, *Soil Sci. Soc. Amer.J.*, 46(1), 1982, pp.3–9.

Arfken, G., *Mathematical Methods for Physicists*, Academic Press Inc., New York, 1966.

Bakr, A. A., L. W. Gelhar, A. L. Gutjhar, and J. R. MacMillan, Stochastic analysis of spatial variability in subsurface flows, 1. Comparison of one- and three-dimensional flows, *Water Resources Research*, 14(2), 1978, pp.263–272.

Barry, D. A., J. Coves, and G. Sposito, On the Dagan model of solute transport in groundwater: Application to the Borden site, *Water Resources Research*, 24(), 1988, pp.1805–1817.

Batchelor,G.K., *Diffusion in a field of homogeneous turbulence, II, The relative motion of particles*, Proc. Cambridge Philos. Soc., 48, 1952, pp.345–363.

Bear, J., *Dynamics of Fluids in Porous Media*, Dover Publications, Inc., New York, 1972.

Bear, J., *Hydraulics of Groundwater*, McGraw-Hill, New York, 1979.

Bellin, A., G.Dagan and Y.Rubin, The impact of head gradient transients on transport in heterogeneous formations: Application to the Borden Site, *Water Resources Research*, 32(9), 1996, pp.2705–2713.

Bellin, A. and A. Rinaldo, Analytical solutions for transport of linearly adsorbing solutes in heterogeneous formations, *Water Resources Research*, 31(6), 1995, pp.1505–1511.

Bellin, A., Rinaldo, A., Bosma, W.J.P., van der Zee, S.E.A.T.M., and Y. Rubin, Linear equilibrium adsorbing solute transport in physically and chemically heterogeneous porous formations, 1. Analytical solutions, *Water Resources Research*, 29(12), 1993, pp.4019–4030.

Berg, P. W. and J. L. McGregor *Elementary Partial Differential Equations*, Holden Day Inc, California, 1966, pp. 421.

Berglund, S., *Groundwater Contamination: Significance of Hydrochemical Processes for Remediation and Impact Evaluation*, Ph.D Dissertation, Dept. of Civil and Environmental Engineering, Royal Institute of Technology, Stockholm, Sweden, 1997.

Black, T.C., and D.L. Freyberg, Stockastic modeling of vertically-averaged concentration uncertainty in a perfectly stratified aquifer, *Water Resources Research*, 23(6), 1987, pp.997–1004.

Brigham, E. O., *The fast Fourier transform and its applications*, Prentice-Hall, Inc., New Jersey, 1988.

Chu, S.Y., and G., Sposito, A Derivation of the Macroscopic Solute Transport Equation for Homogeneous, Saturated, Porous Media, 2. Reactive Solute at Low Concentration, *Water Resources Research*, 17(2), 1980, pp.333–336.

Clifton, P.M., and S.P. Neuman, Effects of Kriging and inverse modeling on conditional simulation of the Avra Valley aquifer in southern Arizona, *Water Resources Research*, 18(4), 1982, pp.1215–1237.

Cvetkovic, V., and A.M. Shapiro, Mass arrival of sorptive solute in heterogeneous porous media, *Water Resources Research*,26, 1990, pp.2057–2067.

Cvetkovic, V., A.M.Shapiro and G. Dagan, A solute flux approach to transport in heterogeneous formation: 2. Uncertainty analysis, *Water Resources Research*,28, 1992, pp.1377–1388.

Cvetkovic, V., and G. Dagan, Transport of kinetically sorbing solute by steady random velocity in heterogenous porous formations, *J. Fluid Mech.*, 265, 1994, pp.189–215.

Dagan, G., Stochastic modeling of groundwater flow by unconditional and conditional probabilities: 1.Conditional simulation and the direct problem, *Water Resources Research*, 18(4), 1982a, pp.813–834.

Dagan, G., Stochastic modeling of groundwater flow by unconditional and conditional probabilities: 2.The solute transport, *Water Resources Research*, 18(4), 1982b, pp.835–848.

Dagan, G., Solute transport in heterogeneous formation, *J. Fluid Mech.*, 145, 1984, pp.151–177.

Dagan, G., Statistical theory of groundwater flow and transport: Pore to laboratory, laboratory to formation, and formation to Regional scale, *Water Resources Research*, 22(9), 1986, pp.120S.

Dagan, G., Theory of solute transport by groundwater, *Ann. Rev. Fluid Mech.*, 19, 1987, pp.183–215.

Dagan, G., *Flow and Transport in Porous Formations*, Springer–Verlag, New York, 1989.

Dagan, G., Transport in heterogeneous porous formations: spatial moments, ergodicity, and effective dispersion, *Water Resources Research*, 26(6), 1990, pp.1281–1290.

Dagan, G., A. Bellin, and Y. Rubin, Lagrangian analysis of transport in heterogeneous formations under transient flow conditions, *Water Resources Research*, 32(4), 1996, pp.891–899.

Dagan, G., V. Cvetkovic, and A. Shapiro, A solute flux approach to transport in heterogeneous formations, 1. the general framework, *Water Resources Research*, 28(5), 1992, pp.1369–1376.

Dagan, G., and S. P. Neuman, Nonasymptotic behavior of a common Eulerian approximation for transport in random velocity fields, *Water Resources Research*, 27(12), 1991, pp.3249-3256.

Dagan, G., and Y. Rubin, Stochastic identification of recharge, transmissivity, and storativity in aquifer transient flow: A quasi–steady approach, *Water Resources Research*, 24(10), 1988, pp.1698–1710.

De Hoog, F. R., J. H. Knight. and A. N. Stokes, An improved method for numerical inversion of Laplace transforms, *SIAMJ. Sci. Stat. Comput.*, 3(3), 1982, pp.357–366.

Delhomme, J.P., Spatial variability and uncertainty in groundwater flow parameters: A geostatistical approach, *Water Resources Research*, 15(2), 1979, pp.269–279.

Deng, F. W., J. H. Cushman, and J.W. Delleur, A Fast Fourier Transform Stochastic Analysis of the Contaminant Transport Problem, *Water Resources Research*, 29(9), 1993, pp.3241–3247.

Deng, F. W. and J. H. Cushman, On higher-order corrections to the flow velocity covariance tensor, *Water Resources Research*, 31(7), 1995, pp.1659–1672.

Destouni, G., and V. Cvetkovic, Field scale mass arrival of sorptive solute into the groundwater, *Water Resources Research*, 27(6), 1991, pp.1315–1325.

Ellsworth, T.R., W.A. Jury, F.F. Ernst, and P.J.,Shouse, A three-dimensional field study of solute transport through an unsaturated layered, porous media, 1. Methodology, mass recovery, and mean transport, *Water Resources Research*, 28, 1991a, pp.951–965.

Ellsworth, T.R., W.A. Jury, F.F. Ernst, and P.J.,Shouse, A three-dimensional field study of solute transport through an unsaturated layered, porous media, 2. Characteristics of Vertical Dispersion, *Water Resources Research*, 28, 1991b, pp.967–981.

Freeze, R.A., A stochastic–conceptual analysis of one–dimensional groundwater flow in nonuniform homogeneous media, *Water Resources Research*, 11(5), 1975, pp.725–741.

Freyberg, D.L., A natural gradient experiment on solute transport on a sand aquifer, 2. Spatial moments and the advection and dispersion of nonreactive tracers, *Water Resources Research*, 22(13), 1986, pp.2031–2046.

Frind, E.O., E.A. Sudicky, and S.L. Schellenberg, Macroscale modelling in the study of plume evolution in heterogeneous media, *Stochastic Hydrol. Hydraul.*, 263(1), 1987.

Garabedian, S., *Large–scale dispersive transport in aquifers: Field experiments and reactive transport theory*, Ph.D Dissertation, Dep. Civ. Eng., Mass. Inst. of Technol., Cambridge, 1987.

Garabedian, S.P., LeBlanc, D.R., Gelhar, L.W., and M.A., Celia, Large–scale natural gradient tracer test in sand and gravel, Cape Cod, Massachusetts: 2. Analysis of spatial moments for a nonreactive tracer, *Water Resources Research*, 27(5), 1991, pp.911–924.

Gelhar, L.W., Stochastic analysis of phreatic aquifers, *Water Resources Research*, 10(3), 1974, pp.539–545.

Gelhar, L.W., The effects of hydraulic conductivity variations on ground-water flows, *2nd Int.Symp. on Stochastic Hydraulics*, Lund, Sweden, 1976.

Gelhar, L.W., Stochastic analysis of flow in heterogeneous porous media, *In Fundamentals of Transport Phenomena in Porous Media*, edited by J.Bear and M.Y.Corapcioglu, M.Nijhoff, Dordrecht, the Netherlands, 1984, pp.673–718.

Gelhar, L.W., Stochastic subsurface hydrology from theory to applications, *Water Resources Research*, 22(9), 1986, pp.135S–145S.

Gelhar, L.W., Stochastic analysis of solute transport in saturated and unsaturated porous media, *In Fundamentals of Transport Phenomena in Porous Media, NATO ASI Series E, No. 128*, edited by J.Bear and M.Y.Corapcioglu, M.Nijhoff, Dordrecht, the Netherlands, 1987a, pp.657–700.

Gelhar, L.W., Applications of stochastic models to solute transport in fractured rocks, Swedish Nuclear Fuel and Waste Management Company, *SKB Tech.Rpt.*, 87–05, Stockholm, Sweden, 1987b.

Gelhar, L.W., *Stochastic Subsurface Hydrology*, Prentice Hall, New Jersey, 1993.

Gelhar, L.W., and C.L. Axness, Three–dimensional stochastic analysis of macrodispersion in aquifers, *Water Resources Research*, 19(1), 1983, pp.161–180.

Gelhar, L. W., A. L., Gutjahr, and R. L. Naff, Stochastic analysis of macrodispersion in a stratified aquifer, *Water Resources Research*, 15(6), 1979, pp.1387–1397.

Gelhar, L.W., A.L. Gutjahr, and R.L. Naff, Reply to comments on "Stochastic analysis of macrodispersion in a stratified aquifer", *Water Resources Research*, 17(6), 1981, pp.1739–1740.

Gelhar, L. W., and A. L., Gutjahr, Stochastic Solution of the one-dimensional convective dispersion equation. *Hydrology Research Program Report H-11*, New Mexico Institute of Mining and Technology, Socorro, 1982.

Geller, J.T., and J.R. Hunt, Mass transfer from nonaqueous phase organic liquids in water–saturated porous media, *Water Resources Research*, 29(4), 1993, pp.833–845.

Gomez-Hernandez, J. J., and S. M. Gorelick, Effective groundwater model parameter values: Influence of spatial variability of hydraulic conductivity, leakance and recharge, *Water Resources Research*, 25(3), 1989, pp.405–419.

Gradshteyn, I.S. and I. M. Ryzhik, *Table of Integrals, Series, and Products*, Academic Press, New York, 1980. pp. 1153

Graham, W.D., and D. McLaughlin, Stochastic analysis of nonstationary subsurface solute transport: 1. Unconditional moments, *Water Resources Research*, 25(2), 1989a, pp.215–232.

Graham, W.D., and D. McLaughlin, Stochastic analysis of nonstationary subsurface solute transport: 2. Conditional moments, *Water Resources Research*, 25(11), 1989b, pp.2331–2355.

Graham, W.D., and D. McLaughlin, A stochastic model of solute transport in groundwater: Application to the Borden, Ontario, tracer test, *Water Resources Research*, 27(6), 1991, pp.1345–1359.

Graham, W.D., and C.D. Tankersley, Forcasting piezometric head levels in the Floridan aquifer: A Kalman filtering approach, *Water Resources Research*, 29(11), 1993, pp.3791–3800.

Graham, W.D., and C.D. Tankersley, Optimal estimation of spatial variable recharge and transmissivity fields under steady–state groundwater flow, Part 1. Theory, *Journal of Hydrology*, 157, 1994, pp.247–266.

Graham, W.D., and C.R. Neff, Optimal estimation of spatial variable recharge and transmissivity fields under steady–state groundwater flow, Part 2. Case study, *Journal of Hydrology*, 157, 1994, pp.267–285.

Gutjhar, A.L., L.W., Gelhar, A.A., Bakr, and J.R., MacMillan Stochastic Analysis of Spatial Variability in Subsurface Flows. 1. Comparison of One- and Three-Dimension Flows, *Water Resources Research*, 14(5), 1978, pp.953–959.

Guven, O., F.J. Molz, and J.G. Melcille, An analysis of dispersion in a stratified aquifer, *Water Resources Research*, 20(10), 1984, pp.1337–1354.

Harter, T., *Unconditional and conditional simulation of flow and transport in heterogeneous, variably saturated porous media*, Ph.D Dissertation, Department of Hydrology and Water Resources, University of Arizona, 1994.

Imhoff, P.T., P.R. Jaffe and G.F. Pinder, An experimental study of complete dissolution of a nonaqueous phase liquid in saturated porous media, *Water Resources Research*, 30(2), 1993, pp.307–320.

James, A.I., Graham, W.D., Hatfield, K., Rao, P.S.C., and M.D. Annable, Optimal estimation of residual NAPL saturation using partitioning tracer concentration data, *Water Resources Research*, 33(12), 1997. pp.2621–2636

Jury, W.A., L.H.Stolzy, and P.Shouse, A field test of the transfer function model for predicting solute transport, *Water Resources Research*, 18(2), 1982, pp.369–375.

Jury W.A., H. El Abd, and M. Resketo, Field study of napropamide movement through unsaturated soil, *Water Resources Research*, 22, 1986, pp.749–755.

Kapoor, V., and L.W. Gelhar, Transport in three–dimensionally heterogeneous aquifers, 1.Dynamics of concentration fluctuations, *Water Resources Research*, 30(6), 1994a, pp.1775–1788.

Kapoor, V., and L.W. Gelhar, Transport in three–dimensionally heterogeneous aquifers, 2.Predictions and observations of concentration fluctuations, *Water Resources Research*, 30(6), 1994b, pp.1789–1801.

Killey, R.W.D. and G.L., Moltyaner, Twin lake tracer tests: setting, methodology, and hydraulic conductivity distribution, *Water Resources Research*, 24(10), 1988, pp.1585–1612.

Leblanc, D.R., Garabedian, S.P., Hess, K.M., Gelhar, L.W., Quadri, R.D., Stollenwerk, K.G., and W.W. Wood, Large–scale natural gradient tracer test in sand and gravel, Cape Cod, Massachusetts: 1. Experimental design and observed tracer movement, *Water Resources Research*, 27(5), 1991, pp.895–910.

Li, L., and W.D., Graham, Stochastical analysis of solute transport in heterogeneous aquifers subject to random recharge *Journal of Hydrology*, in press 1998, pp. .

Li, S-G, and D. B. McLaughlin, A nonstationary spectral method for solving stochastic groundwater problems: Unconditional analysis, *Water Resources Research*, 27(7), 1991, pp.1589–1605.

Li, S-G, and D. B. McLaughlin, Using the nonstationary spectral method to analyze flow through heterogeneous trending media, *Water Resources Research*, 27(7), 1995 pp.541–551.

Mackey, D.M., Freyberg, D.L., Roberts, P.V., and J.A., Cherry, A natural gradient experiment on solute transport on a sand aquifer, 1. Approach and overview of plume movement, *Water Resources Research*, 22(13), 1986a, pp.2017–2029.

Mackey, D.M., Freyberg, D.L., Roberts, P.V., and J.A., Cherry, A natural gradient experiment on solute transport on a sand aquifer, 2, Spatial moments and the advection and dispersion of nonreactive tracers, *Water Resources Research*, 22(13), 1986b, pp.2031–2046.

Mantoglou, A., and L.W.Gelhar, Stochastic modeling of large-scale transient unsaturated flow systems, *Water Resources Research*, 23(1), 1987a, pp.37–46.

Mantoglou, A., and L.W.Gelhar, Capillary tension head variance, mean soil content and effective specific soil moisture capacity of transient unsaturated flow in stratified soils, *Water Resources Research*, 23(1), 1987b, pp.47–56.

Mantoglou, A., and L.W.Gelhar, Effective hydraulic conductivities of transient unsaturated flow in stratified soils, *Water Resources Research*, 23(1), 1987c, pp.57–67.

Matheron, G., and G., De Marsily, Is Transport in Porous Media Always Diffusive? A Counterexample, *Water Resources Research*, 16(5), 1980, pp.901–917.

McLaughlin, D., and E.F. Wood, A distributed parameter approach for evaluating the accuracy of groundwater model predictions, 1. theory, *Water Resources Research*, 24(7), 1988a, pp.1037–1047.

McLaughlin, D., and E.F. Wood, A distributed parameter approach for evaluating the accuracy of groundwater model predictions, 2. application to groundwater flow, *Water Resources Research*, 24(7), 1988b, pp.1048–1060.

Mizell, S. A., A. L. Gutjhar, and L.W. Gelhar, Stochastic analysis of spatial variability in two-dimensional steady groundwater flow assuming stationary and non-stationary heads, *Water Resources Research*, 18(4), 1982 pp.1053–1067.

Neuman, S.P., Eulerian–Lagrangian theory of transport in space–time nonstationary velocity fields: Exact nonlocal formalism by conditional moments and weak approximations, *Water Resources Research,* 29(3), 1993, pp.633–645.

Neuman, S.P., and Y.-K. Zhang, A quasilinear theory of non-Fickian and Fickian subsurface dispersion, 1, Theoretical analysis with application to isotropic media, *Water Resources Research*, 26(5), 1990, pp.887–902.

Press, W.H., Teukolsky, S.A., Vetterling, W.T., and B.P. Flannery, *Numerical Recipes in C, the Art of Scientific Computing*, Second Edition, Cambridge University Press, New York, 1992.

Rehfeldt, K. R., and L. W. Gelhar, Stochastic Analysis of Dispersion in Unsteady Flow in Heterogeneous Aquifers, *Water Resources Research*, 28(8), 1992, pp.2085–2099.

Roth, K., and W.A. Jury, Linear transport models for adsorbing solutes *Water Resources Research*, 29(4), 1993, pp.1195–1203.

Rubin, Y., Stochastic modeling of macrodispersion in heterogeneous porous media, *Water Resources Research*, 26(1), 1990, pp.133–141.

Rubin, Y., and Bellin, A., Effects of recharge on flow nonuniformity and macrodispersion, *Water Resources Research*, 30(4), 1994, pp.939–948.

Rubin, Y., and G. Dagan, Stochastic identification of transmissivity and effective recharge in steady groundwater flow, 1. Theory, *Water Resources Research*, 23(7), 1987a, pp.1185–1192.

Rubin, Y., and G. Dagan, Stochastic identification of transmissivity and effective recharge in steady groundwater flow, 2. Case study, *Water Resources Research*, 23(7), 1987b, pp.1193–1200.

Rubin, Y., and G. Dagan, Conditional estimation of solute travel time in heterogeneous formations: Impact of transmissivity measurements, *Water Resources Research*, 28(4), 1992, pp.1033–1040.

Serrano, S.E., The form of the dispersion equation under recharge and variable velocity, and its analytical solution, *Water Resources Research*, 28(7), 1992, pp.1801–1808,

Smith, L., and Freeze, R.A., Stochastic analysis of steady state groundwater flow in a bounded domain, 1, One dimensional simulations, *Water Resources Research*, 15(3), 1979a, pp.521–528.

Smith, L., and Freeze, R.A., Stochastic analysis of steady state groundwater flow in a bounded domain, 2, Two-dimensional simulations, *Water Resources Research*, 15(6), 1979b, pp.1543–1559.

Sposito, G., and D. A. Barry, On the Dagan model of solute transport through groundwater: Foundational aspects, *Water Resources Research*, 23(10), 1987, pp.1867–1875.

Sudicky, E.A., A natural gradient experiment on solute transport on a sand aquifer: Spatial variability of hydraulic conductivity and its role in the dispersion process, *Water Resources Research*, 22(13), 1986, pp.2069–2082.

Tompson, A.F.B., R. Ababou, and L.W. Gelhar, Applications and use of the three-dimensional turning bands random field generator in hydrology: Single realization problems, *Parsons Laboratory Report 313*, Massachusetts Institute of Technology, Cambridge, 1987.

Tompson, A.F.B., and L.W. Gelhar, Numerical simulation of solute transport in three–dimensional, randomly heterogeneous porous media, *Water Resources Research*, 26(10), 1990, pp.2541–2562.

Valocchi, A., and A.M.Quinodez, Application of the random walk method to simulate the transport of kinetically adsorbing solutes, *Groundwater Contamination, IAHS Publ., 185*, 1989, pp.35–42.

van der Zee, S.E.A.T.M., and W.H. van Riemsdijk, Transport of reactive solute in spatially variable soil systems, *Water Resources Research*, 23, 1987, pp.2059–2069.

Warren, J.E., and H.S. Price, Flow in heterogeneous porous media, *Soc. Petrol. Eng. J.*, (1), 1961, pp.153–169.

Wolfram, S., *Mathematica*, 2nd ed., Addison–Wesley, Reading, Mass., 1991,

Yeh,T.-C., L.W.Gelhar and A.L.Gutjahr, Stochastic analysis of unsaturated flow in heterogeneous soils, 2: Statistically anisotropic media with variable alpha, *Water Resources Research*, 21(4), 1985a, pp.457–464.

Yeh,T.-C., L.W.Gelhar and A.L.Gutjahr, Stochastic analysis of unsaturated flow in heterogeneous soils, 3: Observations and applications, *Water Resources Research*, 21(4), 1985b, pp.465-471.

Zhang, D., and S.P. Neumann, Eulerian–Lagrangian analysis of transport conditioned on hydraulic data, 1. Analytical–numerical approach, *Water Resources Research*, 26(5), 1995a, pp.39–51.

Zhang, D., And S. P. Neuman, Eulerian–Lagrangian analysis of transport conditioned on hydraulic data, 2. Effects of log transmissivity and hydraulic head measurements, *Water Resources Research*, 31(1), 1995b, pp.53–63.

Zhang, D., And S. P. Neuman, Eulerian–Lagrangian analysis of transport conditioned on hydraulic data, 3. Spatial moments, travel time distribution, mass flow rate, and cumulative release across a compliance surface, *Water Resources Research*, 31(1), 1995c, pp.65–75.

Zhang, D., And S. P. Neuman, Eulerian–Lagrangian analysis of transport conditioned on hydraulic data, 4. Uncertain initial plume state and non-Gaussian velocities, *Water Resources Research*, 31(1), 1995d, pp.77–88.

Zhang, Y., *Spatial characterization of a hydrogeochemically heterogeneous aquifer using a three-dimensional distributed parameter extended Kalman filter*, Ph.D Dissertation, Agricultural and Biological Engineering Dept., University of Florida, Gainesville, FL., 1997.

Zhang, Y.-K., and S.P. Neumann, A quasi-linear theory of non-Fickian and Fickian subsurface dispersion, 2, Application to anisotropic media and the Borden site, *Water Resources Research*, 31(1), 1990, pp.903–913.

BIOGRAPHICAL SKETCH

Liyong Li was born in HangZhou, China, on June 12, 1962. He received a Bachelor of Science degree in Physical Geography from HangZhou University of China in July, 1983. He moved to the Beijing Normal University, receiving an M.S. in Environmental Sciences in 1986. After working for six years as a hydrologist for Chinese Research Academy of Environmental Sciences, he went to University of Liverpool of United Kindom as a research associate for the joint project in 1992. He started his Ph.D study in Department of Civil Engineering of Helsinki University of Technology of Finland in 1993. One year later he transfered into a doctoral program in Agricultural and Biological Engineering and Hydrologic Science at the University of Florida in the spring of 1994. His research interests include water resources engineering, contaminant hydrology, stochastic subsurface hydrology, and computer-aided modeling.

I certify that I have read this study and that in my opinion it conforms to acceptable standards of scholarly presentation and is fully adequate, in scope and quality, as a dissertation for the degree of Doctor of Philosophy.

Wendy D. Graham, Chairman
Associate Professor of Agricultural and Biological Engineering

I certify that I have read this study and that in my opinion it conforms to acceptable standards of scholarly presentation and is fully adequate, in scope and quality, as a dissertation for the degree of Doctor of Philosophy.

Palakurthi S.C. Rao, Cochairman
Graduate Research Professor of Soil and Water Science

I certify that I have read this study and that in my opinion it conforms to acceptable standards of scholarly presentation and is fully adequate, in scope and quality, as a dissertation for the degree of Doctor of Philosophy.

Kenneth L. Campbell
Professor of Agricultural and Biological Engineering

I certify that I have read this study and that in my opinion it conforms to acceptable standards of scholarly presentation and is fully adequate, in scope and quality, as a dissertation for the degree of Doctor of Philosophy.

Kirk Hatfield
Associate Professor of Civil Engineering

I certify that I have read this study and that in my opinion it conforms to acceptable standards of scholarly presentation and is fully adequate, in scope and quality, as a dissertation for the degree of Doctor of Philosophy.

Michael D. Annable
Assistant Professor of Environmental Engineering Sciences

This dissertation was submitted to the Graduate Faculty of the College of Engineering and to the Graduate School and was accepted as partial fulfillment of the requirements for the degree of Doctor of Philosophy.

May, 1998

Winfred M. Phillips
Dean, College of Engineering

Karen A. Holbrook
Dean, Graduate School